



University
of Glasgow

Ockelford, Anne-Marie (2011) *The impact of stress history on non cohesive sediment bed stability and structure*. PhD thesis

<http://theses.gla.ac.uk/2577/>

Copyright and moral rights for this thesis are retained by the author

A copy can be downloaded for personal non-commercial research or study, without prior permission or charge

This thesis cannot be reproduced or quoted extensively from without first obtaining permission in writing from the Author

The content must not be changed in any way or sold commercially in any format or medium without the formal permission of the Author

When referring to this work, full bibliographic details including the author, title, awarding institution and date of the thesis must be given.



**THE IMPACT OF STRESS HISTORY ON NON-
COHESIVE SEDIMENT BED STABILITY AND
BED STRUCTURE**

By

ANNE-MARIE OCKELFORD

**Submitted in fulfilment of the requirements for
the Degree of Doctor of Philosophy**

**SCHOOL OF ENGINEERING
UNIVERSITY OF GLASGOW**

ABSTRACT

THE IMPACT OF STRESS HISTORY ON NON-COHESIVE SEDIMENT BED STABILITY AND BED STRUCTURE

Historically the inter-flood period has been disregarded from investigations as it was deemed that the stability of non cohesive beds could only be altered by above threshold flows capable of sediment transport. However, this is at odds with more recent 'stress history' data which provides unequivocal evidence that entrainment thresholds can be delayed to higher shear stresses after being subjected to longer periods of sub threshold flows. The magnitude of this effect appears related to the surface grain size distribution and relative grain size effects, whilst the specific mechanics associated to generating a more resistant bed under sub-threshold flows are merely speculated upon. The aim of the present thesis is therefore to provide a comprehensive and quantitative data set on stress history that specifically address comparative grade effects and provides a detailed mechanistic understanding of the processes responsible for generating a more resistant bed configuration under sub threshold flows.

Using a range of grain size distributions, a series of flume based experiments assess two main aspects of the stress history process. Firstly the effects of grain size distribution on the relationship between stress history duration and entrainment threshold is quantified. This is split into two sets of experiments based on the duration of the applied sub threshold antecedent flow, prescribed as 50% of the critical shear stress (τ_c) of the median grain size (D_{50}). The antecedent durations of first set of experiment ranged from 0 to 60 minutes, whilst the antecedent duration of the second set of experiments ranged from 0 to 960 minutes. To ascertain the effect of the antecedent period on critical entrainment threshold and transported bedload, each experiment is concluded with a stability test composed of incrementally increased flow discharges until critical threshold conditions were reached. Secondly, aspect of stress history investigated uses high resolution laser scanning to assess bed topography and particle repositioning in order to ascertain the granular mechanics underpinning the stability process. The bed is scanned before and after the application of the applied antecedent flow with changes to bed surface structure described using Digital Elevation Models (DEM's), statistical analysis and 1D and 2D semi-variograms to analyse scaling behaviour.

In all experiments, increasing the antecedent flow duration significantly increases river bed stability in that the critical shear stress increases by up to 25% where uniform beds are more responsive to antecedency than bimodal beds. Laser based analysis reveals that vertical settlement, localised changes to bed roughness, pockets of more pronounced development of hiding effects, and particle repositioning are all mechanisms by which the bed reorganises under an applied sub threshold flow. However, the different bed grain size distributions cause significant differences in the importance of each mechanism in determining the magnitude of stress history induced bed stability.

Keywords: Graded, Sediment, Stability, Stress history, Laser scanning, Surface organisation

Dedication

This thesis is dedicated to three people who were instrumental in my decision to continue to pursue a personal goal; Peter Ockelford, Belinda Kent-Lemon and Kirsty Howell.

“Sometimes, if you stand on the bottom rail of a bridge and lean over to watch the river slipping slowly away beneath you, you will suddenly know everything there is to be known”

(Winnie the Pooh)

“Ipsa scientia potestas est”

(Sir Francis Bacon)

Chapter 1 Introduction.....	1
1.1 Research Aims and Objectives.....	3
Chapter 2 Literature Review.....	5
2.1 Sediment Entrainment Thresholds.....	5
2.2 Determination of Entrainment threshold	8
2.2.1 The Impact of Sediment Heterogeneity upon Sediment Entrainment	15
2.2.2 The Impact of Bed Structure and Surface Characteristics	18
2.2.3 Measurement of River Bed Surfaces	22
2.3 Stress history	26
2.3.1 Effects on critical entrainment threshold	26
2.3.2 Importance and application	32
2.4 Summary of the Literature Review	34
Chapter 3 Experimental Set- up and Instrumentation	36
3.1 Experimental Programme	36
3.2 Shields Flume.....	37
3.2.1 Installation.....	37
3.2.2 Bedload visualisation equipment.....	38
3.2.3 Bedload Sampling Equipment.....	39
3.3 Kelvin Flume.....	40
3.3.1 Installation.....	40
3.3.2 Bedload Sampling Equipment.....	41
3.3.3 Laser Displacement Scanning	42
3.4 Bed Materials	45
3.5 Chapter Summary.....	47
Chapter 4 Stress History Experiments in the 0.3m wide Flume.....	52
4.1 Introduction	52
4.2 Hypotheses	53
4.3 Experimental Procedure.....	53
4.3.1 Definition of critical threshold (τ_c)	54
4.4 Results.....	56
4.4.1 Uncertainty analysis	56
4.4.2 Critical entrainment threshold	60
4.4.3 Total Transported Bedload.....	65
4.4.4 Fractional Bedload Transport.....	75
4.5 Discussion	82
4.5.1 The influence of stress history on bed stability.....	82
4.5.2 Literature based explanations of the possible mechanics explaining the differential bed stability gains and response to stress history.	86
4.5.3 Absolute threshold and the role of fines.	87
4.5.4 The relative responsiveness of beds to stress history; the ability of fractions to rearrange.	90
4.5.5 Questions raised from data and discussion of Chapter 4	82
4.6 Chapter Summary	95
Chapter 5 Stress History Experiments in the 1.8m wide flume.....	97
5.1 Introduction	97
5.2 Hypothesis.....	98
5.3 Experimental Procedure.....	98

5.4	Results.....	99
5.4.1	Critical entrainment threshold.....	99
5.4.1	The effect of width depth ratios	102
5.4.2	Total transported bedload	109
5.4.3	Fractional transported bedload.....	122
5.5	Discussion	126
5.5.1	The influence of stress history on bed stability; confirmation of stress history derived trends from Chapter 4?	126
5.5.2	The effect of extending antecedent durations from 60mins (Chapter 4) to 960 minutes?.....	128
5.5.3	The effect of flume width on stress history trends	132
5.5.4	Questions raised from data and discussion of Chapter 5	136
5.6	Chapter Summary	137
Chapter 6 Mechanisms of Bed Stabilisation.....		140
6.1	Hypothesis.....	140
6.2	Experimental Procedure.....	141
6.3	Results.....	142
6.3.1	Visual Analysis.....	143
6.3.2	Global Quantitative Analysis	154
6.3.2.1	Probability Density Functions.....	154
6.3.2.2	Porosity	158
6.3.3	Small scale grain reorientation and displacement	178
6.3.3.1	Digital Elevation Models of Change	178
6.3.3.2	Particle repositioning	182
6.3.4	Large scale structuring.....	187
6.3.4.1	Fractional Analysis.....	188
6.3.4.2	2-D Second Order Structure Functions.....	191
6.4	Discussion	209
6.4.1	Small scale stabilisation processes; the effect of vertical settlement, changes to bed roughness and changes to bed porosity.....	209
6.4.2	Large scale process; the case for bed stabilisation as a result of grain rearrangement	214
6.5	Chapter Summary	220
Chapter 7 Conclusions and Future Research.....		223
7.1	Experimental summary	223
7.2	Effects of stress history upon entrainment threshold.....	223
7.3	Effects of stress history upon transported bedload.....	224
7.4	Effects of stress history upon bed structure	225
7.5	Future Research	227

LIST OF FIGURES

Figure 2-1; Diagram to depict different pivoting angles (ϕ_1 and ϕ_2) and particle surface area exposed to the flow field resulting from a mixed-bed of different particle sizes, shapes, and packing arrangements (Lorang and Hauer, 2001).....	7
Figure 2-2 Thresholds of sediment motion represented by the Shields curve (from Miller <i>et al.</i> , 1977). The black solid line represents the initial Shields curve (Shields, 1936) with the grey shaded envelope of values proposed by Miller <i>et al.</i> , (1977) to take into account the uncertainty surrounding the initiation of motion.....	8
Figure 2-3: Schematic representation of Grass' concept of overlapping shear stress distributions	14
Figure 2-4; Three subsequent time frames showing the bed topography and grain movement linked with the dimensionless streamwise velocity signature (from Bottacin – Busolin <i>et al.</i> , 2008). The boxed grain stops at the position in the second frame before being entrained again. The star box related to the position over which the velocity trace was taken.....	20
Figure 2-5; Continuous record of unit bedload transport expressed as submerged mass i_b , for selected floods from Turkey Brook, 1978- 1980. Floods with short recurrence intervals are noted to have large amounts of sediment generated on the rising limb (25-26 th Jan 1979, 31 st Jan – 1 st Feb 1979, 13-14 th March, marked with a solid black box) whereas floods which follow prolonged periods of low flow generate bedload on the falling limb after the rising limb has loosened the bed structuring and released the fines (10-11 th Dec, 1978, 9th-10 th Dec 1979, marked with a dashed black box)...	29
Figure 3-1; Schematic diagram of flow control devices attached to the Kelvin Flume.	40
Figure 3-2; Diagram depicting how the scanCONTROL 2800 laser records the surface. The top of the two images shows the relationship between x and z whilst the bottom image shows how the light source is projected onto the surface and reflected back onto the CMOS array.	43
Figure 3-3; Graphical representation of the five grain size distributions employed.	46
Figure 3-4 Experimental setup (Shields Flume) indicating the test section of sediments (coloured sections) the sediment trap in the foreground, the glass plate used to still the water surface during image capture and the camera used for video and still image capture.	49
Figure 3-5: Instrument Rig (Kelvin Flume) detailing the video camera and pointer gauge situated over the channel centre line and the sediment set up.	50
Figure 3-6; Sediment trap used for collecting sediment in the Kelvin Flume.	51
Figure 4-1: Variability in the raw threshold counts for all five grain size distributions over five antecedent durations.....	59
Figure 4-2: Relationship for displacements recorded close to threshold (uniform bed). An increasingly steep gradient is noted as antecedent duration is increased with the exception of the 10 minutes date; the gradient is noted next to each line. The numbers of on the graph represent the gradient of the line for the individual experimental runs.	60
Figure 4-3; The relationship between antecedent duration, average critical bed shear stress and grain size distribution. The uniform, unimodal and bimodal beds are fitted with a linear polynomial growth curve with root mean square errors values of 0.09, 0.01 and 0.03 for the uniform, unimodal and bimodal beds respectively.	61
Figure 4-4: First derivative of the fitted trend lines of the response of the uniform, unimodal and bimodal grain size distributions respectively to antecedent flow duration.....	63

Figure 4-5; Stress history relationships with total bedload fitted with an exponential decay function superimposed in a background constant noting R^2 values of 0.99, 0.90, 0.82, 0.92 for the unimodal, bimodal, coarse and fine respectively.	67
Figure 4-6; First derivative of the fitted trend lines of the response of the unimodal, bimodal, coarse and fine grain size distributions respectively to antecedent total transported bedload. Given the different magnitude of response of the unimodal bed it has been plotted separately.	68
Figure 4-7; Critical bed shear stress plotted as a function of geometric standard deviation; the unimodal σ_g is depicted by diamond shaped markers and ranges from 1.41 to 1.49, the bimodal σ_g is depicted by crossed shaped markers and ranges from 1.77 to 1.84, the fine σ_g is depicted by open circle markers and ranges from 1.68 to 1.84, and the coarse σ_g is depicted by square shaped markers and ranges from 1.23 to 1.37 (bold denotes the original σ_g for 0 minutes antecedent flow). The red regression line relates to data collected with 0 minutes of applied antecedent flow whilst the green trend line relates to data collected after 60 minutes antecedent flow.	70
Figure 4-8; Fractional bedload transport rate of the unimodal bed scaled by the abundance of each size (g_i) in the bulk mix(F_i) plotted against dimensionless size for antecedent durations 0-60mins.	77
Figure 4-9; Fractional bedload transport rate of the bimodal bed scaled by the abundance of each size (g_i) in the bulk mix(F_i) plotted against dimensionless size for all five antecedent durations.	79
Figure 4-10; Fractional bedload transport rate of the coarse bed scaled by the abundance of each size (g_i) in the bulk mix (F_i) plotted against dimensionless size for all five antecedent durations.	80
Figure 4-11; Fractional bedload transport rate of the fine bed scaled by the abundance of each size (g_i) in the bulk mix (F_i) plotted against dimensionless size for all five antecedent durations.	81
Figure 5-1; The relationship between antecedent duration, average critical bed shear stress and grain size distribution. The uniform, unimodal and bimodal beds are fitted with a linear polynomial growth curve with root mean square values of 0.03, 0.01 and 0.049 for the uniform, unimodal and bimodal beds respectively.	100
Figure 5-2; First derivative of the fitted trend lines of the response of the uniform, unimodal and bimodal grain size distributions respectively to antecedent flow duration.	101
Figure 5-3; The relationship between antecedent duration, average critical bed shear stress, grain size distribution. The uniform, unimodal and bimodal beds are fitted with a linear polynomial growth curve. Data from the low width depth ratio experiments are plotted using a solid line with a dashed line used to depict the predicted relationship between antecedent duration and shear stress if experiments were to be extended to 960 minutes under low width depth conditions. The results from the higher width depth ratio experiments are plotted using a dot and dash line.	106
Figure 5-4; First derivative of the fitted trend lines of the response of the uniform, unimodal and bimodal grain size distributions respectively to antecedent flow duration. Data from the low width depth ratio experiments are plotted using a solid line with a dashed line used to depict the predicted relationship between antecedent duration and shear stress if experiments were to be extended to 960 minutes under low width depth conditions. The results from the higher width depth ratio experiments are plotted using a dot and dash line.	106

Figure 5-5; Stress history relationships with total bedload fitted with an exponential decay function superimposed in a background constant noting R^2 values of 0.92, 0.95, 0.94, for the uniform, unimodal and bimodal beds respectively.	110
Figure 5-6: First derivative of the fitted trend lines of the response of the uniform, unimodal and bimodal grain size distributions respectively to antecedent flow duration.	111
Figure 5-7; Total transported load at each flow step of the stability test plotted against the average bed shear stress for that flow step for the uniform bed. The graph is plotted on a log log axis.	113
Figure 5-8; Total transported load at each flow step of the stability test plotted against the average bed shear stress for that flow step for the unimodal bed. The graph is plotted on a log log axis.	114
Figure 5-9; Total transported load at each flow step of the stability test plotted against the average bed shear stress for that flow step for the bimodal bed. The graph is plotted on a log log axis.	114
Figure 5-10: Critical bed shear stress plotted as a function of geometric standard deviation (Unimodal σ_g ranging from 1.46 to 1.58 (1.55), and the Bimodal σ_g ranging from 1.55 to 2.10 (1.88), where bold denotes the original σ_g for 0 minutes antecedent flow). Unimodal data points are represented by square markers whilst the bimodal data points are represented by triangular markers.	117
Figure 5-11; Fractional bedload transport rate of the unimodal bed scaled by the abundance of each size in the bulk mix plotted against dimensionless size for all five antecedent durations.	123
Figure 5-12; Fractional bedload transport rate of the bimodal bed scaled by the abundance of each size in the bulk mix plotted against dimensionless size for all five antecedent durations.	124
Figure 6-1; Digital Elevation Models of the uniform bed before and after the antecedent period of 60 Minutes.	148
Figure 6-2; Digital Elevation Models of the uniform bed before and after the antecedent period of 960 Minutes.	149
Figure 6-3; Digital Elevation Models of the unimodal bed before and after 60 minutes of antecedent flow.	150
Figure 6-4; Digital Elevation Models of the unimodal bed before and after the antecedent 960 minutes of antecedent flow.	151
Figure 6-5; Digital Elevation Models of the bimodal bed before and after the antecedent period of 60 minutes.	152
Figure 6-6; Digital Elevation Models of the bimodal bed before and after the antecedent period of 960 minutes of antecedent flow.	153
Figure 6-7; Porosity plotted as a function of elevation in the uniform bed for the 60 and 960 minute experiments.	161
Figure 6-8; Porosity plotted as a function of elevation in the unimodal bed for the 60 and 960 minute experiments.	161
Figure 6-9; Porosity plotted as a function of elevation in the bimodal bed for the 60 and 960 minute experiments.	162
Figure 6-10; Schematic showing a fixed threshold to separate grains from pores (after Rollinson 2006).	163
Figure 6-11; Schematic showing the problems of applying a fixed threshold to a natural gravel bed (after Rollinson 2006).	163
Figure 6-12; Digital elevation model of the uniform bed shown in the left hand image with comparable image of the spatial porosity shown in the right hand image.	165

Figure 6-13; Digital elevation model of the unimodal bed shown in the left hand image with comparable image of the spatial porosity shown in the right hand image.	166
Figure 6-14; Digital elevation model of the bimodal bed shown in the left hand image with comparable image of the spatial porosity shown in the right hand image.	167
Figure 6-15; Schematic showing the dynamic threshold approach to separating gravels from pores (after Rollinson, 2006).....	168
Figure 6-16; Digital elevation model of the uniform bed shown in the left hand image with comparable image of the spatial porosity shown in the right hand image.	169
Figure 6-17; Digital elevation model of the unimodal bed shown in the left hand image with comparable image of the spatial porosity shown in the right hand image.	170
Figure 6-18; Digital elevation model of the bimodal bed shown in the left hand image with comparable image of the spatial porosity shown in the right hand image.	171
Figure 6-19; Image of the gravel bed DEM overlain by the derived watersheds representing the pores using a smoothing radius of 1.0 mm. Close inspection of the derived watersheds appear to show a faithful representation of the delineation of deeper areas representing pores on the bed surface.	174
Figure 6-20; Image of the gravel bed DEM overlain by the derived watersheds representing the pores using a smoothing radius of 0.5mm. Close inspection of the derived watersheds appear to show watersheds which are split into too many unrealistic pore boundaries.....	174
Figure 6-21; Image of the gravel bed DEM overlain by the derived watersheds representing the pores using a smoothing radius of 4.8mm (representative value of the bed D_{50}). Close inspection of the derived watersheds appear to show watersheds which are split into unrealistic larger pores missing some detail at the smaller scale.	175
Figure 6-22; DEM's of difference for the uniform (upper image pair), unimodal (middle image pair) and bimodal (bottom image pair) beds after 60mins (left hand of the image pairs) and 960mins (right of the image pairs) antecedent flow.	181
Figure 6-23; Orientations of the long a-axis of 50 grains manually digitised from laser scans for the uniform bed. Image pairs show the bed before (left hand of the image pair) after (right hand of the image pair) the application of 60 minutes (top of the image pair) and 960 minutes (bottom of the image pair) antecedent flow. Flow is along the 0 – 180 line.	184
Figure 6-24; Orientations of the long a-axis of 50 grains manually digitised from laser scans for the unimodal bed. Image pairs show the bed before (left hand of the image pair) after (right hand of the image pair) the application of 60 minutes (top of the image pair) and 960 minutes (bottom of the image pair) antecedent flow. Flow is along the 0 – 180 line.	185
Figure 6-25; Orientations of the long a-axis of 50 grains manually digitised from laser scans for the bimodal bed. Image pairs show the bed before (left hand of the image pair) after (right hand of the image pair) the application of 60 minutes (top of the image pair) and 960 minutes (bottom of the image pair) antecedent flow. Flow is along the 0 – 180 line.	186
Figure 6-26; Second order structure functions D_b of the bed surface elevations for the uniform bed before and after 60 and 960 minutes antecedent flow duration for the streamwise (top of the image pair) and lateral (bottom of the image pair). D_b is normalised by $2\sigma_{Zb}^2$ for l_x and l_y where σ_{Zb} is the standard deviation of the bed surface elevations and l_x and l_y is the spatial lag in the streamwise and lateral directions respectively.....	195
Figure 6-27; Second order structure functions D_b of the bed surface elevations for the unimodal bed before and after 60 and 960 minutes antecedent flow duration for the	

streamwise (top of the image pair) and lateral (bottom of the image pair). D_b is normalised by $2\sigma_{Zb}^2$ for l_x and l_y where σ_{Zb} is the standard deviation of the bed surface elevations and l_x and l_y is the spatial lag in the streamwise and lateral directions respectively.....	196
Figure 6-28; Second order structure functions D_b of the bed surface elevations for the bimodal bed before and after 60 and 960 minutes antecedent flow duration for the streamwise (top of the image pair) and lateral (bottom of the image pair). D_b is normalised by $2\sigma_{Zb}^2$ for l_x and l_y where σ_{Zb} is the standard deviation of the bed surface elevations and l_x and l_y is the spatial lag in the streamwise and lateral directions respectively.....	197
Figure 6-29; Isopleth plots of $D_b(l_x, l_y)/2\sigma_{zb}^2$ for the uniform bed before (left hand of the image pair) and after (right hand of the image pair) 60 minutes of antecedent flow. Flow is from left to right.	201
Figure 6-30; Isopleth plots of $D_b(l_x, l_y)/2\sigma_{zb}^2$ for the uniform bed before (left hand of the image pair) and after (right hand of the image pair) 960 minutes of antecedent flow. Flow is from left to right.	202
Figure 6-31; Isopleth plots of $D_b(l_x, l_y)/2\sigma_{zb}^2$ for the unimodal bed before (left hand of the image pair) and after (right hand of the image pair) 60 minutes of antecedent flow. Flow is from left to right.	203
Figure 6-32; Isopleth plots of $D_b(l_x, l_y)/2\sigma_{zb}^2$ for the unimodal bed before (left hand of the image pair) and after (right hand of the image pair) 960 minutes of antecedent flow. Flow is from left to right.	204
Figure 6-33; Isopleth plots of $D_b(l_x, l_y)/2\sigma_{zb}^2$ for the bimodal bed before (left hand of the image pair) and after (right hand of the image pair) 60 minutes of antecedent flow. Flow is from left to right.	205
Figure 6-34; Isopleth plots of $D_b(l_x, l_y)/2\sigma_{zb}^2$ for the bimodal bed before (left hand of the image pair) and after (right hand of the image pair) 960 minutes of antecedent flow. Flow is from left to right.	206

LIST OF TABLES

Table 3-1; Grain size distribution for the five test sediment grades. The D_{50} of each distribution is highlighted in green and the D_{84} in blue.	46
Table 4-1; Comparison between the D_{50} : D_{84} ratios of the bulk mix in comparison to the screeded bed surfaces. The D_{50} : D_{84} ratio from the surface is calculated according to the number of individual D_{50} and D_{84} grains counted on the bed surface photographs over a 200x 200mm area.....	57
Table 4-2; Evolution of grain parameters with increasing antecedent duration for the unimodal bed; D_{50} highlighted for ease of analysis.....	72
Table 4-3; Evolution of grain parameters with increasing antecedent duration for the bimodal bed; D_{50} highlighted for ease of analysis.	72
Table 4-4; Evolution of grain parameters with increasing antecedent duration for the coarse bed; D_{50} highlighted for ease of analysis.	73
Table 4-5; Evolution of grain parameters with increasing antecedent duration for the fine bed; D_{50} highlighted for ease of analysis.	73

Table 4-6; Summary of experimental variables for the experiments performed in the 0.3m flume using 5 grain size distributions and 5 antecedent durations (where 0 minutes acted as the benchmark).	97
Table 5-1; Relative depth derived according to equation 24 (R_b/D_i) where z represents the flow depth (m), R_b is the hydraulic radius and D_i is the representative grain size, taken to be the D_{50} . Results are shown for all tested antecedent durations for the uniform, bimodal and unimodal beds respectively.	104
Table 5-2; Relative depth derived according to equation 24 (R_b/D_i) where z represents the flow depth (m), R_b is the hydraulic radius and D_i is the representative grain size, taken to be the D_{50} . Results are shown for all tested antecedent durations for the uniform, bimodal and unimodal beds respectively.	105
Table 5-3; Evolution of grain parameters with increasing antecedent duration for the unimodal bed.	120
Table 5-4; Evolution of grain parameters with increasing antecedent duration for the bimodal bed.	120
Table 5-5- Summary of experimental variables	140
Table 6-1; Summary table of investigated mechanisms of stabilisation and their analytical methodologies	144
Table 6-2; Summary of the bed surface properties of the three beds for experiments running 1 and 16 hours antecedent flow duration where Z_b is the mean surface elevation, k is the range and Sk_b is the skewness of the distribution of bed surface elevations. Differences between 60 and 960 minutes are shown in both absolute and relative terms; red cells indicate a positive change; blue cells a negative change.....	156
Table 6-3; Summary of the pore properties of the three beds for experiments running 60 and 960 minutes antecedent flow duration.....	177
Table 6-4; Analysis of the total number, the total area and the ratio of the $D_{50}:D_{90}$ for the D_{50} and D_{90} at the start and finish of 60 and 960 minutes antecedent flow. Area is in arbitrary units	190
Table 6-5; A summary of the bed surface properties derived from the second order structure functions for the uniform, bimodal and unimodal beds where l_x and l_y are the spatial lags in the streamwise direction in the streamwise and lateral directions respectively, l_{x0} and l_{y0} are the correlation lengths of z_b in the streamwise and lateral directions respectively, σ_b is the standard deviation and H_x and H_y are the Hurst exponents for the streamwise and later variations in Z_b respectively.	197

LIST OF APPENDICIES

Appendix A1; Experimental Programme.....	230
Appendix A2; Data Collected	233
Appendix B; Cumulative Grain Size Distribution Graphs for the Unimodal, Bimodal, Coarse and Fine Beds	236
Appendix C; Cumulative Grain Size Distribution Graphs for the Unimodal and Bimodal Beds	238
Appendix D; Probability Density Functions of Normalised Elevation for the Uniform, Unimodal and Bimodal Beds	239
Appendix E; Cumulative Distribution Graphs plotting pore size as a function of applied antecedent flow for the Uniform, Unimodal and Bimodal Beds	241

LIST OF SYMBOLS

α_2	Particle shape factor
A	Area
b	Flow width
c	Bedload coefficient
C_p	Particle packing coefficient
D	Grain Diameter
D_b	2D Structure function of bed surface elevations
D_i	Grain diameter corresponding to size i
D_x	Particle diameter corresponding to x percentile finer
F_D	Fluid drag
F_{iwt}	Immersed weight force of the particle
f_{ai}	Percentage of size class i on bed surface based on surface area
F_i	Percentage of size class i on bed bulk mix
f_{si}	Proportion of the fraction i in the sub pavement layer
g	Gravitational constant
G_b	Sum of bedload transport
g_i	Fractional bedload transport
H_x	Hurst component in the downstream direction
H_y	Hurst component in the cross stream direction
I	Intensity of sediment movement
k	Roughness height
K	Diameter of the base of the grain
l_x	Spatial lag in the downstream direction
l_y	Spatial lag in the cross stream direction
M_b	Total number of bed elevations in the cross stream direction
m_b	Multiplying coefficient
n	Mannings roughness coefficient; empirical parameter
N	Number of mobile grains
Nm^{-2}	Newton Meters
N_b	Total number of measured bed elevations in the downstream direction
n_b	Multiplying coefficient
n_g	Grain roughness
n_w	Glass roughness
P	Wetted perimeter
P_b	Wetted perimeter of the bed
P_i	Percentage of size class I on bedload sample
P_w	Wetted perimeter of the walls
ρ_s	Particle density
q_{bi}^*	dimensionless mass bedload transport rate of size class i
q_{bi}	transport rate of the i th size fraction
Re^*	Grain Reynolds number
R	Hydraulic radius
R^2	Correlation coefficient
R_b	Bed Hydraulic radius

ACKNOWLEDGEMENTS

The acknowledgements have been one of the most difficult parts of this thesis to write. There are so many people to thank and every time I try to write one of these lists I forget someone. Consequently the list below is long and probably not exhaustive but...

Dr Heather Haynes you have been a source of boundless patient support and encouragement throughout - your professionalism is a credit to you and you have been an outstanding mentor both professionally and personally. Professor Trevor Hoey you have provided a refreshing insight and combined with your knowledge, advice and encouragement you have been influential in the development of this thesis. Professor Bill Sloan your ability to ask critical questions has brought this thesis into a very valuable context. Much valued help during the early stages of this thesis came from Professor Alan Ervine who provided the foundation of knowledge from which this thesis developed. Dr Rebecca Hodge you have been a constant source of help with your input into my PhD being absolutely instrumental to its outcome. Professor Roger Bettess your support, suggestions and overall contribution have always been delivered with enthusiasm and have been greatly valued and appreciated. Dr James Cooper you have provided endless hours of encouragement and support with your thought and insight greatly strengthening the results of this thesis. Professor Simon Tait and Dr Joe Aberle you have been generous with your suggestions and opinions which helped enormously with the development of the laser data analysis. Dr Rick Haynes, Mr James Minto and Miss Katie Whitbread your help with the GIS has saved many hours of frustration! Time spent with Professor Gary Parker and his team at the University of Illinois offered me an unparalleled opportunity to learn with some of the best academics in the world. Dr Steve Rice you have been patient with allowing me to finish writing up during the start of my new job.

Stuart, Bobby, Ian, Tim, Al, and Robert you deserve special recognition for your time and for enduring my continual requests for help even if you did throw me in the flume! Amanda, Eileen and Barbara you have made sure at least someone is in complete control! Thanks are also extended to the rest of the Water and Environment team at Glasgow and my fellow office colleagues who have always been ready with a much needed drink(s) at the end of the day, including that all important 'one for the road'!!

Without the ongoing support from my friends and family I would have found the hard times of this project even more difficult. There are too many of you to thank individually, you know who you are. Dad, thank you for being on the end of a phone with your tolerant descriptions of all things related to engineering and for not saying I told you so (too many times!) during the great data loss of 2010! B, thank you for trusting me and encouraging me to look forward not back. Nikki your ability to give me perspective and make me laugh at myself has made counting stones all the more enjoyable! Becka, your support, friendship and proof reading skills (one day I will learn how to use commas!) have been invaluable. Karen and Clare your proof reading skills have also been much appreciated! Elisa, Jen, Katie and Doug you have been the ones who have made the ups and downs of this PhD bearable with your ability to make me laugh proving invaluable! Kirsty, Mitch, Ana, Charlie and Matt you have provided encouragement and wine in equal quantities over the past few months, both of which have been greatly appreciated! As always Kirsty Howell you have always been there no questions asked with a confidence I don't deserve. Finally, Steve you have been of continual support over the last three years with unwavering patience, encouragement and belief in my abilities throughout - 143.

This is for all of you -thank you.

Authors Declaration

I declare that no portion of the work in this thesis has been submitted in support of any application for any other degree or qualification of this or any other university or institute of learning. I also declare that the work presented in this thesis is entirely my own contribution unless otherwise stated.

Anne-Marie Ockelford

Chapter 1 Introduction

The transport of sediment through river channels has major consequences for public safety, management of water resources and environmental sustainability (Frey and Church 2009). However, as greater constraints are imposed upon sediment management within a sustainable practice framework integrating knowledge on river bed structure and processes in a coherent manner becomes exigent. This is especially true in a hydraulic context where river bed characteristics govern a number of complex inter relationships such as flow velocity, turbulent intensity and sediment transport. In an applied context accurate prediction of the transition between river bed stability and instability is therefore fundamental to many aspects of river management and engineering (Haynes and Pender, 2007), ranging from the success of fish spawning grounds to scour around hydraulic structures.

The disparity between scientific understanding and the more detailed knowledge required for applied practise is highlighted in the discipline of sediment dynamics. This detailed understanding of the fundamental controls on sediment entrainment remains a significant research challenge due to the dynamic duality of two phase flows of both water and sediment. As the boundary over which the fluid flows is deformable if we are to understand how and when sediment is transported researches must crucially ascertain the mechanics by which the boundary may be restructured in response to the imposed flow regime. Indeed, since the research discipline's inception by Gilbert (1914), the proliferation of research efforts continue even over the past decade (e.g. Schmeeckle *et al.* 2007; Vollmer and Kleinhans, 2007; Righetti and Lucarelli, 2007; Detert *et al.* 2008) and are testament to the well-recognised need to improve our understanding in this area.

Although the boundary conditions describing the threshold of motion for uniform sediment are readily available, in a natural river environment the bed is composed of graded sediment, typified by a wide range of size and shaped particles, such that the process of entrainment becomes significantly more complicated. Knowledge of such thresholds is thus contingent upon an understanding of not only fundamental fluid dynamics causing the first motion of a particle from a sediment bed (e.g. average or instantaneous velocity, fluid stresses, fluid shear and shear instabilities) but also of the properties and interactions of the sediment bed itself (e.g. particle packing, orientation, modality, distribution). Given that

different fluvial environments lead to different bed grain size compositions, it is important that research is directed to consider how different graded beds are generated under a range of flow regimes and how these size distributions give rise to variability in particle entrainment threshold.

Empirical descriptions of river bed stability tend to concentrate on describing how a particle of representative grain size (e.g. the median) is entrained from a graded bed surface at a particular critical shear stress (Shields, 1936; Neill and Yalin, 1969; Shvidchenko *et al.*, 2001). Traditionally, these models assumed that the structure of non cohesive sediment beds, and hence the resistance to entrainment, was only modified when the applied shear stress exceeded the threshold for incipient motion (Gomez, 1983). However, an emerging school of thought suggests that sediment beds, whether uniform or graded, also appear to progressively stabilise when subjected to sub-threshold flows (Paphitis and Collins, 2005; Monteith and Pender, 2005; Haynes and Pender, 2007). This implies that the entrainment of a given sediment fraction may, as a result of being exposed to different sub-threshold antecedent flow conditions, be entrained over a range of shear stresses. Therefore, accounting for antecedent flow (stress) history may, to some extent, improve the prediction of, and reduce the uncertainty in, the entrainment threshold.

Both the work by Paphitis and Collins (2005) and Haynes and Pender (2007) inferred that increased bed stability due to stress history may be caused by local particle rearrangement into a structure that was more resistant to entrainment by fluid flow. Yet, the magnitude of stress history effects between these data sets appears to differ between uniform and graded beds suggesting an intrinsic link between antecedent stability and relative grain size effects in terms of hiding, packing density and individual particle orientation. Similarly, field observations by Buffington *et al.*, (1992) and Church *et al.*, (1998) suggested that the resistance of grains to entrainment from naturally-formed gravel beds is not related simply to the grain weight, as described by the surface grain size distributions, but to some other property of the bed, possibly the arrangement of the surface grains and the topography of the bed surface. But, whilst both field and laboratory studies support the concept of stress history there is relatively little evidence to indicate the mechanisms which are responsible for bed stabilisation under sub-threshold flows.

1.1 Research Aims and Objectives

As discussed, initial data sets indicate that the stability of both uniform (Paphitis and Collins, 2005) and graded (Monteith and Pender, 2005; Haynes and Pender, 2007) sediment beds is dependent upon the antecedent, sub-threshold flow regime to which they are exposed. However the limited research into the concept of stress history has been based on datasets that only speculate upon the reason(s) as to why beds stabilise when subjected to prolonged periods of sub-threshold flow. Thus, the aim of this research is to extend the specific findings of Paphitis and Collins (2005), Monteith and Pender (2005) and Haynes and Pender (2007) by firstly directly comparing stress history effects on the entrainment thresholds of different grades of sediment and secondly providing the first quantitative understandings of the mechanisms of stabilisation which the bed undergoes during periods of sub threshold flow. This comprehensive and systematic research is specifically designed to provide quantitative relationships pertaining to stress history which may potentially improve sediment entrainment predictions. The relevance of such insight is especially timely in an era of climate change where the duration of low-flows and the frequency of flood events are predicted to change; stress history research thus has the potential to inform the design and management of new and existing hydraulic structures and catchment management plans.

The research is divided to generate two major data sets. The first was designed to compare and contrast the effect that grain size distribution has upon bed stability following different antecedent durations. Specifically the response of five different grain size distributions were analysed and discussed in terms of visual entrainment threshold analysis together with total and fractional transported bedload results such that the change to entrainment threshold as a result of stress history can be quantified (Chapter 4). Results from this data set allowed for the rational design of the second set of experiments, the results from which are split into two further chapters. Chapter 5 details stress history experiments run with longer antecedent flow time periods using the same analytical techniques as Chapter 4. Chapter 6 then describes how rapid acquisition surface laser scanning was used to understand and quantify the underpinning mechanism of stress history induced change to bed stability; the results are explained using image processing and statistical analysis to generate insights into associated changes to bed topography and particle repositioning.

The results of this study are also presented in a set of conference and journal papers (Ockelford and Haynes, 2008; Haynes and Ockelford, 2009; Ockelford *et al.*,2010 and Ockelford and Haynes, 2011).

Chapter 2 Literature Review

The incipience of motion is the concomitant outcome of driving forces overcoming resisting forces in order that a particle is displaced. However, although theoretically a simple concept and despite numerous empirical studies (Buffington & Montgomery, 1997) there still remains significant uncertainty in defining this threshold. In general, the more natural and hence more complex the environment, the more inter-related the variables become which need to be isolated and analysed to ascertain the process controls on entrainment threshold and reduce uncertainty in threshold definitions. One such potential process control, as described in Chapter 1, is the modification of entrainment threshold as a result of exposure to different sub-threshold flow regimes. Little is known about such effects and consequently this literature review concentrates upon the determination of entrainment thresholds, the effect of graded sediment upon entrainment thresholds and the consequent effect upon large and small scale bed structuring. All three processes will specifically be analysed with regard to the effect of the temporality and magnitude of the flows prior to a sediment transporting event.

2.1 Sediment Entrainment Thresholds

As the fluid velocity or stress it exerts over a bed of sediment increases, a situation is eventually reached such that any additional increase causes particles to be moved from the bed for transport. Threshold of motion is defined when the forces promoting motion are greater than those resisting motion such as to cause a small degree of sediment movement termed incipient motion or entrainment. The circumstances necessary to initiate sediment motion are a function of the characteristics of the sediment (density, size, packing, sorting and shape), the fluid (density and viscosity) and the flow conditions (average velocity or intensity of turbulent stresses) (Miller *et al.*, 1977).

Assuming a simple scenario of a spherical grain on a planar bed, the driving forces must overcome the resisting forces for sediment entrainment to occur. Buffington and Montgomery, (1997) describe this approach through the relationship between the immersed weight (W) of the grains and the flow force, which refers to the threshold shear stress for initial motion. The dominant forces for particle motions can be divided into three variables. Firstly, a drag force, F_D , acts on the particle side facing the flow such that;

$$F_D = \tau_0 D^2 \left(\frac{\alpha^2}{C_p} \right) \quad (\text{Equation 1})$$

where C_p is a particle packing coefficient and α_2 is a shape factor related to particle area. The ratio α_2/C_p describes the surface area of the particle exposed to the flow, which is dependent on the size, shape, and packing of the streambed particles. Secondly, a lift force is resolved by both a time averaged lift force, $F_{L,\text{std}}$ and a short term lift force, $F_{L,\text{turb}}$. Sources of pressure fluctuations are described by flow depth and mean flow velocity. For hydraulically rough beds the velocity and length scales are boundary shear velocity and bed roughness; for hydraulically smooth beds they are the boundary shear velocity and viscosity divided by the boundary shear velocity. Finally particle weight, described as either a driving nor resisting force as this vector can be resolved into two components, the normal component (W_n) and the parallel (downslope) component (W_d). The normal component provides the resisting force while the parallel component is a driving force. It is the relative magnitude of each component of particle weight that will either drive or resist movement; these are a function of bed slope, where a shallow slope will see the normal component be greater than the downslope component thus impeding movement as compared to a steeper slope where the downslope component will dominate to promote movement. When simplified, the immersed weight force of the particle (F_{iwt}) when fully submerged is the weight force in air minus the buoyant force of water, expressed as;

$$F_{iwt} = (\rho_s - \rho)g(\alpha D^3) \quad (\text{Equation 2})$$

where ρ_s is the density of the particle being entrained and α is a shape factor that relates to the particle volume.

However, in reality grains are rarely spherical and unlikely to rest upon a planar bed where there is no interaction between other particles. As a consequence, the complex combination of naturally occurring bed material and bed packing introduces high variance when estimating critical threshold conditions. In this scenario it is the pivot angle of the grain which is of critical importance, whereby critical entrainment threshold occurs when the moment of fluid drag about the pivot point equals the moment of the immersed weight. In both uniform and graded beds the pivot angle is determined by the particle geometry and the gravitational moments acting about the centre of a mass of an individual particle with respect to its neighbouring particles, particularly those immediately downstream. In

graded beds the pivot angle is related to the relative size effects as shown by Figure 2-1 (Lorang and Hauer, 2001).

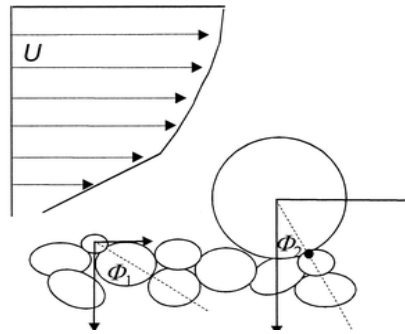


Figure 2-1; Diagram to depict different pivoting angles (ϕ_1 and ϕ_2) and particle surface area exposed to the flow field resulting from a mixed-bed of different particle sizes, shapes, and packing arrangements (Lorang and Hauer, 2001)

Pivot angle and shear stress are commonly investigated together (e.g. Bridge and Bennett, 1992) where pivot angle varies according to the composition of the sediment; typically for uniform spheres the angle is of the order of 30-32° but for heterogenic sediment it depends on the relative particle sizes involved (up to 90°). Adopting an empirical approach, Miller and Byrne (1966) derive a relationship expressing pivot angle as a function of the ration D_i/D_{50} where α and β are coefficients based on grain roundness and bed sorting parameters such that;

$$\Phi = \alpha(D_i / D_{50})^{-\beta} \quad (\text{Equation 3})$$

Additionally, Figure 2-1 suggests that if one considers the case of pivoting angles in simple spheres there is a variability observed where the ratio of D/K , D being the grain diameter and K being the diameter of the base of the grain, will exhibit an inverse relationship with pivot angle; as the D/K ratio increases, the pivoting angle decreases. This is commonly termed the relative size effect; the effect of this in terms of sediment entrainment is discussed in section 2.2.1. Changes to pivot angle and hiding as a result of water working are manifested and hence measurable on the bed surface by way of vertical settlement and grain reorientation; this is explored fully in Chapter 6.

2.2 Determination of Entrainment threshold

In order to better define threshold conditions, a number of early investigations into thresholds of motion produced empirical graphical relationships which are still in use in modern day sediment transport investigations. These have been cast in the form of a critical shear velocity (u_{*c}) or a critical shear stress (τ_c) related to sediment parameters. The most commonly used graphical interpretation is that defined by Shields (1936). Shields developed a dimensionless critical shear stress (θ) to express a relationship between applied bed shear stress and the immersed weight of the grain such that;

$$\theta = \frac{\tau_0}{(\rho_s - \rho)gD} \quad (\text{Equation 4})$$

where D is the grain diameter, g is the gravitational constant, ρ_s is the grain density and ρ the fluid density; θ is commonly referred to as the Shields entrainment function, a non-dimensional variable dependent on the distributions of streambed particle size, shape, and packing (Shields 1936, Allen, 1970). The now commonly recognised Shields threshold curve, shown by Figure 2-2 plots this relationship using the grain Reynolds number (Re_*) against θ .

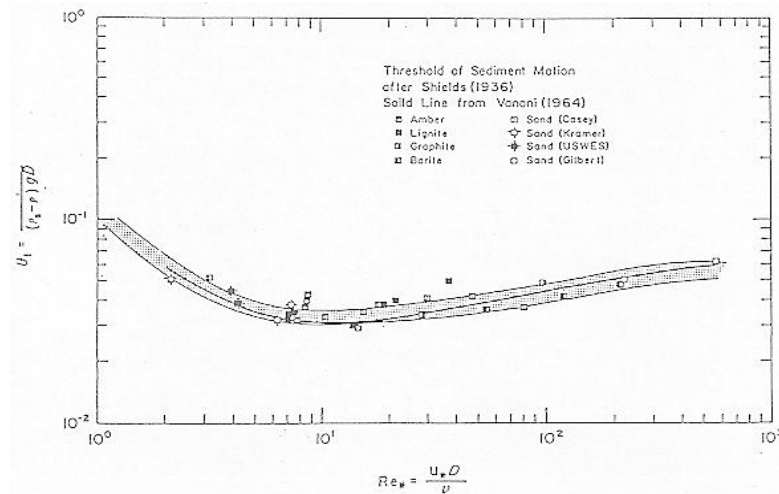


Figure 2-2 Thresholds of sediment motion represented by the Shields curve (from Miller *et al.*, 1977). The black solid line represents the initial Shields curve (Shields, 1936) with the grey shaded envelope of values proposed by Miller *et al.*, (1977) to take into account the uncertainty surrounding the initiation of motion.

The grain Reynolds number represents both the thickness of the viscous sublayer and the hydrodynamic conditions of the flow around the surface grains (Buffington, 1999) and is given as the following:

$$Re_* = \frac{u_* k}{\nu} \quad (\text{Equation 5})$$

where u_* is the shear velocity, ν denotes the kinematic viscosity and k represents the roughness height of the bed material. From Figure 2-2 it is seen that the Shields parameter follows a distinct distribution with Reynolds number (Yang 1996; Chien and Wan 1999; Yalin and daSilva 2001) where there is a deterministic solid line pertaining to threshold as developed by Shields as well as an envelope of values determined from Miller *et al.*, (1977) which represents the uncertainty with which threshold can be predicted. Threshold conditions are not met if data falls below the band and sediment motion is therefore not observed; the converse is true above the band. Specifically, Shields identified that the relationship between critical Shields stress and grain Reynolds number is defined according to the hydraulic roughness of the bed (Graf 1971; Chien and Wan 1999; Yalin and deSilva 2001). Flows with low grain Reynolds numbers are regarded as hydrodynamically smooth such that the viscous forces within the viscous sub-layer dominate the prevailing threshold conditions. As boundary roughness increases, a progressive thinning of the viscous sub-layer is noted where inertial forces dominate the conditions of threshold. The curve reaches a minimum value where the grain diameter equals the height of the laminar sub-layer.

Whilst Shields' work has formed the benchmark of empirical threshold study, discrepancies between experimental observations of particle thresholds and thresholds estimated by the Shields curve have led to numerous revisions of the Shields curve over an eight decade period (Buffington, 1999). Typically such revisions have taken the form of simple empirical functions which have been used to simulate factors such as the relative flow depth, the degree of grain protrusion, sediment shape and the hiding-exposure effect for graded beds (e.g. Egiazaroff, 1965; Ashida and Michue, 1972; Proffitt and Sutherland, 1983; Shvidchenko and Pender, 2000) which are discussed in detail above. However, more fundamentally underpinning much of the uncertainty in Shields' work and more recent threshold studies is the actual definition that researchers employ in determining threshold. From the discussion above and Figure 2-2 it can be seen that the determination

of threshold is complex and as can be seen from the Shields curve, is not a purely deterministic value. Instead, thresholds of motion are seen to occur in a band of theoretical values with this scatter, which is in part due to the manner in which threshold of motion is defined. Shields (1936) discussed two methods of defining incipient motion but did not state which method he used (Buffington and Montgomery, 1997). Typically the determination of threshold falls into two categories, those which define threshold using a deterministic approach and those which use a stochastic approach. The four most common methods are described below; the visual, reference transport and largest grain methods follow a deterministic approach and the probabilistic follows a stochastic approach.

Visual Method: Shields (1936) described using a visual method where he described motion according to a ‘small number of detachments’. This appears related to the slightly earlier definition of first motion provided by Kramer (1935), where weak motion was the proxy for incipient motion such that;

“several of the smallest particles are in motion, in isolated spots and in countable numbers”

As intensity of motion was seen to increase and more particles were beginning to be entrained, Kramer employed three further definitions, with the highest termed “general motion” and described as;

“grains up to and including the largest are in motion and movement is occurring in all parts of the bed at all times. It is sufficiently vigorous to change the bed configuration”

(Kramer, 1935)

However, this method is highly subjective in that, although it is direct, it depends solely on the user defined definition of how much movement constitutes initial motion (Yalin and Karahan, 1979; Wilcock, 1988). Yalin (1972) therefore proposed a method to quantify observed grain detachments from a bed of uniform particle size, denoted the Yalin Criterion (ε) such that;

$$\varepsilon = \frac{n}{At} \left(\frac{\rho D^5}{(\rho_s - \rho)g} \right)^{\frac{1}{2}} \quad (\text{Equation 6})$$

where a lower limit of ε was defined as 1.0×10^{-6} , based on the number of mobile grains (n) observed over a given area (A) over a specified time (t). Since the entrainment threshold of sediment is considered as a spatially and temporally random process of particle displacement under turbulent fluctuations, it is necessary that the area of observation, A , should be ‘large’ in comparison to the grain area and the time, t , of the observation should be ‘large in comparison to the average time period of turbulent fluctuations’ (Yalin, 1972). This method has been successfully employed by both Paphitis and Collins (2005) and Haynes and Pender (2007). However, due to the fact that this criterion employs a scaling with particle diameter it becomes complicated when considering mixed grain problems as it only allows consideration of one specified grain size fraction at a time. The original Yalin Criterion is therefore unsuitable for use in mixed grain problems and hence Wilcock (1988) developed the following equation to account for the individual fractions comprising a graded bed using the D_{65} as the representative grain diameter. In his correction Wilcock defined a new constant value in the same manner as the ε as defined by Yalin (Equation 6) in response to the different percentage of the fraction on the bed surface according to Equation 7;

$$\frac{n_i D_i^2}{f_{ai}} = const. \quad (\text{Equation 7})$$

Given that neither n nor the constant are known n is calculated from Equation 6 and then input into Equation 7 such that the constant can be calculated. The initial constant value should be calculated for the D_{65} as it was deemed that this grain represented a reasonable approximation of the roughness length of the bed surface (Wilcock 1988). Once the constant is known it forms the basis of the correction equation for each size fraction of the bed (D_i) whereby n_i is related to the percentage of desired fraction (f_{ai}) on the bed surface (Equation 7).

Reference Based Transport Method: The second deterministic approach to threshold derivation is the reference based transport method which involves measuring transport rates for individual size fractions at a range of different flows. The relationship between shear stress and transport rates is then used to determine the shear stress that produces a small reference transport rate for that size fraction (Johnston and Andrews, 1998). Parker *et al.* (1982) use a reference transport criterion to provide a deterministic description of the first sediment motion which is now widely used in most investigations of this type

(Wilcock, 1993; Wilcock *et al.*, 1996; Wilcock and McArdell, 1997). Using field data they defined a dimensionless parameter of fractional bedload (W_i^*) such that;

$$W_i^* = \frac{q_{bi}^*}{\theta_i^{\frac{3}{2}}} \quad \text{Equation (8)}$$

where (θ_i) is the Shields stress for the particle fraction of diameter D_i and q_{bi}^* is the normalised Einstein bedload parameter (Einstein, 1942) given by;

$$q_{bi}^* = \frac{q_{bi}}{f_{si} \rho_s \sqrt{\left(\left(\frac{\rho_s}{\rho} - 1 \right) g D_i^3 \right)}} \quad \text{Equation (9)}$$

where q_{bi} is the transport rate of the i th size fraction for a given time and bed width, whilst f_{si} is the proportion of the fraction i in the sub pavement layer (the sub pavement refers to the layer below the surface pavement where the latter is said to be between 1D and 3D of the sub-pavement (Parker *et al.*, 1982). The value of the reference dimensionless volumetric transport rate W_i^* is usually taken as 0.002 (Parker *et al.*, 1982; Wilcock, 1988; Wilcock and Southard, 1988; Kuhnle, 1993; Almedej *et al.*, 2006) which was proposed by Parker *et al.*, (1982). This value is more accurate than extrapolating to a zero sediment transport rate; in justification this is because a small degree of mobility is required for observation and is one way to overcome subjectivity due to the random nature of the impacts of fluid flow upon the boundary (Einstein, 1950; Paintal, 1971; Papanicolaou, 2002). Parker *et al.*, (1982) found this method to be advantageous as it was far easier to determine than empirical relationships, as well as W_i^* being independent of D_i .

More recently, Shvidchenko *et al.*, (2001) developed a different reference transport equation relating the critical value of the Shields stress to a constant value of the normalised Einstein bedload parameter akin to Parker *et al.*, (1982). This was based upon scaling sediment transport rates relative to the size distribution of the bed surface that produces the observed bed load transport. Essentially the difference between the Parker *et al.*, (1982) equation and the Shvidchenko *et al.*, (2001) equation is linked to the use of a volumetric transport rate in the former as compared to a mass transport rate in the latter which was believed to be easier to apply. However, irrespective of the equation used,

reference based methods have been widely employed in studies using mixed beds despite reliability questions. These questions commonly refer to the use of a single reference based transport rate which cannot be valid for situations where size selective entrainment occurs. This was confirmed by Komar (1987) in the re-analysis of data from Oak Creek where it was found that equal mobility was not achieved and hence a single reference transport rate would not be valid for entrainment of all fractions of the bed. Thus, it is clear that such an approach remains sensitive to the extrapolation technique used (Paintal, 1971) and the relationship between sub pavement size.

Largest Grain Method: The third of the deterministic methods is the largest grain method but this is not commonly used nowadays. This method relies on the development of competence functions that relate shear stress to the largest mobile fraction and allows the calculation of critical shear stress for a given grain size that is of interest (Andrews, 1983). Predicting incipient motion in this way assumes that the largest mobile grain size collected in a bed load trap is indicative of the initial motion conditions. But, this method is sensitive to the size and efficiency of sediment trap, sample size, sampling strategy, and availability of coarse grain sizes (Wathen et al., 1995). It is also inappropriate for sediment that exhibits equal mobility, as this approach relies on selective transport (Wilcock, 1988, 1992).

Probabilistic Method: The final method of threshold estimation uses a probabilistic approach to threshold determination. Grass (1970), Gessler (1971) and Paintal (1971) all advocated that incipient motion of a particular grain size was an inherently statistical problem. They deemed that incipient motion was dependent on the probability functions of both turbulent shear stress at the bed and the inter-granular geometry of the bed material, described as a function of grain shape, sorting and packing (Kirchner *et al.*, 1990; Buffington *et al.*, 1992). Thus, the probabilistic approach presents the concept of the likelihood of a grain being mobilised, typically relating threshold to a percentage of bed particles in motion. This method considers the probability distribution of dimensionless critical shear stresses for a particular grain size of interest (Grass, 1970; Papanicolaou *et al.*, 2002; Sarmiento and Falcon, 2006), shown by Figure 2-3. No motion is observed where the curves do not overlap, however where they begin to overlap entrainment threshold is reached; the further the curves overlap the greater the intensity of particle transport (Grass, 1970).

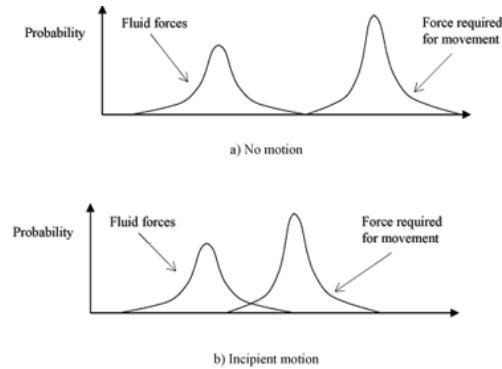


Figure 2-3: Schematic representation of Grass' concept of overlapping shear stress distributions

More recently, Shvidchenko and Pender (2000) advocated the use of a criterion for movement based on the intensity of motion. This is expressed as the relative number of particles moving per unit time;

$$I = \frac{m}{Nt} \quad (\text{Equation 10})$$

where m is the number of particle displacements from an area of bed containing N number of surface grains observed during the time interval t . N can be derived from the following equation:

$$N = \frac{AD(1-\rho)}{\frac{1}{6}(\pi D^3)} \quad (\text{Equation 11})$$

This method allows that a measured bedload transport rate to be expressed as a probability of entrainment or intensity of motion and has advantages in terms of the parameters involved being chosen to suit the conditions of a given experiment. For threshold characterisation in this thesis the visual methodology of the Yalin criterion (derived according to Equation 7 and 8) was used. This method was justified given that it allows direct comparison between the only other two studies which analyse the effects of stress history (Paphitis and Collins, 2005; Monteith, 2005). In addition, it should be highlighted from the discussion of threshold derivation that sediment heterogeneity appears central to the correctness of threshold calculation. As such, the following sections deal with both the direct impact of sediment characteristics and sediment heterogeneity upon entrainment

thresholds as well as the impact of surface structuring which acts to increase bed resistance and hence delay entrainment.

2.2.1 The Impact of Sediment Heterogeneity upon Sediment Entrainment

Traditionally, the majority of flume experiments use uniform sediments where threshold shear stress is observed to increase with particle size. It is rare, however, to find uniform grain size distributions in natural environments. Instead, most natural river reaches contain sediment beds with a wide range of grain sizes depending on the characteristics of the river channel and reflecting the legacy of the past river environments. Of particular interest in many studies in fluvial hydraulics are the effects of these grain parameters upon flow, and *vice versa*. However, opinion is divided as to whether the relative grain size effects (hiding) of a graded bed reduce size selectivity at entrainment and during transport (White and Day, 1982; Komar, 1987) or actually induce a condition of equal mobility (Andrews and Parker, 1987; Wilcock and Southard, 1988). The equal mobility entrainment theory is based on the effect of relative grain size where a bed is composed of grains of a different diameter (e.g. Parker *et al.*, 1982; Wilcock and Southard, 1988; Parker, 1990; Shvidchenko, 2000) and entrainment is independent of grain size. Conversely, the size selective entrainment theory is based upon the absolute size effect of particles within a mixture (e.g. Carling, 1983; Komar and Li, 1986; Wilcock and McArdell, 1993, 1997; Wathen *et al.*, 1995).

The equal entrainment hypothesis proposes that each size fraction within a particular mixed bed will be mobilised at the same threshold of shear stress (Wilcock 1992). The importance of relative size effects in controlling the mobility of sediment mixtures has been described since the work of Einstein (1950) who described a phenomenon known as hiding, viewed as a combination of grain projection and exposure. In a bed composed of mixed sized sediments, finer surface grains typically protrude less into the flow than the surrounding coarser grains which act to increase the pivot angle of fine grains and shelter them from entrainment by flow. Their lower protrusion is both a result of smaller particle size and the greater probability of the finer particles falling into the gaps between surrounding coarser grains, commonly termed microscopic hiding (Parker and Klingeman, 1982). Conversely, coarser grains have a greater relative protrusion into the flow and thus are thus of a lower pivot angle. As such, they are subject to greater fluid shear, offsetting any stability gains that their greater immersed weight may have at resisting entrainment.

Attempts have been made, therefore, to account for the development of the coarse armour layer using empirical devices called ‘hiding functions’ (Sutherland, 1991). Hiding functions modify the mobility of size fractions with respect to their single size mobility as determined by the Shields curve to values more appropriate to mixed grain size beds. Thus, hiding functions generally reduce the transport capacity of the finer fraction of the mixture and increases the transport capacity of the coarser fraction. Hiding functions have been determined empirically under a number of different experimental and field conditions and have been used to numerically adjust the predicted threshold conditions or predicted transport rates and typically take the form of Equation 12.

$$\tau_{ci}^* = \tau_{c50}^* \left(\frac{D_i}{D_{50}} \right)^\beta \quad (\text{Equation 12})$$

where τ_{c50}^* is the critical dimensionless shear stress when $D_i = D_{50}$ and β is a hiding factor which quantifies the dependence of τ_{ci}^* on relative particle size ($\beta < 0$) Equation 12 therefore quantifies the extent to which the relative size effects act to reduce the intrinsic differences in mobility between coarse and fine fractions. Of particular significance are the values of $\beta = 0$ and $\beta = -1$. If $\beta = 0$ then, as Shields suggested, sediment entrainment is dependent solely on particle size (size selective entrainment). However an exponent of -1 indicates that the absolute weight of the particle is completely compensated for by the relative size effects and critical shear stresses for particles composing sediment mixtures are independent of sediment size. In the case $\beta = -1$ all particles are, therefore, entrained at an equal threshold shear stress (τ_{50}^*) and the bedload grain size distribution approximates that of the bed material at all sediment transporting flows.

Parker *et al.*, (1982) corroborated this in their analysis of the data from Oak Creek where they derived an entrainment function with a hiding factor of -0.982. The exponent was considered to be so close to -1 as to render all surface grain sizes equally mobile such that entrainment of even the finest grains required flows in excess of the threshold required to break up the armour; this resulted in the bedload grain size distribution approximating that of the bulk bed material. These data are supported by data from other coarse gravel bed rivers which have shown that at a given shear velocity a mix of grain sizes and shapes can

be entrained and transported together (Ashworth and Ferguson, 1989; Carling, 1989; Wallbridge *et al.*, 1999). The effectiveness of these hiding functions have been demonstrated by Proffitt and Sutherland (1983) who found that the use of hiding functions improved predictions of the size distribution of the transported sediment (Sutherland, 1991). However these functions do not attempt to simulate individual physical processes (sheltering, protrusion and grain arrangement) caused by the interaction between different grain size fractions when a mixed grain size is mobilised. Also, the successful application of the functions generally requires knowledge of the result so that the appropriate hiding function can be selected.

The antithesis of the equal mobility approach is that of size selective entrainment; this assumes a greater dependence of the entrainment threshold on absolute particle size with smaller, lighter particles typically entrained at lower shear stresses than larger grains. Whilst to some degree the effects of hiding are appreciated by researchers pertaining to the selective transport approach, the broad grain size distributions of gravel bed rivers allow for considerable selective transport and dynamic textural response to local perturbations of sediment supply and transport capacity (Dietrich *et al.*, 1989). Specifically, this school of thought denotes that in sediment mixtures larger particles, due to their greater inertia are intrinsically less mobile than the smaller particles that may, to some degree, be sheltered by their coarser neighbours (and thus exhibit a higher critical shear as compared to uniform sediment of the same size). The relative variation of the critical value of the dimensionless bed shear stress for different grain sizes, D_i , within a mixture is largely controlled by their relative size with respect to a central value of the grain size distribution, commonly the median size, D_{50} . It is the differences in sediment grading pertaining to selective transport that may explain some of the scatter in the Shields incipient motion representation (Figure 2-2). Also, many patterns of sediments routing in gravel-bed rivers are consistent with the preferential entrainment of sediment by size. For example, surface coarsening can result from the entrainment of finer, more mobile particles during periods of low flow that are incompetent for coarser, less mobile clasts (Powell, 1998). Wathen *et al.*, (1995) use a similar argument when considering the long profile of a river where there is rapid downstream fining of sediment which they purport can only be attributable to size selective transport due to the resistant nature of the sediment in question. Through analysis of bed load trap data they find there to be preferential movement of sand compared with gravel and fine gravel compared with coarse gravel. This was corroborated by a one dimensional

flow and sediment routing model (Hoey and Ferguson, 1994) which suggested that the high observed degree of downstream fining could be simulated only by size selective bedload transport operating over a number of years.

From the discussion above it is implied that the two schools of thought are mutually exclusive. However, it is now more generally assumed that equal mobility better describes conditions seen where shear stresses are high as compared to conditions with low shear stresses in which a degree of size selectivity is exhibited. This view is supported by published analysis of field data within unimodal channels (Komar and Shih, 1992) and weakly bimodal (Kuhnle, 1992) gravel beds. Wathen *et al.*, (1995) analysed data from a bimodal channel and showed a progressive shift in grain sizes as τ increases, rather than a constant distribution similar to that of the bed as would be expected if perfect equal mobility prevailed. At low stresses, grain size distributions of the bedload were shown to be dominated by sands with no more than 10% gravel. Yet as shear stress increased, the proportion of sand fell whilst that of gravel rose, exceeding 80% in events with peak stresses above 30 Pa. At low shear stresses only sand and fine gravel are mobile with sand transport dominating because, despite low availabilities of sand in the bed surface, the shear stress is well above the threshold for sand. At higher shear stresses, coarser gravel fractions become mobile, and their greater availability, compared with sand, means that their fractional transport rate increases faster than that of sand. A similar view has been expressed by Ashworth and Ferguson (1989) although this was based on less reliable spot measurements of bedload and shear stress measurements. As such, it is increasingly evident that both equal mobility and size selective entrainment theories must be considered when studying sediment entrainment in graded sediment over a range of flows, as in the present thesis.

2.2.2 The Impact of Bed Structure and Surface Characteristics

Instead of the sharp distinction between stability and instability as the Shields diagram (Figure 2-2) would suggest, Grass (1970) proffered a statistical approach to entrainment processes for near uniform sediments in terms of a distribution of applied shear stress (displacement force) and a distribution of critical shear stresses (resistance). The former is determined by the turbulent nature of the flow and the boundary conditions, including the particle geometry, while the critical shear stress distribution is a function of the sediment, with variations in shape, weight and placement of the particles all contributing.

Consequently, since the majority of transport happens at this boundary, it is the characteristics of this boundary which govern a number of complex inter relationships, such as flow velocity and turbulent intensity. The scale at which this boundary changes to accommodate both the overlying fluid flow regime and the upstream sediment supply fundamentally changes the overall stability of the surface. Small scale processes such as particle reorientation act at the grain scale and cause little to no change to the surface grain size distribution yet can still have significant effects upon the overall stability (i.e. the resistance to entrainment) of the surface (Cooper and Tait, 2008). Stabilisation by large scale processes such as river bed armouring occur over vast areas of the sediment bed and act to significantly change both the surface grain size distribution together with the surface characteristics. Despite a tendency towards focusing upon the larger scale processes due to the ease of measurement, the relative importance of each of these processes at both the large and small scale will change with flow regime, sediment supply and the interaction between the two.

Small scale processes act at the particle scale. As such, although small scale processes don't significantly change the surface distribution or characteristics of the bed surface they do serve to increase the structural stability of a bed surface. The concept of textural influences supports previous laboratory evidence by Kirchner *et al.*, (1990) which indicated that the range and size of grain pivot angles within grain size fractions depended on local grain topography as well as the grain size. Supporting this, field observations by Buffington *et al.*, (1992) and Church *et al.*, (1998) suggested that the resistance of grains to entrainment from naturally formed gravel beds is not related simply to grain weight as described by the surface grain size distributions but to some other property of the bed, possibly the arrangement of the surface grains and the topography of the bed surface. For example Church *et al.*, (1998) showed that entrainment thresholds increased by as much as 60% because of the development of grain scale structures. This enhancement of stability is thought to be caused by increased inter-granular friction due to grain to grain contact such that particles interlock and/or shelter in the lee of exposed grains (Schmeeckle and Nelson, 2003). These field observations suggest that the use of models that link transport simply to the surface grain size distribution may over predict sediment transport because they ignore the contribution to bed stability caused by different patterns of grain topography observed in water worked gravels.

There is also evidence that movement of grains alter the fluid flow regime surrounding the bed. Bottacin-Busolin *et al.*, (2008) took simultaneous readings of bed surface structure and near bed local flow field such that grain entrainment could be identified with the corresponding velocity signature. This allowed detailed quantification of the interaction between the bed surface and the fluid flow. Results noted that as a grain is entrained there is a decrease in the dimensionless stream velocity. Figure 2-4 shows the change to the velocity signature as a grain is entrained where the velocity trace is taken from a position above the star box. The grain originally in frame (a) is deposited directly into the area in frame (b) where the trace is being recorded such that the originally stable velocity trace changes when the grain is entrained again (c) where a decrease in the instantaneous streamwise velocity for the duration of the grain movement is noted.

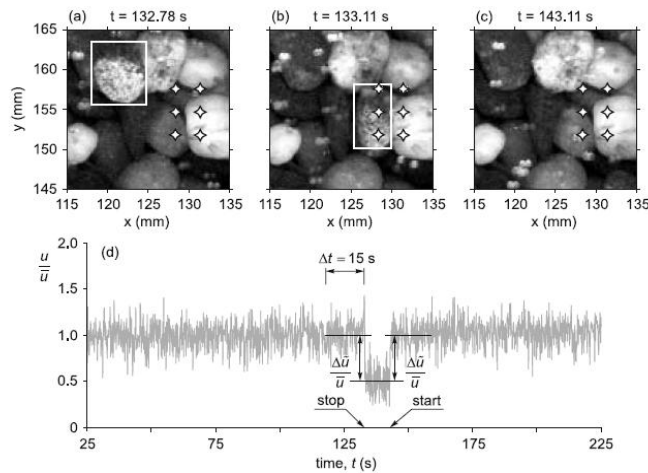


Figure 2-4; Three subsequent time frames showing the bed topography and grain movement linked with the dimensionless streamwise velocity signature (from Bottacin – Busolin *et al.*, 2008). The boxed grain stops at the position in the second frame before being entrained again. The star box related to the position over which the velocity trace was taken.

Figure 2-4 shows that even small scale grain displacements (vibrations and subsequent entrainment) can cause changes to the overlying fluid flow. As such, it would follow that a bed subjected to a prolonged period of low flow has a longer time to interact with the overlying flow such that grains are rearranged *in situ* or moved very locally to become increasingly resistant to entrainment. This concept is developed fully in Chapter 6.

In addition to small scale processes, bed stabilisation by large scale processes also typically occurs in the well-recognised form of bed armouring. Under time varying flow conditions the transport of heterogenous sediments can lead to the development of bed armouring

where armouring is defined as a stratum with a thickness of 1-2 coarse grains, at least part of which are exposed on the bed surface (Gessler, 1971). As such, the median size of the grains at the surface is larger than the median size of the grains in the subsurface (Whiting and King 2003). For armouring to occur, the non uniform characteristics of a sediment must provide a sufficiently wide range of critical shear stresses to allow the stable layer to form; this generally implies a range of sizes. Indeed, armour layers are said to be time dependent in that it is the distribution of critical bed shear stress over time which partially controls armour development. As armouring progresses, a reduction in transport rate is noted, which is said to be proportional to the accumulation of non moving particles, with a less than complete layer being necessary to protect the bed (Liversey, 1963). Indeed, detailed examination of bed load transport rates and compositions by Hassan and Church (2000) inferred that over static armoured gravel beds formed in the laboratory, up to 50% of the fluid forces could be resisted by small, well developed grain scale structures.

Related to this the armour definition has been sub-divided into two types of layer, the static armour layer and the mobile armour layer (pavement), formed depending on the prevailing flow conditions. Firstly, the static armour layer is immobile and developed by the selective entrainment of fines and as such is documented to prevent bed erosion (Gessler 1971). Development takes place at flows strong enough to cause selective entrainment of the smaller sizes but too weak to move the larger ones. Conversely, static armour is said to develop in supply limited conditions such that fine material is winnowed downstream with no upstream supply to replace it, thus leaving the coarse immobile bed surface (Sutherland, 1991; Andrews and Parker, 1987). Selective transport and horizontal winnowing of fines and bed degradation continue until there is sufficient coarse cover to prevent further sediment transport (e.g. Proffitt and Sutherland, 1983, Chin *et al.*, (1994).

Secondly, the alternative mechanism for armouring was suggested by Parker and Klingeman (1982) and Parker *et al.*, (1982) where the mobile armour is proposed to develop as a result of a tendency for 'equal mobility' of various size fractions under partial mobility conditions (Lisle *et al.*, 2000; Hassan and Church, 2000). Equal mobility of all sizes in the sediment supply is sustained by a surface grain size distribution which shelters small particles in the lee and interstices of coarse particles and increases the exposure of larger ones, causing the development of a coarsened surface (Andrews and Erman, 1986; Andrews and Parker, 1987). The process continues until all size fractions are transported

in proportion to their presence in the supply. The mobile armour layer is reported to sporadically interchange with bedload (Wilcock and Southard 1989) with material being washed out from the subsurface and transported through the coarse surface layer (Hunziker and Jaeggi, 2002). However regardless of the mechanism for armouring it is unclear whether or not bed structuring processes akin to armouring, i.e. surface coarsening are possible under sub threshold flow conditions. Whilst Monteith (2005) found that the ratio of D_{50} : D_{90} grains changed such that the surface appeared to be coarsening in response to stress history this remains the only quantitative indication of the effect of stress history upon armour development. As such this concept will be fully developed in Chapter 6 (Section 6.3.4.1).

In more recent studies investigating the structure of gravel beds, statistical methods of analysis of grain rearrangement have noted systematic patterns which are thought to be dependent on whether they were formed under static or dynamic armouring (e.g. Koll *et al.*, 2008; Cooper *et al.*, 2008; Cooper *et al.*, 2009; Mao *et al.*, 2009). For static armour layers, grains are seen to rest with their a (longest) axis parallel to the flow direction, their b (intermediate) axis transverse to the flow and with their c (shortest) axis orthogonal to the flow direction (Allan, 1982; Komar and Li, 1986; Abele and Nikora, 2006). Conversely, during mobile armouring the rolling particles tend to rest with their b-axis parallel to the flow and their a-axis transverse to the flow direction (Komar and Li, 1986; Robert, 1991; Nikora *et al.*, 1998; Bulter *et al.*, 2001; Nikora and Walsh, 2004). However, regardless of the type of armour and unlike small scale particle rearrangement, this type of large scale process does affect the grain size distribution on the surface. As a consequence, parameters such as roughness are changed significantly such that an armoured bed becomes more resistant to entrainment in this manner (Papanicolaou *et al.*, 2001).

2.2.3 Measurement of River Bed Surfaces

Since river bed characteristics govern a number of complex inter relationships such as flow velocity, turbulent intensity and sediment transport, gaining an understanding of the 3D structure of river beds is essential, yet difficult to measure without invasive techniques. Traditionally, this difficulty has been overcome in one of two ways; either avoiding the difficulty by making simplifying assumptions which are often conceptually limited, or as seen more recently, through the acquisition of 2D and 2.5D data where 2.5D refers to a surface in which coordinate points can be extruded along an axis perpendicular to the main

2D viewing plane (Jones *et al.*, 2008). An example of this is the use of laser displacement scanning which has been used across a variety of scales to provide quantitative 2.5D descriptions of river bed surfaces both within the field (Hodge *et al.*, 2009) and flume environment (Rumsby *et al.*, 2008; Measures and Tait, 2008). Most recently, it has been possible to use MRI scanning to acquire a fully 3D non-invasive, non-destructive analysis of the internal structure of opaque materials such as to define structural parameters e.g. void ratio, pore size distributions and permeability (Kleinhans *et al.*, 2008; Haynes *et al.*, 2009). However, given that these 3D techniques are only at their inception and access to the equipment needed to undertake such scans is limited, hence this study concentrates on the more mainstream analytical technique of laser displacement scanning.

In the past, characterisation of gravel beds in both the laboratory and field environments has relied on photogrammetry techniques to collect image data (Bulter *et al.*, 1998, 2001, 2001) which can be processed to gain quantitative and qualitative information (McEwan *et al.*, 2000; Sime and Ferguson, 2003). Typically, stereo images are taken of the surfaces which are then used to reconstruct a digital terrain model interpretation of the surface (e.g. Butler *et al.*, 2001; Smart *et al.*, 2004) through knowledge of the geometry of the cameras and the surfaces over which the images were taken. In order to generate the required stereo pair of images two separate cameras are needed together with a number of control points placed on the surveyed surface which act as an external reference system. Computer software is then used to stereo match the images, eliminate radial lens distortion and conduct further adjustments before the final Digital Elevation Model (DEM) is generated (Butler *et al.*, 1998, 2001). In this manner the method has been used successfully both within the laboratory and field and for imaging both dry surfaces and surfaces through water. Lane *et al.*, (2001) and Chandler *et al.*, (2001) used photogrammetry to describe a 300mm by 400mm patch within a flume where the D_{50} of the measured material was 24mm; a DEM was created with a resolution of 3mm. Results were then compared with a laser profiler where the latter was used to record the same material but over an area of 250mm by 250mm at a resolution of 0.5mm; elevation differences between the two techniques were within 2mm. Similarly, within the field, Butler *et al.*, (1998) used photogrammetry to create DTMs of gravel patches where the D_{50} was 10mm; DTMs were interpolated from the photogrammetry with a point spacing of 3mm where 75% of the residuals were within ± 10 mm. Yet, together with resolution issues there are other known limitations inherent to this photogrammetry method, typically

including image contrast, the photographic resolving power of the camera and lens, variable lighting and maintaining camera position which can significantly alter the picture and DEM quality (Bulter *et al.*, 1998).

More recently, a moveable 3D photogrammetric system has been employed to capture information about sub aqueous dune field topographies yielding an x and y resolution of 25mm and a vertical precision of ± 1 mm (Golding *et al.*, 2003; Henning *et al.*, 2008, 2009). This system uses camera units to record instantaneous images of the channel bed from three different positions with a grid projected onto the bed surface via a slide projector acting as a co-ordinate system. However, despite being a significant advance in the field of photogrammetry, the system has been limited to Froude numbers of 0.3 with negligible disturbances to the bed surface plane. Application of this system to environments with larger Froude numbers without a planar surface remains untested. In addition, due to the light absorbance of the water body, the accuracy of the system is decreased at higher flow velocities due to greater turbulence.

An alternative methodology to photogrammetry is laser displacement scanning. This has been used across a variety of scales to provide quantitative 2.5D descriptions of river bed surfaces, with resolutions typically in the region of 1mm. Packman *et al.*, (1997) and Packman and Brooks (2001) demonstrated the potential of such techniques within their flume investigations relating to the interactions of solutes and colloids. Marion *et al.*, (2003) demonstrated the capacity of 2.5D laser altimetry for capturing high resolution and high accuracy elevation data in an experimental study of gravel surface texture and changes in bed topography. Their topography was measured over a 192mm x 192mm area at a resolution of 0.5mm with a vertical accuracy of 0.1mm. Along a similar vein Rumsby *et al.*, (2007) used this technique to investigate mechanisms of fine sediment infiltration and preservation in gravel beds. More recently the resolution and accuracy of laser scanned surfaces within a flume environment have been assessed in detail. For example, Aberle and Nikora (2006) used a point laser to record longitudinal bed profiles of bed topography under differing armouring regimes where the D_{50} of the measured material ranged from 5.2mm to 25.3mm. Here, a sampling interval of 1mm in the x direction was recorded with a lateral spacing of 4mm and a vertical precision of ± 0.1 mm with the differing sampling intervals in the x and y directions reflecting the footprint of the laser. Cooper *et al.* (2008, 2009) also used a point laser to measure a 250mm x 250mm area at a resolution of 0.5

microns in the vertical dimension with each measurement being integrated over an area of 20x45microns. In addition to being able to achieve greater resolution and accuracy in comparison with photogrammetric methods, laser scanning is found to be more accurate where the elevation to be recorded falls within a crevice in the bed. Studies by Carbonneau *et al.*, (2003), Lane *et al.*, (2001) and Chandler *et al.*, (2001) noted that photogrammetric methods were unable to record elevations in crevices due to perspective errors. Here, the matching algorithm used to correlate the two stereo images was unable to find matching points in the crevices of the two images and, therefore, could not measure any elevations. Lane *et al.*, (2001) and Chandler *et al.*, (2001) noted a significant correlation between whether a pixel was at a grain edge or grain centre with more successful algorithm matches noted at the grain centres. As such, this formed a key limitation of photogrammetry use in rough beds, whilst in contrast the vertical viewpoint of the alternative method of laser scanning meant that it was able to record elevations in crevices without these problems.

However, despite these highlighted examples, 2.5D analytical applications of such technologies within fluvial sedimentological contexts are limited. One fundamental issue still to be resolved is the resolution with which surfaces can be described. The experiments by Marion *et al.*, (2003) indicated that the best surface resolution attainable was similar to that of the smallest grains ($D_{16} \sim 1\text{mm}$, resolution of 0.5mm) making an accurate understanding of surface processes difficult. Also, often high image resolution has often been traded off against the lengthy acquisition time for data collection (where lengthy data collection times are only viable for highly stable bed surfaces, uncommon in flow-sediment environments). Typically laser, scanners have been run overnight where Chandler *et al.*, (2001) and Lane *et al.*, (2001) scanned an area of 250mm by 250mm over an 8 hour period. Although Smart *et al.*, (2004) used a different kind of laser scanner (a hand held 'wand' which uses two cameras to record the cross section of a laser strip projected onto the surface) where 50 cross sections per second could be measured, this speed was still traded off against accuracy, typically in the region on 1mm. Given the importance of data resolution for accurate bed structure analysis, it is evident that improved instrumentation/methodology is still required by researchers; this thesis therefore strives to demonstrate new equipment that reduces the compromise required (Chapter 3).

Once collected, data from both photogrammetric and laser topography measurements can be used to quantitatively describe the bed surface. It is possible to analyse grain

protrusion, pivot angles (Kirchner *et al.*, 1990) and roughness elements (Gomez, 1983) as well as characteristic length scales (Nikora *et al.*, 1998; Smart *et al.*, 2004); details of such techniques are explicitly defined and explored within Chapter 6. It is a combination of understanding derived from all these indicators which is needed if a full understanding is to be gained of bed surface evolution under differing flow regimes and sediment distributions.

2.3 Stress history

What has become apparent within the preceding review of the literature is the uncertainty which surrounds the onset of entrainment. This has been linked to a number of factors, most importantly the impact of sediment heterogeneity. Accounting for the sediment properties, however, only acts to reduce some of the uncertainty surrounding the onset of transport. In order to understand and ultimately reduce this uncertainty, there is a need to take into account both the graded sediment dynamics as well as the fundamental flow properties. One of these properties is the time between events capable of transporting sediment. Richards (1982) describes this problem as;

“ the morphological impact of events is partly a queuing problem, with the inter-arrival times between peaks being as significant as peak magnitudes. The cumulative effect of a succession of low magnitude flood peaks may equal that of a single major flood in terms of sediment transport.”

Despite this recognition that the inter-flood period might be of significance, historically only one flood has been looked at and it has been assumed that the response of the bed would be the same. Over the past six years, however, the effect of the inter-flood period has started to be the specific focus of academic investigation. This research into the effect of the duration and magnitude of the applied shear stress that a sediment bed experiences prior to reaching entrainment threshold has been termed ‘stress history’ (Paphitis and Collins, 2005).

2.3.1 Effects on critical entrainment threshold

The traditionalist school of thought logically determined that non-cohesive sediment beds are only able to modify their structure, and hence resistance to entrainment, when the shear stress applied is above the threshold for incipient motion (Gomez, 1983). Controversially

counter to this, an emerging school of thought more recently has shown that both uniform and graded beds appear to progressively stabilise even when subjected to sub-threshold shear stress (Paphitis and Collins, 2005; Monteith and Pender, 2005; Haynes and Pender, 2007). Researchers postulate that it is the rearrangement of grains on the bed surface into a more stable structure which was responsible for an increase in the critical entrainment shear stress. This implies that where a bed goes on to experience higher flows which are capable of entraining grains, entrainment of a given fraction may, as a result of different antecedent conditions, be entrained over a range of shear stresses. Therefore, accounting for flow history may, to some extent, reduce the uncertainty in entrainment threshold prediction.

Reviewing the temporality of hydrographs further, the effect of hydrograph shape upon the changing relationship between flow and bedload transport has been recognised for some time. Hassan *et al.*, (2006) noted that hydrographic regimes characterised by relatively flat, long hydrographs saw the development of an armoured bed surface, whereas regimes characterised by short flashy floods tended to subdue or destroy the armour layer. This latter regime was believed to be due to strong vertical interchange of sediment throughout the active layer with continuous exposure and entrainment of the fine sediment from the surface. Yet, whilst flood hydrographs of sediment transporting capability have been analysed, the effect of the inter-flood period upon bed stability has received relatively little attention despite indirect support from the field suggesting that this period is of fundamental importance to the onset of entrainment. The closest that field research has come to answering how inter-flood periods affect transported bedload is through the work undertaken by Reid and Frostick (1984) and Reid *et al.*, (1985) who published field data for Turkey Brook, England. Their work showed that entrainment thresholds were up to three times higher during isolated flood events as compared to floods which occurred over a shorter recurrence period. It was reasoned that isolated flood events allowed a greater period for bed re-structuring during the inter-flood period such that the bed became increasingly consolidated (due to the particles interlocking on the bed surface and the infiltration of finer grains into the matrix) and hence more able to resist entrainment. Counter to this, floods with short recurrence intervals note bed material being comparatively loose such as to offer less resistance to entrainment. In this case, substantial amounts of bedload are generated on the rising limb which is the opposite of floods with longer inter-flood periods. This is exemplified by Figure 2-5 where the events of 10th

December 1978 and 9th December 1979 come after more than four months of low flows; data is plotted on the abscissa and discharge and total bedload plotted on the primary and secondary ordinates respectively. During this time the bed material underwent some consolidation and thus the floods failed to generate bedload until the bed shear stress was 3 and 1.5 times the average shear stress at initial motion respectively.

Whilst Reid's work hinted at stress history effects this was not the focus of his publications and chronological developments in antecedent-related sediment research were still biased towards sediment transporting flows. Flume research by Willetts *et al.*, (1987) found that the rate of sediment transport is a function of antecedent flow conditions moulding the current bed state; the significance of this finding was thus subsequently researched in more depth by Saadi (2002). Saadi investigated bedload transport rates following periods of between 1 and 12 hours of both steady and unsteady flow capable of transporting sediment. Results noted that the bedload transport rate following these periods of flow were lower following longer durations of antecedent flow transport. Similar to Reid's suggestion, Saadi attributed this to an increased period of time for the grains to attain a more stable position on the bed surface and thus form a stronger bed. More recently, the field study of Oldmeadow and Church (2006) compared a control reach ($D_{50} = 67\text{mm}$) with a treated reach ($D_{50} = 59\text{mm}$) in which all cluster bedforms were broken down so structural development of bedform clusters could be analysed; here it was also noted that the degree of structural development depended on the recent history of flow and sediment supply, again suggesting that temporality of antecedent flow warrants more detailed investigation with respect to entrainment studies.

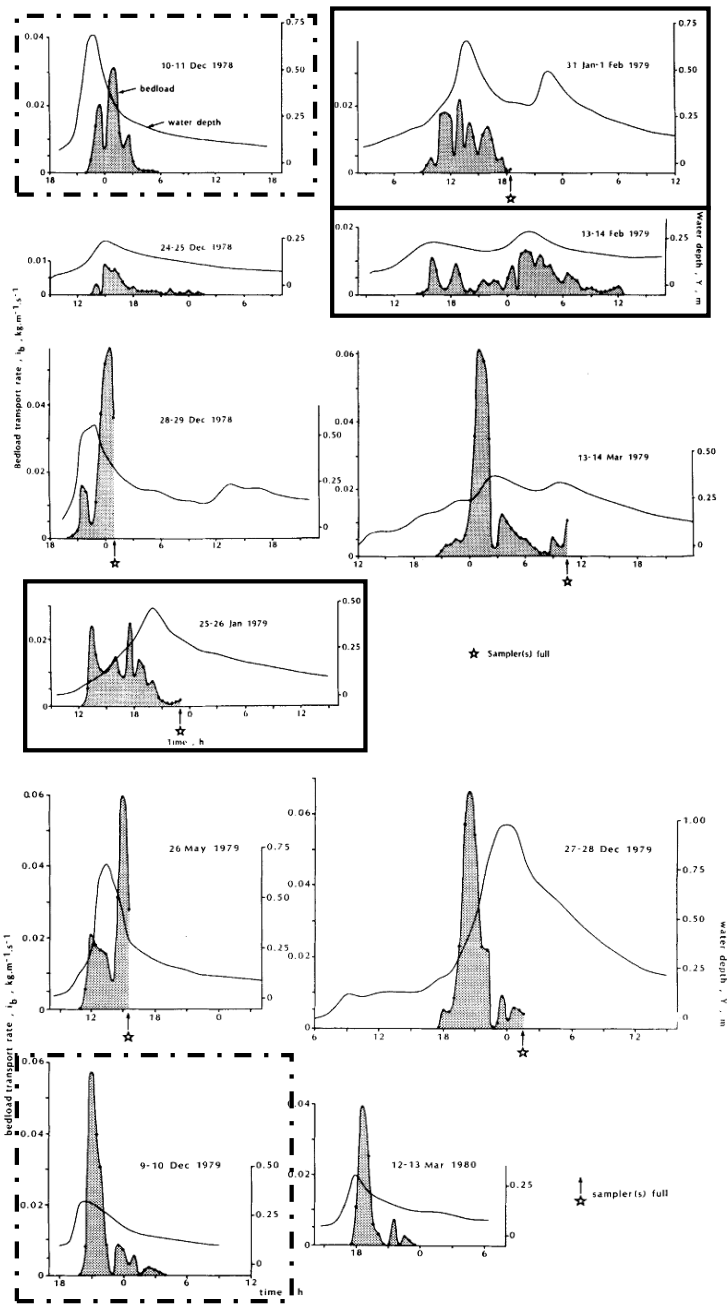


Figure 2-5; Continuous record of unit bedload transport expressed as submerged mass i_b , for selected floods from Turkey Brook, 1978- 1980. Floods with short recurrence intervals are noted to have large amounts of sediment generated on the rising limb (25-26th Jan 1979, 31st Jan – 1st Feb 1979, 13-14th March, marked with a solid black box) whereas floods which follow prolonged periods of low flow generate bedload on the falling limb after the rising limb has loosened the bed structuring and released the fines (10-11th Dec, 1978, 9th-10th Dec 1979, marked with a dashed black box).

Specific to sub-threshold antecedence analysis, direct laboratory evidence supporting the concept of stress history has now been specifically determined by Paphitis and Collins (2005), Monteith and Pender (2005) and Haynes and Pender (2007). Paphitis and Collins (2005) experimentally studied the entrainment threshold for uniform sand beds ($0.194 < D_{50} < 0.774\text{mm}$) subjected to antecedent flow durations (0 - 120 minutes). Their data indicated beds were up to 27% more stable following exposure to prolonged durations and higher magnitudes of antecedent shear stress. This was attributed to the erodability of a particle being dependent on particle rearrangement under sub threshold flow conditions into a more stable bed configuration. Similarly, Monteith and Pender (2005) and Haynes and Pender (2007) undertook flume-based analysis of a bimodal sand-gravel mixture ($\sigma_g = 2.08$). Beds were exposed to antecedent conditioning flow durations of 0, 15, 30, 60, 1140 and 5760 minutes where sub-threshold flow was set at 50% of the critical bed shear stress required to entrain the D_{50} . Bed stability was measured via a stability test which ran immediately after the antecedent flow period; flow in this stage was increased so as to expose the bed to a constant shear stress of 110% of that required to entrain the D_{50} . In terms of the findings from the antecedent duration experiments, their results indicated up to a 48% increase in critical bed shear stress by increasing antecedent duration from 0 to 5760 minutes. These data were augmented by experiments also documenting the effect of antecedent magnitude upon bed stability, in that beds were exposed to antecedent flow magnitudes of 50%, 75%, 80%, 90% and 100% of the critical bed shear stress required to entrain the D_{50} . The effect of the antecedent flow magnitude appeared to govern stability via the alteration of the proportions of the framework gravel and the matrix sand compromising the bed surface due to selective entrainment processes (Section 2.2.1); specifically their results showed that beds conditioned by high antecedent bed shear stresses offer low residual stability and require longer to re-stabilise following a change in flow conditions. Both sets of Haynes' results suggest that the level of stability offered by a graded bed is specific to the stress history. Whilst Haynes' finding suggest that grade may play a role in stress history induced stability, neither the work of Paphitis and Collins (2005) and Monteith (2005) provide definitive data sets pertaining to quantification of the underpinning mechanics causing stability change. In addition, past research has been specific to the one specific grade chosen by the researcher; data sets do not overlap size ranges and methodological differences mean that data may not be directly comparable. Therefore, when considered with respect to grade influences discussed in Section 2.2 there is a clear need to directly compare and contrast the effect of grain size distribution when

beds are exposed to different antecedent durations, as well as a need to provide a detailed look at the mechanisms which are responsible for bed stabilisation under below-threshold flows.

Both the work by Paphitis and Collins (2005) and Haynes and Pender (2007) inferred that increased stability was caused by local particle rearrangement into a structure more resistant to entrainment by fluid flow. Consequently, both surmise that stabilisation due to stress history effects are intrinsically linked to surface grain size distribution, packing density and individual particle orientation. Experimental observations of Monteith (2005) noted that a bed which had not been subjected to water-working of any kind is mixed, poorly structured, loosely packed and unstable. When subjected to flow, energy is imparted to the grains such that they rearrange locally even under sub threshold flow; the longer this period of flow the more reorganisation that can occur. During this period it was postulated that fine grains settled into lower relief areas of the bed via exploitation of the voids in the surface layer such that the coarser grains became more and more exposed to the overlying flow. This was further evidenced from photographic analysis of the D_{50} and D_{90} present on the bed surface, where the proportion of the D_{90} increased with increasing antecedent duration (countered by a decrease in the number of D_{50} particles) and this supports the theories of vertical winnowing and hiding effects creating a more stable bed. Experimental observations also note that the coarser particles pivot around an axis until they are streamlined with the flow, such that they offer the least resistance to the fluid and are less likely to be transported. Consequently, by the end of a prolonged period of sub-threshold flow the bed surface is composed of coarser particles which are exposed, streamlined and stable as compared to the finer grains which are in low relief, in the sheltered downstream lee of coarse particles. In addition, it is also suggested that a proportion of fines are completely 'lost' from the surface as they are vertically winnowed through the bed so that they are not just sheltered from the flow but are deep enough within the bed such that they would only be transported if the whole matrix were to be entrained. However, these are primarily assumptions based upon literature and uncorroborated by stress history data sets specifically. Whilst selective entrainment, hiding effects and pivoting angles are discussed, direct quantification of vertical settlement, reorientation or bed structuring is not provided, yet would be expected to be important.

2.3.2 Importance and application

The concept of stress history has significance for the accurate prediction of the transition between river bed stability and instability; the longer the inter flood period, the more stable the bed and hence the greater the increase to critical entrainment threshold. As such, there are several avenues in terms of the strategic output of this work which must be recognised by both academic researchers and applied practitioners of sediment-related science and engineering.

In an applied engineering context, such as within river engineering where hydrographs are artificially maintained, flow regimes including volume, duration, timing, frequency and lapse time since last flooding, are the key driving variables. The UK Environment Agency's River Habitat Survey showed that less than 10% of sample river reaches in the UK were free from channel and bank structural modification. It has also been estimated that 95% of the UK gauging stations are affected by regulation (Sear *et al.*, 2000). Typically, such regulation involves direct modification of hydrology, flow regimes and sediment systems in a river channel (Acreman 2000; Hamill 2002). In regulated rivers, flows are rarely seen to drop to natural summer levels yet disturbance events caused by periods of discrete high flow events interspersed in the stable flow regime of the river are a natural and important feature of such environments (Sousa 1984). Such regulation is exemplified through an understanding of freshet releases from dams. Typically, reservoir releases are governed by the Environment Agency and take the form of block releases of water. However, it is widely recognised that there is a need to alter this release regime in order to meet the instream and environmental flow requirements (Bullock and Gustard 1992; Acreman *et al.*, 2000; Gibbons *et al.*, 2001). The adoption of the compensation flows have taken over from the continuous minimum flow release maintained throughout the year used in past management practice. However, more recently release regimes aim to mimic natural seasonal variation in flow with Gilvear (1994) suggesting that the release hydrograph should be representative of natural flows, both on the rising and falling limbs with Acreman *et al.*, (2000) suggesting that there should be a release of high flows so as to maintain channel form and function. Therefore predicting the amount and timing of sediment delivery as a result of the imposed flow regime is of fundamental importance; the effects of stress history upon such timing and delivery is liable to have a significant effect but as of yet has not been researched.

In addition, ecological integrity of river ecosystems is dependent on the variation in flow regime to which they are adapted with the spatio-temporal heterogeneity of river systems responsible for a diverse array of dynamic aquatic habitats. Hence, ecological diversity is maintained by the natural flow regime such that any disturbance to the regime will impinge upon the natural function of the ecosystem. However, since floods cause hydraulic disturbances that determine the composition of biotic communities within the channel, the riparian zone and the floodplain (Junk *et al.*, 1989; Webb *et al.*, 1999) engineering of fluvial systems to regulate flow often cause hydraulically optimal but ecologically poor systems (Petts 1994). The biological changes associated with river engineering are widely reported to reduce diversity and abundance of biomass amongst fish and macrophytes, especially those that are associated with coarse substrate, shallow water and high velocity (Swales 1989; Hey 1996). Consequently, alteration of the discharge and sediment regime of the river has fundamentally important effects upon river habitat diversity which can ultimately have financial consequences e.g. sport fishing revenue, tourism, research activities and adoption of the Water Framework Directive.

This becomes particularly important in the light of climate change acting to change inter-flood periods. Estimates by the Hadley and Tyndall Centres through the UK Climate Impacts Programme (UKCIP02) predict that that the UK winters will become wetter and summers drier, with the likelihood that heavy winter precipitation will increase (UKCIP02). Essentially this translates as higher extremes of flow but also an increase in the frequency of high flows in winter and decrease in the frequency in summer. Thus, long inter-flood periods of low flow during the summer may give the sediment bed of a river more of a chance to rearrange under sub threshold conditions resulting in a bed more resistant to entrainment and lower sediment transport rates during a subsequent high flow event. There is, therefore, a need to direct research at understanding how climate change will manifest as differences in the riverine environment, specifically how the flow hydrograph, sediment transport and hydromorphology will change. Thus, it is vital that research is driven by a desire to answer such fundamental questions.

In addition to predicting and understanding the impact of stress history within the field, attention should also be paid to the possible effects upon the set up of future experimental programmes (and understand the potential reasons for data scatter in past programmes). Since Paphitis and Collins (2005), Monteith and Pender (2005) and Haynes and Pender

(2007) all advocate the importance of stress history, it seems important that care must be taken in the set up procedure of experiments. Experiments where flow is either increased slowly or the observational period is relatively long will produce a bed that is more compact (than the original bed) as compared to sediment beds where flow is increased rapidly or the observational time periods are short, where beds will be comparatively unstable. This will be further exacerbated where differing threshold criteria are employed; a criterion that requires a significant amount of movement before it is satisfied will be subjected to increased effects of stress history. The importance of this to laboratory-derived data should not be unstated.

Finally, as increases are seen in the complexity of the scenarios being investigated, research work becomes the primary domain of river morphological modelling through which an attempt is made to answer complex, integrative scenarios that are beyond the realms of standard investigative science. Such models incorporate restrictive assumptions pertaining to spatial variability, dimensionality and interaction of various components of flow and transport processes. At the heart of most of these models are sediment transport equations. Since an incipient motion term forms the basis of most sediment transport equations, there is a need to reduce associated uncertainty so as to form accurate predictions. One possible way of reducing this is to vary the critical shear stress associated with an applied antecedent duration so as to modify incipient motion. Yet, to do so requires more comprehensive data sets upon which to base the correction. Thus, not only is the outcome of this research pertinent to wider investigations in fluvial engineering, management of regulated rivers, the sensitivity of river morphology to climate change and flume-based experimental technique, but it may also form a basis from which to improve the reliability of sediment transport models used increasingly within both the academic and industrial domain of our subject field.

2.4 Summary of the Literature Review

Discussion within this literature review has concentrated upon the factors which determine incipient motion and how incipient motion is affected by graded sediment dynamics and bed surface structuring. This has been discussed in the light of the effects of antecedent flow duration and the effects upon entrainment threshold.

Incipient motion has been shown to be a function of both particle and flow parameters where much research has concentrated on viewing the threshold of motion as deterministic processes. However, significant uncertainty still surrounds the determination of threshold which has led to the development of stochastic methods of threshold prediction. Both paradigms of thought are additionally complicated in the light of graded sediment dynamics where inter granular effects serve to confound difficulties in the prediction of entrainment threshold. Such dynamics are controlled at a fundamental level by the properties of the grains themselves such as size, shape and packing, together with their interaction with the surrounding bed and the overlying fluid flow regime. Due to the inter-granular effects, where a graded bed is exposed to a fluid flow there is therefore potential to form structures on the bed surface which serve to increase the beds resistance; these have been shown to be both active at the large and small scale with the relative importance of each a facet of both the grain and fluid properties. Furthermore the fluid flow regime has also been seen to be especially important in terms of the duration and magnitude of antecedent flows. Here there is a growing body of evidence showing that these low flows are of fundamental importance to entrainment prediction, whereby the longer the inter-flood period, the more stable the bed and hence the more resistant to entrainment. However, little is known about the inter-grade effects of stress history or the specific mechanisms which are responsible for the observed increase in bed stability.

As with all academic research, the purpose of this thesis is to aid resolution of some of the holes and inconsistencies found within existing research. Given the evidence of the relationship between the grain size distribution and the overlying fluid flow properties this thesis is dedicated specifically to further understand the relationship between stress history, entrainment thresholds and bed structure. The following Chapters not only provide new data and analysis (Chapters 4-6), but also advance the measurement techniques within experimental research of this kind (Chapter 3) and raise questions that are signposted for future research in related fields of sediment entrainment.

Chapter 3 Experimental Set- up and Instrumentation

The experimental programme detailed below was designed to generate the most comprehensive dataset to-date on the effect of stress history on sediment entrainment. In subsequent chapters the methods described in this chapter are analysed to yield a deeper understanding of the effects of stress history. Specifically, stress history effects were analysed using three methods. Firstly, visual threshold analysis was undertaken to quantify the critical entrainment threshold of the D_{50} of different sediment grain size distributions. Secondly, total and fractional bedload data was collected such that the magnitude of the total bedload transported could be evaluated to provide proxy data on the stability of each bed. Lastly, the specific mechanisms responsible for stability changes due to stress history were quantified through rapid acquisition high resolution laser scanning of the bed surface.

3.1 *Experimental Programme*

The experimental laboratory programme was conducted using flumes in the Department of Civil Engineering, University of Glasgow, United Kingdom. Two sets of experiments were run between August 2007 and March 2010, including a 2 month period of calibration within the new 1.8m wide ‘Kelvin’ flume (Section 3.3). The first set of experiments, completed in the 0.3m wide ‘Shields’ flume were designed to provide data to inform the main experimental programme (Section 3.2), whilst the second set of experiments (Section 3.3), completed in the ‘Kelvin’ Flume, formed the main experimental programme and were designed to understand the mechanisms underpinning the stabilisation of the bed due to stress history. Three justifications follow for using the two different flume facilities; firstly, the only two previous stress history studies available for comparison have been conducted in 0.3m wide flume facilities (Paphitis and Collins and Monteith, 2005), making data gathered from the ‘Shields’ flume directly comparable to both data sets. Secondly, the different hydraulic conditions experienced in each flume offered two specific conditions under which to test the effects of antecedent flow duration, especially focussing upon width depth ratios and sidewall influences. Finally, the practical constraints made using the ‘Shields’ flume an easier alternative for the development and refinement of techniques that were to be used within the larger flume facility whilst the thesis focus on particle rearrangement required areal analysis of the bed surface which, due to sidewall effects, was better performed in the larger ‘Kelvin’ flume. A detailed breakdown of all experiments undertaken is given in Appendix A1.

The variables measured included: transported bedload, bed surface topography, flow velocity and bed surface composition; a detailed breakdown of the variable sampling strategy is given in Appendix A2. Information on the sediments employed in this research is given in section 3.4. In order to standardise experiments, a repeatable procedure was established with only one variable altered per experiment to allow isolation of driving variables within the experiment. Whilst the present Chapter discusses the general instrumentation required for each experiment, more detailed methodology is provided specific to the analysis undertaken in Chapters 4-6; this format is elected due to subtle, yet essential and justifiable, differences in the experimental procedures of the data sets collected. A total of 75 experiments were completed within the Shields flume and 36 experiments with the Kelvin flume.

3.2 *Shields Flume*

3.2.1 *Installation*

The first set of stability experiments were performed within an *Armfield* flow-recirculating, tilting flume (15m long x 0.3m wide x 0.45m deep). The glass-sided flume was rectangular in cross section with a smooth, steel floor. The flume slope was controlled by a mechanical screw jack at the upstream end, which acted via a pivot point at the flume centre allowing slopes to range from -0.005 and 0.035. Running rails extending along the length of the flume ran parallel to the floor of the flume (and thus at the same gradient as the flume floor); minor adjustments to the running rails were made via screw gauges set along each side of the flume.

The flume was a closed system with water re-circulated by means of a *Calpeda* pump capable of discharging up to 30 litres per second. Water was pumped from the header tank at the upstream end of the flume, down the flume to discharge over the tail gate before being returned to the header tank via a return pipe. The flow velocity in the water return system is controlled via a *Portaflow SE* flow controller which is linked to the pump via a power inverter. Flow information is recorded by the *Portaflow* by two sensors which are attached to the outside of the return pipe which emit acoustic signals; the transmit sensor emits an acoustic pulse which is then backscattered via small particles in the return pipe and returned to the second, receiver sensor. This allows measurement of the flow velocity

within the pipe to within ± 0.1 m/sec of the recorded velocity. The quality of the received signal was assessed via monitoring of the signal strength value; within all experiments these values were in excess of 80% (a minimum value of 40% is recommended by the manufacturers).

To prevent scour and induce turbulent boundary conditions 2 metres of immobile sediment (approximately $D = 20$ mm) were placed directly downstream of the flume inlet. The remaining length, comprising the test sediments, was immediately downstream of this immobile bed. Using a flume slope of 1/200, the bed was screeded to a depth of 60mm using a wooden board run along the running rails of the flume in the downstream direction. Preparing the bed as described can introduce bias (Cooper and Tait, 2008) such that although the surface of the volumetric grain size distribution may be similar, the statistical distribution of bed elevations is different. Typically the surfaces of screeded beds have been characterised by a relatively flat, uniform surface with visible pore spaces between grains. However also noted have been the protrusions of random, irregular grain scale protrusions around the mean elevation causing the surface distribution of elevations to be characterised by a negative skew (Nikora *et al.*, 1998). This bias was minimised by one operator preparing all the beds, and by checking the surface grain-size distributions on photographs of the prepared bed surface of screeding the bed (section 4.4.1). Water and bed slope profiles were taken at periodic intervals throughout the experiments using a *Mitutoyo SD Series 572* vertical scale pointer gauge mounted on a moving instrument carriage mounted on the running rails; this ensured that quasi-uniform flow was maintained in each flow period. Output data from this instrument are accurate to ± 0.01 mm and measurements were taken at 0.5m intervals along the length of the flume relative to an arbitrary datum established at the upstream end of the flume. This procedure was carried out in all calibration runs (i.e. prior to the main experimental runs) such that uniform flow was established for each discharge; this set up was then employed during the main set of stress history experiments.

3.2.2 Bedload visualisation equipment

Entrainment threshold was estimated using visual techniques using images recorded by a digital Sony HD 4 Mega pixel camera mounted on the instrument carriage. This was aimed vertically downwards to view an area 200m by 200mm (named the 'texture square'), approximately 11m from the inlet (Figure 3-4). Although there is no definitive definition of

the correct size of texture square to be used (in terms of the ratio of observation area to the number of grains) it has been noted that the area of observation should be 'large' in comparison with the grain diameter and the length of the time of observation should be 'large' in comparisons with the average period of turbulent fluctuations (Yalin, 1972). The choice of both the area and the time of observation in any particular study depends on the flume dimensions, measuring equipment, method of observation, the range of grain sizes investigated and the flow conditions employed (Shvidchenko and Pender, 2000). In this research the size of the observation areas was constrained by the width of the flume thus, given the choice of sediment size, the observation areas permitted approximately 3900 D_{50} grains to be analysed per image in the uniform bed, 1563 in the unimodal bed (based on 40% of the distribution composed of D_{50} grains) and 312 in the bimodal bed (based on 8% of the distribution composed of D_{50} grains); this was sufficient for the statistical analysis undertaken given that the maximum number of grains needed to satisfy the Yalin count at threshold approximate to 4 % of the theoretical grains available on the bed surface . In addition, it is worth highlighting that a 4MPx resolution over this observation area implies 0.1mm pixel size, which permits a minimum of 10 pixels per grain (1mm is the smallest grain size used) and therefore sufficient resolution to identify fractions of the bed surface (Humphreys *et al.*, 1999). Video recordings were taken under natural light conditions for a period of 3 minutes which allowed the entrainment threshold to be calculated (as detailed in Section 4.3.1). In order to take both the still photographs and video recordings, a glass plate was lowered onto the water surface so as to remove ripples in the water surface and enhance image clarity. For bed compositional analysis, still photographs were also taken under UV light in order that both the D_{50} and D_{90} fluoresced, allowing ease of recognition during more detailed compositional analysis.

3.2.3 Bedload Sampling Equipment

Transported bedload was sampled by collecting sediment in a removable transparent sediment trap located 12m downstream of the inlet (Figure 3-4). The trap was 1000mm deep, 150mm wide with a streamwise length of 70mm in the downstream direction. Control was via a brass quarter turn valve at the top of a removable Perspex collecting chamber. This allowed the top valve to be opened permitting sediment to be collected for the required sampling period before being closed at the end of the sampling period. The collecting box was then removed, sediment extracted and the collecting box replaced.

Sediment was then air dried overnight and analysed by sieving the sample at 0.5 phi sieve intervals in order to establish fractional entrainment thresholds.

3.3 Kelvin Flume

Given similarity of the infrastructure and instrumentation of many features of the two flume facilities, this section only highlights components distinct to the Kelvin flume. For reference, the following aspects of the facilities are identical: flume fabric, instrument rails, turbulent boundary layer induction, screeding technique, basic flow control and monitoring, flow recirculation, basic bedload trap components and sampling.

3.3.1 Installation

The stress history experiments of the main experimental programme were performed within a glass-sided, flow-recirculating flume of rectangular cross-section (13 m long \times 1.8 m wide \times 0.35 m deep) (Figure 3-5). The glass-sided flume was rectangular in cross section, with a concrete screed covering a steel floor. As the flume could not be tilted by mechanical means, the concrete screed was configured to produce a slope of 0.005. The bed was screeded to a depth of 50mm using a wooden screed board in a cross stream direction in 0.5m sections for the working section of the flume. Three mobile instrument carriages ran along the length of the flume. The first carried the video camera, the second carried the glass plate over which the video camera was focused and the third carried the laser displacement scanner.

Flow was controlled in the same manner as with the Shields flume except that three pumps were used, each with a maximum capacity of 50 litres per second thus giving a combined maximum of 150 litres per second; the required flow velocities were programmed to be split equally between the three pumps. Additional control was afforded to flow within the Kelvin flume via the use of a closed-loop, feedback system as detailed in Figure 3-1.

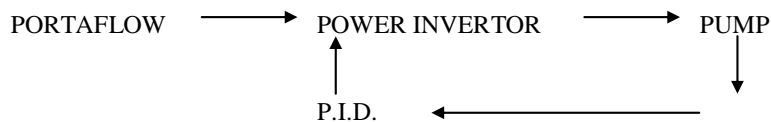


Figure 3-1; Schematic diagram of flow control devices attached to the Kelvin Flume.

The Proportional Integrative Derivative (P.I.D) device was used to increase the accuracy of the flow by calculating the ‘error’ in the system recorded as the difference between a measured process variable, in this instance flow velocity, and a desired setpoint, in this instance the programmed flow velocity. As such the P.I.D allows a closed loop feedback to be set up such that the required flow velocity is programmed into the P.I.D. controller, which feeds into the power inverter to control the pump speed. The speed from the pump and, hence, flow velocity is recorded by the Portaflow. The recorded flow velocity is then fed in a feedback loop to the P.I.D controller until the desired and achieved flow velocities are the same. The desired flow can be achieved to a 1% accuracy of that required. Similarly to the Shield’s, flume water was pumped from the header tank at the upstream end of the flume, down the flume to discharge over the tail gate before being returned to the header tank via a return pipe.

To prevent scour and induce turbulent boundary conditions, 2 m of immobile sediment was placed directly downstream of the flume inlet. Immediately downstream of the immobile sediment the bed comprised the mobile test sediments (effective working length 8 m). During the flume calibration water and bed slope profiles, results were recorded at three discrete locations across the flume width; at the channel centre line and then equidistant between the channel centre line and channel sides. These results established that recordings taken at the channel centre line were representative of the flow occurring over the channel width thus calibration runs to establish uniform flow for each discharge used during the experiments were only carried out at the channel centre line.

3.3.2 Bedload Sampling Equipment

The bedload visualisation equipment used with the Kelvin flume was the same as that used within the Shields flume (3.2.2). The transported bedload was sampled by collecting sediment in a transparent sediment trap located 12m downstream of the inlet (Figure 3-6). The trap 75mm wide in the downstream direction with the sampling slot covering 1.5m of the flume width. In Figure 3-6 the trap was also divided into three collecting chambers so that the spatial variation of the sediment transport in the cross stream direction could be investigated although this was not investigated within this thesis. The trap was controlled by two quarter turn valves, one at the top of the Perspex collecting chamber and one at the bottom. This allowed the top valve to be opened thus allowing sediment to be collected for the required sampling period and closed at the end of the sampling period. Sediment could

then be purged by opening the bottom valve. Water from the trap was re-circulated into the flume storage tanks using submersible scavenger pumps. Water was re-fed back into the Perspex collecting boxes via small taps opening into the collecting chambers in order to fill the collecting chamber with water before the top valve was opened; this ensured that minimal air was released when the valve opened as this could have acted to displace sediment located near the trap margins. Sediment transport was measured for ten minutes and then purged during discrete measurement intervals throughout the experiment.

3.3.3 *Laser Displacement Scanning*

Crucial to the present investigations was the laser displacement instrumentation. Given that the single point laser systems of past studies (e.g. Tait *et al.*, 1997; Marion *et al.*, 2003) required many hours to scan even a small area of bed, if multiple beds of multiple stress histories were to be analysed within the timeframe of this PhD it was essential that an alternative state-of-the-art system was sought, tested and adopted that was capable of much faster acquisition times. As such bed topography measurements were carried out using a *Micro Elipson scanCONTROL2800*. Initially the scanCONTROL 2800 was designed for applications in industrial environments where a high measurement rate combined with a high degree of accuracy made the system ideally suited for applications requiring high precision data acquisition within short cycle times. As such it has more commonly been employed to inspect the surface of the tyres for production defects, inspecting the surface geometries of rotary pistons as well as checking for flaws in car windscreens (Micro - Epsilon handbook, 2010). However the functionality of the system and adaptability to different applications meant that it is now possible to employ such a technology to river bed science.

The scanCONTROL 2800 makes use of the triangulation principle for two-dimensional acquisition of profiles. In contrast to familiar point laser sensors, a linear optical system projects a laser line onto the surface of the object to be measured which typically makes the scanning a lot quicker. Specifically a laser beam is projected onto the bed surface in the cross-stream (x) direction via a linear optical system. This profile uses the laser light that is diffusively reflected back to the sensor to simultaneously read the x, z co-ordinates (z = vertical displacement) of 1024 discrete points along the laser beam; this is then replicated on a CCD array for quantitative evaluation. The CCD array is composed of a grid of 8 by 8 individual measurement squares over which the signal is replication with

each able to record up to 256 pixels. As such the maximum number of pixels which can be measures is 1024 x 1024 pixels. The area over which the data is recorded (and thus the number of pixels) is preselected by the user where altering the portion of the array used increases data acquisition speed. Consequently, the geometry of the measuring field (height z and width x) can be varied and can be adapted to the measurement application. In order to generate the y component an *Arrick Robotics* stepper table and motor system was used which automatically moved the laser in the downstream direction at a prescribed speed, hence a known number of steps per distance.

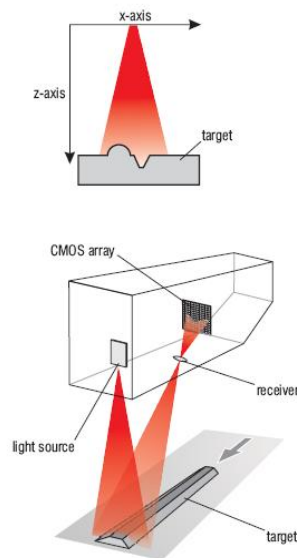


Figure 3-2; Diagram depicting how the scanCONTROL 2800 laser records the surface. The top of the two images shows the relationship between x and z whilst the bottom image shows how the light source is projected onto the surface and reflected back onto the CMOS array.

The resolution of the laser is controlled by the maximum number of data points which can be exported per second (limited to 256000) which is linked to the area of the surface to be scanned; the larger the area the coarser the resolution with which the surface can be described. For the purpose of this thesis typical resolution values derived with the literature provided the foundation for resolution justification where there is an emerging argument which suggests that in order to accurately represent a single grain 10 points are needed per grain (e.g. Humphreys *et al.*, 1999). Given the smallest grain was 4.8mm in the uniform bed the minimum sampling resolution needed was 0.48mm however within the bimodal bed the smallest grain size was 1mm and therefore, in order to resolve the smallest particles the sampling interval should be 0.1mm.

Specifically, in this thesis, along a single laser profile the x-direction resolution ranged from 0.109 mm in the centre of the beam (with a standard deviation of 0.09 mm) to 0.120 mm at the edges of the beam (with a standard deviation of 0.150 mm); this was due to the lateral splay in the emitted beam trajectory and the roughness of the bed surface. As explained, in the z direction the resolution is controlled by the capabilities of the CCD array of the sensor. Although the maximum number of points that can be collected in the z direction is 1024 given the x and y dimensions (100mm by 116mm) the number of data points gathered in the z direction had to be reduced so was set at 512 over 122.9 mm vertical distance; this yielded a resolution in the z direction of 0.239 mm. The y component was controlled by the configuration of the stepper motor such that, in the present investigation the stepper motor was configured to approximately maintain the aspect ratio of the x, y, z image; 800 profiles were, therefore, taken per 100 mm length translating into a y-direction grid resolution of 0.125 mm. With the laser reading 204,800 data points per second, the prescribed y-direction resolution resulted in a scan rate of 25 mm downstream distance per second; as such, a 116 mm (x) by 100 mm (y) area took only 4 seconds to scan. Although in total 9 scans were taken each time the bed was drained (an area of 300x300mm) only one scan was used per experiment for full analysis; this was partly due to the post processing time which was required for each scan and partly due to the difficulty in stitching the individual scans together. The use of one scan is justified in terms of analysis of the 2D structure functions (Section 6.3.4.2) which saturated at scales much smaller than 100mm suggesting that the structure on the bed surface could accurately be represented by a 100x100mm texture patch. The resolutions gained are within the same range as those previously noted within the literature (e.g. Aberle and Nikora, 2006; Rumbsby *et al.*, 2008; Cooper and Tait, 2008) however the acquisition time of the sample is significantly less. Given that the longer a flume is drained for the more likely it is that changes will happen to the bed surface (e.g. the surface drying out and vertically settling) the quicker the acquisition time the more accurate the representation of the surface is likely to be. Information regarding the analytical techniques employed once the data was collected is given in Chapter 6.

According to the manufacturers the overall accuracy of the data derived from the laser is contingent upon five main factors; the degree of reflection on the target surface, colour differences on the target surface, extraneous light surrounding the target surface,

mechanical vibrations and surface roughness. As high levels of light were scattered from the surface due to the moisture retained in some pore spaces the exposure time was increased so as to increase the uniformity of light across the image and maximise the image quality and was set to 5 ms; this value was chosen based by iteratively changing the exposure time and analysing the resultant output scan until an optimum exposure duration was found based on visual inspection of the output scan. Additionally, in order to reduce both the scatter of light and the extraneous light, a blackout curtain was built to enclose the laser scanner. Whilst it was noted that the scan quality was better over a dry bed as compared to a wet bed a trade off had to be made between the quality of the scan and the time that the bed was drained for given the impact of draining on bed structure; justification for this methodology is given in Section 6.2. Colour differences in the sediment being scanned could not be controlled although there was not vast difference between the individual grains. The laser scanner was fixed to the x,y, table such as to increase stability and dampen the mechanical vibrations. The effect of the surface roughness would be expected to be at its greatest over the graded beds and has been highlighted earlier where it is shown that the x resolution ranged from 0.109mm at the centre of the beam to 0.120 mm at the edge of the beam; this difference was deemed so small and the effects of surface roughness upon scan accuracy could therefore be ignored.

3.4 Bed Materials

Five grades of sediment were employed using natural sand and gravel ranging from 1 to 16mm in diameter and of approximately sub-rounded shape. Near-uniform, unimodal and bimodal grain size distributions were used using a common median grain size (4.8mm). Two further grades were employed, a coarse distribution and a fine distribution to assess the impact of fines on the distribution. The uniform distribution was chosen to act as a benchmark distribution, with the D_{50} equal to 4.8mm. The compositions of the unimodal, fine and coarse distributions were established in accordance with Shvidchenko, Pender and Hoey (2001) and the bimodal in accordance Shvidchenko (2000); these flume-based grades were specifically selected: (i) to ascertain whether stress history results were affected by bed modality and end-fraction grain sizes, and; (ii) to provide inference on the underpinning bed mechanics responsible for any sub threshold changes in bed stability that should be further analysed using laser displacement data. A summary of the parameters for each distribution are shown in Table 3-1 and graphically in Figure 3-3. Sediments were sieved to obtain eight size fractions at standard $\frac{1}{2}$ phi size intervals and then recombined

into the desired composition. In order to be able to assess fractional composition and fractional mobility the D_{50} and D_{84} were painted with ultra violet paint in different colours to allow easy identification during later analysis.

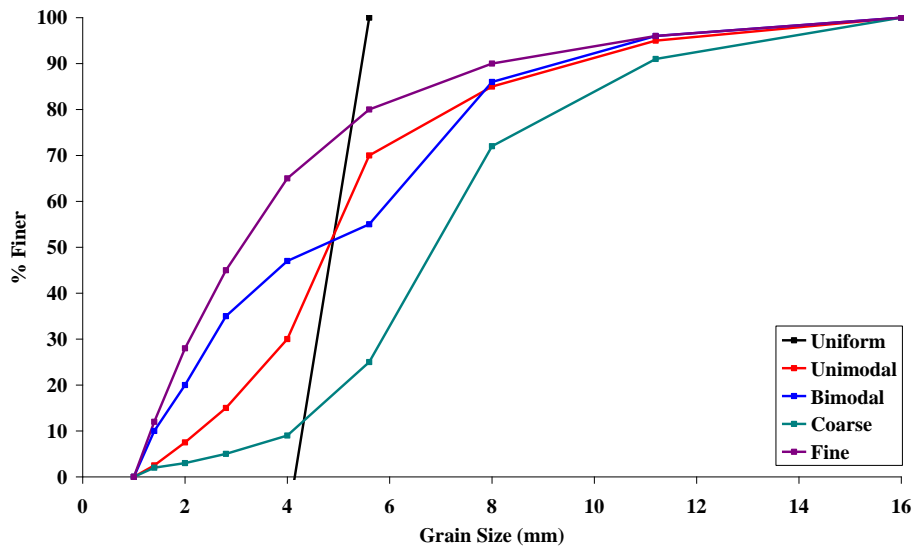


Figure 3-3; Graphical representation of the five grain size distributions employed.

		Near Uniform	Unimodal	Bimodal	Coarse	Fine
Grain Size (mm)	1 - 1.4	0	2.5	10	2	12
	1.4 - 2	0	5	10	1	16
	2 - 2.8	0	7.5	15	2	17
	2.8 - 4	0	15	12	4	20
	4 - 5.6	100	40	8	16	15
	5.6 - 8	0	15	31	47	10
	8 - 11.2	0	10	10	19	6
	11.2 - 16	0	5	4	9	6
	D_{50}	4.8	4.8	4.8	6.8	3.1
	σ_g	1.13	1.63	2.12	1.36	2.05
	Graphic skewness	0	-0.05	-0.25	-0.07	0.04

Table 3-1; Grain size distribution for the five test sediment grades. The D_{50} of each distribution is highlighted in green and the D_{84} in blue. The σ_g is calculated according to $\sigma_g = (D_{84}/D_{16})^{0.5}$ and graphic skewness according to $S = \frac{\phi_{84} + \phi_{16} - 2(\phi_{50})}{2(\phi_{84} - \phi_{16})} + \frac{\phi_{95} + \phi_5 - 2(\phi_{50})}{2(\phi_{95} - \phi_5)}$

3.5 Chapter Summary

This chapter has provided an overview of the basic infrastructure and instrumentation employed in this research, where many of the methods used are standard practice in flume investigations. More detailed methodology is provided in later Chapters (Chapter 4-6), as specific to the objectives analysed in each. However, there are three factors which are worthy of specific note. Firstly the use of 2 widths of flumes permits assessment of aspect ratios on stress history data sets which, in all past studies, only employed narrow 0.3m flumes. Given that the width depth ratio has been seen to be important in the development of both the turbulent structure of the fluid and the structure of the bed surface it is important that the effect of width depth ratio upon stress history be quantified (Chapter 5). Secondly the use of five grades of bed material permits the first assessment of granular mechanics underpinning stress history induced stability; research has previously only looked at one graded in singularity and hence there is no firm understanding of the comparative effects of grain size distribution on the effects of stress history (Chapters 4-6). Finally the high-resolution laser displacement methodology dramatically reduces the time for bed scanning (compared to past research) and is specific to the research employed during this thesis which was critical given that the main focus of the thesis relates to understanding sub threshold particle mechanics (Chapter 6).

Results are summarised in three chapters. Firstly Chapter 4 assesses the effects of stress history on bed stability in terms of the critical bed shear stress and the transported bedload in the 0.3m wide flume. Results are presented for five grain size distributions and for five short antecedent flow durations (0, 10, 20, 40 and 60 minutes). Chapter 5 also assesses the effects of stress history on bed stability in terms of the critical bed shear stress and the transported bedload however experiments are run in the 1.8m wide flume over lengthened antecedent flow durations (0, 60, 120, 240, 960 minutes). This allowed the effect of width ratio to be quantified as well as exploring the effect of longer antecedent durations. A truncated data set of the three comparable (based on equivalent D_{50}) distributions of sediment were used; near-uniform, weakly bimodal and unimodal. Chapter 6 presents the main findings from the laser scanner and form the main focus of the thesis. In Chapter 6 the focus is on providing a quantitative, mechanistic understanding of the processes responsible for bed stabilisation under sub threshold conditions. This will offer the first real insights into the relationship between stress history and the associated changes to bed

topography, particle repositioning and possible structure formation. data compares results from the 60 minute and 960 minute antecedent flow durations, i.e. the extremes of the time distribution in three grades; near-uniform, unimodal and bimodal.



Camera mounted to record still and video images of the test sediments

Glass plate used to still the water surface

Test section (coloured sediments)

Sediment trap

Figure 3-4 Experimental setup (Shields Flume) indicating the test section of sediments (coloured sections) the sediment trap in the foreground, the glass plate used to still the water surface during image capture and the camera used for video and still image capture.

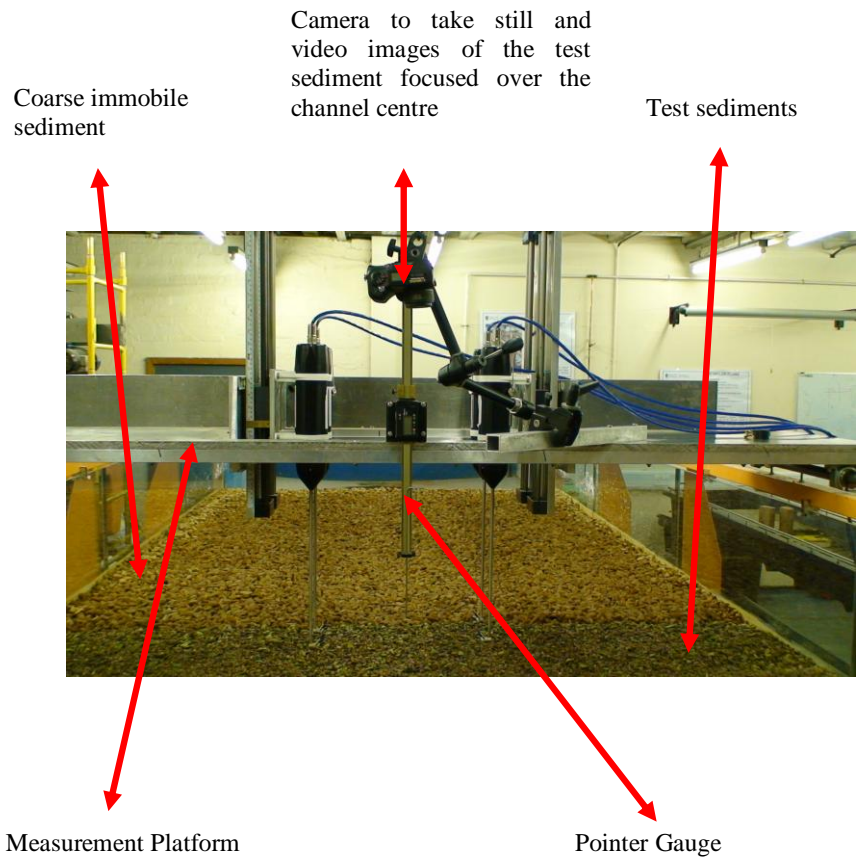


Figure 3-5: Instrument Rig (Kelvin Flume) detailing the video camera and pointer gauge situated over the channel centre line and the sediment set up.

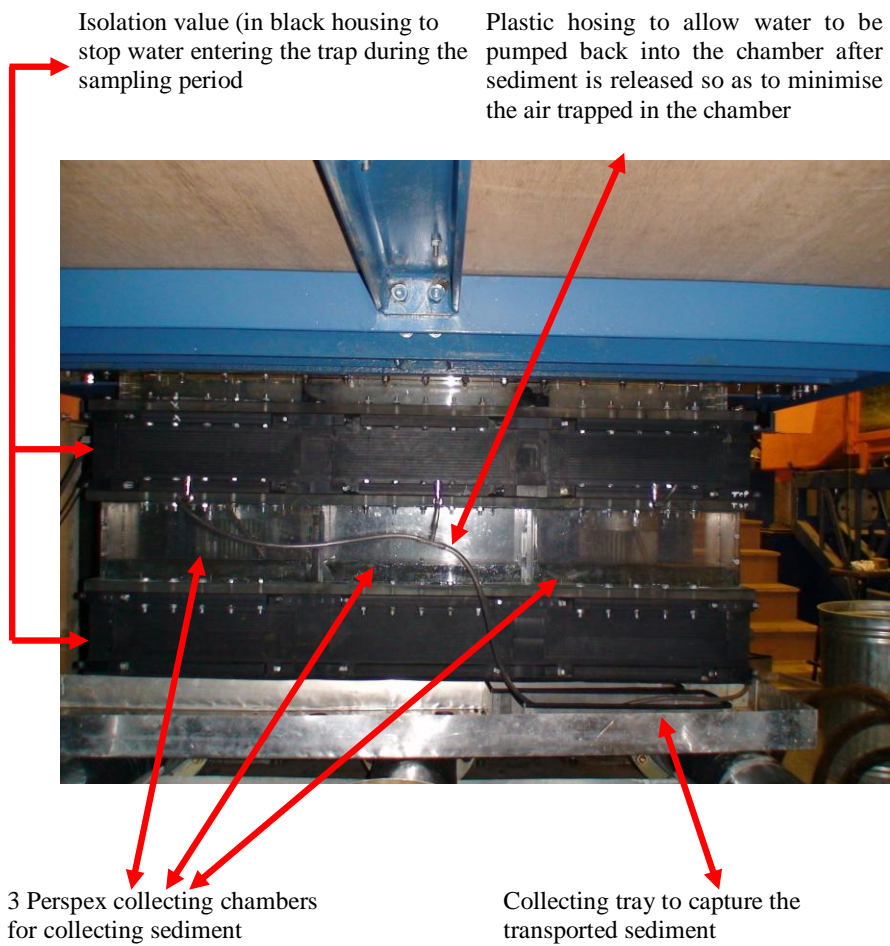


Figure 3-6; Sediment trap used for collecting sediment in the Kelvin Flume.

Chapter 4 Stress History Experiments in the 0.3m wide Flume

4.1 Introduction

The restricted data sets that are available for analysis indicate that the accurate determination of entrainment threshold requires a greater knowledge of the effect that various combinations of ‘stress’ (magnitude) and ‘history’ (temporality) have upon sediment stability. Crucially, no comprehensive analysis has been performed into how stress history response is influenced by sediment grade and this is fundamental if we are to apply experimental or theoretical data to real river systems. This chapter therefore aims to take a similar approach to previous flume-based stress history research to specifically assess the effects of grain size distribution on the relationship between stress history duration and entrainment threshold.

The results from 75 experiments use the five distributions of sediment described in Section 3.4 (Table 3-1 and Figure 3-3). Justification for use of these grades is as follows: three grain size distributions (near-uniform, weakly bimodal and log normal) with a common median grain size (D_{50}) were used to assess the effects of distribution; two additional grain size distributions with extended coarse and fine tails were used to determine the influence of the presence/absence of fines on bed stability. In addition, the D_{50} of the first three grades was akin to that employed in previous stress history research using a 0.3m wide flume by Haynes and Pender (2007); this permitted direct comparison of data in analysis. The temporal effects of stress history on bed stability were examined using a range of short antecedent flow durations (0, 10, 20, 40 and 60 minutes) for an applied antecedent shear stress equal to 50% of critical shear stress of entrainment (τ_c). Given that the purpose of data presented in Chapter 4 was to confirm the existence of grade influence on stress history, these short timeframes were selected to be commensurate with the range of durations employed in similar work by Paphitis and Collins (2005) and to include the two shortest durations assessed by Haynes and Pender (2007). Similar to this past research, this Chapter reviews critical shear stress of entrainment and bedload transport data as indicators of the relationship between stress history and bed stability; fractional bedload data are utilised to infer the processes of stability and possible influence of grade (as undertaken by Haynes and Pender, 2007).

4.2 Hypotheses

Primarily this chapter aims to address three main working hypotheses:

- Increasing the duration of antecedent flow will increase the structural resistance of the bed to entrainment by fluid flow
- Total transported sediment will be inversely related to the duration of the applied antecedent duration
- As any increased hydraulic resistance of the bed will be unique to the grain size distribution employed, it would be expected that graded beds would exhibit a greater potential response to stress history given their relative grain size effects. Using σ_g as an indicator, it would be expected that the response to stress history would be positively correlated with σ_g such that hierarchy of response would be bimodal > fine > unimodal > coarse > uniform ($\sigma_g = 2.12, 2.11, 2.05, 1.36, 1.13$ respectively)

4.3 Experimental Procedure

Using the experimental setup for the ‘Shields’ flume as detailed in Chapter 3, the following methodological procedure was followed:

- Bedding-in Period: An initial bedding-in period employed a flow depth of 10mm for 10 minutes duration; this was designed to remove any air pockets or unstable grains generated within the bed screeding process.
- Antecedent Period: Flow was then increased to apply a shear stress of magnitude 50% that of the critical threshold for entrainment of the median grain size for a bed where no stress history was applied (derived in section 4.3.1). This constituted the stress history phase over durations of 0, 10, 20, 40 and 60 minutes; runs with no antecedent flows were used as benchmark runs for stress history assessment.
- Stability Test: In order to ascertain the effect of the antecedent period on entrainment threshold, flow was further increased by a series of incremental short flow steps of constant discharge. Each step of the stability test was 5 minutes in duration to allow flow stabilisation and then visual assessment of whether or not the new threshold had been reached.

In order to increase the reliability of the dataset, experiments were repeated three times for runs without an antecedent period (benchmark runs) and twice for all runs including an antecedent period; sensitivity analysis is presented in section 4.4.1.

4.3.1 Definition of critical threshold (τ_c)

Paphitis and Collins (2005) describe the ‘threshold’ of sediment movement as the “specific point within the sequential process of transport where a small (arbitrary) amount of sediment grains are entrained or set in motion”. Typically the reference size of threshold for a graded bed has been assumed to be the median grains size (D_{50}) of that distribution (Proffitt and Sutherland, 1983) and consequently can be used to calculate the reference critical bed shear stress for the entrainment of particles from the bed. Whilst it is recognised that the use of the D_{50} as the representative grain size is controversial within the literature (e.g. Sambrook Smith *et al.*, 1997) it is common practise and was used in the only other two studies of stress history which are available (Paphitis and Collins, 2005; Haynes and Pender, 2007), thus allowing direct comparison of results. Additionally given that the uniform, unimodal and bimodal beds all have the same D_{50} (section 3.4) it allows direct comparison of the effects stress history has upon the three different beds.

The boundary or bed shear stress (τ_0) can be defined as the force applied tangentially to the sediment surface (Bauer *et al.*, 1992) and is commonly used in sediment entrainment and transport studies in terms of critical shear stress (τ_c) being used to compare entrainment threshold data. Traditionally bed shear stress is difficult to derive (Wilcock, 1996) and can either be measured directly or inferred indirectly; this thesis employs an indirect method of derivation using the relationship with depth and slope. The depth slope product uses the energy slope and the hydraulic radius, or water depth, to compute an average shear stress from the section of channel studied; this is a common technique in river sediment studies, in particular where it is inappropriate or unfeasible to obtain velocity profiles that are spatially restricted, time-consuming and require expensive instrumentation (e.g. Powell and Ashworth, 1995; Hassan and Churuch, 2000, Measures and Tait, 2008). Monteith and Pender, (2005) and Haynes and Pender, (2007), have already set precedent by using the depth-slope methodology in stress history research; thus this thesis uses the same method for comparability of data. Bed shear stress, using this methodology was calculated for all five antecedent time periods and for all five grain size distributions according to Equation 13;

$$\tau_{c50} = \rho g R_b S_0 \quad (\text{Equation 13})$$

where, S_0 is the channel slope (0.005) and R_b is the hydraulic radius, corrected for the sidewall effects of the flume using Equation 14 and Equation 15 through the application of the Manning's formula to each part of the fluid area, derived according to the following:

$$R_b = R \left(\frac{n_g}{n} \right)^{\frac{3}{2}} \quad (\text{Equation 14})$$

$$n = \frac{\left[P_b (n_g)^{\frac{3}{2}} + P_w (n_w)^{\frac{3}{2}} \right]^{\frac{2}{3}}}{P^{\frac{2}{3}}} \quad (\text{Equation 15})$$

Where (n_g) is the grain roughness calculated according to the Strickler formula where $n_g = 0.048D^{\frac{1}{6}}$ using median grain size as D (Carson and Griffiths, 1987), (n_w) is the roughness of the glass surface assumed to be 0.01 (Chow, 1959), P_b is the wetted perimeter of the bed (equal to that of the flow width b), whilst P_w is the wetted perimeter of the walls (given as twice the flow depth z_0). The total wetted perimeter is given by $P = P_b + P_w$. In this way, the cross-section of fluid flow is divided into a bed area and wall area that exhibit the same energy gradient and mean velocity yet account for different frictional effects.

In line with previous stress history studies (Paphitis and Collins, 2005; Monteith and Pender, 2005; Haynes and Pender, 2007), for the purpose of research within this Chapter the critical shear stress of entrainment was established using a quantitative visual technique presented in Equations 7 & 8 (Section 2.2.1). The area of observation (A) was set as 0.04m^2 and located 11m downstream from the inlet and was located over the channel centreline in order to minimize the effects of the side walls. The time of observation (t) was set to 180 seconds, both to minimise the flow step duration of the stability test (and thus minimise additional stress history effects) and to be commensurate with Haynes and Pender (2007) who used similar beds and methodology.

4.4 Results

4.4.1 Uncertainty analysis

The aim of section 4.4 is to analyse the effects of stress history upon entrainment threshold, concentrating on quantifying the revised critical entrainment threshold of the D_{50} due to the stress history duration. Before an analysis of the critical entrainment threshold can be undertaken, it is important to undertake an uncertainty analysis associated with the chosen method of derivation. This is especially true since previous studies have indicated variability in the frequency of granular dislodgement over 0.04 units of the ordinate of the Shields curve (Figure 2-2; Graf and Pazis, 1977; Van Rjin, 1989). This variability has been linked to both the error associated with the experimental methodology as well as the variability in the nature of the system being measured (e.g. Wilcock, 1988; Buffington and Montgomery, 1997). In the context of this research error in the experimental methodology can be primarily linked to two main factors. Firstly, inaccurate screeding may lead to the development of bed surfaces in which the bed surface distribution varies between the different experiments and, secondly, the derivation of threshold according to the Yalin Criterion can be subjective as described in section 2.2.1. Consequently, this section provides data to specifically analyse the impact of both factors upon the reliability of the data set.

Screeding can have an effect of the bed surface by introducing bias (Cooper and Tait, 2008) such that although the surface of the volumetric grain size distribution may be similar, the statistical distribution of bed elevations is different. This potential bias was reduced as much as possible by using one operator only to screed the beds for all experiments as well as taking photographs of the bed surface after the initial screed. To quantify the effects of screeding two methods have previously been used within the literature; destructive sampling (e.g. wax sampling (Haynes and Pender, 2007)) or image thresholding to delimit the grain boundaries and attain a surface grain size distribution (e.g. McEwan *et al.*, 2000). The former was unsuitable in the present thesis as it would destroy the surface of the bed (i.e. the focus of this research); the latter was too time consuming given the nature of the analysis that would be required to produce reliable results. Thus, the effects of screeding were analysed using bed surface photographs taken after the initial screed; the D_{50} and D_{84} grains were coloured on the bed surface and could thus be counted and the ratio of $D_{50}:D_{84}$ used as an indication of the distribution of the bed surface. Comparison is therefore made between both the bulk mix (Table 3-1) and the surfaces of

the individual beds following screeding. Where a similar $D_{50}:D_{84}$ is noted, screeding is shown to have a negligible effect and beds are a faithful representation of the target bulk distribution.

		Bulk Mix	0 Minutes	10 Minutes	20 Minutes	40 Minutes	60 Minutes
Unimodal	$D_{50}: D_{84}$	2.67	2.63	2.67	2.71	2.65	2.69
Bimodal	$D_{50}: D_{84}$	0.26	0.26	0.24	0.26	0.27	0.28
Coarse	$D_{50}: D_{84}$	2.47	2.43	2.49	2.47	2.49	2.5
Fine	$D_{50}: D_{84}$	1.70	1.68	1.72	1.74	1.71	1.71

Table 4-1; Comparison between the $D_{50}:D_{84}$ ratios of the bulk mix in comparison to the screeded bed surfaces. The $D_{50}:D_{84}$ ratio from the surface is calculated according to the number of individual D_{50} and D_{84} grains counted on the bed surface photographs over a 200x 200mm area.

Results from Table 4-1 show that all four graded grain size distributions are a good representations of the bulk mix. Typically results taken from the surface photographs have higher $D_{50}:D_{84}$ than those of the bulk mix; this supports the theory that screeding causes a coarser bed surface (e.g. Copper and Tait, 2008) and is logical given that pore spaces can be exploited by the finest of fractions such that some may be sieved away from the surface. The magnitudes of these differences are small, where the maximum difference noted between the bulk mix and the screeded bed surface calculated as 1.49%, 2.10%, 1.61% and 2.35% for the unimodal, bimodal, coarse and fine beds respectively. Repeatability between beds of the same grade is also acceptable at 3.04%, 3.96%, 2.88% and 3.97% respectively. Screeding therefore has a negligible measureable effect on the surface. Importantly, this gives confidence that any differences in bed composition stem solely from the active processes pertaining to the experiment itself, rather than different starting conditions.

Secondly the use of the Yalin Criterion as a measure of threshold has been described as being subjective. To minimise this, data was collected using a single operator and comparison of multiple repeats of runs was undertaken (Section 4.3). Threshold counts were performed during each step of the stability test and Figure 4-1 demonstrates variability of count between 0% to 46% when compared to the average. Reviewing this in more detail, two main findings are apparent from Figure 4-1. Firstly, intra-grade repeatability was similar, independent of the antecedent duration applied. Secondly, inter-

grade comparison of count variability indicates that beds with a higher number of detachments needed in order to satisfy threshold conditions had a higher variability in threshold count. Specifically, the greatest variability in threshold count (up to 46% of the average value; equivalent to 22 grain movements) is associated with the fine distribution which requires 47 grains to satisfy threshold; conversely, the least variability is seen in the bimodal distribution (up to only 13% of the average value; equivalent to only 1 movement) which requires only 7 grains to satisfy threshold. In explanation an argument similar to that presented by Paintal (1971) is proffered. His study noted that sediment entrainment occurred even when low values of shear stress theoretically below that required to entrain the grain. This supports the concept of Miller *et al.*, (1977) who noted that rather than the discrete value of entrainment as proposed by Shields (1936) an envelope of threshold values exists. Paintal (1971) described movements at the lowest shear stresses as being ‘random’ in space and time and there did not seem to be a limit below which there was no movement. Consequently, in the context of this research it is possible that the critical entrainment threshold could be underestimated since the number of movements required to satisfy the threshold criterion would be reached but because of random particle displacements rather than the attainment of threshold conditions. It is postulated that this effect would be exacerbated where there are a larger number of grains which are needed to satisfy the threshold criterion since there is an increased likelihood of these ‘random’ movements being recorded; this has the propensity to register greater variability in the results.

Whilst at first glance the count variability (up to 46%) appears statistically significant, it is important to note that the present thesis considers entrainment threshold as the critical shear stress. As such, threshold count variability translates as only 0% to 3% variability in terms of average critical shear stress; this is in line with experimental data errors of similar laboratory studies (e.g. Paphitis and Collins, 2005) and suggests that methodology appropriate to the aim of the thesis was employed.

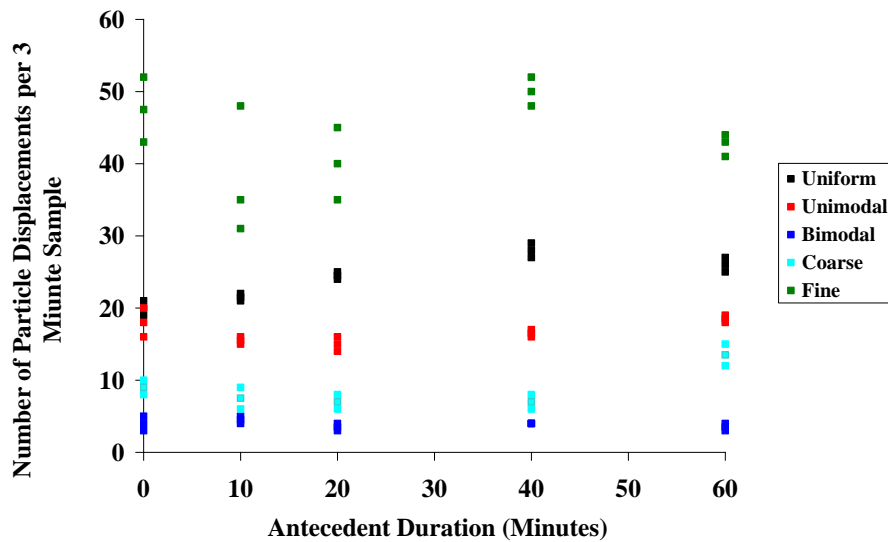


Figure 4-1: Variability in the raw threshold counts for all five grain size distributions over five antecedent durations.

A second component of sensitivity analysis reviewed the threshold count data sets either side of threshold (Figure 4-2). The gradient of the straight line fitted between these data indicates the transition between bed stability (sub threshold) and instability (above threshold); the steeper the line, the more rapid the transition between stability and instability. From Figure 4-2 it is evident that as antecedent duration is increased, the transition between stability and instability is described by steeper line gradients and thus becomes more pronounced. As this transition is more marked, it acts to reduce the uncertainty associated with the derivation of critical entrainment threshold. Only the 10 minute data appears as an outlier from this overall trend; in explanation, it may be that the proximity of the above threshold movement (n) value of these data is so close to the threshold (as compared to the four other antecedent durations) that the trend appears falsely skewed. In summary, the stability transition data show that beds subjected to longer durations of sub threshold flow are subject to a more sudden breakdown of surface structure at threshold, releasing a large number of median sized grains (commensurate with the sharp rise in particle counts on Figure 4-2). Conversely, when the bed is subjected to shorter antecedent durations, the transition between stability and instability is more gradual and seems to suggest that it is the occasional movement of discrete grains from the loosely packed surface. Whilst this type of sensitivity analysis of threshold is not new, the

relationship to stress history is of interest in aiding our understanding of the bed mechanics causing stress history induced stability.

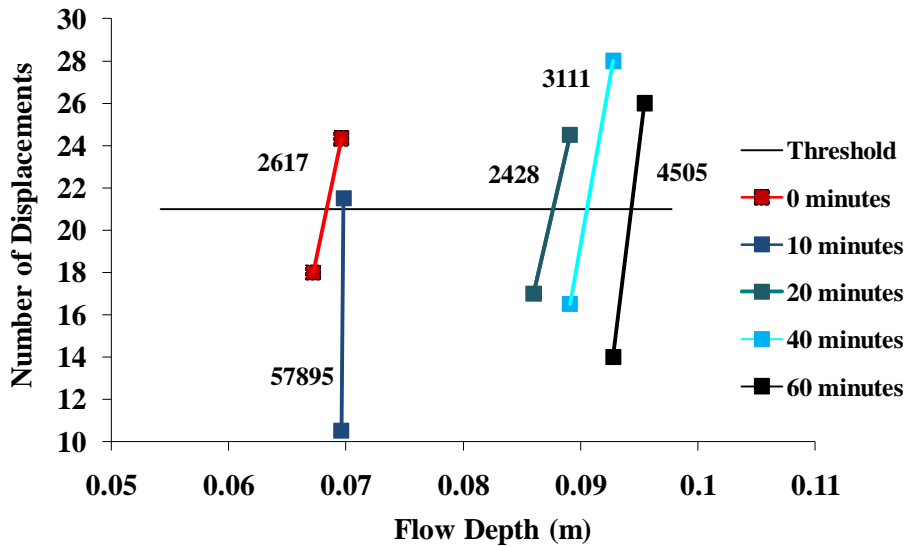


Figure 4-2: Relationship for displacements recorded close to threshold (uniform bed). An increasingly steep gradient is noted as antecedent duration is increased with the exception of the 10 minutes date; the gradient is noted next to each line. The numbers of on the graph represent the gradient of the line for the individual experimental runs.

Thus the sensitivity analysis undertaken for each sediment grade reveals three inferences;

- The screeding technique is consistent and produces beds which are similar both to the bulk mix as well as to each other at the beginning of each experiment such that any differences noted at the end of the experiment are as the result of the applied antecedent period and not different initial starting conditions.
- The Yalin Criterion was deemed to accurately determine the threshold of motion since the variability in terms of average critical shear stress was only 0% to 3%.
- A more rapid transition between stability and instability is noted in bed subjected to the longest antecedent durations; this suggests that these beds undergo more catastrophic failure at threshold.

4.4.2 Critical entrainment threshold

Analysis in this section concentrates on describing the relationship between critical entrainment threshold and antecedent duration, summarised by Figure 4-3. For ease of

analysis, section 4.4.2 provides detailed results on the following: (i) absolute critical shear stress trends with respect to grain size distribution; (ii) general stress history trend analysis; (iii) relative stress history responses of different grain size distributions.

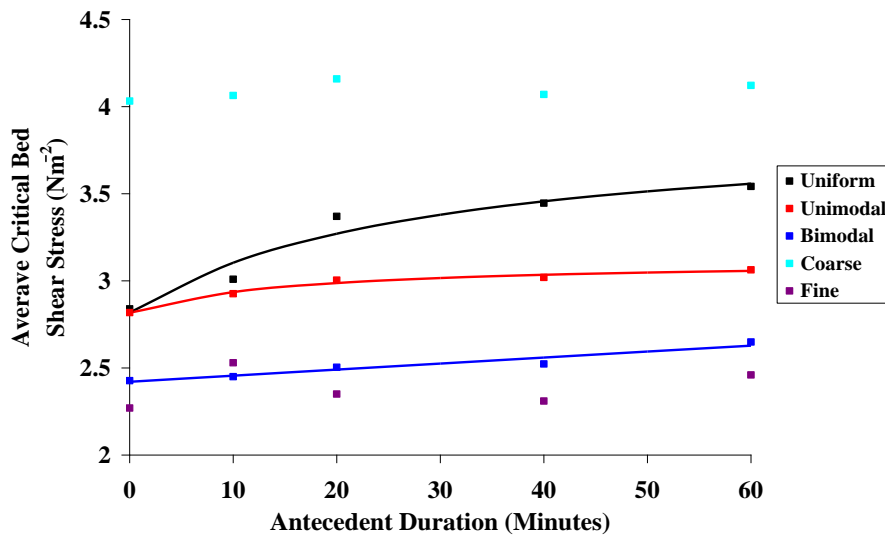


Figure 4-3; The relationship between antecedent duration, average critical bed shear stress and grain size distribution. The uniform, unimodal and bimodal beds are fitted with a linear polynomial growth curve with root mean square errors values of 0.09, 0.01 and 0.03 for the uniform, unimodal and bimodal beds respectively.

Absolute critical shear stress values for all five grain size distributions under benchmark conditions (i.e. no antecedent period) clearly show a hierarchy to stability (Figure 4-3). The coarse distribution requires the highest critical shear stress (4.03Nm^{-2}) and is most able to resist entrainment. Conversely, the fine bed has the lowest entrainment threshold (2.27Nm^{-2}) and is the least stable under an applied flow (Figure 4-3). These results are expected due to the submerged weight of the particles employed in the distributions; i.e. the coarser bed ($D_{50} = 7.2\text{mm}$) comprises particles of greater submerged weight which increases grain resistance to entrainment, whilst the lighter grains of the finer bed ($D_{50} = 3.1\text{mm}$) are inherently more mobile. More interestingly, comparison between the other three beds of identical D_{50} (Figure 4-3) show that whilst near-uniform and unimodal beds offer similar critical thresholds under benchmark conditions (2.84 and 2.82Nm^{-2} respectively), the bimodal threshold is 14% lower (2.43Nm^{-2}). This implies that the bimodal bed is therefore, more susceptible to entrainment. In explanation, data presented highlight that absolute critical shear stress of entrainment values may conceivably be

linked to the relative percentage of the D_{50} in the bulk mix or the tightness of the distribution around the D_{50} value. Specifically, the D_{50} comprises just 8% of the bimodal bed with σ_g values of 2.12 as compared to 40% D_{50} in the unimodal bed of $\sigma_g = 1.63$ and 100% D_{50} of the near-uniform bed of $\sigma_g = 1.13$. Given this finding, it appears appropriate that this study is focussed on the influence of grade and continues to consider the influence of modality.

Stress history analysis reviews the general relationship between threshold and antecedence as shown on Figure 4-3 where two findings are evident. Firstly, the coarse and fine distributions show a variable response to antecedent duration; no discerning stability trend is observed. Secondly, beds of comparative D_{50} (near-uniform, unimodal and bimodal) typically indicate a distinct positive correlation between applied antecedent duration and average critical bed shear stress. For these beds, a linear polynomial growth curve best describes the data;

$$\tau_c = \left(\frac{p_1 t + p_2}{t + q_1} \right) \quad \text{(Equation 16)}$$

where τ_c represents the critical shear stress, antecedent duration represents time and p_1 , p_2 and q_1 are coefficients. This growth form represents the initial rapid increase in bed stability and is followed by a more gradual increase in response to the imposed flow regime. This is confirmed by the first derivative of the regression curve, derived according to Equation 17 and plotted on Figure 4-4;

$$\frac{d\tau_c}{dt} = \frac{p_1(t + q_1) - (p_1 t + p_2)}{(t + q_1)^2} \quad \text{(Equation 17)}$$

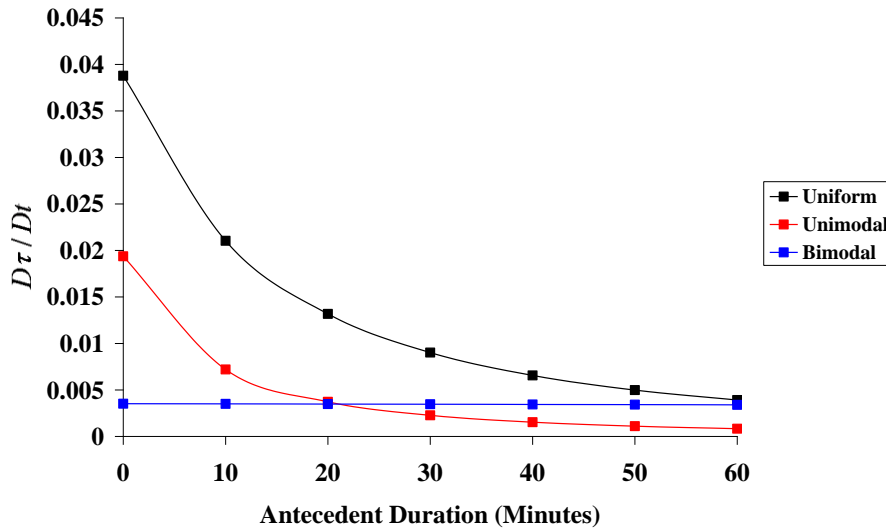


Figure 4-4: First derivative of the fitted trend lines of the response of the uniform, unimodal and bimodal grain size distributions respectively to antecedent flow duration.

It is evident from Figure 4-4 that both the uniform and unimodal curves exhibit a greater rate of change to average critical bed shear stress for the shortest applied antecedent durations. That both data sets tend towards an asymptote at infinity suggests that data may approximate to stability maxima for very long antecedent durations (in excess of the 60 minutes tested); this supports previous data by Paphitis and Collins (2005) and Haynes and Pender (2007). Wider review of Figure 4-3 may also support this interpretation in that the coarse fraction may have reached a stability maximum after 20 minutes antecedent duration; however these data are within the bounds of experimental error and discernable trends are difficult for this data set. Yet, it is important to note that Figure 4-4 does not show as strong a polynomial relationship in the bimodal bed as that of the uniform or unimodal beds of equivalent D_{50} ; instead, the more linear response of this data set suggests that the processes underpinning stability gains for bimodal beds are more progressive.

The effect of grain size distribution on bed responsiveness to stress history shows the following hierarchy to 60 minute stress history responsiveness as compared to benchmark experiments: near uniform (+25%) > bimodal (+9%) > unimodal (+8%) > fine distribution (+8%) > coarse distribution (+2%). Whilst benchmark runs indicate that the threshold

shear stress of uniform sediment is only 0.7% higher than that of unimodal beds, following an antecedent duration of 60 minutes this difference increases to 14%. Similarly, compared to bimodal beds of equivalent D_{50} and subjected to 60 minutes antecedence, the critical shear stress for the uniform bed is 25% greater than for the bimodal bed. It is interesting to note that, whilst the type of modality (uni- or bi-) affects absolute values of critical threshold, it has very little effect on the relative degree of stabilisation attained during the antecedent period (+8 to +9%); with reference to Table 3-1 this may be due to the similar proportions of fractions comprising the fine and coarse ends of the grain size distributions, hence similar relative grain size effects and hiding may occur during the antecedent period.

In contrast to the obvious responsiveness of the three beds described above, the two grades employed to qualify the stress history effect on fine and coarse dominated distributions indicate more variable relationships between antecedent duration and critical threshold. Specifically, the fine distribution illustrates a similar magnitude of stability gain as the unimodal and bimodal beds (~ +9%). From Table 3-1 it is evident that the fine and bimodal beds have a similar and significant proportion of fine material that appears likely to explain the similarity in their response to stress history. Data indicate that the increase in average critical bed shear stress of the fine distribution was up to 3.5 times more responsive to stress history than the coarse distribution. This suggests that the fine fraction of a graded bed is overall more reactive to antecedent flow than the coarser fractions and is a logical suggestion given their lower submerged weight and potential ability to respond to the sub-threshold shear stress imparted (as based on the D_{50}). In addition, the finer grains can also infiltrate into the pore spaces of the bed and hence become unavailable for transport. As such it is their size as well as their mobility which appears an important controlling factor (Ferguson *et al.*, 1989; Wilcock and Crowe, 2003).

Thus results derived at the point of critical entrainment threshold for each sediment grade reveal three clear inferences.

- Increasing the duration of antecedent flow increases the threshold of entrainment for all five grain size distributions. The magnitude of these responses (2% to 25%) is however significantly lower than the 56% increase in critical entrainment threshold determined by Paphitis and Collins (2005) for the same 60 minute period of applied flow.

-
- Following applied stress history, the response of average critical shear stress associated with the uniform beds is at least twice that of the graded beds.
 - The influence of modality is shown to be significant with respect to absolute threshold values where critical bed shear stress is higher for tighter distributions (i.e. the unimodal bed) of equivalent D_{50} .
 - The effect of stress history appears independent of modality for beds of equivalent D_{50} with bimodal beds more responsive than unimodal beds.
 - Data indicate that the fine fractions in a graded bed are more responsive to antecedent flow than the coarser fractions; this is explained in terms of their lower submerged weight and potential ability to infiltrate into the pore spaces.

4.4.3 Total Transported Bedload

Previous stress history analysis has used total transported load and an indicator of bed stability (Haynes and Pender, 2007) with the underpinning theory that an inverse correlation should exist between the two variables, that is, a more stable antecedent bed will be associated with lower subsequent bedload transport (Monteith and Pender, 2005). As such, trends of the magnitude of the total bedload transported during the stability test were evaluated for the four graded beds to provide proxy data on bed stability response to antecedent flow durations. Care must however be taken in interpretation of these results because of the different durations of the stability test (60 minutes through to 170 minutes, depending on grade; Appendix A Table 2) and the change in this duration due to stress history per individual grade (10 to 25 minutes; Appendix A Table2). Given the different durations of the stability tests, there is the potential for more transport if the stability test is longer and it is expected that different grades will demonstrate different fractional stabilities in response to stress history, such that there is the potential for finer fractions to be more mobile in higher flow steps. If bedload data indicates a relationship to these variables then inter-grade comparison of stress history effects on bedload is compromised however the presented bedload data (Fig 4-5 y-axis) does not show any relationship to the stability test duration applied.

In addition, since the stability test only collects the pre-threshold bedload (because the stability test is stopped once threshold is reached) total bedload transport rates are small and would be expected to be dominated by the fractions $<D_{50}$ in size if selective entrainment is the dominant process. Grades are therefore treated as comparable in terms

of the following definition ‘the total bedload transported in the stability prior to and including threshold, but not beyond’. As such, this section focuses on trend and statistical analysis of the bedload data sets with the structure of data analysis being: (i) total bedload transport trends with respect to grain size distribution; (ii) stress history regression analysis; (iii) bedload composition analysis, specific to detailed fractional analysis and comparison to the initial bulk mix.

Stress history effects on total bed transport are given in Figure 4-5. This illustrates an inverse relationship between bedload transport and stress history showing that beds subject to prolonged periods of antecedent flow are increasingly resistant to entrainment manifested through lower sediment transport rates. This is in agreement with previous stress history research (Monteith and Pender, 2005; Haynes and Pender, 2007). Extending the antecedent period from 0 to 60 minutes resulted in the total bedload transported reducing by the following grade-specific hierarchy: bimodal (-94%) > unimodal (-90%) > fine (-70%) > coarse (-59%). Here it appears important to note that modality defined beds (unimodal and bimodal) behave similarly, whilst end-fraction defined beds (fine and coarse) give significantly reduced responses. Observations during the stability test noted the progressive development of low-relief, low-resistance troughs within the beds most reactive to stress history (i.e. unimodal and bimodal). The troughs appeared to stabilise the coarse fractions as ridges and preferentially route finer material through the troughs. This suggests that these two beds stabilise by some degree of size selective sorting and that this stabilisation process occurs more rapidly in response to an applied sub-threshold flow than the stabilisation processes occurring in the other two grain size distributions tested. This notion and its implications are examined further within the discussion (Section 4.5).

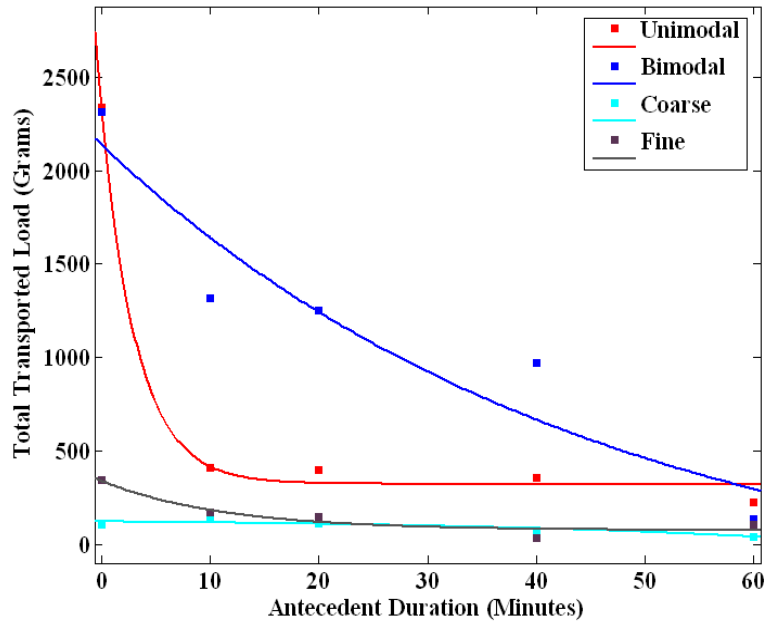


Figure 4-5; Stress history relationships with total bedload fitted with an exponential decay function superimposed in a background constant noting R^2 values of 0.99, 0.90, 0.82, 0.92 for the unimodal, bimodal, coarse and fine respectively.

Regression analysis for all grades is shown in Figure 4-5. This demonstrates that the relationship between antecedent duration and total bedload transport can be defined by an exponential function superimposed on a background constant transport fitting a relationship of form;

$$\sum G_b = A \exp(-bt) + K \quad (\text{Equation 18})$$

where $\sum G_b$ is the sum of bedload transport, t is antecedent duration and A , $-b$ and K are coefficients. This type of relationship yields strong R^2 values 0.82 to 0.99 and therefore is preferred over the power-law form of Haynes and Pender (2007) which yielded weaker R^2 values for a first order polynomial fit of only 0.3 to 0.8.

Grade-dependency of stress history response (as defined by total bedload) can therefore be examined using the first derivative of the regression curve (Figure 4-9). From this it is evident that the rate of bedload reduction is greatest during the early part (0-10mins) of the applied antecedent period. This trend is far more pronounced for the unimodal bed than the

other grades (Figure 4-6) and as such is plotted separately; such a finding appears to support earlier results from threshold data on unimodal beds given in Section 4.4.2. This suggests that, although a continual decrease in the rate of sediment transport with increased antecedency of flow is likely to be noted for unimodal beds, very little additional stability is likely to be afforded by extended sub-threshold flow durations. This implies a very rapid generation of a stable unimodal bed configuration in response to applied antecedent flow durations; this is akin to the entrainment analysis in section 4.4.2.

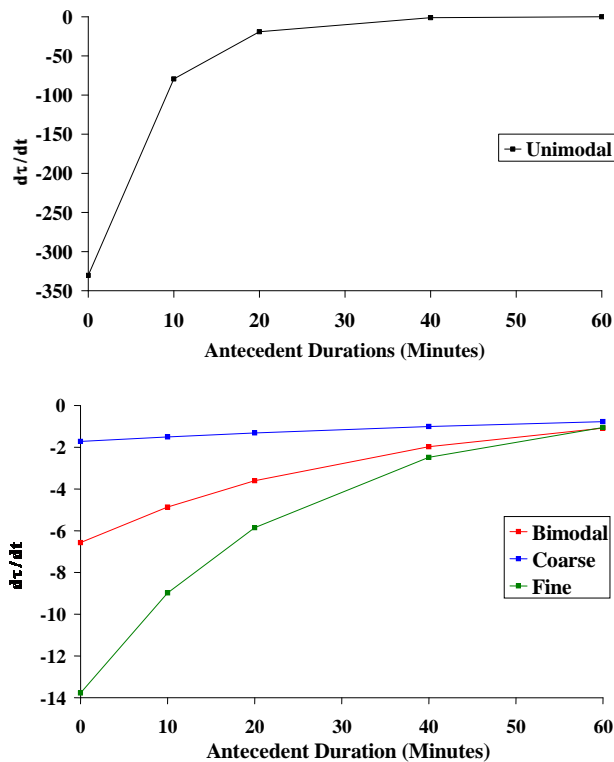


Figure 4-6; First derivative of the fitted trend lines of the response of the unimodal, bimodal, coarse and fine grain size distributions respectively to antecedent total transported bedload. Given the different magnitude of response of the unimodal bed it has been plotted separately.

Although total transported load analysis yields information regarding the stability of the bed induced by antecedent flows, it does not give information regarding which fractions of the bed are most influenced by this antecedent flow period. Thus, the following analysis concentrates on the temporal development of the grain size distribution of the transported bedload. This allows an assessment of the development of the transported load as

compared to the parent population, identifying temporal differences and making inferences about the processes underpinning stabilisation.

Bedload composition analysis is therefore performed using two distinct techniques. Firstly, the change in geometric standard deviation (σ_g) of the bedload following each antecedent duration is analysed; this acts as a proxy indicator of the degree of selective entrainment caused by stress history in a manner similar to White and Day (1982), Pender and Li (1995) and Patel and Ranga Raju (1999). Secondly, raw bedload data is subsequently provided for each fraction and corrected for relative abundance with respect to the bulk mix; this more detailed data set specifically reviews the response of the D_{50} as an indicator of graded bed response before assessing the role of individual fractions in generating bed stability under antecedent conditions.

Figure 4-7 plots average critical bed shear stress against geometric standard deviation (σ_g) for the four graded grain size distributions. This seeks to demonstrate two things: (i) the relative effect of σ_g on average critical bed shear stress; and (ii) the evolution of σ_g with increasing antecedent flow duration. Three key findings stem from this analysis. Firstly, an inverse relationship is noted between σ_g and critical bed shear stress that approximates to an exponential decline. This indicates that as the resistance of beds to entrainment increases, there is a narrower range of particle sizes in transport purporting to enhanced size selectivity. However, given the nature of the exponential decline these data suggest that there is a stronger relationship at higher critical shear stresses and lower σ_g values. The regression analysis in Figure 4-7 appears to be dependent on antecedent duration where the gradient of the line is -0.97 without flow antecedency and -0.88 with 60 minutes antecedency. Thirdly, there is a general inverse relationship between σ_g and antecedent duration in the unimodal, bimodal and coarse beds; this directly supports to the first finding relating σ_g to threshold bed shear stress. Specifically for the unimodal, bimodal and coarse beds σ_g decreases by -16%, -21% and -29% respectively after 60 minutes antecedent duration as compared to the original bulk mix; this indicates that stress history reduces the particle size range in transport such as to suggest enhanced size selectivity. However, whilst the fine bed demonstrates significant data scatter there is some

evidence that a converse response is found with up to a 12.8% increase in σ_g as antecedent duration increases.

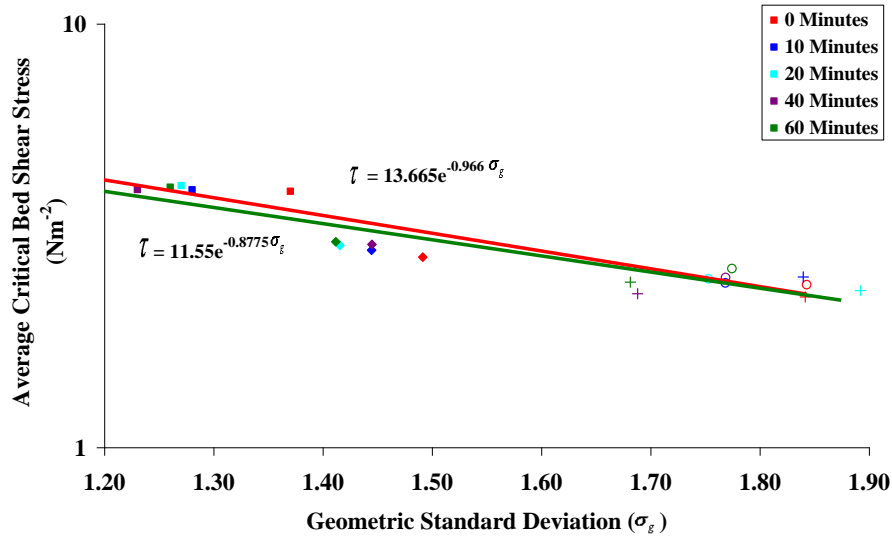


Figure 4-7: Critical bed shear stress plotted as a function of geometric standard deviation; the unimodal σ_g is depicted by diamond shaped markers and ranges from 1.41 to **1.49**, the bimodal σ_g is depicted by crossed shaped markers and ranges from 1.77 to **1.84**, the fine σ_g is depicted by open circle markers and ranges from 1.68 to 1.84, and the coarse σ_g is depicted by square shaped markers and ranges from 1.23 to **1.37** (bold denotes the original σ_g for 0 minutes antecedent flow). The red regression line relates to data collected with 0 minutes of applied antecedent flow whilst the green trend line relates to data collected after 60 minutes antecedent flow.

The general reduction in the spread around the mean indicates that there are relatively fewer grains present within the transported bedload from the extremes of the distribution i.e. fewer smaller and larger grains. This implies that these fractions are less available for transport after longer periods of antecedent flow. Two mechanisms may be used to explain this; firstly the development of structures on the bed surface such that larger grains act as stable keystones around which smaller grains are sheltered or, secondly the infiltration of finer grains vertically into the bed matrix such that they are unavailable for transport as bedload. It is likely that both processes are occurring but the relative importance of each is unknown. However, it is essential to remember that σ_g analysis looks only at relative grain sizes, rather than absolute. As such the analysis above can only suggest greater or lesser size selectivity of bedload. What is not known is whether there has been a change in the

mean (D_{50}) value of the bedload composition which would indicate whether the distribution has significantly fined or coarsened due to stress history effects; it is this more detailed fractional analysis which is critical to understanding which grain sizes are influential in stabilising the bed during antecedent flow.

Detailed fractional analysis of the change in individual fractions of the total bedload transported in the stability test are provided in Table 4-2 through Table 4-5 (with cumulative frequency distribution graphs shown in Appendix B). D_{16} and D_{84} data were used in calculation of geometric standard deviation values presented earlier in this section. D_5 and D_{95} data provide an indication of end member response of the grain size distribution. Initial analysis reviews the effect of stress history on the D_{50} fraction to ascertain whether the bedload fines or coarsens in response to stress history. This provides complementary information to the σ_g analysis. Specifically, this section analyses the percentage change between: (i) the bulk mix and bedload subsequent to 60 minutes of applied antecedent flow and, (ii) 0 and 60 minutes antecedency data sets; the former is more commonplace in past literature as most flume experiments only have bulk mix composition available as a benchmark, whilst the latter provides more specific analysis of stress history effects on water-worked beds. As a point of note, although the stability test is terminated at the attainment of threshold for the D_{50} , it is identified that grains coarser than this fraction appear to be mobile on the bed surface. This is either due to equal mobility conditions or a one off instability caused by turbulent fluctuations in the overlying fluid flow. The transport of these grains, even in low proportions, is notable due to the analysis of bedload by weight. The movement of one of two of these coarser grains may skew the overall observed pattern of transport due to the greater overall weight compared to smaller grains.

Parameter	Bulk Mix	0	10	20	40	60	% difference between bulk mix and 60 minutes	% difference between 0 and 60 minutes
D₅	1.68	1.70	1.80	1.98	1.70	1.72	1.95	1.16
D₁₆	2.89	2.38	2.33	2.42	2.31	2.22	-30.12	-7.21
D₅₀	4.76	3.58	3.33	3.38	3.33	3.22	-47.73	-11.18
D₈₄	7.82	5.30	4.86	4.85	4.82	4.43	-76.36	-19.64
D₉₅	11.31	7.77	6.85	6.62	7.00	6.31	-79.43	-23.14

Table 4-2; Evolution of grain parameters with increasing antecedent duration for the unimodal bed; D₅₀ highlighted for ease of analysis.

Parameter	Bulk Mix	0	10	20	40	60	% difference between bulk mix and 60 minutes	% difference between 0 and 60 minutes
D₅	1.19	1.65	1.25	1.20	1.21	1.18	-1.13	-39.83
D₁₆	1.74	2.12	1.60	1.52	1.52	1.50	-16.21	-41.33
D₅₀	4.72	3.44	2.98	2.37	2.37	2.29	-98.64	-50.22
D₈₄	7.82	7.19	5.01	4.68	4.77	4.72	-65.87	-52.33
D₉₅	10.93	9.74	5.58	5.45	5.57	5.55	-96.85	-75.50

Table 4-3; Evolution of grain parameters with increasing antecedent duration for the bimodal bed; D₅₀ highlighted for ease of analysis.

Parameter	Bulk Mix	0	10	20	40	60	% difference between bulk mix and 60 minutes	% difference between 0 and 60 minutes
D ₅	2.71	3.13	4.78	3.00	2.94	3.37	19.69	7.76
D ₁₆	4.26	4.03	5.81	3.98	3.60	4.24	-0.45	5.21
D ₅₀	6.38	4.83	6.73	4.95	4.65	5.58	-14.24	15.53
D ₈₄	8.91	6.09	7.79	6.61	5.58	7.13	-24.97	17.08
D ₉₅	13.11	7.35	9.46	7.54	7.04	7.72	-69.82	5.03

Table 4-4; Evolution of grain parameters with increasing antecedent duration for the coarse bed; D₅₀ highlighted for ease of analysis.

Parameter	Bulk Mix	0	10	20	40	60	% difference between bulk mix and 60 minutes	% difference between 0 and 60 minutes
D ₅	1.44	1.14	1.15	1.17	1.21	1.27	-12.78	11.40
D ₁₆	1.89	1.50	1.55	1.59	1.66	1.95	2.96	30.00
D ₅₀	3.10	2.95	3.29	3.48	2.93	3.50	11.53	18.64
D ₈₄	5.65	5.08	5.23	5.69	4.74	5.52	-2.46	8.66
D ₉₅	9.39	6.56	6.70	7.19	5.76	7.09	-32.57	8.08

Table 4-5; Evolution of grain parameters with increasing antecedent duration for the fine bed; D₅₀ highlighted for ease of analysis.

Comparison with the bulk mix indicates that, whilst grades maintain their general distribution form, there is a positive correlation between antecedent flow duration and a finer bedload composition. It is postulated that this change cannot stem from enhanced total transport of fines (due to total bedload decreasing after longer stress history durations, (Figure 4-5) hence, by proxy it most likely results from the progressive decrease in the availability of coarser fractions for transport following longer antecedent flow periods. In that the unimodal, bimodal and coarse beds generally a progressively greater magnitude reduction of transport with increasing particle size is noted. This shows more pronounced selective entrainment of smaller, lighter particles for transport (winnowing) during the increasing flows of the stability test.

As stress history duration lengthens from 0 to 60 minutes, data indicate a progressive fining of the bedload D_{50} by 48%, 99% and 14% respectively as compared to that of the original bulk mix. D_{50} statistics in Table 4-2 and Table 4-3(unimodal and bimodal) indicate that the largest degree of fining (+27.11% and +24.79 for the unimodal and bimodal beds respectively) occurs during between the 0 and screeded bulk mix and the start of the antecedent period (i.e. the bedding in period) but there remains a general progressive trend in the fining of D_{50} as antecedent duration increases to 60 minutes. This is in line with longer-duration stress history runs of Haynes and Pender (2007) in bimodal beds and the more commonplace degradational experiments performed using more active sediment-transport conditions (e.g. Hassan and Church, 2000). Although the coarse bed (Table 4-4) also indicates D_{50} fining relative to that of the bulk mix, the magnitude of fining is less than in the unimodal or bimodal beds; this may be a facet of the tightness of grading around coarser fractions which are inherently more stable due to submerged weight. In support of this statement, an additional observation is that there is no clear relationship between bedload fining and the temporality of stress history within the coarse bed.

Finally, when related to bulk mix data, the pattern of bedload evolution with antecedent duration for the fine bed (Table 4-5) is contrary to the other three grain size distributions discussed. The D_{50} coarsens by +11.53% with increasing stress history implying that the high proportion of available fines are less available for transport than expected from bulk mix data. Wider analysis of Table 6 indicates the development of something akin to hiding, in that both end fractions of the distribution appear to stabilize during flow antecedency

whilst the middle sizes are thus over exposed, entrained and more abundant in the transported load (Fenton and Abbott, 1977).

Secondly, analysis comparing the distribution to that at the start of the antecedent period (0 minute data) was undertaken; technically this was a more accurate representation of stress history changes specific to the antecedent period (as it removed the bedding-in period from analysis). This data shows a less pronounced bedload response to the stress history imparted (0-60 minutes), compared to the previous bulk mix data analysed above. This finding is expected as the water-working period is, to some degree, akin to the application of subsequent sub-threshold stress history which has been demonstrated to change bed stability. Direct stress history relationships with fractional bedload are statistically presented in Table 4-2 to Table 4-5. Unimodal and bimodal data show an 11.18% and 50.22% fining of the D_{50} , with general trends and explanations similar to those already outlined in the previous analysis undertaken with bulk mix. However, the coarse and fine bed response both indicate a coarsening of bedload with increased antecedent duration; data for the D_{50} are 15.53% and 18.64% finer respectively. Whilst the fine bed data shows progressive coarsening trends in relation to antecedent duration, the coarse bed demonstrates significant variability in compositional response. However, counter to both the unimodal and bimodal beds in which the coarser fractions showed the greatest response, review of the fractional data set does however suggest that it is the middle fractions of the bedload distribution which show the greatest response to stress history. A summary of total and median data is provided at the end of Section 4.4.

4.4.4 Fractional Bedload Transport

Analysis to date in this section reveals that, as the total bedload transported decreases, as a function of stress history there is also a change to the selectivity of the transport which is occurring and that this response appears grade-specific. Whilst geometric standard deviation and median grain size trends have already been considered (augmented by very general trend analysis pertaining to specific parameters provided in Table 4-2 to Table 4-5), there appears a need to specifically analyse the stability-mobility patterns of every individual fraction within each grade in order understand why the stress history response differs from one grade to another. Since graded sediment beds demonstrate a surface comprising of a mixture of different size fractions in unequal proportions, it is possible to

scale derived results either by the transported load for a specific fraction or by the original proportion in the bulk mix.

The degree to which mixture effects on fractional transport rates are evident depend on the manner in which the data are presented. Most commonly used is a dimensionless plot of transport rate (W_i^*) versus fractional Shields parameter (τ_i^*). A simple similarity transformation can then be used to collapse the data to a single thread (e.g. Parker *et al.*, 1982; White and Day, 1982) by replacing τ_i^* with τ_i^* / τ_{*ri}^* . However, Wilcock (1992) noted that this type of plot obscures large differences in q_{bi} from fraction to fraction which can lead to errors of greater than an order of magnitude when predicting fractional transport rates. As such, previous stress history studies (e.g. Haynes and Pender, 2007) used the relationship between the changing bedload composition (p_i) as a fraction of the original mix (F_i) to account for the changes in size selectively; p_i/F_i was thus plotted against antecedent flow duration giving individual temporal trends for each fraction. Yet, the p_i/F_i representation is not commonplace in fractional bedload analysis and the whole grain size distribution cannot easily be interpreted for any given stress history. Therefore, this thesis presents detailed fractional bedload data by scaling the fractional bedload transport rate, g_i , by the abundance of each size in the bulk mix, F_i , and then plotting against dimensionless size (fraction D_i scaled by the bulk D_{50}) for each of the antecedent flow durations. This plot is well suited to establishing whether fractions are being transported under equal mobility conditions or are being selectively entrained (White and Day, 1982; Parker and Klingeman, 1982; Andrews and Parker, 1987; Wilcock, 1992) as true equal mobility would appear as a horizontal line parallel to the abscissa, with any deviation from this depicting selective transport. As such, data sets typically have 'n' shape, tending to equal mobility in the middle of the distribution and selective transport for sizes at the extremes of the distribution due to both hiding effects and sampling inefficiency for smaller grain sizes (Wilcock, 1992). The position of the distributions on the graph give an indication of the rates of transport, meaning that the spacing of the lines and their slopes can be used to interpret changes in size selectivity and grain size distribution as stress history changes. It is worth reiterating at this point that the experiments were stopped at the threshold of entrainment for the D_{50} grain fractions. As such it would be expected that if size selective entrainment were strong in these experiments no grains greater than the D_{50} should be moving, however if grains greater than the D_{50} are moving then there is a tendency towards equal mobility conditions.

Fractional bedload transport, g_i , of each size fraction is presented for each grade of bed subjected to stress histories 0-60 minutes in Figure 4-8 to Figure 4-11. Results obviously corroborate the general analysis undertaken from Tables Table 4-2 to Table 4-5 above. Within the unimodal bed (Figure 4-8) the 'n' shape distribution pertaining to selective entrainment, especially of 1.4mm to 5.6mm grains, is observed. With the finest fraction (1-1.4mm) and those above the median size underrepresented in the bedload, hiding effects are well developed in the unimodal bed (even after water-working alone). The finest grains 'lost' to entrainment due to infiltration or sheltering by the more stable grains greater than the D_{50} which offer greater submerged weight. That the 'n' shaped distribution is noted at all suggests that even although the experiments are stopped at the threshold of the D_{50} grains there is significant size selective entrainment with Figure 4-8 showing that the nature of the size-selectivity remains preserved regardless of applied antecedent duration, possibly implying progressive stability of the bed as a whole (i.e. all fractions equally). The displacement of distributions along the ordinate axis indicates progressive stability with increasing antecedency; this is in line with the entrainment data presented in Figure 4-3 and consistent with other degradational experiments (e.g. Hassan and Church, 2000).

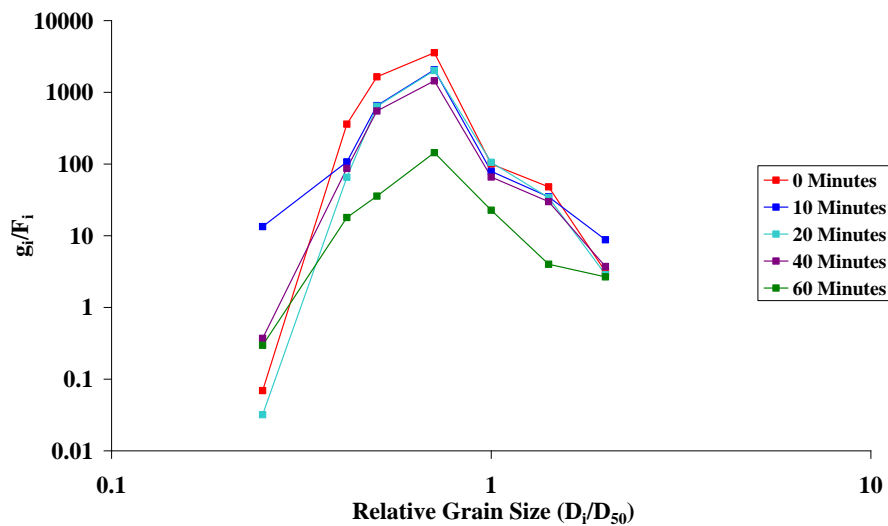


Figure 4-8; Fractional bedload transport rate of the unimodal bed scaled by the abundance of each size (g_i) in the bulk mix(F_i) plotted against dimensionless size for antecedent durations 0-60mins.

Bimodal bed data (Figure 4-9) shows a more complex fractional bedload response following stress history. Only fractions finer than or equal to the D_{50} are entrained for transporting relatively high proportions, although the 5.6-8mm fraction is the coarsest fraction mobile in all experiments. This indicates both: (i) a general winnowing process and, (ii) that coarse particles are highly stable in the bimodal distribution even without significant water-working. The general trend of winnowing appears independent of the antecedent duration applied with the exception of the 60 minute data which appears to be showing a move towards equal mobility of the mobile fractions with the exception of the coarsest fraction. The displacement is most pronounced between 40 and 60 minutes of antecedent flow (as also found for the unimodal bed). Interestingly it is clear is that the bimodal bed does not have obvious hiding effects of fine end member fractions (this is counter to that found for the unimodal bed). Instead both the finer of the two modal fractions (2 – 2.4mm) and the fraction containing the D_{50} demonstrate the greatest relative mobility of all fractions. The mobility of the finer fraction is easy to explain in terms of its greater relative abundance in the distribution combined with their low submerged weights which both act to increase its relative ability. However the mobility of the fraction contain the D_{50} is harder to explain given that it constitutes only 8% of the overall distribution. One explanation may be methodological related in that the low abundance of this fraction in the bulk mix over-inflates statistical representation of this fraction's mobility using analysis of bedload by weight. Regardless of this the D_{50} appears to stabilise after the longest antecedent durations and there is less of a marked difference between this fraction and the other finer fractions. This finding raises the possibility that, starting with the coarsest fraction, there may be hierarchical stabilisation of progressively finer fractions under antecedent flow conditions in the development of something akin to an armour layer development.

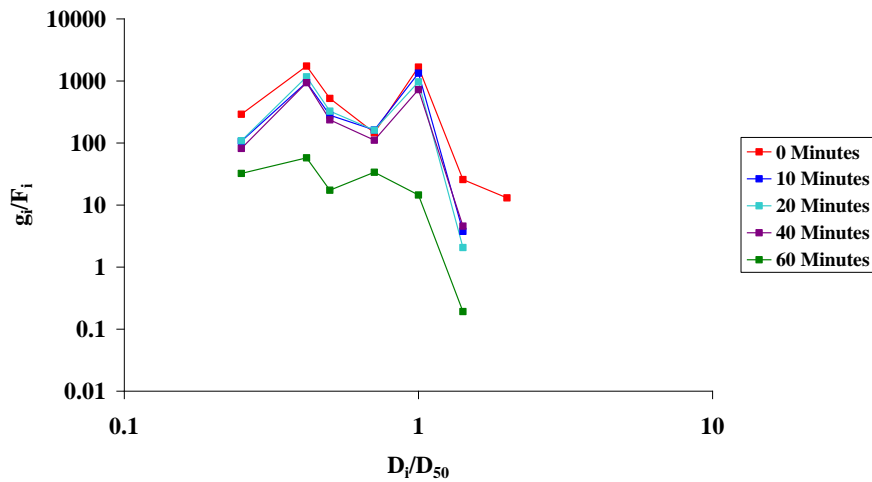


Figure 4-9; Fractional bedload transport rate of the bimodal bed scaled by the abundance of each size (g_i) in the bulk mix (F_i) plotted against dimensionless size for all five antecedent durations.

The coarse bed (Figure 4-10) identifies that only fractions up to the D_{50} are selectively entrained; this indicates a stable coarse fraction and the preferred winnowing of particles $< D_{50}$. As postulated in the introduction to this section, this relationship is expected given that the stability test is only using flows up to entrainment thresholds of the D_{50} . There is some evidence towards a truncated ‘n’ shaped distribution in that the finest fractions are also affected by hiding for all stress histories applied. Although there is no clear relationship of fractional bedload response to stress history, the reduction in g_i/F_i of the 5.6-8mm fraction (i.e. the coarsest fraction found to be mobile) subsequent to longer stress history durations (40 minutes) may indicate that this fraction is starting to stabilise akin to the bimodal bed where the coarse grains begin the stabilisation process.

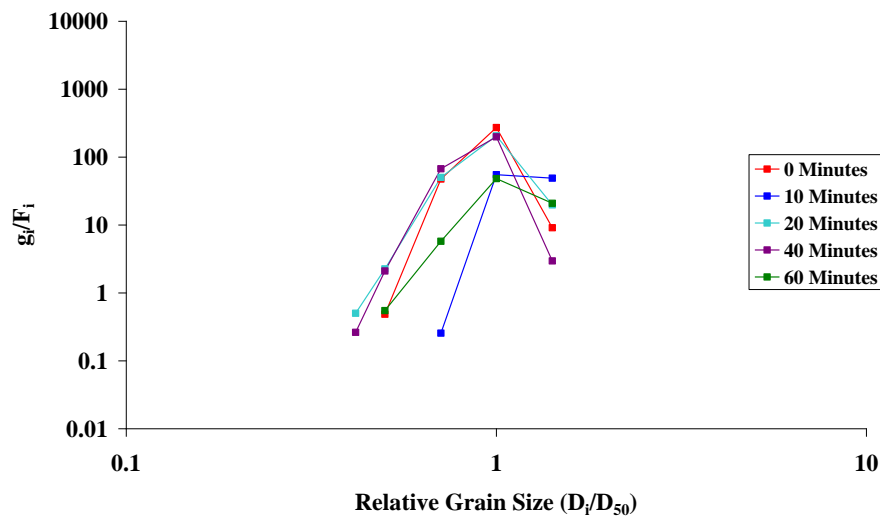


Figure 4-10; Fractional bedload transport rate of the coarse bed scaled by the abundance of each size (g_i) in the bulk mix (F_i) plotted against dimensionless size for all five antecedent durations.

The fine bed (Figure 4-11) is unique in indicating near equal-mobility of the mobile fractions with the exception of the coarsest mobile fraction (5.6–8mm) which begins to exhibit size selective entrainment. With increasing stress history, there is a negative displacement of the g_i/F_i data which is particularly noticeable in the end member fractions (1-1.4mm and > 5.6mm) indicating the progressive development of hiding as antecedent duration increases from 0 to 60 minutes. This antecedent-related trend is most discernable for these coarser end member fractions where there is a sequential reduction between 0 and 60 minutes (10 minute data is the outlier from the trend). The largest response is noted between 20 and 40 minutes suggesting that longer antecedent durations are needed to fully stabilise the coarsest mobile fractions. The finest mobile fraction also shows a sequential reduction in transport rates with antecedent duration between 0 and 60 minutes (40 minutes being the outlier from the trend). However there appears to be a two stage stabilisation process where the fine grains initially stabilise quickly between 0 and 10 minutes but it then takes the longest antecedent durations (40 and 60 minutes) to stabilise the grains further. This suggests that the finer grains are initially winnowed deeper into surface pores such they are protected from entrainment. The second response suggests that the finer grains may be protected, by sheltering, as a result of the stabilisation of the coarsest fractions.

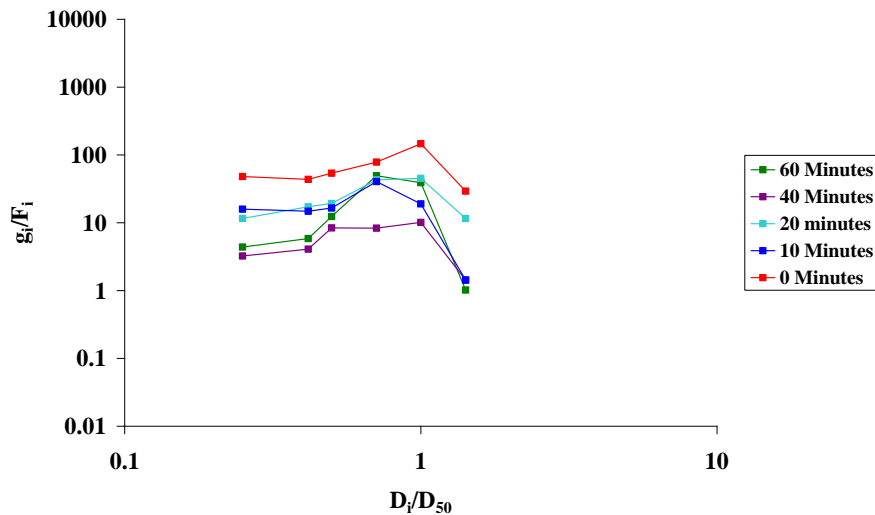


Figure 4-11; Fractional bedload transport rate of the fine bed scaled by the abundance of each size (g_i) in the bulk mix (F_i) plotted against dimensionless size for all five antecedent durations.

In summary of the total and fractional transported bedload analysis, results derived for each sediment grade reveal five clear inferences.

- Increasing the duration of the antecedent flow decreases the total transported load for all four grain size distributions; this is taken as a proxy indicating increased stability of the bed. This supports the entrainment threshold analysis presented earlier in this Chapter and is in general agreement with total bedload findings from the stress history data of bimodal beds undertaken by Haynes and Pender (2007).
- The response of total transported load to the imposed stress history regime shows significant grade dependency. Extending the antecedent flow period results in the transported bedload reducing by the following grade-specific hierarchy: bimodal (-94%) > unimodal (-90%) > fine (-70%) > coarse (-59%). The similarity in magnitude response of the unimodal and bimodal bed is highlighted; again, this is supportive of earlier entrainment threshold analysis.
- Increasing the duration of antecedent flow typically results in a systematic decrease in the geometric standard deviation suggesting enhanced size selectivity of transport. There is, however, a significant grade dependency thus suggesting that there is also a dependence on the relative position of a grain fraction within the grain size distribution rather than σ_g alone.

-
- Selective entrainment is found for the unimodal, bimodal and coarse beds, independent of the antecedent duration applied, however it is the coarse bed which shows the strongest degree of size selectivity. As this typically goes hand-in-hand with hiding development, the effect is on mobility of the middle fractions of the transported distribution. Data for the fine bed is subtly different in that, from a start point of equal mobility, selective entrainment only develops progressively during the antecedent period.
 - The fine bed (directly), coarse and bimodal bed (indirectly) data support the theory of initial stabilisation of coarse particles being the trigger mechanism for progressively more enhanced bed stability of other fractions after longer antecedent durations. Yet, unimodal data is counter to this, suggesting that progressive stabilisation of all fractions may occur uniformly for this specific grade.

It should be highlighted that these results are derived from data only taken over the stability test. Specifically, stability test flows increased only up to the critical threshold for the D_{50} when the test was stopped; this means that the durations and final shear stresses of the stability tests vary for each grade and time combination (Appendix A1). As such comparison of data should be treated with caution.

4.5 Discussion

Based on past literature the aim of Chapter 4 was to determine if stress history influences could be confirmed in both uniform and graded beds, and if there was an obvious influence of grade on the magnitude of stress history effects (section 4.1). As such, this discussion seeks to use past research papers to support the findings from Chapter 4 in the wider context of sediment transport knowledge, to speculate on explaining why these trends may occur and, importantly, direct further research within this thesis. Specifically, the hypotheses set at the beginning of this chapter (Section 4.2) will be used as a framework to highlight the findings presented in this chapter in terms of: (i) magnitude of stress history induced stability; (ii) possible general mechanics of stress history induced stability gains; (iii) questions arising pertaining to differential response of grades.

4.5.1 The influence of stress history on bed stability.

This Chapter has provided evidence demonstrating the stabilising influence of sub-threshold flows on non cohesive sediment beds. This directly refutes the findings of

Gomez (1983) who claimed that the stability of non cohesive beds could only be altered by above-threshold flows capable of sediment transport. Instead it is supportive of field (e.g. Reid and Frostick, 1984; Reid *et al.*, 1985; Willetts *et al.*, 1987; Oldmeadow and Church, 2006) and more recent laboratory (Paphitis and Collins, 2005; Monteith and Pender, 2005; Haynes and Pender, 2007) data which have both indirectly and directly suggested that antecedency may be an important control on entrainment thresholds. In line with previous literature specific to stress history, two metrics of stability have been used in this chapter to assess the stability gains as a result of stress history; direct entrainment threshold analysis (similar to Paphitis and Collins, 2005) and proxy bedload analysis (similar to Monteith and Pender, 2005; Haynes and Pender, 2007) .

Firstly, using direct entrainment threshold analysis, data in the present thesis shows that critical shear stress of the median grain size increases by between +2% and +25% due to the applied stress history of 60 minutes at τ_{c50} . Equivalent data by Paphitis and Collins (2005) showed a +56% change after 60 minutes for 0.19 to 0.77 mm uniform sand beds. Thus, the present thesis indicates a lesser response; uniform gravel response is half that cited by Paphitis and Collins (2005), whilst graded bed response is significantly lower. This may be explained by a number of factors. Firstly, the estimates of critical bed shear stress from Paphitis and Collins (2005) were calculated using the log law derivation methodology (e.g. Wilcock, 1996; Graf, 1998) as compared to derivation using the depth-slope methodology in this thesis. Previous research has suggested that shear stress estimates calculated using the log law derivation method are consistently higher compared to those obtained using the depth slope methodology (Buffington and Montgomery, 1999). Secondly, the method of bed preparation used by Paphitis and Collins (2005) differed in that the sand grains were allowed to settle naturally under still water conditions. This method of bed preparation would form a looser packing arrangement of the bed surface (hence more scope for rearrangement during stress history), than the more consolidated beds generated by the screeding methodology associated with the present thesis (e.g. Cooper and Tait, 2008). Thirdly, Paphitis and Collins (2005) make no mention of the length of their bedding in period prior to their experiment; if this was longer than 30 minutes (as used in this thesis), then a more resistant bed may result. Finally, the studies differ in terms of grain size, demonstrating that uniform gravels are less responsive

to stress history than uniform sands. This has been linked to the influence of packing within the literature, where the larger the grain size the lower the packing density and hence stability (Brayshaw *et al.*, 1996; Rollinson, 2006), supporting the findings noted within this thesis where the larger uniform gravels are less responsive than uniform sand grains used by Paphitis and Collins (2005).

Secondly, using bedload data as a proxy for stress history response shows that longer antecedent periods reduce subsequent bedload. This is in agreement with the general finding for the bimodal bed research of Monteith and Pender (2005) where they noted a 63% reduction in bedload after 60 minutes of antecedency. This is in comparison with a 94% reduction in total load noted within this thesis. Whilst the grade employed is comparable between the two studies, the methodology of the stability test is not, as not only did Monteith and Pender (2005) use a steady flow stability test for a prescribed duration, but their discharge was above-threshold for the D_{50} . Application of their method in the present thesis was inappropriate as assessment of entrainment to be calculated using visual entrainment would not have been possible; thus, a stepped stability test akin to Paphitis and Collins (2005) was used. In doing so this leads to variable duration and magnitude stability tests and may explain the observed differences between this study and that of Monteith and Pender (2005). In this thesis bedload response is particularly notable in the unimodal bed where a very rapid generation of a stable unimodal bed configuration in response to applied antecedent flow durations is noted; this is akin to the entrainment analysis. This is in agreement with Cooper *et al.*, (2009) who assessed the comparative stability of unimodal and bimodal deposits of similar D_{50} by linking stability with the organisation of the surface deposits. Results indicated that in bimodal beds a higher degree of mobility, and hence a lower overall stability, was due to a higher proportion of the fluid force being carried by the finer grain fractions. As flow periods were increased a higher proportion of the fluid force was carried by the larger grains due to grain sheltering (Schmeeckle and Nelson, 2003) and the development of grain structures (Hassan and Church, 2000) such that the differences in the stability of the two beds decreased. This is in line with the findings in this thesis where the initial difference in the critical entrainment threshold decreases with increasing antecedent duration. The underpinning mechanisms behind the change to response are likely to be similar to those noted by (Cooper *et al.*, 2009) and are discussed in more detail below.

The rate of response of the imposed stress history regime in terms of both average critical bed shear stress and total transported load consistently shows greater changes at the start of antecedent periods (typically within the first 10 minutes of the new applied flow). This indicates that beds directly and rapidly respond to a new flow regime, even if the applied flow is sub-threshold. Such behaviour is similar to that of many degradation experiments (Tait *et al.*, 1992; Proffitt and Sutherland, 1983; Pender *et al.*, 2001). Haynes and Pender (2007) attributed this decay not only to the loss of initially unstable grains from a screeded surface, but also to the progressive stabilisation of larger areas of the bed surface such that grains became unavailable for transport; this appears to be supported in the present thesis. In an applied context this essentially means that even relatively short inter flood periods may substantially affect the entrainment threshold and that each flow magnitude change in the flow history of a hydrograph should be identified and analysed for the effect it has had on the bed surface. Further, the magnitude of response of the bedload is significantly (~9 fold) greater than critical shear stress threshold response. This suggests that bedload is not a simple function of bed shear stress (Cooper *et al.*, 1995) but is governed by interdependent mechanisms, the most significant being the interaction between bed roughness, surface layer composition and near bed flow (Nelson *et al.*, 2005; Drake *et al.*, 1988). Specifically, the increase in critical bed shear stress appears best characterised by a growth rate that will continue to occur with increasing antecedent duration but that the growth will occur at a smaller and smaller rate such that a maximum value can effectively be assumed to be reached after the longest antecedent durations; this general response appears supported by Paphitis and Collins (2005). However, despite a similar pattern in the decay of the curve fitted to the bedload data, a zero transport rate will never be reached. This is supported in the literature where it has been suggested that even under the lowest flow velocities sediment transport is possible due to turbulent fluctuations in the flow (e.g. Grass, 1970; Paintal, 1971; Graf and Pазis, 1977; Lavelle and Mofjeld, 1987; McEwan *et al.*, 2004; Paphitis and Collins, 2005; Bottacin *et al.*, 2008). This means that although the bed will continue to transport sediment it may be at its most stable granular configuration as evidenced by the attainment of a stability maxima in the shear stress values. This may begin to explain the differences in the rate of change in bedload transport as compared to shear stress. The distinction between the response of the critical bed shear stress and total transported load is important for stress history research application; whilst correcting for entrainment threshold will determine whether there is (or isn't) transport in any high flow

event, a different correction for bedload would be needed to determine the amount of material transported.

4.5.2 *Literature based explanations of the possible mechanics explaining the differential bed stability gains and response to stress history.*

The question arises as to how sub-threshold flows are capable of enhancing a bed's resistance to entrainment, particularly in very short timeframes at the start of a new applied flow. Possible mechanisms are discussed in detail by Paphitis and Collins (2005) who emphasise the role of particle vibration, serving to permit grain reorientation, increased imbrication and higher packing density whereby the consequence of reduced frictional drag would increase in the bed's structural resistance to entrainment. In particular, research by Church (1978) noted that 'loose' un water-worked beds record lower values of the Shields entrainment function ($\theta=0.02$) than 'compacted' water worked surfaces ($\theta=0.01$). Kirchner *et al.*, (1990) corroborates these findings showing that water-working a non-cohesive bed increased friction angles, leading to a tighter packing arrangement and thus created a smoother bed. Kirchner *et al.*, (1990) note that pivot angles are typically up to 20-25° higher than those of unworked beds (Miller and Bryne, 1966; Fenton and Abbott, 1977; Komar and Li, 1986). For these reasons a water worked bed is less liable to be modified by the overlying fluid flow regime and hence exhibit a higher critical shear stress (Church, 1978). In the context of stress history, the change of flow at the start of the antecedent period is likely to cause increased pressure (due to increased flow depth) and short-term turbulence instabilities which directly impact the sediment bed causing a level of vibration in excess of that imparted by the more steady flow regime. This may explain why stability gains are more pronounced immediately subsequent to a new flow being imposed. Whilst the degree of vibration (and thus bed restructuring) reduces with longer antecedent durations, the continuation of progressive stability gains of the bed may still be attributed, in part to observed vibrations caused by the inherent turbulent properties of the flow and the subsequent grain rearrangements (Leeder, 1983; Kaftori *et al.*, 1995). The effects of turbulent instabilities causing grain vibrations and reorientations will be complicated in graded beds which are typically composed of a coarser framework and a matrix of finer material (Reid *et al.*, 1997). As a consequence it is likely that grain vibrations at flows below the entrainment threshold will cause a differential fractional response as a result of relative grain size effects (Dietrich *et al.*, 1989). This would imply the possibility of not only a temporal response to the underpinning mechanism responsible for bed stabilisation as a result of stress history but also a grade dependent response to

stress history even under benchmark conditions. This will be discussed in turn below both under benchmark conditions and with applied antecedent flow. Whilst the mechanistic processes suggested above cannot be (dis)proven by the data from Chapter 4 (and therefore form the focus of Chapter 6), grade response can to some extent be explained by fractional bedload during the pre-threshold stability test.

4.5.3 *Absolute threshold and the role of fines.*

Under benchmark conditions a hierarchy of stability in terms of critical bed shear stress is noted (section 4.4.2) which is consistent with the postulations of a grade dependent response as proposed above. In this thesis, absolute critical shear stress values are highest in the coarse bed (and hence it is most stable) and lowest in the fine bed (so it is the least stable). Given that the coarse bed has the smallest proportion of fines within the distribution and the fine bed the highest proportion, the hierarchy of stability seems to suggest that it is the proportion of fines within the distribution which fundamentally control the stability of the bed surface. The effect of fines within a distribution has been noted to have two effects. Firstly, in response to the overlying fluid flow, finer material exploits the interstices of the bed surface and initially settles into the lee of larger particles whilst still remaining part of the bed surface composition (Reid *et al.*, 1985; Marion *et al.*, 2003; Haynes and Pender, 2007). The small absolute size of the sand in relation to the larger grains results in comparatively higher pivot angles which serve to stabilise the grain (Miller and Byrne, 1966). In addition to lateral winnowing, fine grains can also be vertically winnowed from the bed surface such that they become isolated from the bed surface but act to consolidate the framework gravels (e.g. Reid *et al.*, 1985; Allan and Frostick, 1999; Haynes and Pender 2007). Thus in terms of relative mobility, the end fractions of the grain size distribution are comparatively more stable than the medium grain size fractions on the bed surface, leaving the latter to be comparatively more mobile. Logically, using the mechanisms above, it is clear to see how, by varying the proportion of sand within a mixture and hence altering the relative size effects, it is possible to change the overall stability of a bed and the subsequent entrainment patterns. However there is a body of literature which suggests that as the proportion of sand is increased in a sand gravel mixture a smaller bed shear stress is needed to transport the sand gravel mixture (Jackson and Beschta, 1984; Ikeda and Iseya, 1988; Wilcock, 1988). These observations seem to lend support to the hierarchy of stability noted within this study where an increase in the proportion of fine grains in the distribution is mirrored by lower critical shear

stresses required for entrainment (coarse bed is the most stable with the lowest percentage of fines in the distribution and the fine bed is least stable with the highest percentage of fines in the distribution). Consequently, the competing effects of stabilisation by vertical winnowing of fines and consolidation of the bed and the increased instability as a result of an increasing proportion of fines in the distribution appear complicated. The results in this thesis however advocate that the initial response of the bed under benchmark conditions (i.e. no antecedent duration) is controlled by the proportion of fines within the distribution.

In terms of the transported bedload under benchmark conditions, the expected relative effects of grade are noted where selective entrainment is clearly found for the unimodal and bimodal beds as evidenced by the relative mobility of the middle fractions of the transported distribution and the relative immobility of the end members of the distribution, akin to previous findings (Wilcock and McArdell, 1993; Kuhnle, 1993; Wilcock and McArdell, 1997; Monteith, 2005). The most notable difference between the two beds is the relative mobility of the D_{50} in the bimodal bed as compared to the relative immobility of the D_{50} in the unimodal bed. Although the mechanisms of why this difference should be so are not clear, given that the D_{50} of both beds is identical it seems to suggest that stability is intrinsically linked not to the absolute percentage of the D_{50} in a mixture but to the relative proportion of the D_{50} to the other grain fractions (D_i/D_{50}). These results fit well with those found within the literature, which note that critical entrainment thresholds are well explained by D_i/D_{50} (White and Day, 1982; Wilcock, 1992; Shvidchenko, 2000) as compared just using the D_{50} . This has important implications for studies which use the D_{50} as a descriptor of stability and an argument is made for explicit consideration of the modality of the grain size distribution rather than simply relying on more traditional descriptors of sediment distributions. The coarse and fine beds show a more complicated pattern of bedload transport under benchmark conditions. Although the coarse bed response exhibits size selectivity akin to the unimodal and bimodal beds, a truncated response is noted where only fractions up to the D_{50} are selectively entrained; this indicates a stable coarse fraction and the preferred winnowing of particles $< D_{50}$. Whilst this could be a facet of the stability test being truncated at the threshold of the D_{50} , the comparative degree of size selectivity as compared to the other three distributions is much greater. This concept is well supported in the literature where, typically even if the sand content of the bed is small (between 10% to 30% , akin to the coarse distribution used in this thesis) and the bed is composed of a framework of gravel clasts, sand transport dominates because not only are the shear stress above that of the sand threshold (Wathen *et al.*, 1995) but sand

fractions can bridge between the gravel clasts thus reducing the hiding effects and increase its ease of transport (Diplas and Parker, 1985; Wilcock and Kentworthy 2003). Further, Wilcock and Kentworthy (2002) support the appearance of a truncated response in the coarser fractions suggesting that as the pore spaces between the grains fill with sand, the gravel may be partially or temporarily buried with sand suppressing the transport rates. Conversely, data for the fine bed is subtly different in that, under benchmark conditions equal mobility conditions are noted. It is reasoned that, the finer sand grains are small and of low submerged weight making them readily mobile and, due to smaller pore sizes, they cannot effectively 'hide'. Given that the coarser grains are in a low relative proportion within the bed they will be isolated on the bed surface (Ikeda and Iysea, 1988) such that their entrainment is liable to be linked to the undercutting of the surrounding finer grains and once in motion, the gravel will be able to keep moving over the relatively smooth sand bed leading to a case of equal mobility of the sand and gravel fractions (Kuhnle, 1992; Wilcock and Kentworthy, 2003).

Thus, results tend towards suggesting that it is percentage of fines in a distribution which is responsible for the overall stability of the bed surface which is linked to the relative stability/mobility patterns of grains during entrainment. Specifically highlighted is the link behind the change to the mechanisms underpinning this stability and the change from size selective entrainment to equal mobility as the bed changed from a clast supported grain size distribution (akin to the coarse bed in this thesis) to a matrix supported distribution (akin to the fine bed in this thesis) even under benchmark conditions. This supports the noted transport patterns here where, as the sand content of the bed is increased (fine>bimodal>unimodal>coarse), there is a change from equal mobility (in the fine bed) to size selective entrainment (in the bimodal, unimodal and coarse beds) with the degree to which the bed adheres to either transport pattern a facet of the proportion of coarse to fine within the distribution. However, if the sand content was the only responsible mechanism for the beds response to stress history it would be expected that the responsiveness of each grain size distribution would follow this original hierarchy as antecedent duration was increased and transport patterns would not change with applied antecedent flow durations. Whilst the order of the absolute threshold data hierarchy is maintained (i.e. the coarse bed always requiring the highest bed shear stresses to be mobilised and the fine bed requiring the lowest), there appears to be no relationship between fine content and relative stability changes to the duration of stress history applied.

4.5.4 *The relative responsiveness of beds to stress history; the ability of fractions to rearrange.*

The relative responsiveness of the graded bed to stress history reveals that it is the uniform bed which is more responsive to stress history as compared to the graded beds in terms of average critical bed shear stress (+25%, +9%, +8%, +8%, +2% for the uniform, bimodal, unimodal, fine and coarse beds respectively). This appears related to the grain size distribution and its influence on the ability of a grain to rearrange in response to the applied antecedent flow. It is this rearrangement which is believed to alter the stability/mobility patterns of the grains fractions such as to alter the pattern of entrainment following periods of prolonged antecedent flow.

It is suggested that in uniform beds there is a greater potential for re-arrangement to occur and hence a greater potential responsiveness to stress history. This is argued to be due to the larger pore spaces in the framework permitting greater potential for movement, where larger pore spaces allow particles to streamline in the fluid flow (Brayshaw *et al.*, 1983; Li and Komar, 1986; Dietrich *et al.*, 1989; Fenton and Abbott, 1997;), serving to increase both grain imbrication and pivot angles such as to decrease surface roughness and enhance resistance. This change to surface roughness has been observed to cause a decrease in both the shear stress magnitude and variability across the bed (Rollinson, 2006). In terms of the relative effects of stress history the literature supports the findings noted above where, in non-cohesive sediment beds, not only do pore spaces tend to be larger in beds that are un-water worked and hence less structured but that beds with more uniform grain sizes have larger pore spaces (e.g. Kirchner *et al.*, 1990; Haynes *et al.*, 2009). In a similar study to experiments reported herein, Rollinson (2006) specifically compared a uniform bed (D_{50} 8mm) and graded (bimodal) bed of comparative D_{50} and found that the pore spaces were both larger (by up to 3%) and deeper (by up to 5%) in the uniform bed after being exposed to up to 4361 minutes of sub-threshold flow duration. In graded beds it is the relative grain effects which cause a reduction in overall bed porosity (Kleinhans *et al.*, 2008; Frings *et al.*, 2008; Haynes *et al.*, 2009) such that finer particles within graded beds serve to reduce pore space size and restrict in-situ particle movement of the larger grains (Frostick *et al.*, 1984; Allan and Frostick, 1999). Under the longest antecedent flow durations, vertical winnowing of the finer grains from the bed surface in graded beds becomes exacerbated such as to increase the relative projections of the larger grains. A greater surface area of the coarse grains is projected as antecedent flow duration is

increased such as to allow the particle to reorientate and streamline itself with the flow direction (Carling *et al.*, 1992, Gomez, 1995). The reorientation of larger surface grains then disturbs surface fines and increases their vertical movement serving to increase roughness. It is therefore logical that the different pore sizes and hence ability of the bed to rearrange will be grade dependent and may explain the different relative response of each distribution to stress history and the deviation from the hierarchy of stability noted under benchmark conditions. This is especially important since the magnitude of the response to stress history within the unimodal, bimodal and fine beds are similar.

Given the change to the relative stability/instability of particles in response to particle rearrangement, it follows that the patterns of entrainment would also be different from those noted under benchmark conditions. Indeed, the pattern of entrainment is temporally responsive to antecedent duration in both the bimodal and fine beds. In the bimodal bed the progressive stabilisation of the D_{50} sees the entrainment patterns tending to become more equally mobile with increased antecedent duration. The progressive stabilisation of the D_{50} is noted in conjunction with a decreased in the σ_g which indicates that there is a narrower range of particle sizes in transport purporting to enhanced size selectivity. Using the same bimodal distribution as in this thesis, flow durations of up to 3.3 hours and flow discharges of up to 30.4 Ls^{-1} , Shvidchenko (2000) supports the findings here where it was noted that the degree of size selectivity of the finest fractions increased with lower σ_g values, consistent with the findings of Naskagawa *et al.*, (1982). Conversely, although the fine bed shows a temporally sensitive response, from a starting point of equal mobility the fine bed becomes progressively described by size selective entrainment as antecedent duration is increased. However, despite different patterns of mobility, in both beds, in response to the stabilisation of the coarse grains there is a sequential reduction of the finest grains in the distribution; this is particularly notable in the fine bed.

These results raise the possibility that starting with the coarsest grains there maybe a hierarchal stabilisation of progressively finer fractions under antecedent flow in the development of something akin to an armour layer development. This is indirectly supported within the literature where both Gomez (1995) and Marion *et al.*, (1997) note a reduction in the probability of movement of the coarser clasts such that the availability of the finer and medium sized fractions is reduced due to both direct and remote sheltering (McEwan *et al.*, 2004). The initial, preferential stabilisation of the coarser grains is in part

due to their relatively higher submerged weight making them more difficult to entrain, however once stabilised these clasts, which have been termed ‘keystones’ in previous research, and have been noted to cause a change to the flow field causing the stabilisation and deposition of fine grain fractions in the lee side (e.g. Brayshaw *et al.*, 1983). This is supported by Monteith (2005) who notes this to be the cause of the under representation of the finer grains in the transported bedload, akin to transport patterns noted in this thesis. This suggests that the coarser grains act to stabilise a significantly larger area of the bed than their plan area seems to suggest, a trend also noted by Pender *et al.*, (2000) and Hassan and Church (2000). This was attributed to passive or active structuring which serves to protect, and hence stabilise, areas of finer material on the bed surface (Tait and Willetts, 1991). However, in the present thesis observations during the sub threshold antecedent period noted no observable grain scale structures; thus, a more appropriate rationale may be that of Marion *et al.*, (1997) and Pender *et al.*, (2000) who linked increased bed stability to changes in the bed topography (but without the requirement for structures to form) given that flows are sub-threshold and hence active entrainment is not occurring on the bed surface. In agreement with Tait and Willetts (1991) and Hassan and Church (2000) this shows the need for understanding of how bed surface texture and topography controls overall bed stability (Chapter 6).

Counter to the bimodal and fine beds, the unimodal and coarse beds do not show a change to the transport patterns with increased antecedent duration. This suggests that stability is more related to the organisation of grains on the bed surface. This would seem to indicate that the mechanisms responsible for arrangement of the grains in the unimodal bed is different to that of both the bimodal and fine beds, a difference highlighted by Cooper *et al.*, (2009). The possibility of the organisation of the surface being the controlling mechanism is exemplified using the results gained from the coarse bed where, despite similar size selective entrainment patterns as those noted in the unimodal and bimodal beds, and despite an apparent preferential stabilisation of the coarsest grain fractions, akin to the fine and bimodal beds the coarse bed does not stabilise in response to the applied antecedent flow. This is feasibly linked to the organisation of the bed surface where the greater overall roughness, due to the initially higher proportion of the coarse grains on the bed surface, the resultant turbulent interactions will act to destabilise the bed (Nakagawa and Nezu, 1977; Paphitis and Collins 2005). This effect is exacerbated since the larger pore spaces resulting from the larger framework of the coarse grains allow penetration of

turbulent eddies into the bed in-between the spaces between grains. This flow within the bed will allow winnowing of fine grains from the surface, exposing the coarse grains framework such that they destabilise. This is contrary to the argument of Paphitis and Collins (2005) that, as turbulent eddies began to penetrate into the bed, grains were shifted and vibrated into a position deeper within the bed, in turn causing the sediments to become more compacted thus creating a more resistant bed. Although the winnowing of fines into the bed to consolidate the coarser clasts may offset this destabilisation to some degree it is liable that the finer grains will winnow deeper into the bed due to the larger pore spaces such that they offer only minimal support to the coarser grains. This may explain the less pronounced increase in the stability in comparison with the other beds.

4.5.5 Questions raised from data and discussion of Chapter 4

Therefore from the discussion above, it is possible to see that there is a clear influence of prolonged periods of sub threshold flow upon antecedent duration. There are also clear influences of grade upon the stability attained by individual beds in response to stress history which is temporally sensitive. This is evidenced by the difference between the hierarchy of stability under benchmark conditions and the hierarchy of response in relation to increased antecedent flow durations. The changes to the bed stability have been linked to changes in the relative mobility/stability patterns of different grain fractions on the bed surface. These patterns have also been noted to be highly grade and temporally dependent. Although these findings have been clearly highlighted and justified throughout the discussion, there are still questions which have arisen as a result of the reported investigations which need developing throughout the remainder of this thesis. As such there is a short section below which briefly identifies the essential next steps of this research and justifies the direction taken in the coming chapters based on the findings gained in this research. This is primarily linked to three main findings; the possible achievement of a stability maxima if the antecedent timeframes were to be increase, the effect of grain size distribution and the link between stability of the bed surface and surface organisation.

- The stability gains in response to stress history reported have been described with two metrics; directly using critical bed shear stress and indirectly using proxy bedload analysis. Both metrics have noted the stabilisation in response to stress history irrespective of grain size distribution, however there have been important questions highlighted which have not been answered in this set of experiments. Specifically, it

appears that a stability maxima may be reached if the antecedent durations were to be extended, in line with previous stress history findings. Thus the question arises as to what time frames would be needed in order for these maxima to be reached and provides justification for the research undertakings reported in Chapter 5 where antecedent durations are extended to 960 minutes.

- Despite consistent overall trends in response to stress history, it has been highlighted throughout this current Chapter that the responses are grade dependent. This becomes particularly relevant given the apparent unexpected response of the uniform and graded beds where the former appear to be more responsive to stress history than the latter. The results shows that modality has a fundamental effect upon the stability gained by a sediment bed and provides the justification for the further analysis of these three beds in Chapter 5 and Chapter 6. Specifically, three main justifications are valid for concentrating on analysing the uniform, unimodal and bimodal beds throughout the remainder of this thesis; (i) they are of equivalent D_{50} and are thus readily comparable (ii) they are the most responsive to stress history in terms of both response to average critical entrainment shear stress and transported bedload (section 4.4.2 and 4.4.3) (ii) they are the most comparable to the previous, limited field and laboratory data (Paphitis and Collins, 2005 (uniform); Montheith and Pender, 2005 and Haynes and Pender, 2007 (bimodal)). Given that this thesis concentrates on the temporal aspect of low flow periods it appears pertinent to analyse beds which are both comparable in terms of the D_{50} (in this case the uniform, unimodal and bimodal beds) manner.
- Both of the above findings have consistently been linked to the possibility that it is the textural influences (surface organisation and topography), which are important in explaining the stability gains of the beds in response to stress history. Only a very limited number of studies have examined the link between surface topography, grain entrainment and bedload transport explicitly and none have combined these effects in relation to stress history. It is therefore a logical step that the structure of the surface be investigated in order that the mechanisms responsible for increased entrainment threshold as a result of stress history be identified and quantified. As such Chapter 6 will concentrate on the development of this understanding in light not only of the overall response to stress history but also to the possible difference in the mechanisms which arise as a facet of grain size distribution.

4.6 Chapter Summary

The results from this chapter have provided clear evidence demonstrating a stabilising influence of sub threshold flow on non cohesive sediment beds. This confirms the concept of stress history as previously defined by Paphitis and Collins (2005) in uniform sand beds and by Haynes and Pender (2007) in graded (bimodal) sediment beds. Akin to both studies, increasing the duration of antecedent flow increases the structural resistance of the bed to entrainment by fluid flow. Although beds subjected to the longest antecedent duration are the most stable, the greatest response to antecedent flows appears to occur for the shorter flow durations such that it is viable to assume a stability maxima would be reached if the antecedent duration were to be increased; this is in line with Monteith and Pender (2005).

Importantly this chapter has extended these findings through the analysis of the grade dependent response of bed stability to stress history regimes. Under benchmark conditions stability has been linked to the overall sand content of the mixture, where the coarse bed (least sand content) was more able to resist entrainment and the fine bed (greatest sand content) was the least able to resist entrainment. However, interestingly it has been shown that uniform beds are comparatively more responsive to stress history than graded beds. It is argued that this is primarily linked to the potential for greater rearrangement of the bed as compared to graded beds, where finer particles restrict in situ particle movement of the larger grains. Bedload data has been used to support these findings, acting as a proxy for bed stability, where increasing bed stability as a response to stress history is mirrored by decreased transported bedload. Specifically a change in the size selectivity of certain fractions in the transported load acts to alter the availability of certain fractions for transport and, hence, alter overall bed stability. A justified choice of questions has been highlighted in the latter part of the discussion based on the findings of the present Chapter where it has been suggested that there needs to be further investigation of the possible attainment of a stability maxima if the antecedent duration were to be extended (Chapter 5). In addition, it has been suggested that the influence of the bed surface texture and organisation may have a significant effects upon the stability of the bed, the exact mechanisms of which have only been postulated upon in this present chapter. There is therefore a need to fully quantify these effects such that the underpinning granular mechanics be understood (Chapter 6). Both questions need to be investigated in the light of the effect which grain size distribution has upon stress history induced stability.

Experiment Number	Grain Size Distribution	Antecedent Period Duration (Minutes)	Stability Test Duration (Minutes)	Average Critical Bed Shear Stress (Nm ⁻²)
1,2,3,4	UNIFORM	0	85	2.84
5,6,7		10	90	3.01
8,9,10		20	120	3.37
11,12,13		40	125	3.45
14,15,16		60	130	3.54
17,18,19,20	UNIMODAL	0	90	2.82
21,22,23		10	100	2.92
24,25,26		20	110	3.00
27,28,29		40	110	3.02
30,31,32		60	115	3.06
33,34,35,36	BIMODAL	0	60	2.43
37,38,39,		10	65	2.45
40,41,42		20	75	2.50
43,44,45		40	75	2.52
46,47,48		60	80	2.65
49,50,51,52	COARSE	0	155	4.03
53,54,55		10	155	4.06
56,57,58		20	170	4.16
59,60,61		40	160	4.07
62,63,64		60	170	4.12
65,66,67,68	FINE	0	60	2.27
69,70,71		10	70	2.53
72,73,74		20	65	2.35
75,76,77		40	60	2.31
78,79,80		60	70	2.46

Table 4-6; Summary of experimental variables for the experiments performed in the 0.3m flume using 5 grain size distributions and 5 antecedent durations (where 0 minutes acted as the benchmark).

Chapter 5 Stress History Experiments in the 1.8m wide flume

5.1 Introduction

The data set presented in Chapter 4 clearly indicates stress history does have an appreciable effect upon that entrainment threshold, acting to increase the threshold of entrainment by up to 25% over short antecedent time frames. Additionally, results presented in Chapter 4 noted a grade dependent response of bed stability where it was noted that uniform beds are comparatively more responsive than graded beds. This supports previous postulations by Haynes and Pender, (2007) and Reid *et al.*, (1985) who both implied that response to stress history is intrinsically linked to both relative grain size and surface grain size distribution.

Given that the implication behind the grade specific response to stress history appears to be linked to the development of bed structure, Chapter 6 uses high resolution laser scanning to specifically assess the impact stress history has upon bed structure. However, since the experiments for this were run in the wide flume facilities as described in Section 3.3 it was first necessary to confirm the stress history patterns observed in Chapter 4. This chapter therefore aims to compare the results derived from the wider flume facility with the trends presented in Chapter 4. In addition longer timeframes were used in this set of experiments which were chosen since results from Chapter 4 supported the notion of a stability maxima being reached if the timeframes of the antecedent duration were to be extended. From Chapter 4 it was noted that the coarse bed does not appear to respond to stress history and whilst the fine bed does respond the temporal aspect of this response is not clear. As such, given the time taken for each experiment and the associated post processing time these two grain size distributions were not analysed further. Consequently this chapter details 48 experiments using three distributions of graded sediment; near-uniform, weakly bimodal and unimodal which were contrasted using a common median grain size (D_{50}) (Section 3.4). As with Chapter 4, the temporal effects of stress history on bed stability were examined using a range of antecedent flow durations (0, 60, 120, 240 and 960 minutes) for a conditioning shear stress equal to 50% of critical shear stress of entrainment (τ_c). Akin to Chapter 4 this Chapter reviews critical shear stress of entrainment and bedload transport data as indicators of the relationship between stress history and bed stability; fractional bedload data is utilised to infer the processes of stability and possible influence of grade.

5.2 Hypothesis

Given that the general experimental set-up and grain size distributions remain the same as Chapter 4, the main distinction is that longer durations of antecedent flow are tested and, given the difference between the two flume facilities, the effect of width depth ratio is also explored. This chapter will therefore aim to address following working hypotheses;

- The stress history relationships with entrainment threshold, bedload and grade will be the same as Chapter 4
- Longer periods of antecedent flow will tend to a stability maxima.
- Given the difference in width of the two flumes and the consequent difference in flow characteristics, the response to stress history will be evidenced through a change in response to the change in width depth ratios.
- Higher width:depth ratios and reduced sidewall effects will influence the absolute data, compared to that of Chapter 4. Based on the literature these will decrease the absolute value of the critical entrainment threshold due to relative depth effects (Shvidchenko and Pender, 2000).

5.3 Experimental Procedure

The set of experiments employed within this chapter used the 1.8m wide flume facility as detailed in section 3.3 with the experimental procedure employed the same as that used within the threshold experiments presented in Chapter 4 (section 4.3) and will not be repeated here. The only difference between the two sets of experiments was the antecedent period duration where beds were exposed to stress histories of 0, 60, 120, 240 and 960 minutes duration in these sets of experiments. Runs of 0 minutes antecedency were again used as benchmark runs for stress history assessment. Finally the duration of each step in the stability test was increased to 10 minutes in duration to allow flow stabilisation, visual assessment of whether or not the new threshold had been reached and the collection of bedload in each step; the bedload sampling interval was set at 8 minutes in order to allow for the trap to be emptied during the time period of each stability step. Total load was then calculated as the sum of the total transported load collected during each step of the stability test. Although not detailed in this chapter, two laser scans (results detailed in Chapter 6) of the bed surface were taken prior to and after the antecedent period to quantify any changes to surface topography and composition. The implications of this are described in section 6.2. In order to increase the reliability of the dataset, experiments analysing entrainment

threshold were repeated three times for runs without an antecedent period and twice for all runs including an antecedent period. A total of 48 experiments (including repeats) were undertaken during which sediment was not re-circulated or fed into the flume.

5.4 Results

5.4.1 Critical entrainment threshold

Annalagous to Chapter 4, analysis in this section concentrates on describing the relationship between critical entrainment threshold and antecedent duration, summarised by Figure 5-1. Section 5.4.1 provides detailed results on; (i) absolute critical shear stress trends with respect to grain size distribution; (ii) general stress history trend analysis; (iii) relative stress history responses of different grain size distributions. These trends are highlighted within the context of the trends noted within section 4.4.2. Direct comparison of the comparative stress history trends between data sets generated in the narrow flume (smaller width depth ratios) under shorter antecedent durations and the wider flume (larger width depth ratios) over longer antecedent durations are discussed in section 5.4.1.

Absolute critical shear stress values for all three grain size distributions under benchmark conditions (i.e. no antecedent period) clearly show a hierarchy to stability (Figure 5-1). The unimodal bed requires the highest critical shear stress (3.09 Nm^{-2}) and is most able to resist entrainment followed by the bimodal bed (2.57 Nm^{-2}) with the uniform least able (2.41 Nm^{-2}) to resist entrainment. Specifically the threshold of the unimodal bed is 31.53% higher than the uniform bed and 23.35% higher than the bimodal bed. Within section 4.4.2 the opposite trend was noted where it was the uniform bed which was comparatively more stable than the graded beds under benchmark conditions.

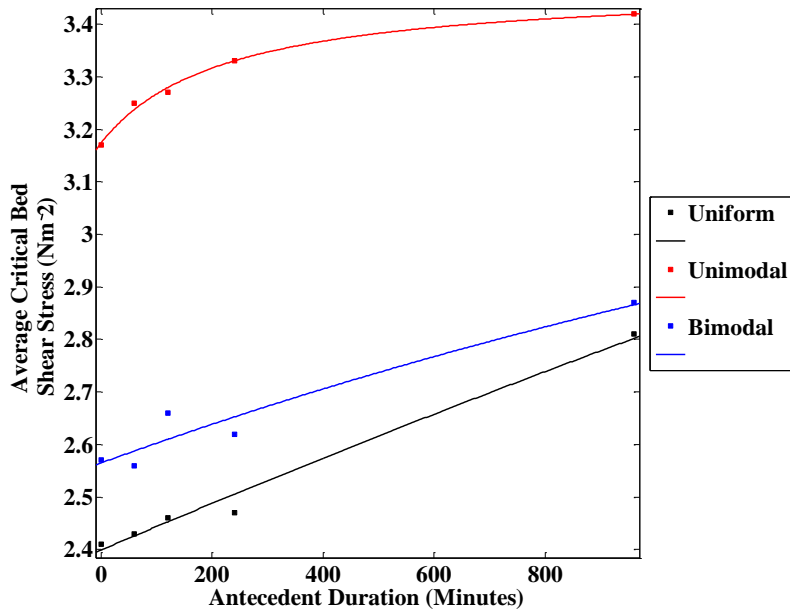


Figure 5-1; The relationship between antecedent duration, average critical bed shear stress and grain size distribution. The uniform, unimodal and bimodal beds are fitted with a linear polynomial growth curve with root mean square errors values of 0.03, 0.01 and 0.049 for the uniform, unimodal and bimodal beds respectively.

Stress history trend analysis reviews the general relationship between threshold and antecedence as shown in Figure 5-1. Akin to Chapter 4, results show a positive correlation between applied antecedent duration and average critical bed shear stress. A rational linear growth curve as described by equations 17 and 18 has been fitted to the data (Figure 5-1); this trend suggests that the initial rapid increase in bed stability is followed by a more gradual increase in response to the imposed flow regime. This is confirmed by the first derivatives of the fitted trend lines which are plotted in Figure 5-2. The greatest rate of change is noted within the unimodal bed where the most progressive response to stress history, especially after the shortest antecedent durations is clearly noted. However although increasing antecedent duration increases the resistance of the bed, data tends towards approximating to a stability maxima for the longest antecedent durations. Interestingly however a maximum has still not been reached supporting the notion that the bed will continue to evolve during sub threshold flow but that the growth may be increasingly small. Conversely in the uniform and bimodal beds an almost linear trend

with antecedent duration is noted suggesting that the development of resistance is occurring more progressively than for the other two beds.

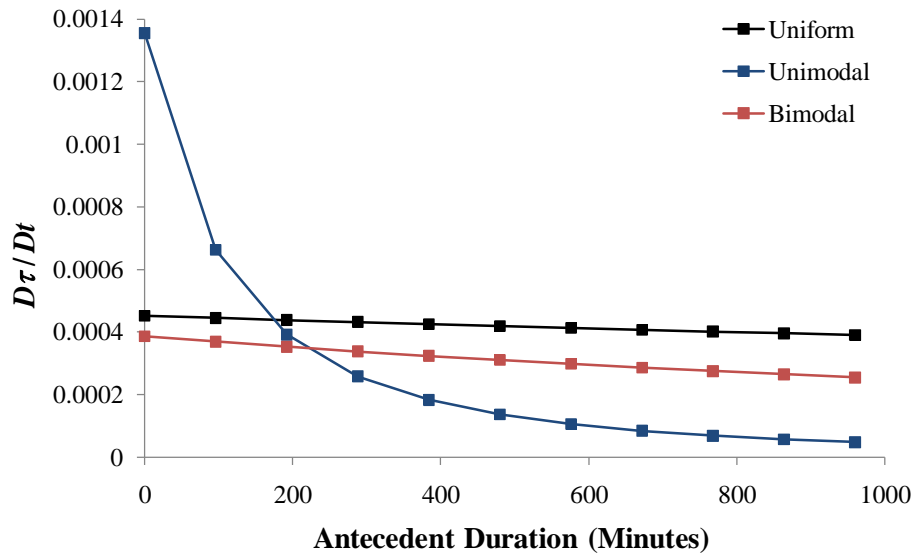


Figure 5-2; First derivative of the fitted trend lines of the response of the uniform, unimodal and bimodal grain size distributions respectively to antecedent flow duration.

The effect of grain size distribution on bed responsiveness to stress history shows the following hierarchy to 960 minutes of antecedent flow as compared to benchmark experiments; uniform (+14.2%) > bimodal (+11.5%) > unimodal (+7.3%). Specifically, whilst benchmark runs indicate that the threshold shear stress of unimodal bed sediment is 31.53% higher than that of uniform bed and 23.35% higher than the bimodal bed, following an antecedent duration of 960 minutes this difference decreases to 12.81% in the uniform bed and 10.45% in the bimodal bed; the difference between the three beds becomes less pronounced with increasing antecedent duration. This decrease in the magnitude of difference between the grades within increased antecedent duration could be important in terms of future application and the development of a stress history term into critical entrainment equations. It has been postulated in Chapter 4 that, given the differential response of each grade to stress history, and the apparent influence of modality, using the depth slope method based on the D_{50} to estimate the revised critical entrainment threshold in response to stress history needed revision to account for modality. However if the inter-flood period is long (as in the field and exemplified by the 960 minutes data in

this thesis) the shear stresses become more similar in magnitude. As such an initial analysis of shear stress change based on a D_{50} depth-slope estimate may be a good initial starting point with future research needed to fully develop an understanding of this effect.

5.4.1 *The effect of width depth ratios*

Given the use of the different flume facilities and the different shear stress values derived in section 4.4.2 as compared to that in section 5.4.1 in accordance with which flume was used it is vital to begin to postulate as to why the different trends are manifested. This is vital since it is liable that the fluid flow characteristics experienced between the two flumes will be different and hence may account for any observed differences in the stress history trends between the two flumes. A number of variables are likely to change in response to the different flume widths with the most obvious being a change to the width depth (z/b) ratio; for the experiments described, the Shields flume (0.3m wide) has lower width depth ratios and the Kelvin flume (1.8m) has higher width depth ratios. Data are detailed in Table 5-1 (Shields flume) and Table 5-2 (Kelvin flume). Further, given that the same grain sizes have been used within both flumes one of the manifestation of the change in channel width will be a change in the depth to grain size ratio otherwise known as the relative depth. This is particularly important when relatively shallow depths are being used as with the experiments described herein; it is often argued that depth to grain size ratio has little or no effect on the initiation of sediment motion in relatively deep flows (Gessler, 1971; Yalin, 1972) but conversely, flume studies (Misri *et al.*, 1983 and Shvidchenko and Pender, 2000, Cooper *et al* 2005; Legleiter *et al* 2007) demonstrated that the influence of relative depth on reported values of critical shear stress can be significant.

Typically the depth to grain size ratio is measured according to;

$$Rd_{gs} = \frac{z}{D_i} \quad \text{Equation (19)}$$

Where z is the flow depth at threshold and D_i is a representative grain size, in this case assumed to be the D_{50} . However more recently relative depth has been defined as the relationship between depth and hydraulic radius (e.g. Shvidchenko, 2000) derived according to Equation 20;

$$Rd = \frac{R_b}{D_i} \quad \text{Equation (20)}$$

Where R_b is the hydraulic radius as derived according to Equations 14 and 15 and D_i is a representative grain size, in this case assumed to be the D_{50} . Via the inclusion of the hydraulic radius, specific account is taken of the differences in flume width and is this equation which is deemed more accurate within the context of this thesis and is analysed below. Results are detailed in Table 5-1(Shields flume) and Table 5-2(Kelvin flume).

	Antecedent Duration (Minutes)	0	10	20	40	60
	b	0.30	0.30	0.30	0.30	0.30
Uniform	z	0.07	0.07	0.08	0.08	0.09
	τ_c	2.84	3.01	3.37	3.45	3.54
	b/z	4.29	4.29	3.75	3.75	3.33
	R_{dgs}	1.40	1.45	1.70	1.74	1.78
	R_b	0.06	0.06	0.07	0.07	0.07
	R_d	1.25	1.27	1.44	1.46	1.52
Unimodal	z	0.07	0.07	0.07	0.07	0.07
	τ_c	2.82	2.93	3.00	3.02	3.06
	b/z	4.29	4.29	4.29	4.29	4.29
	R_{dgs}	1.37	1.43	1.43	1.49	1.59
	R_b	0.05	0.05	0.05	0.05	0.05
	R_d	1.15	1.23	1.25	1.25	1.29
Bimodal	z	0.05	0.06	0.06	0.06	0.06
	τ_c	2.43	2.45	2.50	2.52	2.65
	b/z	6.00	5.00	5.00	5.00	5.00
	R_{dgs}	1.17	1.18	1.21	1.22	1.25
	R_b	0.06	0.06	0.06	0.06	0.06
	R_d	1.04	1.06	1.08	1.08	1.10

Table 5-1; Relative depth derived according to equation 20 (R_b/D_i) where z represents the flow depth (m), R_b is the hydraulic radius and D_i is the representative grain size, taken to be the D_{50} . Results are shown for all tested antecedent durations for the uniform, bimodal and unimodal beds respectively.

	Antecedent Duration (Minutes)	0	60	120	240	960
	b	1.8	1.8	1.8	1.8	1.8
Uniform	z	0.04	0.05	0.05	0.05	0.05
	τ_c	2.36	2.44	2.46	2.47	2.76
	b/z	40.91	40.00	39.13	39.13	36.00
	R_{dgs}	0.09	0.09	0.1	0.1	0.11
	R_b	0.02	0.02	0.02	0.02	0.03
	R_d	0.04	0.05	0.05	0.05	0.52
Unimodal	z	0.05	0.05	0.06	0.06	0.06
	τ_c	2.96	2.99	3.19	3.33	3.22
	b/z	33.96	33.96	31.58	32.14	30.00
	R_{dgs}	1.33	1.34	1.43	1.5	1.45
	R_b	0.03	0.03	0.03	0.04	0.04
	R_d	0.63	0.65	0.69	0.729	0.79
Bimodal	z	0.06	0.06	0.07	0.07	0.07
	τ_c	2.52	2.56	2.66	2.62	2.81
	b/z	28.57	28.13	26.09	25.00	26.09
	R_{dgs}	1.11	1.11	1.12	1.12	1.25
	R_b	0.02	0.02	0.03	0.03	0.03
	R_d	0.54	0.54	0.58	0.56	0.63

Table 5-2; Relative depth derived according to equation 20 (R_b/D_i) where z represents the flow depth (m), R_b is the hydraulic radius and D_i is the representative grain size, taken to be the D_{50} . Results are shown for all tested antecedent durations for the uniform, bimodal and unimodal beds respectively.

Two specific aspects of Table 5-1 and Table 5-2 are analysed below both in terms of the overall comparative trends and then for both data sets after 60 minutes of antecedent flow for the width depth ratio and relative depth term (R_b). Width depth ratios are consistently higher in the Kelvin flume (1.8m wide) for all three grain size distributions and decrease with increasing antecedent duration in both sets of experiments reflecting the increase in critical threshold depth. Comparative width depth ratios after 60 minutes antecedent duration are 89.28%, 87.58% and 82.22% higher in the Kelvin flume for the uniform, unimodal and bimodal beds respectively. Conversely the relative depths where ratios are consistently higher in the Shields flume (0.3m wide) for all three grain size distributions and increasing with increasing antecedent duration in both sets of experiments reflecting the increase in critical threshold depth. Comparative relative depth ratios after 60 minutes

antecedent duration are 63.93%, 47.15% and 49.06% higher in the Shields flume for the uniform, unimodal and bimodal beds respectively. According to Shvidchenko and Pender (2000), for a given bed shear stress and sediment size, a decrease of relative depth of 25 to 5 caused an almost twofold increase of Shields stress. This was deemed to be due to an increase in friction with decreasing relative depth for shallow flows is due to the increased effect of the wake eddies, shed by the bed particles on the overall flow resistance. As such a decrease in relative depth is associated with a decrease in both flow velocity, shear stress and bedload transport rate. From this it would be expected that the higher width depth ratio data (Kelvin flume) would have a lower shear stress in comparison with the data from the low width depth ratio data (Shields flume). This is however the opposite of the trend noted here where shear stress is noted to decrease with increasing relative depth such that data collected from the high width depth conditions exhibit the lower critical shear stresses of entrainment. This has been linked in the literature to a growing body of evidence (Cooper *et al.*, 2005; Legleitier *et al.*, 2007) which suggests that this trend might be due to the relationship between the flow depth and flow structure through its influence on the spatial persistence of the flow characteristics. It is therefore suggested that it is the flow characteristics which control the effects of relative depth rather than purely the resistance. This lends support to the findings here where bed shear stress increases with increasing antecedent duration; this is discussed in detail in the section **Error! Reference source not found.**

Given this relationship, the final section of the critical entrainment analysis uses both critical entrainment data sets plotted on the same graph to allow direct comparison of the shear stress relationships as a result of the different width depth ratios; this is plotted in Figure 5-3. On each figure data from the uniform, unimodal and bimodal beds are shown. Data from the low width depth ratio experiments are plotted using a solid line with a dashed line used to depict the predicted relationship between antecedent duration and shear stress if experiments were to be extended to 960 minutes under low width depth conditions. The results from the higher width depth ratio experiments are plotted using a dot and dash line. Figure 5-4 plots the first derivatives of the derived trends. This allows (i) direct comparison between the different experiments after 0 and 60 minutes antecedent flow; (ii) direct comparison between the predicted results using extrapolated trends from the low width depth experiments with collected data over the longest antecedent timeframes for the higher width depth ratio experiments.

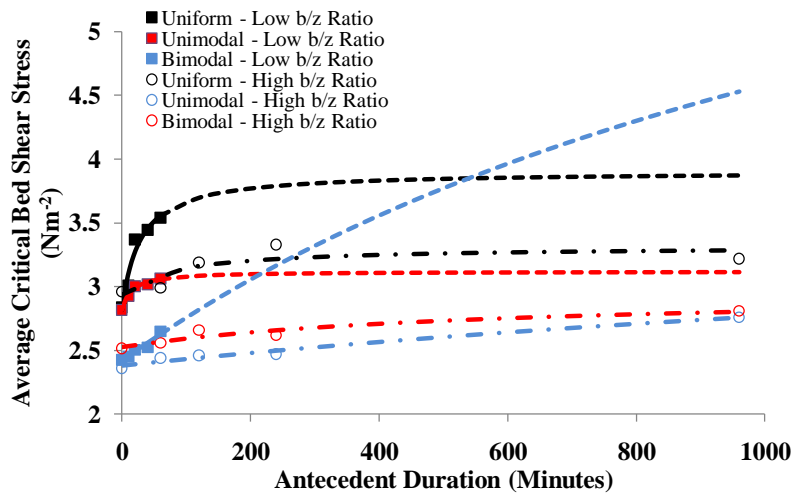


Figure 5-3; The relationship between antecedent duration, average critical bed shear stress, grain size distribution. The uniform, unimodal and bimodal beds are fitted with a linear polynomial growth curve. Data from the low width depth ratio experiments are plotted using a solid line with a dashed line used to depict the predicted relationship between antecedent duration and shear stress if experiments were to be extended to 960 minutes under low width depth conditions. The results from the higher width depth ratio experiments are plotted using a dot and dash line.

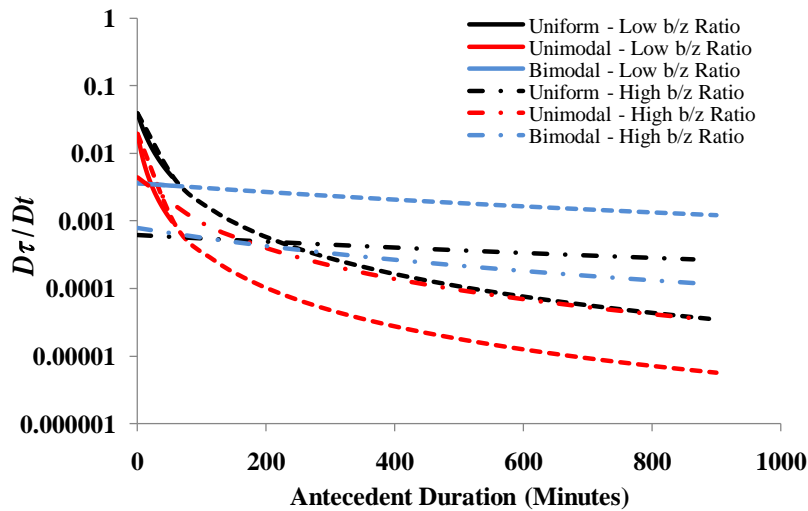


Figure 5-4; First derivative of the fitted trend lines of the response of the uniform, unimodal and bimodal grain size distributions respectively to antecedent flow duration. Data from the low width depth ratio experiments are plotted using a solid line with a dashed line used to depict the predicted relationship between antecedent duration and shear stress if experiments were to be extended to 960 minutes under low width depth conditions. The results from the higher width depth ratio experiments are plotted using a dot and dash line.

From Figure 5-3 and Figure 5-4 a number of similarities are noted with the data derived from both sets of experiments. Firstly, the trend analysis shows that although the magnitudes of response are different between the two sets of data, the response of all three beds to the applied antecedent flow can be described by a linear polynomial growth curves as described by equation 16 in section 4.4.3 by the same type of growth curves fitted to the separated data. This suggests that both data sets tend towards a stability maxima in excess of 960 minutes (low width depth results trend is based in extrapolation of the trend in critical shear stress noted after 60 minutes of antecedent flow). This is particularly noticeable in extrapolated values for the bimodal bed using the relationship from the low width depth ratio experiments with data suggesting that the stability maxima would be far in excess of the 960 minute data collected during this thesis; clearly further research is required to fully understand this difference. Secondly the rate of change is greatest during the early part of the experiment as described by equation 17 in section 4.4.3. This is especially noticeable in the uniform and unimodal beds. The bimodal bed shows a more progressive stabilisation regardless of the width depth ratio. Finally, both data sets note a hierarchy to stability where the uniform bed is most responsive to antecedent duration in comparison with the graded beds.

However, more interestingly a number of differences are manifested as the result of a change to the width depth ratios of the experiments. Under benchmark conditions critical bed shear stress is 16.87% higher in the uniform bed for the low width ratio experiments. Conversely in the graded beds a lower average critical bed shear stress is noted for the low width depth ratio experiments; a -3.70% and -5.04% reduction is noted for the unimodal and bimodal beds respectively. It is unclear as to why this grade dependent response should be noted with the only difference to the observed results being linked to the presence or absence of longitudinal ridges and troughs. In both graded beds for experiments run with lower width depth ratios such bedforms were present however in the uniform bed experiments bedforms were absent. Bedforms were absent in all experiments run for the higher width depth ratios. This suggests it is the overlying fluid flow regime (the streamwise vortices set which cause the bedforms to form) which are responsible for the observed trends; this is discussed in section **Error! Reference source not found.**

In terms of the relative response to stress history, comparative values of shear stress after 60 minutes of antecedent flow reveal that data from the low width depth experiments are

+21.83%, +7% and +7.32% higher than those measured in the higher width depth ratio experiments. Extrapolated trends reveal that after 960 minute it would be expected that a + 27.18%, +9.55% and 46.56% increase would be expected for the uniform, unimodal and bimodal beds respectively. The increases in the uniform and unimodal beds are similar to what is reported after 60 minutes (+ 25.00% and +8.00%) suggesting that increasing the antecedent duration would have only minimal affects upon the overall critical bed shear stress. In the bimodal bed, extrapolating the 60 minute data trend to 960 minutes increases the critical bed shear stress by 46.56%; this is 37.56% increase over the recorded data after 60 minutes of antecedent flow suggesting that by increasing the antecedent duration a significant change would be noted to overall bed stability. However in comparing all three results with the results collected after 960 minutes flow during the higher width depth ratio experiments deviations between these expected trends are noted. Specifically, the extrapolated critical shear stress values based on the lower width depth ratio experiments are 12.98%, -1.45% and +39.26% different from those reported from the higher width depth experiments.

Finally in terms of the overall hierarchy to stability whilst the uniform bed remains the most responsive to stress history regardless of width depth ratio the type of modality (unimodal or bimodal) affects the relative degree of stabilisation attained during the antecedent period. In the low width depth ration experiments whilst the type of modality affects absolute values of critical threshold, it has very little effect on the relative degree of stabilisation attained during the antecedent period (+8 to +9%) after 60 minutes of antecedent flow. This was deemed to be due to the similar proportions of fractions comprising the fine and coarse ends of the grain size distributions, hence similar relative grain size effects and hiding may occur during the antecedent period (Table 3-1). However in the higher width depth ratio experiments the type of modality not only affects the absolute critical values (bimodal shear stress is up to 19.68% higher than the unimodal bed) it also affects the relative degree of stabilisation attained during the antecedent period (+3.58% to +4.68%) after 60 minutes of antecedent flow and +11.5% and +7.3% for the unimodal and bimodal beds respectively after 960 minutes of antecedent flow. This suggest that increasing the antecedent duration to 960 minutes has a greater effect upon the bimodal bed (as evidenced by a higher overall response to stress history) when the width depth ratios are higher as compared to the unimodal beds. Specifically, that whilst the majority of the change occurs during the first 60 minutes stability the bed is still

rearranging and gaining in stability after the longest antecedent durations. This is in comparison with the unimodal bed which seems to stabilise under different time frames; this will be quantified mechanistically in Chapter 6.

Results comparing the two different flume facilities in terms of width depth ratio and relative depth together with their influence upon critical bed shear stress can be summarised as;

- Width depth ratios are consistently higher in the Kelvin flume; after 60 minutes of antecedent flow width depth ratios are 89.28%, 87.38% and 88.22% higher in the Kelvin flume as compared to the Shields flume
- This is manifested as a difference in the relative depth ratio where ratios are consistently higher in the Shields flume; after 60 minutes of antecedent flow width depth ratios are 63.93%, 47.15% and 49.06% higher in the Shields flume as compared to the Kelvin flume.
- Shear stress trends noted that shear stress increases with with decreasing relative depth such that data collected from the low width depth conditions are +21.83%, +7% and +7.32% higher than those measured in the higher width depth ratio after 60 minutes of antecedent flow.

5.4.2 Total transported bedload

Trends of the magnitude of the total bedload transported during the stability test were evaluated for the three beds to provide proxy data on bed stability response to antecedent flow durations from 0 to 960 minutes. However as discussed in section 4.3, given the different stability test durations (40 minutes through to 140 minutes, depending on grade; Appendix A Table 1) and the change in this duration due to stress history per individual grade (10 to 55 minutes; Appendix A Table 1) direct comparison of absolute bedload data is not made. The justification for using total bedload as a proxy indicator has already been discussed in section section 4.3 and so will not be repeated here. This section focuses on trend and statistical analysis of the bedload data sets with the structure of data analysis being: (i) total bedload transport trends with respect to grain size distribution; (ii) stress history regression analysis; (iii) total bedload transport trends with respect to shear stress; (iv) bedload composition analysis, specific to detailed fractional analysis and comparison to the initial bulk mix. These findings are considered in light of the trends noted in Chapter 4 for similar analysis over shorter antecedent durations.

Stress history effects on total bedload transport are given in Figure 5-5. This analysis illustrates the expected inverse relationship between bedload transport and stress history; this shows that beds subject to prolonged periods of antecedent flow are increasingly resistant to entrainment as manifested through lower sediment transport rates. Extending the antecedent period from 0 to 960 minutes resulted in the total bedload transported reducing by the following grade-specific hierarchy: bimodal (-89%) > near uniform (-65%) > unimodal (-50%). Regression analysis of total transported load as a function of antecedent duration (Figure 5-5) for all three grades can be defined by an exponential function superimposed on a background constant transport fitting as derived by Equation 19 in section 0 Grade-dependency of stress history response (as defined by total bedload) is examined using the first derivative of the regression curve (Figure 5-6). From this it is evident that the rate of bedload reduction is greatest during the early part (0-60 minutes) of the applied antecedent period. This data supports earlier results from threshold data (given in Section 5.4.1) suggesting that, although a continual decrease in the rate of sediment transport with increased antecedency of flow is likely to be noted, very little additional stability is likely to be afforded by extended sub-threshold flow durations.

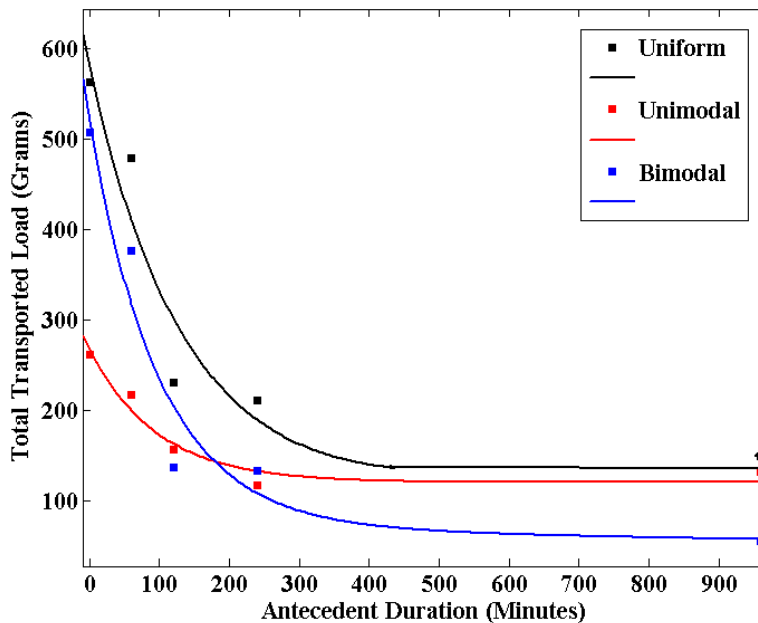


Figure 5-5; Stress history relationships with total bedload fitted with an exponential decay function superimposed in a background constant noting R^2 values of 0.92, 0.95, 0.94, for the uniform, unimodal and bimodal beds respectively.

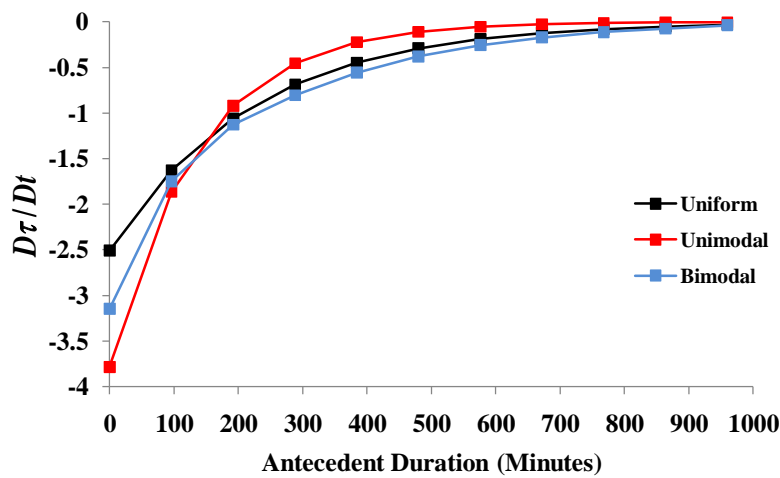


Figure 5-6: First derivative of the fitted trend lines of the response of the uniform, unimodal and bimodal grain size distributions respectively to antecedent flow duration.

In terms of the comparative effects between the two flume facilities at 60 minutes it is only possible to directly compare the response of the unimodal and bimodal beds. This is because uniform bedload data was not collected in Chapter 4 and coarse and fine data were not analysed in Chapter 5. Comparison of the absolute total load data reveals that for experiments run in the flume with the lower width ratios (Shields Flume) total loads are up to 78% higher in the unimodal bed and 91% higher in bimodal bed as compared to experiments run with higher width ratios (Kelvin Flume). This difference is feasibly linked to the difference in the duration of the stability test, where more steps in the stability test were needed in experiments run under low width depth ratios (as a facet of the greater stability gains in overall critical bed shear stress). Consequently the stability test durations used for experiments with the lower width depth ratios were up to 25 minutes longer in the unimodal bed experiments and up to 30 minutes longer in the bimodal bed experiments; this may explain the greater absolute transport values. In terms of the comparative response to stress history, whilst the hierarchy to response of the bimodal and unimodal beds is the same as those reported in section 4.4.2 the comparative responses after 60 minutes of antecedent flow shows that the reduction in bedload for experiments run with the lower width depth ratios are up to 25% and 9% greater as compared to experiments run with the higher width ratios for the unimodal and bimodal beds respectively. Both differences between the data sets, are in part, likely to be due to the development of bedforms within the narrow flume (as discussed previously) acting to increase the total transported load. Specifically, the progressive development of low-relief, low-resistance

troughs within unimodal and bimodal beds appeared to stabilise the coarse fractions as ridges and preferentially route finer material through the troughs. Such development is usually attributed to the lateral transport of particles by a series of streamwise – oriented vortices (Prandtl, 1952; Karcz, 1973; Nezu and Nakagaw, 1993; McLelland *et al.*, 1999) where secondary flow cells are developed such that upwelling flow is noted over the smoother parts of the bed and downwelling over the rougher ridges (Hinze, 1973; Colombini and Parker, 1995). Such bedforms were not noted in the experiments carried out in the wider flume as reported in this chapter. This is the likely effect of the side wall influence where the lateral vortices set up due to sidewalls; in the Shields flume the side wall influence is much greater and therefore sets up stronger secondary flows however in Kelvin flume the sidewall influence is far less and therefore the same cross flume series of secondary flow structures are not as readily developed.

In addition to analysing stress history effects upon total bedload trends, analysis of total bedload as a function of shear stress was also possible within this set of experiments since bedload data was also collected in each step of the stability test. Whilst the trends observed during the stability test are not the explicit focus of this thesis they do provide information on how the antecedent period may affect the onset of entrainment when a bed is exposed to higher shear stresses following the antecedent period. Typically, such analysis uses data collected from a wide range of shear stresses; at low shear stresses marginal transport is observed however as shear stress increases partial mobility is noted which extends to full equal mobility at the highest shear stresses (e.g. Wilcock and Southard, 1989). Although data here was only recorded up unto threshold the relationships derived are still useful and can be compared to patterns typically found during the progression of an experiment. Figure 5-7, Figure 5-8 and Figure 5-9 plot average bed shear stress of each step of the stability test as a function of the total transported load for the uniform, unimodal and bimodal beds respectively. It is postulated that increasing antecedent duration would lead not only to lower total loads per step of the stability test (as inferred by Figure 5-5) but that the onset of transport would occur later on within the stability test as antecedent duration is increased as a result of a stronger antecedent bed. Within the uniform bed (Figure 5-7) although large amounts of scatter appear in the data two trends are defined. Firstly, a positive correlation between average bed shear stress and total load is noted such that increased average bed shear stress (i.e. increased time into the stability test) is correlated with an increase in transported load for each step of the stability

test. The outlier to this trend is the data for the lowest shear stress (1.35Nm^{-2}) where transported load for the 120 and 960 minute experiment is at least one order of magnitude higher than would be expected according to the trend of the other data. This is conceivably linked to the displacement of sediment at the trap margins by air pockets which are released as the trap is opened to purge the sediment. Secondly, an inverse relationship is noted between antecedent duration and transported load in each step of the stability test whereby a decrease in total load is correlated to an increase in antecedent duration. This suggests that a stronger bed, more able to resist entrainment, is formed as the duration of antecedent flow duration is increased such that smaller amounts of sediment, is transported at a comparable shear stress. Thirdly there is no observable delay to the onset of entrainment, so although bed shear stress is increased with the application of an antecedent flow period, the bedload appears to be independent of the relationship with antecedent flow. This supports the notion that bedload is governed by interdependent mechanisms such as interaction with bed roughness, bed surface composition and near bed flow characteristics (Nelson *et al.*, 1995; Drake *et al.*, 1988; Cooper *et al.*, 2009).

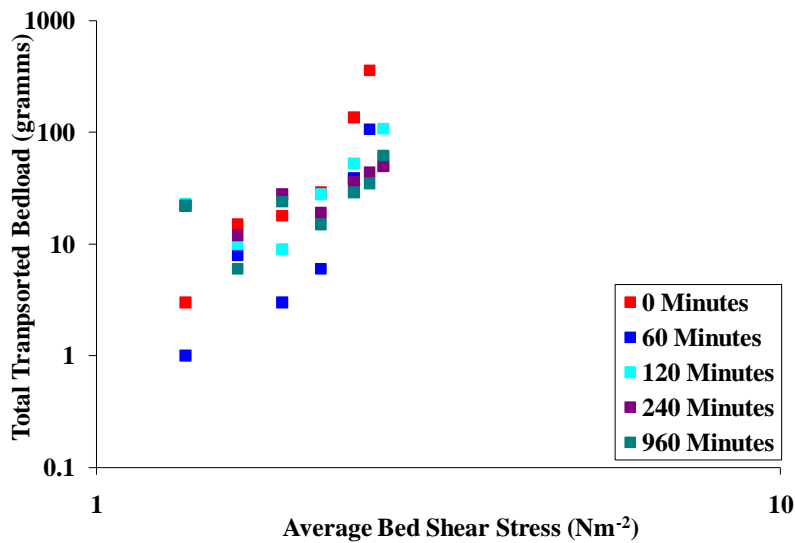


Figure 5-7; Total transported load at each flow step of the stability test plotted against the average bed shear stress for that flow step for the uniform bed. The graph is plotted on a log log axis.

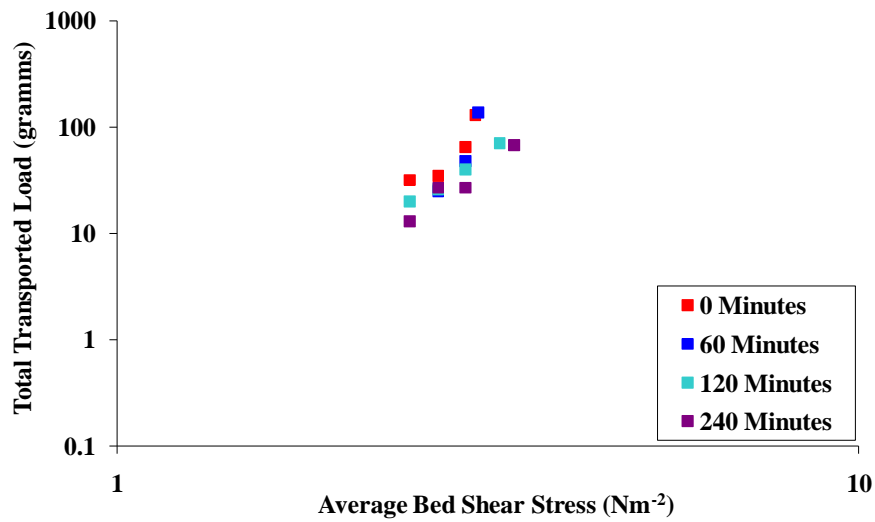


Figure 5-8; Total transported load at each flow step of the stability test plotted against the average bed shear stress for that flow step for the unimodal bed. The graph is plotted on a log log axis.

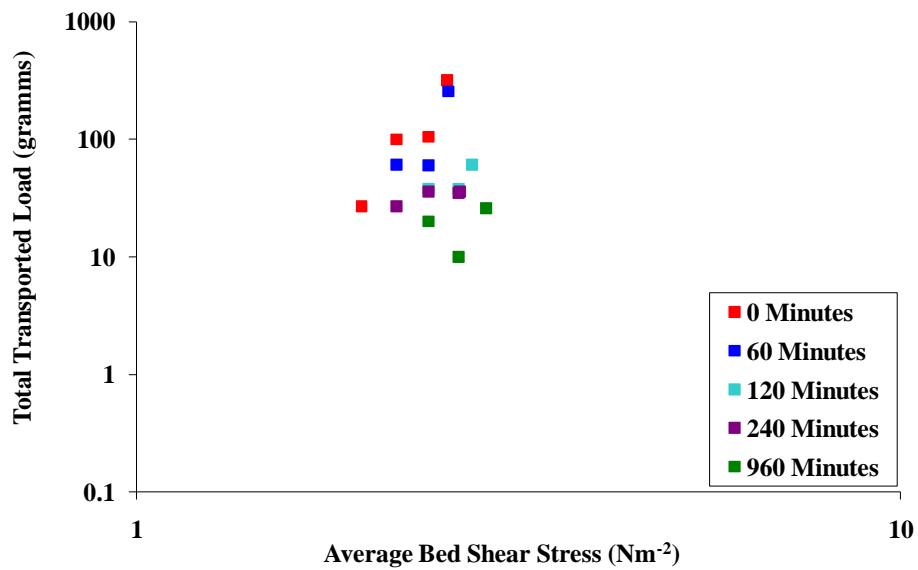


Figure 5-9; Total transported load at each flow step of the stability test plotted against the average bed shear stress for that flow step for the bimodal bed. The graph is plotted on a log log axis.

In both the unimodal (Figure 5-8) and bimodal bed (Figure 5-9) a much clearer pattern is noted as compared to the uniform bed (the 960 minute data is not presented for the

unimodal bed as failure of the submersible pump during the experiment meant the sediment trap could not be opened and closed allowing only total load to be collected for that experiment). Three trends are discernable; firstly an increase in transported load is positively correlated with an increase in time into the stability test (i.e. increase in average bed shear stress) and an increase in antecedent duration is mirrored by a decrease in the transported load for the same shear stress at each step of the stability test. This is akin to the uniform bed. Secondly in the bimodal bed an offset is noted on the abscissa such that transport does not commence until later in the stability test (i.e. at higher average bed shear stresses) as antecedent duration is increased; this is not noted for the unimodal bed. This suggests that although the uniform bed is more responsive to stress history than the bimodal bed in terms of average critical bed shear stress, the bimodal bed generates a bed surface which affects the transported bedload to a greater extent. This begins to suggest that the organisation of different bed surfaces is, in part, responsible for the overall responsiveness of the bed to the applied antecedent flow. Finally, for both the unimodal and bimodal bed an increase in the spread of the data on the ordinate axis is noted with increasing bed shear stress is noted; scatter within the unimodal data seen to span just under one order of magnitude at the lowest shear stresses which increase to just over one order of magnitude at threshold. Comparatively at lower shear stress conditions in the bimodal bed bedload spans approximately 1 order of magnitude which increases to just under 2 orders of magnitude at threshold conditions. The change in scatter may be related to the postulation that, under threshold conditions, particle mobility is more sensitive to flow turbulence and local grain characteristics such as imbrication, orientation and protrusion (Carling, 1983; Andrews and Parker, 1987; Church *et al.*, 1998). This suggests that antecedent duration has a greater effect upon bimodal beds as compared to unimodal beds which is analogous to the entrainment data in section 5.4.1. Conversely, although the uniform bed exhibits scatter this does not change with increased bed shear stress. This is likely to be linked to the fact that the uniform bed cannot structure in terms of the development and hiding as with this the uniform beds. As such the susceptibility of a grain to entrainment on a uniform bed essentially remains similar in response to antecedent duration such that scatter in the entrainment data remains similar irrespective of antecedent duration.

Relationships derived between both total load with antecedent duration and total transported load with average bed shear stress suggest the effects of antecedent duration are twofold; not only are smaller amounts of sediment transported where beds are exposed

to prolonged periods of antecedent duration but entrainment can also be delayed such that higher shear stresses are needed to initiate motion. In part, this is believed to be because of the development of structuring on the bed surface acting to alter the overlying flow characteristics so as to change entrainment threshold. However neither analytical method yields information regarding which fractions of the bed are most influenced by the antecedent flow period. Thus the following analysis concentrates on the temporal development of the grain size distribution of the transported load. This allows assessment of the development of the total load as compared to the parent population, identifying temporal trends and making inferences about the processes underpinning stabilisation. Bedload composition analysis is therefore performed using two distinct techniques. Firstly, the change in geometric standard deviation (σ_g) of the bedload following each antecedent duration is analysed; this acts as a proxy indicator of the degree of selective entrainment caused by stress history. Secondly, raw bedload data is subsequently provided for each fraction and corrected for relative abundance with respect to the bulk mix; this more detailed data set specifically reviews the response of the D_{50} as an indicator of graded bed response before assessing the role of individual fractions in generating bed stability under antecedent conditions.

Figure 5-10 plots average critical bed shear stress against geometric standard deviation (σ_g) for the bimodal and unimodal distributions. This seeks to demonstrate two things (i) the relative effect of σ_g on average critical bed shear stress; and (ii) the evolution of σ_g with increasing antecedent flow. Three key findings stem from this data. Firstly an inverse relationship is noted between σ_g and critical bed shear stress which approximates to a logarithmic reduction; this is akin to the findings noted in Figure 4-7. Given the nature of the exponential decline, this data suggests that there is a stronger relationship at higher critical shear stresses and lower σ_g values (i.e. the unimodal bed). Secondly, the nature of the regression seems to be independent of antecedent duration where it is not possible to differentiate the antecedent duration effects. Finally, there is an inverse relationship between σ_g and antecedent duration; a -6.16% reduction in σ_g is noted within the unimodal bed as antecedent duration is increased from 0 to 960 minutes and a -26.67 % reduction is noted within the bimodal bed over the same antecedent durations. A reduction in the spread around the mean is indicative of fewer grains being present within the transported bedload from the extremes of the distribution i.e. fewer smaller and larger grains which, in

turn, imply that there are significant hiding effects and hence selective entrainment of the middle fractions occurring. Two mechanisms were used to explain this in Chapter 4; firstly the development of structures on the bed surface such that larger grains act as keystones around which smaller grains are sheltered or secondly the infiltration of finer grains vertically into the bed matrix such that they are unavailable for transport as bedload. The latter may explain the reduction of smaller grain sizes within the transported load. It is likely that both processes are occurring but the relative importance of each is unknown; laser data from Chapter 6 will begin to address these questions.

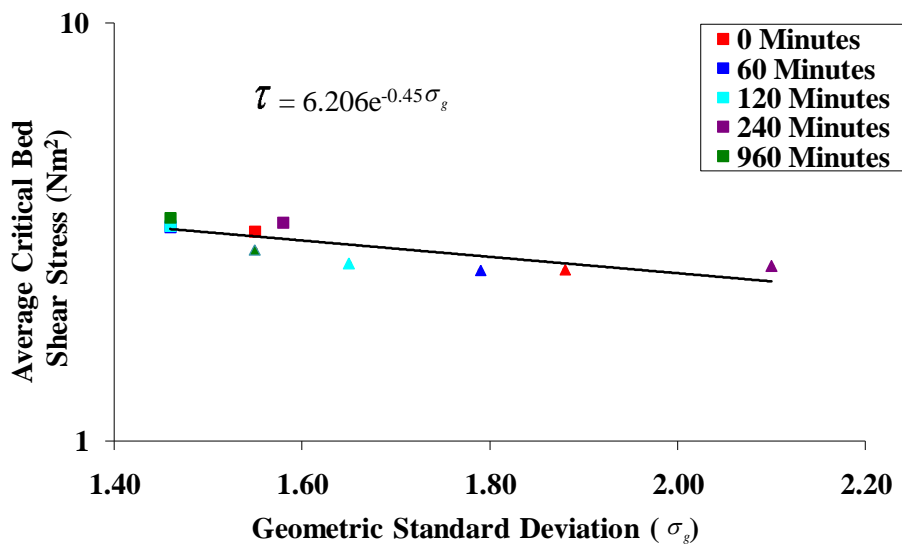


Figure 5-10: Critical bed shear stress plotted as a function of geometric standard deviation (Unimodal σ_g ranging from 1.46 to 1.58 (**1.55**), and the Bimodal σ_g ranging from 1.55 to 2.10 (**1.88**), where bold denotes the original σ_g for 0 minutes antecedent flow). Unimodal data points are represented by square markers whilst the bimodal data points are represented by triangular markers.

In terms of the comparative responses between those noted in Chapter 4 and those noted within this Chapter the percentage reduction is greater in the experiments run in the flume with the low width depth ratios (shorter antecedent durations) at comparative time periods (60 minutes antecedent flow); a -16% and -21% reduction for the unimodal bed and bimodal beds respectively as compared to a -4.73% and -14.69% reduction in the larger width depth flume experiments. However a similar inverse relationship is noted between σ_g and critical bed shear stress which approximates to a logarithmic reduction; this is akin to the findings noted in Figure 4-7. Given the nature of the exponential decline, this data

suggests that there is a stronger relationship at higher critical shear stresses and lower σ_g values (i.e. the unimodal bed), again akin to trends noted in section 4.4.3. This supports the earlier differences in both the average critical bed shear stress and total load data. Finally, similar to the results in Chapter 4, there is an inverse relationship between σ_g and antecedent duration where the bimodal bed shows the greatest reduction in σ_g over time although more interestingly the nature of the regression noted in Figure 5-10 seems to be independent of antecedent duration where, unlike Figure 4-7, it is not possible to differentiate the antecedent duration effects.

Given that σ_g only considers relative grain sizes rather than absolute grain sizes the last section analyses the change in individual fractions of the total bedload transported in the stability test. Data is provided in Table 5-3 and Table 5-4 (with cumulative frequency distribution graphs shown in Appendix C). Initial analysis reviews the effect of stress history on the D_{50} fraction to ascertain whether the bedload fines or coarsens in response to stress history; by proxy this provides complementary information to the σ_g analysis. Specifically, this section analyses the percentage change between: (i) the bulk mix and bedload subsequent to 960 minutes of applied antecedent flow and, (ii) 0 and 960 minutes antecedency data sets; the latter provides more specific analysis of stress history effects on water-worked beds, as reasoned in Chapter 4.

Comparison with the bulk mix in both beds indicates that whilst grades maintain their general distribution form there is a positive correlation between antecedent duration and bedload fining. This shows that fine grains become relatively more mobile compared to coarse particles. Data from Figure 5-5 has already shown that this change cannot stem from enhanced total transport of fines; hence by proxy it most likely results from the progressive decrease in the availability of, coarser fractions for transport as they become more stable following longer antecedent flow periods. In both beds data indicates a progressive fining of the bedload D_{50} by -7.58% and -10.70% as compared to that of the original unimodal and bimodal bulk mix. However D_{50} statistics in Tables 8 and 9 indicate a variable temporal relationship with no obvious progressive trend in the fining of D_{50} as antecedent duration increases to 960 minutes. The comparatively larger response of the D_{50} in the bimodal bed as compared to the unimodal bed is in line with findings from section 0 where the greater instability noted in the bimodal bed was postulated to be due to either the

lower proportion of D_{50} within the mixture making this fraction less stable in the bulk mix or the relationship with the geometric standard deviation response noted previously. In addition it is possible that this trend is caused as a facet of the analysis-by-weight technique which has the ability to skew the data when the bedload transport rates are very low as in this thesis.

Parameter	Bulk Mix	0	60	120	240	960	% diff between bulk mix and 960 minutes	% diff between 0 and 960 minutes
D₅	1.91	1.55	1.74	1.74	1.92	1.94	1.55	20.10
D₁₆	2.83	2.34	2.83	2.86	3.57	2.45	-15.51	4.49
D₅₀	4.97	5.18	4.74	4.65	5.27	4.62	-7.58	-12.12
D₈₄	10.08	10.33	9.11	7.84	8.5	10.22	1.37	-1.08
D₉₅	14.71	13.89	14.36	12.83	10.35	13.22	-11.27	-5.07

Table 5-3; Evolution of grain parameters with increasing antecedent duration for the unimodal bed.

Parameter	Bulk Mix	0	60	120	240	960	% difference between bulk mix and 960 minutes	% difference between 0 and 960 minutes
D₅	1.68	1.83	1.67	1.43	1.69	1.98	15.15	7.58
D₁₆	2.89	2.83	1.82	2.48	3.07	3.23	10.53	12.38
D₅₀	4.76	4.13	3.72	4.50	4.42	4.30	-10.70	3.95
D₈₄	7.82	6.16	6.32	6.77	7.17	6.08	-28.62	-1.32
D₉₅	11.31	9.88	9.56	9.66	11.07	9.18	-23.20	-7.63

Table 5-4; Evolution of grain parameters with increasing antecedent duration for the bimodal bed.

Comparison with the water worked bed (0 minute data) shows a more complicated and less pronounced response as compared to the pervious bulk mix analysed above. This finding is expected as the water-working period is, to some degree, akin to the application of subsequent sub-threshold stress history which has been demonstrated to change bed stability. Direct stress history relationships with fractional bedload are statistically presented in Table 5-3 and Table 5-4 as a percentage change in grain diameter as antecedency progresses from 0 to 960 minutes. In the unimodal bed the finest fractions increase in the transported load and the coarsest fractions decrease in the total transported load as compared to the benchmark proportions; this suggests the stabilisation of the coarsest fractions on the bed surface and the instability of the finest grains. The mobility of the finest fractions is perhaps surprising as it would be expected that the grains would be winnowed vertically through the bed surface and hence become unavailable for transport. As such their increased mobility suggests that other mechanisms possibly linked to the change in the overlying turbulent flow regime are responsible for their instability. The fraction containing the D_{50} shows greater magnitude decrease than compared to the relationship with the bulk mix; this is akin to the findings in section 0 where the D_{50} was seen to be stable on the bed surface. Conversely the bimodal data generally shows the same pattern as that compared to the bulk mix with the exception of the fraction containing the D_{50} which becomes relatively more mobile. Again this relative mobility of the D_{50} is akin to analysis in section 4.4.3.

Thus results derived from the total transported load for each sediment grade reveal four inferences.

- Increasing the duration of the antecedent flow decreases the total transported load for all three grain size distributions which is taken as a proxy indicating increased stability of the bed.
- Akin to the threshold analysis dataset, the response of total transported load to the imposed stress history regime shows significant grade dependency. Extending the antecedent flow period results in the transported bedload reducing by the following grade-specific hierarchy: bimodal (-89%) > uniform (-65%) > unimodal (-50%).
- There is an inverse relationship between the change in the geometric standard deviation and the length of antecedent flow duration although

the relationship between antecedent duration and geometric standard deviation is not well defined.

- In both beds data indicates a progressive fining of the bedload D_{50} as compared to that of the original bulk mix. However D_{50} statistics indicate a variable temporal relationship with no obvious progressive trend in the fining of D_{50} as antecedent duration increases to 960 minutes.

Thus comparative results after 60 minutes antecedent duration for low and high width depth ratio experiments) derived from the total transported load for each sediment grade reveal three inferences.

- Whilst the hierarchy to response of the bimodal and unimodal beds is the same as those reported in section 4.4.2 the comparative responses after 60 minutes of antecedent flow shows that the reduction in bedload for experiments run with the lower width depth ratios are up to 25% and 9% greater as compared to experiments run with the higher width ratios for the unimodal and bimodal beds respectively. This is likely to be due to the development of bedforms in experiments run with lower width depth ratios acting to increase the total transported load. Such bedforms were not noted in the experiments carried out for experiments where width depth ratios were higher. This is the likely effect of the side wall influence where the lateral vortices responsible for the development of these bed forms are generated in response to the influence of the sidewalls; in the Shields flume the side wall influence is much greater and set up stronger secondary flows however in Kelvin flume the sidewall influence is far less and therefore the same cross flume series of secondary flow structures are not as readily developed.
- There is an inverse relationship between the change in the geometric standard deviation and the length of antecedent flow duration in both sets of experiments however the experiments run with smaller width depth ratios note a greater overall reduction in geometric standard deviation (an 11.27% and 6.31% greater reduction for the unimodal and bimodal beds respectively).
- The comparatively larger response of the D_{50} in the bimodal bed as compared to the unimodal bed is in line with findings from section 0 however the fining of the D_{50} is up to 43.37% and 71.04% greater in the experiments run using the lower width depth ratios for the unimodal and bimodal beds respectively.

5.4.3 *Fractional transported bedload*

Analysis to date both in this chapter as well as that presented in Chapter 4 reveals that, as the total bedload transported decreases as a function of stress history there is also a change to the selectivity of the transport which is occurring. Thus, in order to be able to begin to understand why the response to stress history differs from one grade to another, there is a need to specifically analyse the stability-mobility patterns of individual fractions within each grade. As in Chapter 4 results in this section concentrate on analysing fractional bedload transport rate, g_i , (scaled by the abundance of each size in the bulk mix, F_i) plotted against dimensionless size (fraction scaled by the bulk D_{50}). These plots tend towards having an 'n' shape, tending to equal mobility in the middle of the distribution and selective transport for sizes at the extremes of the distribution due to both hiding effects and sampling inefficiency for smaller grain sizes (Wilcock, 1992). The position of the distributions on the graph give an indication of the rates of transport, meaning that the spacing of the lines and their slopes can be used to interpret changes in size selectivity and grain size distribution as stress history changes.

Within the unimodal bed (Figure 5-11) a decrease in the transport rate as a function of antecedent duration is noted with the exception of the 960 minute data which appears to be the outlier from the trend. Under benchmark conditions (0 minutes antecedent duration) there is a trend towards equal mobility, especially in the intermediary size fractions. Increasing the antecedent duration from 0 to 240 minutes (the 960 minute data is not used as it is the obvious outlier from the trend) exacerbates size selective entrainment tendencies where fractions up to the D_{50} and the coarsest mobile fractions (8-11.2mm) show size selective mobility. This effect is more noticeable in the fine end of the distribution and it is these fractions which show the greatest response to antecedent duration. The intermediary fractions between those two extremes remain characterised by equal mobility. As antecedent duration is increased mobility of particles finer than the D_{50} decreases where, after 240 minute antecedent duration, fractional transport rates are seen to decrease by up to 2 orders of magnitude in these grain fractions. Conversely, although the coarsest fractions decrease in relative abundance as antecedent duration is increased the reduction in mobility spans approximately one order of magnitude such that the reduction in the mobility of the fines is nearly twice that of the coarsest fractions. This is in line with the

degradational experiments of Hassan and Church (2000) who note fractional transport rates were seen to decrease by up to several orders of magnitude as degradational armouring periods were increased. The greatest decrease in the fractional mobility of the smaller grains is noted to occur between the 0 and 60 minute data suggesting that the majority of surface compositional change occurred early in the experiment allowing surface modification and rearrangement later in the experiments in line with Marion *et al.*, (2003) suggesting that it is the change in the flow at the beginning of the experiment which is more critical than the timeframe of the flow.

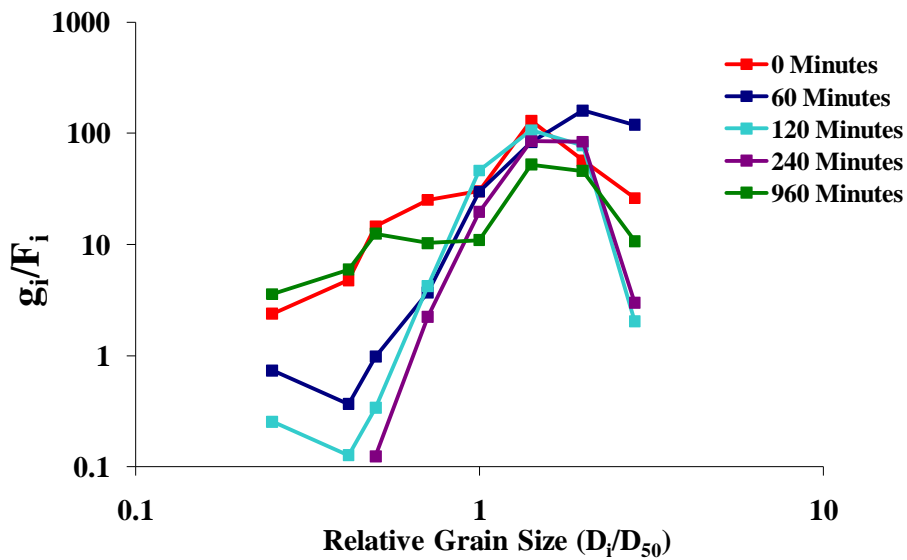


Figure 5-11; Fractional bedload transport rate of the unimodal bed scaled by the abundance of each size in the bulk mix plotted against dimensionless size for all five antecedent durations.

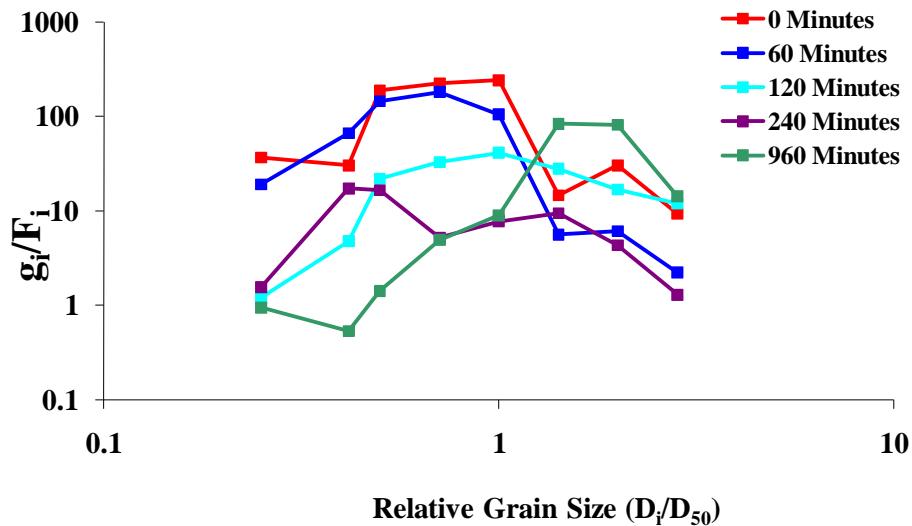


Figure 5-12; Fractional bedload transport rate of the bimodal bed scaled by the abundance of each size in the bulk mix plotted against dimensionless size for all five antecedent durations.

Within the bimodal bed (Figure 5-12), akin to the unimodal bed, a decrease in the transport rate as a function of antecedent duration is noted. Under benchmark conditions selective entrainment of the finest and coarsest fractions is noted with size fractions around the mean (2.4-5.6mm) being transported in equal mobility conditions. The finest fractions and those above the median are underrepresented in the bedload which suggests that hiding effects are present. The temporal trends note a clear inverse relationship between total transport rate and the duration of the antecedent flow is noted where the bed after 960 minutes antecedent duration is most stable and least sediment is transported. The degree of size selective transport increases with increasing antecedent duration such that fine and coarse fractions become increasingly transported by size selective transport as compared to the median fractions which are transported in equal mobility proportions. The 960 minute data is the outlier from this trend where it appears that the pattern of transport is shifted along the abscissa as compared to the other four experiments. This shift shows that particles up to the coarsest fractions are transported under size selective conditions indicating that not only has the total transported load decreased but the distribution of grain sizes being transported has become over represented by the coarser fractions. Antecedent duration seems to have the greatest effect upon the transport of the finest fractions ($<D_{50}$) as it is these fractions which decrease to a greater extent as compared to the coarser fractions.

This can be explained by the infiltration of finer grains into the bed such that they become unavailable for transport (Allan and Frostick, 1999; Brasington *et al.*, 2000). However the degree to which the fine end members of the distribution stabilise is not as significant as that seen within the unimodal bed; this is evidenced from the very different shape of the distribution evolution between Figure 5-11 and Figure 5-12.

Results derived from the fractional transported load and for each sediment grade reveal three inferences;

- Increasing the duration of antecedent flow reveals a reduction in the transport rate as a function of antecedent duration irrespective of grain size distribution. This supports wider transport analysis both within this thesis as well as with previous studies (Monteith and Pender, 2005).
- The unimodal bed is strongly characterised by size selective entrainment irrespective of antecedent duration however the bimodal bed is characterised by equal mobility conditions which become more strongly size selective with increased antecedent duration
- g_i/F_i data indicates that as antecedent duration is increased the total load becomes increasingly dominated by size selective entrainment in the coarse and fine end members of the distribution in both distributions; as this typically goes hand-in-hand with hiding development the effect is on mobility of the middle fractions of the transported distribution. Selective entrainment develops progressively in these grain fractions as the antecedent period is extended, particularly notable in the unimodal bed.

Results derived from the comparative (after 60 minutes antecedent duration for low and high width depth ratio experiments) fractional transported load and for each sediment grade reveal two inferences;

- Typically the unimodal bed shows a similar pattern of mobility regardless of width depth ratio employed in the unimodal bed. Comparatively the bimodal bed is characterised by a tendency for greater equal mobility in the higher wider depth ratio experiments particularly noticeable in the coarser end members.
- After 60 minutes of antecedent flow results from the low width depth ratio experiments show similar hiding effects in the fine end members of

the distribution in the unimodal bed. However the D_{50} is proportionally stable and the coarser end members are selectively entrained. This is in comparison with the relative instability of the D_{50} and the entrainment of the coarser end members in equal mobility proportions in the higher wide depth ratio experiments. This suggests that the bed has stabilised in the former set of experiments whilst the bed in the latter experiments are still evolving in response to applied antecedent flow. In the bimodal bed a similar fine member response is noted after 60 minutes of antecedent flow with both sets of experiments noting equal mobility and both beds have a relatively unstable D_{50} fraction. However there is a much more obvious stabilisation of the coarser fractions in the low width depth ratios suggesting that the coarser grains run in the higher width ratio experiments still have not stabilised, akin to the unimodal bed.

5.5 Discussion

Based on past literature and the results derived in Chapter 4, the aim of Chapter 5 was to determine if stress history influences could be confirmed in both uniform and graded beds over extended time frames of antecedent flow (section 5.2). As such, this discussion seeks to use past research papers and the findings from Chapter 4 in the wider context of sediment transport knowledge to speculate on explaining why these trends may occur and, importantly, direct further research within the final chapter of this thesis. Since explicit, detailed discussion regarding the possible general mechanics of stress history induced stability gains has already been forwarded in Chapter 4 discussion here will focus on; (i) similarity of the trends derived in Chapter 5 with those found in Chapter 4 (ii) the influence if increasing the antecedent duration from 60 minutes to 960 minutes (iii) the influence of the different flume width on stress history trends and (iv) questions arising pertaining to differential response of grade.

5.5.1 *The influence of stress history on bed stability; confirmation of stress history derived trends from Chapter 4?*

This Chapter has provided further evidence demonstrating the stabilising influence of sub-threshold flows on non cohesive sediment beds; this is directly in line with results presented in Chapter 4. As before, two metrics of stability have been used in this chapter

to assess the stability gains as a result of stress history; direct entrainment threshold analysis (akin to Paphitis and Collins, 2005) and proxy bedload analysis (akin to Monteith and Pender, 2005; Haynes and Pender, 2007). Firstly, using direct entrainment threshold analysis, data in the present Chapter shows that critical shear stress of the median grain size increases by +14.2 % in the uniform bed, +11.5 % increase in the bimodal bed and +7.3% in the unimodal bed due to the applied stress history (960 minutes at τ_{c50}) (section 5.4.1). In comparison with previous stability gains in response to stress history, particularly results presented earlier in this thesis, the magnitudes of response are higher in the low width depth ratio experiments. Specifically, after 60 minutes of antecedent flow the magnitude of response of uniform, unimodal and bimodal beds are 21.83%, 7.00% and 7.32% higher respectively than for the same time period in the higher width depth ratio experiments (section 5.4.1). Given that the grain size distributions are the same as those used within Chapter 4 the difference can be logically linked to the relative depths between the two flumes (Shvidchenko and Pender, 2000; Cooper and Tait, 2008); the explicit reasoning behind these differences are explained in section 5.5.3. Secondly, proxy data analysis of bedload response to stress history is noted to have an appreciable effect upon the total transported load, directly comparable to results generated in Chapter 4. Extending the antecedent flow period results in a reduction in the transported bedload by the following grade-specific hierarchy: bimodal (-89%) > uniform (-65%) > unimodal (-50%). Two overall trends are thus of notable importance. Comparison of the absolute total load data reveals that for experiments run in the flume with the lower width ratios (Shields Flume) total loads are up to 78% higher in the unimodal bed and 91% higher in bimodal bed as compared to experiments run with higher width ratios (Kelvin Flume) after 60 minutes of antecedent flow. This is the likely results of the generation of longitudinal ridge trough structures in the low width ratio experiments which act to route finer sediment in the troughs and stabilise coarse sediment in the ridges (Shvidchenko, 2000); these bedforms were not present in the Kelvin flume with the reasoning behind this is discussed at length in section 5.5.3. The second trend worthy of note is the relative response of the shear stress and bedload to the applied antecedent flow. Akin to findings within Chapter 4 a greater magnitude of response to stress history is noted within the bedload in comparison to the critical shear stress; this was attributed to the stochastic nature of sediment entrainment such that, even under the lowest flow velocities sediment transport is possible due to turbulent fluctuations in the flow (e.g. Gras, 1970; Paintal, 1971; Graf and Pазis,

1977; Lavelle and Mofjeld, 1987; McEwan *et al.*, 2004; Paphitis and Collins, 2005; Bottacin *et al.*, 2008.

The mechanisms responsible for the stabilisation of the bed in response to applied antecedent flow have already been discussed in detail in section 4.5.2 and will not be repeated here especially given the similarity in the trends of response noted in this Chapter. Instead the remainder of this chapter will highlight the difference and potential reasoning behind why these differences may arise under both under benchmark conditions and in response to the applied antecedent flow.

5.5.2 *The effect of extending antecedent durations from 60mins (Chapter 4) to 960 minutes?*

Under benchmark conditions a hierarchy of stability is noted where the unimodal bed requires the highest critical shear stress (3.09 Nm^{-2}) and is most able to resist entrainment followed by the bimodal bed (2.57 Nm^{-2}) with the uniform least able (2.41 Nm^{-2}) to resist entrainment; this is consistent with the postulations of a grade dependent response as proposed throughout the thesis thus far. However this is the opposite trend to that noted in section 4.4.2 where the uniform bed was seen to be most stable (critical bed shear stress is 16.87% higher in the uniform bed for the low width ratio experiments). Possible reasoning for this is discussed in terms of the effect of relative depth (Shvidchneko and Pender, 2000; Cooper *et al.*, 2005; Cooper and Tait, 2008) in section 5.5.3 and to the development of longitudinal ridges (Nezu and Nakagawa, 1993; McLelland *et al.*, 1999; Shvidchenko, 2000;) and troughs in the graded beds which were absent in the uniform bed for the experiments run with lower width depth ratios, discussed in section 5.5.4. Akin to findings in Chapter 4, in response to increased antecedent duration, whilst the order of the hierarchy to stability is maintained (the unimodal bed always requiring the highest bed shear stresses to be mobilised and the uniform bed requiring the lowest) the uniform bed is more responsive to antecedent flows than the graded beds (+14.5%, +11.5%, +7.3%, for the uniform, bimodal and unimodal beds respectively). This appears related to the grain size distribution and its influence on the ability of a grain to rearrange in response to the applied antecedent flow, as discussed in section 4.5.2.

The response of the bedload is also similar to that reported in Chapter 4 where it is noted that there is a grade dependent reduction of total transported load with increased antecedent duration which occurs most rapidly after the application of the shortest

antecedent periods, akin to findings in section 4.4.3. As the reasoning behind this reduction has already been discussed at length in section 4.5.1 it will not be repeated here however since bedload data were taken during every step of the stability test in this set of experiments it is possible to examine change in total load with increasing shear stress; this was not possible in Chapter 4 and so this analysis furthers the understanding of the effects of stress history upon transported bedload. Typically the relationship between bed shear stress and total load is linked to a transition from marginal transport rates at low shear stress which increase to partial and full mobility transport conditions as shear stress increases (e.g. Wilcock and McArdell, 1993, Shvidchenko and Pender, 2001). In explanation, using the probabilistic approach to entrainment as a framework (Grass, 1970; Gessler, 1971; Paintal, 1971), under low flow conditions transport will be controlled by the probability functions of both turbulent shear stress at the bed and the intergranular geometry of the bed material, described as a function of grain shape, sorting and packing (Kirchner *et al.*, 1990; Buffington *et al.*, 1992). As shear stress is increased, the greater the overlap in the probability functions of the turbulent shear stress and the bed and intergranular geometry, and the greater the intensity of sediment movement such that marginal transport conditions occur. Marginal transport conditions give way to full bed mobility under the highest shear stress values (Paintal, 1971; Lavelle and Mofjeld, 1987). However the effects of stress history may complicate this trend such that two schools of thought are proposed to describe the effects.

Firstly it is suggested that the onset of entrainment could be delayed as a result of increasing antecedent duration but that this would not delay the transition between partial and full mobility and the higher flows associated with the development of full mobility conditions would break up any bed structure (Parker, pers comm.). As a consequence, at some values of τ / τ_c the bed structure would be broken up and the total transported load would not change in magnitude at threshold; this is consistent with field data (e.g. Wilcock *et al.*, 1996). The antithesis of this essentially relates to the development of a hysteresis loop whereby, due to bed structuring smaller amounts of bedload are transported as antecedent duration is increased at the same shear stresses under which bedload would be transported if no antecedent durations were applied. Typically hysteresis loops have been discussed in the light of rising and falling limbs of hydrographs where different magnitudes of bedload transport have been produced by the same flow magnitude, depending on whether the flow occurs on the rising or falling limb of a hydrograph (Reid

et al., 1985; Church *et al.*, 1991; Hassan *et al.*, 2006). These studies have proved an intrinsic link between bed structure characteristics and the total load transported (Reid *et al.*, 1985; Reid *et al.*, 1997). Overall it is postulated that not only would stress history serve to delay entrainment (as evidenced by an offset in the initiation of motion as compared with beds not exposed to stress history) but that the total loads would also be reduced for comparable shear stresses. This is of fundamental importance in the application of this study to the field environment.

Results indicate that in all three beds a reduction in total load for each step of the stability test is noted with increasing antecedent duration. Specifically up to a 86%, 59% and 63 % decrease in total load for each step of the stability test is noted for the uniform, unimodal and bimodal beds. This means smaller amounts of sediment are transported at a comparable shear stresses to that of a bed which hasn't been exposed to a prolonged antecedent flow. This suggests that a stronger bed, more able to resist entrainment, is formed antecedent flow duration is increased; this is in line with the literature which pertains to the effect of water working on bed stability (Kirchner *et al.*, 1990; Monteith and Pender, 2005; Rollinson, 2006; Haynes and Pender, 2007). Secondly in the bimodal bed an offset is observed such that transport does not commence until later in the stability test (i.e. at higher average bed shear stresses) as antecedent duration is increased in line with the entrainment data discussed earlier which supports the notion of a grade dependent response. Both trends support the latter hypothesis described above in which it was postulated that smaller amounts of bedload would be transported as antecedent duration is increased. This is in line with the findings of Reid and Frostick (1986) who note that the initiation of motion on the rising limb and cessation of motion on the falling limb such that cessation thresholds were noted as being 20% of those of initiation. They attributed this change to be a facet of changes to particle imbrication, surface structures and relative sizes surrounding the grain i.e. bed structuring), which appear to be affected by the recent previous flows to which the bed material has been exposed (Reid and Frostick, 1986; Church *et al.*, 1998). This would thus suggest that the effects of the antecedent flow serve to re organise the bed into a similar structure as that noted in previous field experiments and that the stability of that bed is enough to not reduce total transported loads but, in some cases, delay the onset of entrainment. However that there is a grade dependent response suggests that not only are the mechanisms which are responsible for the differences generated between uniform and graded beds different but so are the

differences noted between beds with comparable median grain sizes but different modalities. The former concept has been linked in this thesis to a change in the serving to permit grain reorientation, increased imbrication and higher packing density (Fenton and Abbott, 1977; Komar and Li, 1986; Paphitis and Collins, 2005). Whilst the latter has been linked to the relative grain effects allowing the development of roughness and hiding effects (Dietrich *et al.*, 1989; Reid *et al.*, 1997; Haynes and Pender, 2007). The fact that the bimodal bed seems more reactive in terms of a delay to the onset of entrainment supports the critical entrainment data in section 5.4.1 where the bimodal bed is more responsive than the unimodal bed. This has recently become a focus of attention within the literature where for example Cooper and Frostick, (2009) compare the relative changes to bed structure of a unimodal and bimodal bed of comparative D_{50} (4.8mm, akin to those reported in this thesis). They note that the structure of both deposits is in response to increasing degradational armouring durations is as the result of a change to the fluid force distribution experienced by the different grains fractions; this concept is developed fully in Chapter 6 where the underpinning mechanisms behind such a change are discussed. Finally, since the experiments reported here were only run until threshold of motion was reached, it is not possible to comment on a potential similarity with previous findings from conditions above critical threshold.

In terms of the fractional pattern of bedload transport under benchmark conditions similar trends are noted to those in Chapter 4. In the unimodal bed there is a trend towards equal mobility in the intermediary size fractions with selective entrainment of the end members of the distribution (Ashworth and Ferguson, 1989; Wilcock and Southard, 1988; Kuhnle, 1992; Wilcock and McArdeil, 1993; Laronne *et al.*, 1994). Conversely in the bimodal bed the selective entrainment is not as clearly developed although the finest fractions and those above the median are underrepresented in the bedload which suggests that hiding effects are present. This follows the size selective entrainment patterns noted within Chapter 4. The difference in the response between the two beds is also consistent with previous findings where it was believed that stability is intrinsically linked not to the absolute percentage of the D_{50} in a mixture but to the relative proportion of the D_{50} to the other grain fractions (D_i/D_{50}).

5.5.3 *The effect of flume width on stress history trends*

This final section will concentrate on explain the effects that the different flume widths have upon the stress history trends. This will be discussed in terms of the effects of relative depth, the effects of bedform development and the effect of the method of shear stress generation.

Results have shown bed shear stress to be highly dependent upon relative depth with a grade dependent response shown; in the uniform bed a negative correlation is noted between relative depth and critical shear stress such that the shear stress exhibited in the Shields flume (low width depth ratio) is higher than that exhibited in the Kelvin flume (higher width depth ratios). Conversely in the two graded beds the opposite is true such that an increase in relative depth is associated with an increase in critical bed shear stress where the shear stresses experienced in the Kelvin flume are higher than those experienced in the Shields flume. Shvidchneko and Pender (2000) specifically assess the impact of relative depth upon the incipient motion of sediments and assume that the relationship between relative depth and shear stress is a function of flow resistance. In their experiments they use the same width flume as the Shields flume used in this study with uniform grain size distributions (grain sizes ranging from 1 to 14mm) with the duration of experiments ranging from between 10 to 90 minutes. They noted that a decrease in relative depth is associated with a decrease in both flow velocity and bedload transport rate and hence the need for a higher shear stress to cause incipient motion. This relationship was attributed to the increased effect of the wake eddies, shed by the bed particles on the overall flow resistance as relative depth decreases. Whilst this trend holds true for the two graded beds and there is a positive relationship between relative depth and shear stress the same is not true of the uniform bed where the opposite trend is noted.

Cooper *et al.*, (2005) support this finding indirectly where they note that as relative depth increases the flow structure above the bed changes significantly which they postulate to be irrespective of the bed topography and consequently that the flow depth controls flow characteristics rather than flow resistance. Specifically, their research uses two different graded beds of comparative D_{50} (~4.8mm) and responses them to a range of different flow depths to investigate the spatial persistence of flow properties under different relative depth ratios. They note that despite clear differences in the bed surface topography of the

unimodal and bimodal beds, they both displayed a similar spatial organisation of $\bar{u}(\bar{u})$.

On average an increase in relative submergence caused a decrease in the number of high speed streaks and an enlarging of the low speed spots. This has the effect of homogenising the distribution of time averaged streamwise velocities (Legleiter *et al.*, 2007). Similar trends in the changes in spatial pattern of $\bar{u}(\bar{u})$ were observed where the same z/k ratios used were demonstrating that the effect of roughness of the bed cannot fully account for the variability in the spatial pattern. It was therefore postulated that the bed surface topography at the grain scale exerts less of an influence on the spatial organisation of $\bar{u}(\bar{u})$ than relative submergence (Cooper *et al.*, 2005). This is in line with the findings of Legleiter *et al.*, (2007) who concluded that as flow stage increased the spatial structure of \bar{u} became smoother and more continuous i.e. an increase in relative depth caused an overall increase in the homogeneity of the distribution of \bar{u} over the bed. Furthermore they discovered that, even in flows where the flow depth was in the same order as the D_{84} , the individual roughness elements were found to have little linear correlation with flow. This implies that flow depth had a fundamental control on flow structure through its influence on the spatial persistence of the flow characteristics. This is in line with findings presented here for the uniform bed. In the context of this research the only method of accurately determining the spatial nature of bed shear stress would be to use techniques such as PIV to link the overlying flow properties to grain moment and bed characteristics to give a spatial estimate of bed shear stress with the local bed rearrangement (e.g. Bottacin *et al.*, 2008); this is the next logical step to be taken in this research field.

In addition to the potential differences linked to the effects of relative depth the presence and absence of bedforms in the low width depth ratio experiments may also be used to explain some of the differences noted between the two data sets, specifically related to the transported load (McLelland *et al.*, 1999; Shvidchenko, 2000). Typically, the formation of sediment troughs and ridges is usually attributed to the lateral transport of particles by a series of streamwise orientated vortices (Karcz, 1973). Prandtl (1952) distinguished two fundamental mechanisms responsible for the generation of these streamwise secondary circulation cells; (i) the skewing of mean shear stress by either a transverse pressure gradient or body force ; (ii) anisotropy of turbulent fluctuations in the plane perpendicular

to the axis of the rotation. In straight channels, where planform channel configuration cannot skew the mean flow direction, the latter mechanisms may be initiated. Typically this is reported to be due to either irregular cross section morphology or variations in boundary roughness (Nezu and Nakagawa, 1993). It is likely that given the uniform cross section of both flume facilities it is the change in roughness at the boundary which causes the development of such secondary flow cells i.e. the change between the sediment bed and the glass side walls.

Further, research has shown that not only are the number and size of these bedforms controlled by channel width but also by grain size distribution. In narrow channels ($z/b < 5$, akin to the low width depth experiments run in the Shields flume) without a deformable bed Nezu and Rodi, (1985) note that secondary currents generated at the channel boundaries extend into the central region of the flow whereas the centre of wider and shallower channels (as in the experiments run in the Kelvin flume) with $b/d > 5$ remain free of secondary currents. This supports the findings in this thesis where the narrower flume (Shields) generated longitudinal ridges and troughs akin to those noted by Nezu and Rodi (1985) but that the wider and shallower flows experienced in the Kelvin flume did not generate such bed structures. However that a grade dependent result was noted in the Shields flume where the bedforms were generated in the graded sediment beds and not in the uniform bed suggests that there are also grade dependent controls on their generations. With poorly sorted sediments, streamwise vortices generate a pattern of alternate coarse and fine grained sediment stripes (Karcz, 1973; Culbertson, 1967). Lateral variations in the boundary roughness associated with these bedforms generate secondary flows with upwelling fluid over the smoother parts of the bed and downwelling over the rougher stripes (Hinze, 1973;; Muller and Studerus, 1979) which has been noted to act as a feedback and amplify the instability process within the turbulent flow (Colombini and Parker, 1995). Visual observation of these bedforms during the current experiments note that the bedforms appear to route finer material and stabilise coarser grains, consistent with the findings of Nezu and Nakagawa, 1993 and Shvidchenko, 2000 with the latter study using the same grain size distribution as that used in this current thesis. This was attributed to higher streamwise velocity and bed shear stresses in the troughs (Shvidchenko, 2000). McLelland *et al.*, use bimodal sand beds ($D_{50}, 1.07$) to show that the development of these bedforms is temporally dependent such that the greatest rate of development occurred within the first 40 minutes of a 15 hour experiments; whilst the grain sizes used are significantly smaller than those used in this thesis, their results indirectly supports the

bedload data collected in this thesis where it is noted that the majority of the bedload stabilisation occurs after the shortest antecedent time periods. Conversely in the uniform bed where the topography is similar (as discussed at length in Chapter 6) the cross stream instabilities generated as a result of non-uniform distribution of Reynolds stresses are not as strong and hence will not generate the same bedforms (Ikeda, 1981; Colombini, 1993).

Finally although a reasoned argument can be made to attribute the differences in the observed shear stress between the two flumes to the differences in flow structure as a result of relative depth effects and the generation of bedforms, the differences could also be a facet of the method of derivation of bed shear stress. In both flume facilities bed shear stress is calculated according to the depth slope method corrected for the influence of the side walls which provides a width averaged estimate of shear stress. There is a body of evidence to suggest that width averaged shear stress estimates underestimate the actual critical shear stress due to the spatial heterogeneity of the surface. Even in uniform beds, Ferguson (2003) states that failing to account for lateral variation in flow will underestimate factors such as critical entrainment shear stress and bedload flux (Paola and Seal, 1995; Paola, 1996; and Nicholas, 2000). In the context of this research, the wider the channel the greater the difference between the calculated width averaged bed shear stress and the actual bed shear stress due to the increased spatial variability of the bed surface, this may explain why the bed shear stress values are lower in the wider flume where the lateral variation is likely to be greater than in the narrower flume; such variation will of course be lower in the uniform bed and may explain the differences in the critical shear stress values. Caution is advised though, in the interpretation of such results, as many of the results described above have been calibrated using field data (e.g. Hoey and Ferguson, 1994; Wathen *et al.*, 1995 and Powell *et al.*, 1999)- in a natural channel variation of flow depth and hence shear stress laterally and longitudinally across bars, thalwegs pools and riffles, planimetric convergence and divergence of flow and secondary circulation of flow exacerbates the spatial differences in shear stress. In addition, support for using the depth slope method to estimate bed shear stress can be found using the results of Legleiter *et al.*, (2007). They note that the flow field at a small scale was influenced by local topographic variability at high spatial frequencies, most noticeably at lower depths but that the large scale flow pattern primarily reflected the bulk morphology of the channel. Essentially they concluded that the flow primarily responds to the gross morphology of the channel and that flow depth is the primary control on flow structure and hence overall bed stability.

It has already been stated that the shear stress estimates have been corrected for sidewall effects in both sets of experiments may also introduce some discrepancies in the data. The sidewall correction procedure used in this thesis is in line with previous stress history studies (Monteith and Pender, 2005; Haynes and Pender, 2007). Whilst there are other methods of correcting for side wall influences (e.g. Vanoi and Brooks, 1971), in his work using the same size distributions as used in the thesis, Shvidchenko (2000) used the same side wall correction procedure and found that the shear stress estimates derived according to this methodology were comparable to the results of the more commonly used Vanoi and Brooks method (Vanoi *et al.*, 1971) differing by less than 5%. Shvidchenko deemed that this correction procedure was more accurate as it was chosen to avoid the use of mean flow velocity. In design practise, flow velocity is usually to be determined, and the Manning formula is widely used for the calculations. Thus the employment of the roughness coefficients for the sidewall correction provides direct applicability of the results to solving practical problems (Shvidchenko, 2000). In this thesis the side wall correction was applied in both the flume facilities. Whilst it is accepted that in the wider flume facility (1.8m) measurements are only in the centre of the channel such that the effect of the side walls are negligible, the correction applied is deemed valid, because it accounts for the hydraulic radius which includes width and depth information.

5.5.4 Questions raised from data and discussion of Chapter 5

So from the discussion above it is possible to see that there is a clear influence of prolonged periods of sub threshold flow upon antecedent duration as observed in section 4.4.2. There are also clear influences of grade upon the stability attained by individual beds in response to stress history which is temporally sensitive. This is evidenced by the difference between the hierarchy of stability under benchmark conditions and the hierarchy of response in relation to increased antecedent flow durations. The changes to the bed stability have been linked to changes in the relative mobility/stability patterns of different grain fractions on the bed surface, akin to section 4.4.4. These patterns have also been noted to be highly grade and temporally dependent. Although these findings have been clearly highlighted and justified throughout the discussion there are still questions which have arisen as a result of the reported investigations which need developing throughout the final chapter of this thesis. As such there is a short section below which briefly identifies the essential next steps of this research and justifies the direction taken in the final chapter

based on the findings gained in this research. As a point of note, whilst it is recognised that the different flume facilities have generated different results in terms of the effects of width depth and relative depth effects they were not the main focus of this thesis and as such the pointers below are primarily linked to developing the relationship between stability of the bed surface and surface organisation.

- It has been noted that antecedent flow duration increases the resistance of the bed to the overlying fluid flow regime both under short (Chapter 4) and long antecedent durations (Chapter 5). This increased resistance acts to both increase critical bed shear stress but also modify the transported bedload regime. However until now the limited available literature pertaining to stress history induced stability gains have only been qualitative postulations. As such it is vital to quantify these qualitative postulations in order to identify and understand the mechanisms which are responsible for the bed stabilisation.
- It has been noted that antecedent flow duration has the greatest effect upon bed stability after the shortest applied antecedent flow durations. It is therefore fundamental to quantify how the mechanisms responsible for stabilisation change with increased antecedent duration such as to control the rate of bed stabilisation.
- Uniform beds are consistently more responsive than graded beds. This appears to be related to the grain size distribution and its influence on the *in situ* repositioning of grains. It is suggested that uniform beds may have the freedom to rearrange to a greater extent due to larger pore spaces and poorer imbrication, whilst the finer particles within graded beds reduce pore space size and restrict *in-situ* particle movement of the larger grains. However these speculative postulations need to be quantified; this can only be done using high resolution scanning of the bed surface.

5.6 Chapter Summary

The results from this chapter have confirmed the stress history trends derived in Chapter 4 further demonstrating the stabilising influence of sub threshold flows on non cohesive sediment beds. Akin to both studies, increasing the duration of antecedent flow increases the resistance of the bed to entrainment by fluid flow. Although beds subjected to the longest antecedent duration are the most stable, the greatest response to antecedent flows appears to occur for the shorter flow durations such that it is viable to assume a stability maxima would be reached. This chapter has also confirmed the graded dependent response

of sediment beds to stress history; uniform beds are found to be consistently more reactive to antecedent flow as compared to the graded beds.

Bedload data has been used to support these findings, acting as a proxy for bed stability, where increasing bed stability as a response to stress history is mirrored by decreased transported bedload and a change to the characteristics of the bedload. Specifically, in the graded beds, an increase in size selective entrainment with increasing antecedent duration is noted which is particularly prominent within the finest fractions in both beds. In addition a clear relationship exists between total load and increasing bed shear stress such that smaller amounts of sediment transported where beds are exposed to prolonged periods of antecedent duration. Entrainment is also delayed such that higher shear stresses are needed to initiate motion in the bimodal bed. In part this is believed to be because of the development of structuring on the bed surface acting to alter the overlying flow characteristics such as to change entrainment threshold. However only a very limited number of studies have examined the link between surface topography, grain entrainment and bedload transport explicitly and none have combined these effects in relation to stress history. It is therefore a logical next step that the structure of the surface be investigated in order that the mechanisms responsible for increased entrainment threshold as a result of stress history be identified and quantified. As such Chapter 6 will concentrate on the development of this understanding.

Finally both the critical bed shear stress and total transported bedload data have shown significant dependency upon width depth ratios through the relationship with relative depth. Higher relative depth (lower width depth) ratios affect the critical bed shear stress in all grain size distributions with average critical bed shear stress being lower in the graded beds and higher in the uniform bed in comparison with lower relative depth (higher width depth) ratios. In addition the presence or absence of bedforms have affected the total transported bedload such that experiments where bedforms were present (high relative depth, graded beds) experienced higher transported bedload rates. Further exploration into these effects is beyond the scope of this thesis and will form the natural next step in the research.

Experiment Number	Grain Size Distribution	Antecedent Period Duration (Minutes)	Stability Test Duration (Minutes)	Average Critical Bed Shear Stress (Nm-2)
81,82,82,84	UNIFORM	0	85	2.36
85,86,87		60	90	2.44
88,89,90		120	120	2.46
91,92,93		240	125	2.47
94,95,96		960	130	2.76
97,98,99,100	UNIMODAL	0	70	2.82
101,102,103		60	70	2.92
104,105,106		120	80	3.00
107,108,109		240	80	3.02
110,111,112		960	80	3.06
113,114,11,116	BIMODAL	40	40	2.52
117,118,119		60	40	2.56
120,121,122		120	50	2.66
123,124,125		240	50	2.62
126,127,128		960	50	2.81

Table 5-5- Summary of experimental variables

Chapter 6 Mechanisms of Bed Stabilisation

The results presented in Chapters 4 and 5 show that prolonged periods of antecedent flow cause an increase in average threshold bed shear stress. Data also indicates that the magnitude of response is related to the bed's grain size distribution and, interestingly, graded beds are observed to be less responsive to antecedence than uniform beds. Given that the antecedent flows applied are sub - threshold, it is reasoned that the bed's increase in stability cannot be attributed to active bed structuring by particle transport; instead in-situ or local alteration to bed packing or grain positioning are proposed. However, data presented so far in this thesis suffers from the same uncertainties as previous research (Paphitis and Collins, 2005; Haynes and Pender 2007), in that threshold and bedload data provide only limited, qualitative and mainly speculative information on the mechanisms that underpin the stabilisation processes pertaining to applied antecedency.

This Chapter will therefore focus on providing a quantitative, mechanistic understanding of the processes responsible for bed stabilisation under sub - threshold conditions. This will offer the first real insights into the relationship between stress history and the associated changes to bed topography, particle repositioning and possible structure formation. Based on the outcome of Chapter 5, the data set is truncated to compare and contrast: (i) the 60 minute and 960 minute antecedent flow durations, i.e. the extremes of the time distribution; (ii) three grades; uniform, unimodal and bimodal. This decision was taken to maximise understanding of bed mechanics, whilst being realistic in terms of the available computational processing power of the vast data sets stemming from laser-based data acquisition.

6.1 Hypothesis

Time-dependent stabilisation of antecedency is hypothesised to occur through four main mechanisms acting at different scales; this forms the focus of investigation and discussion within this Chapter;

- *Vertical settlement* of the bed so as to consolidate the bed into a tighter packing arrangement which is more resistant to entrainment; for graded beds this specifically includes the infiltration of fines into low relief pore spaces of the bed surface, with associated increases in hiding effects and grain pivot angles.

-
- *Porosity* reduction (i.e. increased packing density) due to reorientation, settlement and infiltration of fines; this is dependent on the surface grain size distribution as different pore sizes will control each process.
 - *Reorientation* of grains on the bed surface such that they reposition into a more stable location on the bed surface, so as to offer decreased resistance to the overlying fluid flow.
 - *Multi-particle structure* development (i.e. larger than grain scale bedforms), such as particle clusters and/or the creation of an armoured bed surface which serve to increase resistance of the bed; the former will act via the trapping of fine grains by coarser clasts such that noticeable ‘clusters’ are formed on the bed surface, the latter will occur such that the surface becomes coarser over time and more stable.

6.2 *Experimental Procedure*

In this Chapter the results of six experiments are presented; the variables employed are shown for these runs in Table 5-5 (referenced as experiment numbers 87, 96, 103, 112, 119, 128). Section 3.3 details the instrumentation, methodology and experimental variables pertaining to Chapter 6. Two laser scans of the bed surface were taken; one immediately prior to and one subsequent to the antecedent period. However, given that stress history is the focus of this thesis an important point to justify is the flow reduction required to attain each scan, in particular the reduction-reflooding cycle at the end of both the bedding in period and the antecedent period. Specifically, the accuracy of laser data is maximised on a drained bed; if, alternatively, this were to be performed through a depth of water medium the laser light would be scattered and the return signal would be of poor quality. As such, the bed was drained as slowly as possible until a water table was established just below the bed surface; this minimised disruption to the bed surface, in particular the settlement of fines to depth. The duration of the scan was also very short (4 seconds per 116x100mm section) and reflooding increased the flow only very slowly back to the pre-scan discharge for the prescribed duration of the antecedent period. Measurement of bed surfaces in this manner is the accepted norm (Tait *et al.*, 1997; Marion *et al.*, 2003; Cooper and Tait, 2008) and every known precaution was taken to minimise bed surface disruption.

6.3 Results

In order to assess the organisation of the bed surface, laser displacement data was post-processed by linear interpolation in *Matlab* onto a 0.1 mm grid; the grid size was chosen as the smallest resolution (0.1mm) measured in any axial direction, however it is possible to resample the data at any given resolution dependent upon the analysis required. This produced a Digital Elevation Model (DEM) measured in mm above an arbitrary datum. Interpolation was necessary since the laser beam was sometimes occluded returning no data for a given point (<0.01% of scan data). These null data points were returned as “NaN” by the software and thus were easily identifiable. Once identified the null data points were replaced by an average value calculated from the surrounding 9 cells; this is normal practice in this type of analysis (Aberle Pers. Comm. 2010). Using this method, non returned values have negligible effect on scan quality, post-processing or analysis.

Once the scans were post-processed a number of qualitative and quantitative analytical techniques were employed to specifically assess the four mechanistic hypotheses in Section 6.1. In terms of assessing the micro-topography of gravel bed rivers there is no consensus regarding the most appropriate measure of surface structure or bed roughness. Thus, it is accepted that a number of different metrics are required to describe coarse-grained sediment structure comprehensively (Hodge *et al.*, 2009). Four general classifications of analysis are elected for this thesis:

- Section 6.3.1 qualitative visual morphometrics
- Section 6.3.2 quantitative aspatial; i.e. bulk properties of the bed surface
- Section 6.3.3 quantitative small-scale spatially-resolved, i.e. particle rotation, fines infiltration and porosity
- Section 6.3.4 quantitative large-scale spatially-resolved, i.e. cluster development, armouring, imbrication.

This order of analysis incrementally increases the level of analytical complexity and computational expense, whilst providing a progressively more detailed and quantitative understanding of the grain mechanics required. Whilst morphometric analysis has often been overlooked in favour of statistical analysis, for the purpose of this thesis it provides a good preliminary basis for visual inspection of the bed surfaces. In terms of aspatial characterisation, probability density functions (pdfs) of surface elevations and their statistical moments will be used to evaluate the degrees of particle reorganisation and bed

stability. Although pdfs are a relatively crude descriptor of microtopography, they provide a means of linking surface conditions to surface forming processes because they are expected to change in a manner which reflects the processes responsible for bed evolution (Aberle and Nikora, 2006). However, since such distributional data does not provide any information on the spatial structure or the scale of the topographic variation a suite of geostatistical tools will be used to further characterise the spatial structure of the surface microtopography (e.g. preferential grain orientations and the length scales associated with grain and form roughness). Given the extensive nature of the analysis within this chapter the mechanisms investigated and the analytical techniques employed are summarised in Table 6-1.

Mechanism	Analytical Method	Thesis Section	Page Number
Vertical Settlement	Visual Analysis	6.3.1	143
	Probability Density Functions	6.3.2.1	154
Porosity	Porosity	6.3.2.2	158
Reorientation	Visual Analysis	6.3.1	143
	D.E.M's of Change	6.3.3.1	178
	Particle Repositioning	6.3.3.2	182
Multi Particle Structures	Fractional Analysis	6.3.4.1	188
	2D Second Order Structure Functions	6.3.4.2	191

Table 6-1; Summary table of investigated mechanisms of stabilisation and their analytical methodologies

6.3.1 Visual Analysis

Digital Elevation Models of the uniform, unimodal and bimodal beds are shown in Figure 6-1 to Figure 6-6. Each figure shows the DEM generated before and after a period of 60 and 960 minutes antecedent flow respectively. The x and y axis are labelled in mm with the elevation measured in mm above an arbitrary datum; in this case the horizontal datum which was taken as the base of the laser scanner. The channel centre line is located at x =

0 with flow direction from $y = \max$ (upstream) to $y = \min$. Red regions are of highest elevation, blue regions are of lowest elevation. Changes to the bed surface are likely to be visually manifested through three notable overall changes to the bed surface between the consecutive image pairs:

(i) Increased area of blue with increased antecedent duration. In explanation, the bed is likely to settle vertically due to the pressure of an overlying fluid flow being imposed. The overall area affected gives some indication of the settlement process. If the majority of the image is affected by negative displacement, then both the 'framework' of the bed (typically the coarse structure of a graded bed) and by proxy the supporting finer matrix must have settled. However, if only local regions of the bed have settled, then either specific pockets of the bed which were unstable and less supported (e.g. specific fraction settlement) will change or a grain has re-orientated and re-positioned most likely disturbing surrounding grains.

(ii) Change to the intensity of blue with increased antecedent duration. This could represent vertical settlement of localised pockets of already low-lying regions of the bed surface (commensurate with the increased area of blue); be as the result of a one-off grain movement essentially leaving a hole in the bed surface; or, show the development of hiding effects within the bed. The latter occurs as finer grains settle into the interstices of the bed and root around the base of larger grains and is controlled by a number of essentially linked to the grain size distribution (e.g. bed porosity). Alternatively, if the intensity of blue decreases between consecutive image pairs this represents filling of pores so as to raise the local elevation of the bed surface; for example, this may be via a grain being deposited to fill a deep pore.

(iii) Small scale movement of individual grains in terms of: particle re-positioning (grain scale); structure formation (local scale); or, movement within, into or out of the field of view. This will affect those particles which are highly unstable on the bed surface (either as a facet of water-working, or as a product of vertical settlement causing increased relative exposure/projection). This type of displacement can result in either a positive (increased red) or negative (increased blue) elevation change depending upon where the grain comes to rest.

The extent to which each mechanism can be visualised on the images will be dependent upon the magnitude and extent of change; the greater the change, the easier it is to identify. Specific analysis of Figures 6.1-6.6 indicates that all three beds exhibit at least some (or

all) of the observations (i) - (iii) noted above. Yet, the magnitude to which each is found varies with antecedent duration and the grade of the bed surface.

In the uniform bed there is no obvious change to the overall 'hue' of the image after 60 minutes of applied antecedent flow (Figure 6-1); this indicates no overall vertical settlement of the bed surface. However, closer inspection yields evidence of movement of individual grains on the bed surface (labelled C on Figure 6-1). The displacement of individual grains is visualised in three examples; two are related to the movement of an individual grain, the other is the displacement of a 'cluster' of grains. These particles were those of the highest elevation on the bed surface and hence were most exposed to higher shear stress promoting displacement. Increasing the antecedent duration to 960mins (Figure 6-2) still does not show vertical settlement, yet clear areas of active movement of individual grains are observed. Interestingly, in this image pair displacement of over-exposed grains (upper highlighted area on Figure 6-2) as well as in-migration of grains is noted. This causes both a positive and negative change in the intensity of the images to be recorded.

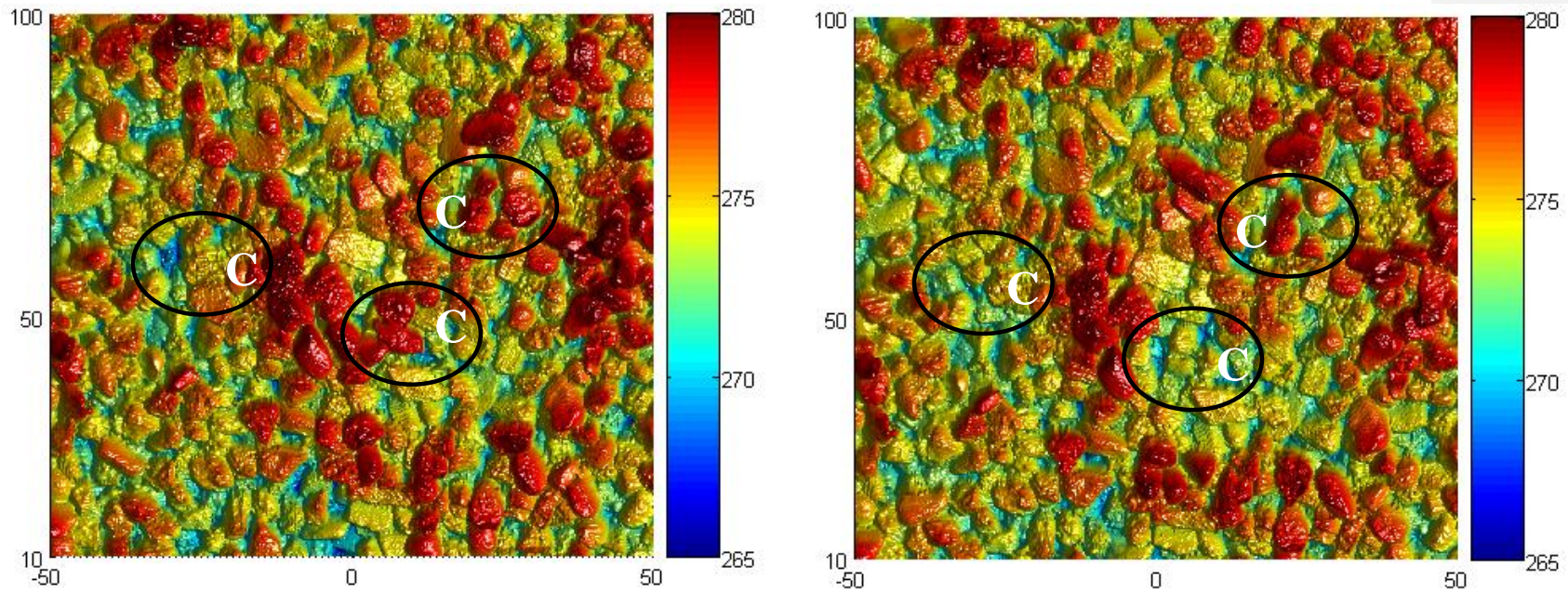
In the unimodal bed after 60mins of antecedent flow (Figure 6-3) there is evidence of individual grain movement within and out of the field of view; no obvious settlement of the bed is observed either locally or generally. Whilst the two highlighted areas to the right of the image both show displacement of over-exposed grains, the highlighted zone to the left of the image indicates in-migration and deposition of a grain into a sheltered low-relief pocket of the bed. Figure 6-4 shows similar changes after 960 minutes; individual grain displacement, deposition and rotation/flipping. The similarity of mechanisms in the unimodal bed to those observed in the uniform bed seems surprising given their significant difference in entrainment threshold response to an applied stress history. However, it may be that the similarity in how the scans 'look' show that both beds have a high proportion of coarse grains on the bed surface pertaining to a distinct coarse supporting framework for the bed; this appears to prevent notable vertical settlement of the bed with changes instead manifesting as exposed particle movement.

Finally, the bimodal bed after 60 minutes of antecedent flow also shows changes only by way of movement of individual grains; in this case into the field of view (Figure 6-5). However, after 960 minutes of antecedent flow there are far more obvious changes to the

bed surface (Figure 6-6) with all three mechanisms evidenced; wholesale settlement, local settlement and grain mobility. Firstly, there is an increase in the blue 'hue' of the image, as labelled 'A' on the image pairs; this shows areal settlement of the whole bed surface and is most easily observed where exposed (red) grains have decreased in elevation (yellow/blue) after prolonged application of antecedent flow. Secondly there are localised pockets of blue on the bed surface where the depth of colour intensity has decreased ('B' on Figure 6-6); this suggests that an area which was originally a deep pore on the bed surface has risen to a slightly higher elevation. This seems surprising and does not appear to be explained by in-migration of fines filling up pores; two possible explanations are proposed: (i) draining-refilling has a greater effect on fine material hence, in beds where the coarse framework is less dominant, draining causes settlement of the whole bed before refilling increases the pore-water pressure causing the lighter fine grains to respond by localised dilation; or (ii) independent of draining-refilling, overall settlement of the coarse framework particles causes a displacement reaction of the surrounding fines augmented by increased porewater pressure causing dilation of the fine areas of sediment (Allan and Frostick, 1999). Finally, localised particle reorientation ('C' on Figure 6-6) and displacement are observed for grains more exposed to flow. Overall, Figure 6-6 clearly indicates that the bimodal bed does visually respond to sub-threshold flow, but only following longer antecedent timeframes.

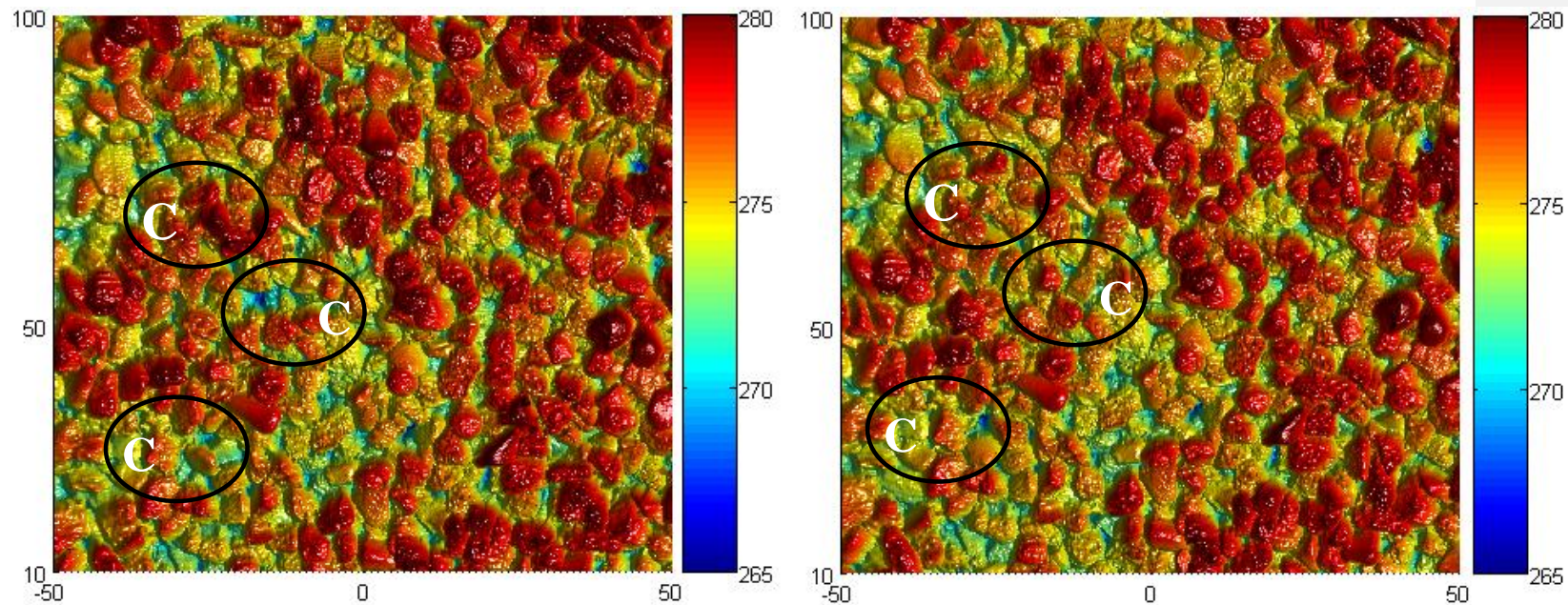
In summary the greatest changes evident within all three beds are related to particle reorientation (flipping of a grain on an axis is most notably observed) and occasional displacement of over-exposed grains on the bed surface. Typically this affects only discrete particles, yet within the uniform beds there is also evidence of unstable 'clusters' of grains being removed en-mass. This may therefore suggest more wholesale rearrangement towards stability within a uniform bed; partially explaining why uniform bed response to stress history, as defined by the change in entrainment thresholds (Chapter 4 & 5), is greater than in graded beds. A secondary, yet important, finding is the vertical displacement observed within the bimodal bed after long durations of applied flow; this is distinct from uniform and unimodal beds, neither of which showed this process. As such, the fine-coarse proportion of the bed surface appears important. Specifically, the disconnected coarse gravel framework and more extensive areas of fines of the bimodal bed are more reactive to antecedent flow. One important aspect appears to be dilation within the fines; however whether these findings result from stress history or draining-re-

flooding of the flume is unclear and a cautionary approach to this data is advocated. In summary of the visual analysis of laser displacement scan DEMs, it is clear to see that changes do not appear great in magnitude or extent; yet, it is difficult to both read the colour-scale to quantify changes in elevation accurately and describe areal and localised changes. Thus, more quantitative analytical methods for investigation of all three mechanisms (bulk settlement; local displacement; particle reorientation/displacement) are required for further development.



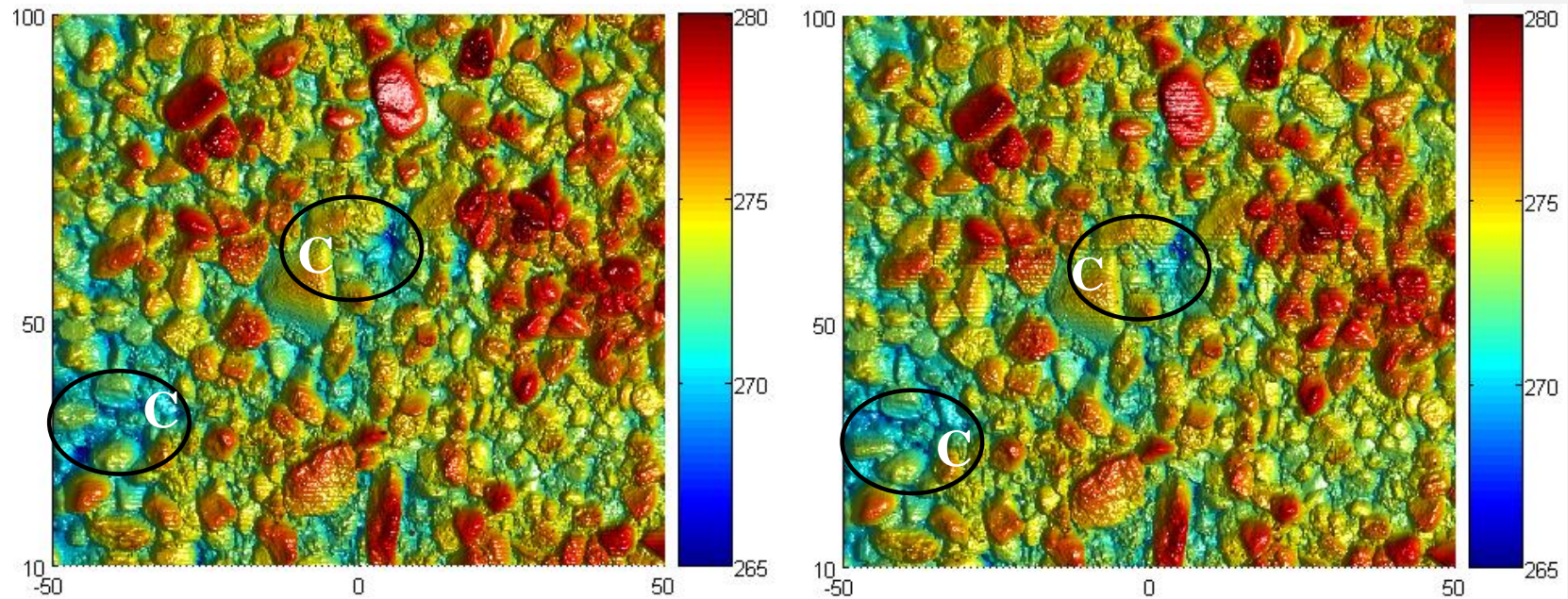
Visual inspection to the scanned surfaces observe notable changes to the bed surface through three main mechanisms; (A) increased areas of blue i.e. areas of low relief on the image, (B) changed intensity of the blue regions; both of these mechanisms signify regions of localised vertical settlement of the bed and (C) small scale movement of individual grains into and out of the field of view.

Figure 6-1; Digital Elevation Models of the uniform bed before and after the antecedent period of 60 Minutes.



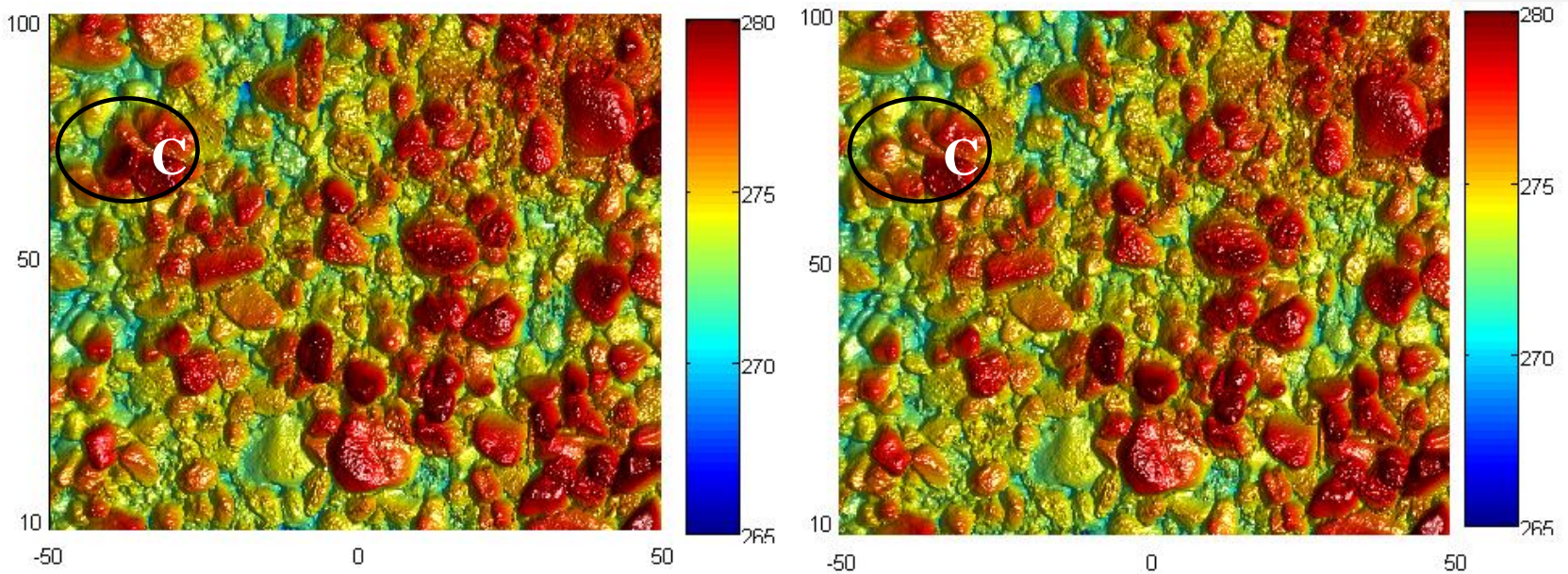
Visual inspection to the scanned surfaces observe notable changes to the bed surface through three main mechanisms; (A) increased areas of blue i.e. areas of low relief on the image, (B) changed intensity of the blue regions; both of these mechanisms signify regions of localised vertical settlement of the bed and (C) small scale movement of individual grains into and out of the field of view.

Figure 6-2; Digital Elevation Models of the uniform bed before and after the antecedent period of 960 Minutes.



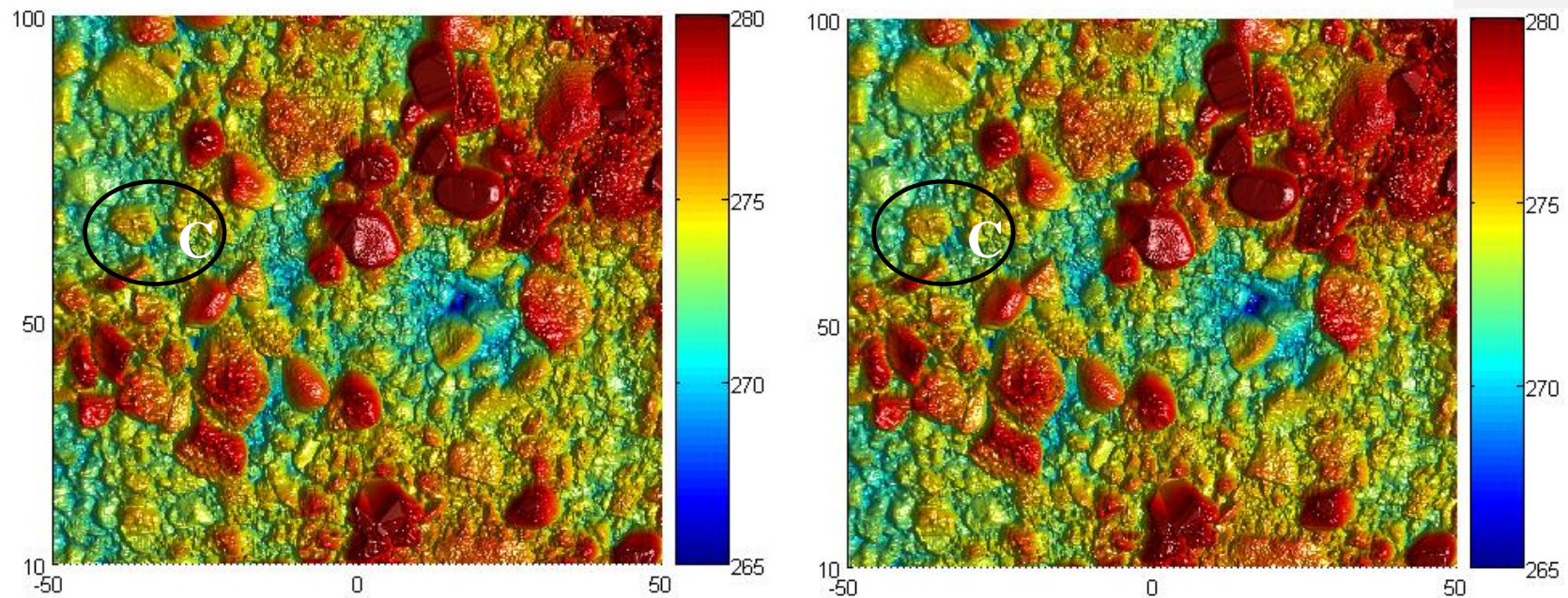
Visual inspection to the scanned surfaces observe notable changes to the bed surface through three main mechanisms; (A) increased areas of blue i.e. areas of low relief on the image, (B) change intensity of the blue regions; both of these mechanisms signify regions of localised vertical settlement of the bed and (C) small scale movement of individual grains into and out of the field of view.

Figure 6-3: Digital Elevation Models of the unimodal bed before and after 60 minutes of antecedent flow.



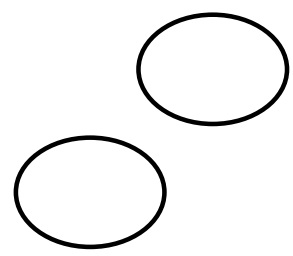
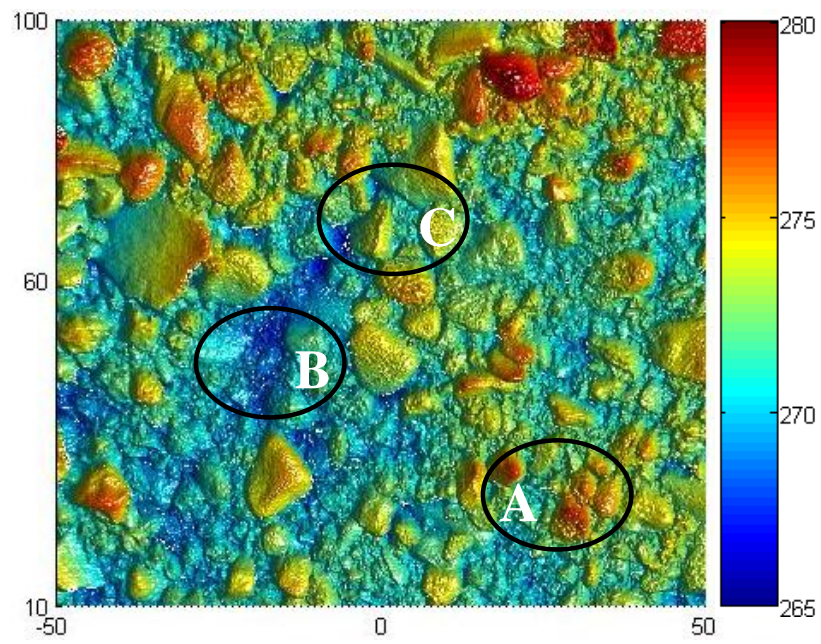
Visual inspection to the scanned surfaces observe notable changes to the bed surface through three main mechanisms; (A) increased areas of blue i.e. areas of low relief on the image, (B) changed intensity of the blue regions; both of these mechanisms signify regions of localised vertical settlement of the bed and (C) small scale movement of individual grains into and out of the field of view.

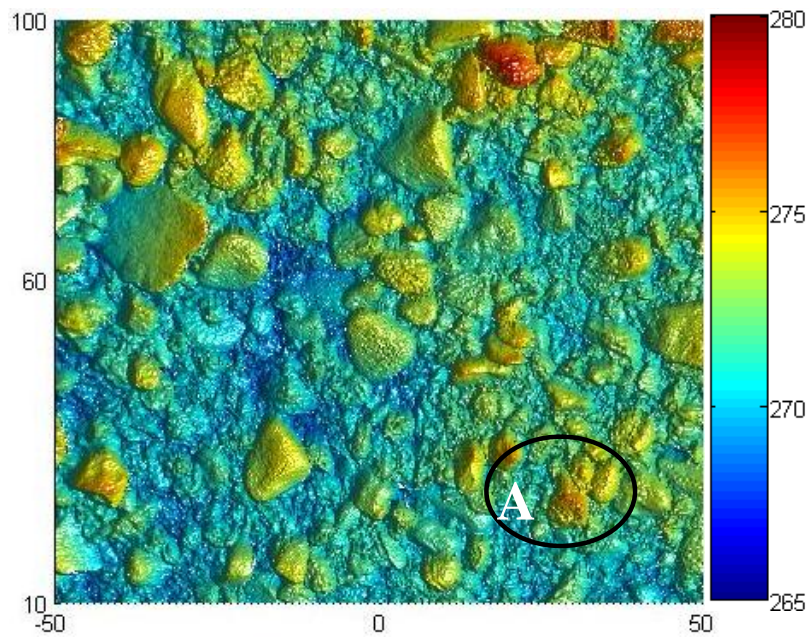
Figure 6-4: Digital Elevation Models of the unimodal bed before and after the antecedent 960 minutes of antecedent flow.



Visual inspection to the scanned surfaces observe notable changes to the bed surface through three main mechanisms; (A) increased areas of blue i.e. areas of low relief on the image, (B) increased intensity of the blue regions; both of these mechanisms signify regions of localised vertical settlement of the bed and (C) small scale movement of individual grains into and out of the field of view.

Figure 6-5; Digital Elevation Models of the bimodal bed before and after the antecedent period of 60 minutes.





Visual inspection to the scanned surfaces observe notable changes to the bed surface through three main mechanisms; (A) increased areas of blue i.e. areas of low relief on the image, (B) changed intensity of the blue regions; both of these mechanisms signify regions of localised vertical settlement of the bed and (C) small scale movement of individual grains into and out of the field of view.

Figure 6-6; Digital Elevation Models of the bimodal bed before and after the antecedent period of 960 minutes of antecedent flow.

6.3.2 Global Quantitative Analysis

6.3.2.1 Probability Density Functions

PDFs change in response to the processes occurring responsible for bed stabilisation such that they are useful in providing a means of linking surface conditions to surface forming processes (Aberle and Nikora, 2006). However they only give bulk descriptors for the area as a whole and are thus incapable of spatially-resolved analysis. In addition, they do not show the degree of surface particle organisation on the bed surface. Yet, for all *pdfs*, this visual interpretation is deemed too crude for the purpose of this thesis in terms of providing a detailed mechanistic understanding of sub-threshold rearrangement processes within the sediment beds. *PDFs* are included in Appendix D for reference.

Whilst *pdfs* of the surface elevations have been interpreted visually in past literature (e.g. Cooper and Tait, 2008), the small magnitude changes between data sets make it difficult to apply qualitative analysis. Thus, Table 6-2 presents quantitative analysis of the statistical moments with attention given to three variables of the DEM data:

- mean bed elevation (Z_b) relative to that of the laser sensor height; the difference in measurements at the start and end of the antecedent period gives a bulk statistic of whether the degree of vertically settlement of the bed.
- range of bed elevations (k); this is a recognised surrogate for geometrical roughness, where a smaller range indicates a smoother bed (e.g. Aberle and Nikora, 2006; Cooper and Tait, 2008).
- skewness of bed elevations (sk_b); a positive skew to the data (i.e. a spread of the data to the right of the zero mean on the *pdf*) is related to an armoured bed surface (e.g. Nikora *et al.*, 1998; Smart *et al.*, 2004) whereas a negative skew suggests no such structural form.

Grain Size Distribution	Descriptor	Ant. Duration (Minutes)	Start of Ant. Period	End of Ant. Period	Absolute Difference	Relative Difference
Uniform	Z _b (mm)	60	275.32	275.29	-0.03	-0.01
	k (mm)		22.16	19.52	-2.64	-13.52
	Sk _b		-0.11	-0.15	-0.04	-26.67
	Z _b (mm)	960	276.21	276.11	-0.1	-0.04
	k (mm)		18.35	17.41	-0.94	-5.40
	Sk _b		-0.17	-0.20	-0.03	-15.00
Unimodal	Z _b (mm)	60	274.30	274.10	-0.2	-0.07
	k (mm)		20.07	23.04	2.97	12.89
	Sk _b		0.10	0.07	-0.03	-42.86
	Z _b (mm)	960	275.44	274.30	-1.14	-0.41
	k (mm)		20.07	21.65	1.58	7.30
	Sk _b		0.06	0.07	0.01	14.29
Bimodal	Z _b (mm)	60	275.95	275.93	-0.02	-0.01
	k (mm)		11.46	16.06	4.6	28.64
	Sk _b		0.04	0.03	-0.01	-33.33
	Z _b (mm)	960	268.21	268.06	-0.15	-0.06
	k (mm)		17.43	21.40	3.97	18.55
	Sk _b		0.34	0.42	0.08	19.05

Table 6-2; Summary of the bed surface properties of the three beds for experiments running 1 and 16 hours antecedent flow duration where Z_b is the mean surface elevation, k is the range and Sk_b is the skewness of the distribution of bed surface elevations. Differences between 60 and 960 minutes are shown in both absolute and relative terms; red cells indicate a positive change; blue cells a negative change.

Mean elevations (Z_b) in Table 6-2 show that mean for the all three grades indicates a small degree of vertical settlement during the applied antecedent period, with increased antecedent duration increasing the degree of settlement. Specifically, absolute data indicate a 0.03, 0.20 and 0.02mm decrease in elevation after 60 minutes for the uniform, unimodal and bimodal beds respectively. After 960 minutes the degree of vertical settlement increases to 0.10, 1.14 and 0.15mm supporting the hypothesis that increasing the antecedent duration allows the bed a greater chance to rearrange. When calculated against mean bed diameter these changes are < 1% to 27% of the median grain size of beds, yet even these small changes may contribute to the sizeable stability gains to the bed surface as found in Chapters 4 and 5. Logically, vertical settlement results in increased packing density within the sediment bed (as solids are compacted into a smaller volume); this may result in higher pivoting angles and enhanced particle stability, thus explaining some of the stability gains.

The range of elevations (k) on the bed surface clearly indicates the difference between response of the uniform and graded beds. Absolute data indicates that k is similar for uniform and graded beds; however there is distinction in their reactions to antecedent flow. The uniform bed decreases the range, and by proxy the geometrical roughness (e.g. Aberle and Nikora, 2006; Cooper and Tait, 2008), by 13.5% and 5.4% as antecedent duration is increased from 60 to 960 minutes respectively. As particles are of equal size, the smoothing of the bed surface can only result from enhanced packing density. Given only the slight change in Z_b data, this appears related more to small scale grain reorientation or loss of exposed particles (see Section 6.3.1). Conversely, the application of antecedency generates increased k values (Table 12) for the unimodal and bimodal beds, respectively; +12.89% and +28.64% after 60 minutes and +4.59% and +18.55% after 960 minutes. For graded beds, response has to be due to the fractional response of the grains where the vibration of the smallest particles during the antecedent period permits their infiltration into the bed pores spaces of the largest particles so that the bed becomes rougher and develops hiding effects (Section 6.3.1). Specifically, the data set indicates that bimodal beds show the greatest response of k . In terms of stress history effect on k , all three beds show an inverse relationship with antecedent duration; longer durations show less change in k than shorter periods. This is surprising, as intuitively the trend of k would be expected to develop progressively. It therefore seems that bed response may be two-stage: (i) rapid evolution of the bed surface as a ‘first response’ to the new imparted flow which appears linked to vertical settlement; this supports the entrainment analysis (Chapter 4) which notes the greatest rate of change in bed stability at the start of the flow antecedent period; (ii) a counter secondary response to temper the roughness change caused by vertical settlement; dilation; repositioning/loss of surface grains, changes to the overlying turbulence and/or infill of bed pores by fines (Aberle and Nikora, 2006; Cooper and Tait, 2008) would be likely responsible mechanisms.

Skewness (Sk_b) analysis reveals that the distributions of elevations (as shown by Figure 6-7 through Figure 6-9) cannot be described by a Gaussian distribution. Instead the data shown in Table 6-2 indicate two trends. Firstly the uniform beds are characterised by a negative skew in the absolute data (Sk_b -0.11 to -0.20) suggesting that there is no armour present; this is independent of antecedent duration and is logical since structuring via the development of a coarser bed surface (akin to armouring) cannot develop without a range of sizes present on the bed surface. Conversely, graded beds indicate a positive skew in the absolute data (Sk_b 0.03 to 0.42) subsequent to longer applied antecedent durations; this

is seen to reflect a structured surface layer composed of larger grains with finer particles filling the depressions between, thus reducing the magnitude of the surface elevations below mean bed level (Aberle and Nikora, 2006) and supporting the earlier rationale of k values for longer duration experiments. Specifically, most absolute data of positive skew are between 0 to 0.1, however, the bimodal bed subsequent to long durations of applied sub threshold flow are significantly more structured with values three to four times those of other grade-time combinations; this shows that the bimodal bed undergoes surface structuring (akin to static armour formation) more significant than the unimodal bed (Section 5.4.1) and suggests differences in the underpinning mechanics of stability gains. The second trend to note is the relationship with antecedent duration which also shows grade dependency. After 60 minutes of antecedent flow, all beds have more negative skewness than at the start of the antecedent period; the uniform bed decreases by -26.67%, the unimodal by -42.86% and the bimodal by -33.33%. Conversely, for the longest antecedent duration (960 minutes), uniform beds shift to more negative skewness (-15.00%) continuing to suggest unstructured surfaces, whilst the graded bed change is progressively positively skewed with a 14.29% increase in the unimodal bed and a 19.05% increase in the bimodal bed. This suggests that, although the greatest change of elevations (Z_b and k) are noted after 60 minutes, graded beds have a requirement for much longer antecedent durations (960 minutes) before any skewness (Sk_b) is developed pertaining to formation of significant bed structuring of the bed surface.

Data within this section describing the *pdf's* and their statistical moments reveal three main findings.

- Mean bed elevation data (Z_b) for all beds clearly indicate small vertical settlement (by up to $0.27D_{50}$) during applied sub threshold flow. Increased antecedent duration increases the degree of settlement in all beds, however graded beds show a greater degree of vertical settlement and the unimodal bed data are most pronounced.
- The range of data (k) is a proxy for bed roughness with uniform beds generating a smoother surface, whilst graded beds become rougher; this data shows that unimodal beds develop the greatest roughness and hiding effects. Yet, a temporally dependent two-stage process is advocated in that rapid roughness changes are subsequently tempered following longer applied duration of antecedent flow.

-
- Skewness (Sk_b) data indicates that only graded beds structure via the development of a coarser bed surface (akin to static armouring); absolute data suggest this is most developed for the bimodal bed after long periods of sub threshold flow.

6.3.2.2 Porosity

Section 6.3.2.1 speculates that increased bed stability could manifest in terms of changes to the packing density of the bed; this is most easily measured in terms of porosity, defined as the ratio of the space taken up by voids to the total volume (e.g. Bunte and Abt, 2001, Kleinbans *et al.*, 2008). The underpinning scientific principle of porosity change is well-established for sediment research; i.e. where a bed undergoes water-working the packing density will increase (Kirchner *et al.*, 1990) resulting in a decrease in bed porosity. Data presented in Section 6.3.1 and 6.3.2.1 suggest that: within uniform beds the reduction in porosity occurs by particle repositioning and slight framework settlement to form a smoother surface where grains ‘fit’ together in a tighter packing formation; within graded beds framework settlement and fine disturbance appears to enhance hiding effects and packing density with fines possibly ‘rooting’ around larger clasts to increase their stability (Velickovic, 2005). Specific to this section of analysis, it is important to highlight that it is only bed surface porosity that is considered; this is commonplace in sediment bed analysis primarily due to depth restrictions of instrumentation through opaque media (such as the laser displacement system of this thesis; Chapter 3). Alternative, more accurate descriptions of porosity via assessment of 3D surface-subsurface cores are possible (Kleinbans *et al.*, 2008; Haynes *et al.*, 2009) but are only at inception for applied sediment research; this is therefore beyond the scope of this thesis and traditional methods of surface based porosity derivation are therefore applied and detailed below.

Porosity was calculated using two standard methods; an aspatial roughness geometry function (Aberle, 2007) and a spatial alternative (Rollinson, 2006). The following methodology is relevant:

1. Roughness Geometry Function; this method plots porosity as a function of elevation. Two steps are used in the calculation where the first step is to assume that the surface is composed of pillars with the ground area identical to the sampling resolution (0.1mm) and height of the corresponding reading in the vertical (z) direction. Secondly the DEM is sliced into 100 vertical segments where, for a

given segment, porosity is calculated according to the ratio of the fraction occupied by solids to the fraction occupied by voids as defined above; this follows the methodology of Aberle and Koll (2004) and Aberle (2007). The top most vertical segment corresponded to the highest recorded elevation and the bottom most to the lowest recorded elevation. The range of elevations, measured from the roughness tops to where the lowest layer tends to a constant zero porosity, is assumed to correspond to the active layer of the bed (Aberle, 2007). Specific to this thesis, elevation was normalised against the mean to allow direct comparison between the different antecedent durations. This aspatial method is interpreted as a statistical measure of the random geometry of the bed surface (e.g. Nikora *et al.*, 2001. Aberle and Koll, 2004) and provides a simple yet effective method to determine aspatial porosity. However no information is given about the spatial nature of the distribution, the change of the spatial characteristics of the distribution over time or the properties of the pores themselves.

2. Spatial porosity; this uses three different types of thresholding technique (of increasing complexity) to define pore spaces from grains. These methods are useful in that they provide information of the spatial nature of the bed porosity (of fundamental importance given the complex topography of the examined surfaces) and quantity features such as pore number, absolute depth and depth relative to the certain bed parameters e.g. the D_{50} . However, these methods can be computationally expensive and thus a trade off is often made between the complexity and therefore the accuracy with which the surface is described and the run time required for each technique.

Results of the roughness geometry function (where porosity is plotted as a function of elevation) for the 60 and 960 minute experiments are shown in Figure 6-7 to Figure 6-9. In all cases, the porosity curve decays monotonically from a porosity = 1 (i.e. air) at the roughness tops to a porosity = 0 (i.e. solid) at the lowest measured elevation. The observed decay curve represents the change in the sediment matrix with depth, where it is implied that at the upper most elevations the bed is composed of a greater proportion of pore space as compared to grains however as packing density increases with depth the ratio of pores to solid grains decrease. In all cases the roughness height over which the porosity is measured is between 8.75mm and 12.3mm. This is equivalent to $2D_{50}$ (or $2D_{max}$) for the uniform bed and $2-3D_{50}$ (or $0.5-0.7D_{max}$ in line with Parker and Sutherland, 1990; Hassan

and Church, 1992; Hoey and Ferguson, 1994) for graded beds. Strictly taking Aberle's (2007) definition of the active layer based on D_{max} , this would seem to suggest that the active layer within the uniform bed is deeper than that of the graded beds. Although this information does not give information about the absolute size of the pores in the surface of the uniform bed it would suggest that the porous structure of the bed is such as to allow greater rearrangement at a greater depth. This permits higher stability gains of both in the surface and sub-surface layers such that at threshold the bed is more stable, even if surface grains are progressively removed; this supports the results in Chapters 4 and 5 where it was noted that uniform bed is most responsive to stress history. In comparison, graded beds seem only to be adjusted to one layer depth and this may explain the greater overall response of the uniform beds to stress history.

The majority of data indicate identical trends and magnitudes, regardless of applied antecedent duration. This is in line with findings from Nikora *et al.*, (1998, 2001, 2006), Aberle and Koll (2004) and Aberle (2007); although these papers were researching the effect of degradational armouring, rather than the effects of antecedent flow, the authors noted very little change to the plotted porosity decay curve which they attributed to two mechanisms. Firstly by normalising the elevation data by the mean the effect of the outliers (i.e. essentially the influence of the range) is reduced such that any changes to the bed surface will be comparatively smaller; although this is a downfall of this technique normalisation is a standard procedure for this kind of analysis and allows direct comparison between different data sets Nikora *et al.*, (1998, 2001, 2006), Aberle and Koll (2004) and Aberle (2007). Secondly it was assumed that the changes to porosity were so small in relation to the overall elevation range that the changes would not be noticeable on the porosity decay curves. Data from the present thesis agrees with these findings.

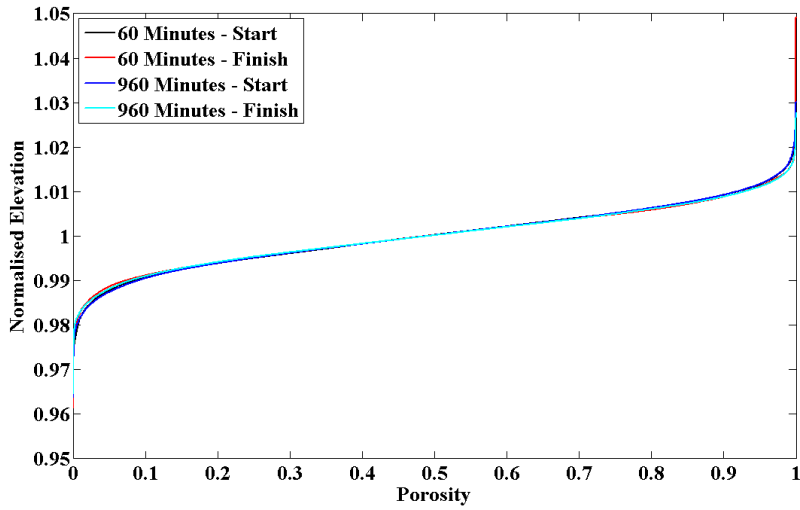


Figure 6-7; Porosity plotted as a function of elevation in the uniform bed for the 60 and 960 minute experiments.

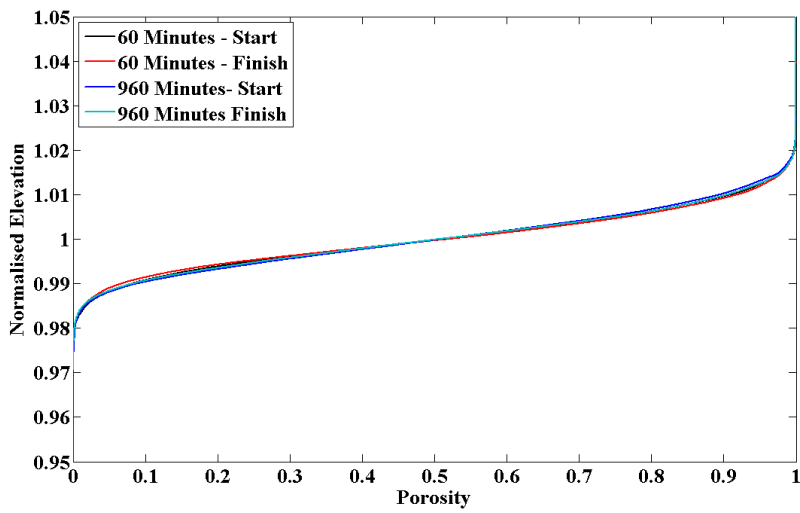


Figure 6-8; Porosity plotted as a function of elevation in the unimodal bed for the 60 and 960 minute experiments.

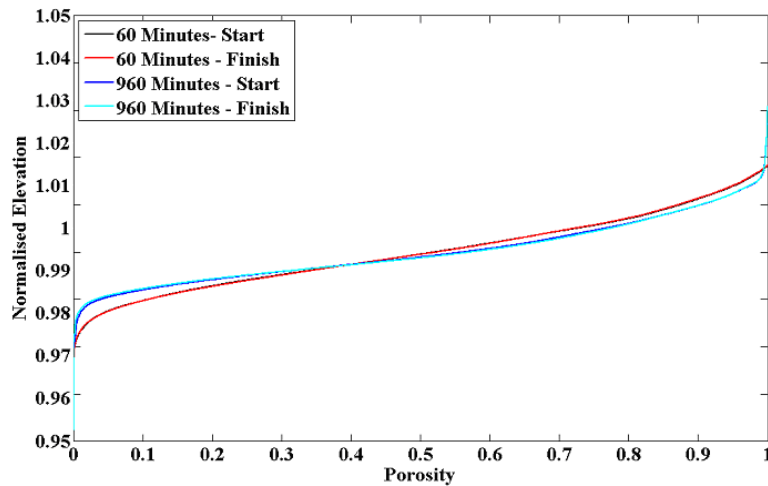


Figure 6-9; Porosity plotted as a function of elevation in the bimodal bed for the 60 and 960 minute experiments.

This method is useful in that it statistically indicates the geometry of the bed surface (Aberle, 2007). Yet, the interpretation of the porosity estimates using aspatial derivation needs to be treated with some caution because porosity calculation is restricted to the surface; in reality porosity tends to a non zero value deeper into the bed, but this is below the range capability of the laser measurements. In addition this method does not give any information about the spatial nature of that porosity and can only be used as a useful first pass estimate of bed surface porosity; thus more advanced data analysis is proposed in subsequent analysis.

One advance is that spatial porosity can be calculated through the use of thresholding techniques based on surface topography; this provides a much more detailed description of the spatial coherence of the surface pores and the evolution of porosity over time. Three threshold techniques are applied in this thesis: (i) a fixed threshold; (ii) a dynamic threshold; (iii) and water-shedding (Rollinson, 2006; McEwan *et al.*, 2000; Sime and Ferguson, 2003). An increase in complexity in the derivation of porosity is noted in progression through each of the types of thresholding technique; the advantages and disadvantages of each are discussed fully below.

(i) *Fixed thresholds* – this essentially applies a plane across the bed surface at the specified elevation, in this case the mean; values above the threshold value are counted as a grain,

whereas those below the threshold value are accounted for as a pore. This technique is based on a single layer of gravel (Figure 6-11; McEwan *et al.*, 2000; Sime and Ferguson, 2003) and therefore assumes that there is no topography on the bed surface; it is similar to the aspatial porosity methodology described earlier, yet replaces porosity with a spatially-resolved function of elevation.

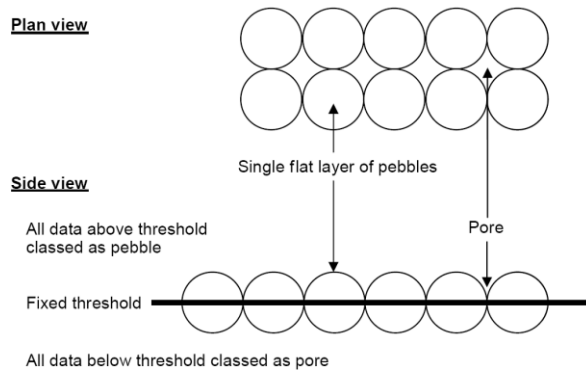


Figure 6-10; Schematic showing a fixed threshold to separate grains from pores (after Rollinson 2006).

However, both uniform and graded beds indicate a wide range of elevations representative of bed roughness greater than one grain diameter (k values; Section 6.3.2). Thus, a fixed threshold oversimplifies boundary roughness, in that roughness patterns persistently laying above/below the threshold are ignored and classed as grains/pores respectively (Figure 6-11); consequently, a lower/higher than actual porosity would be recorded.

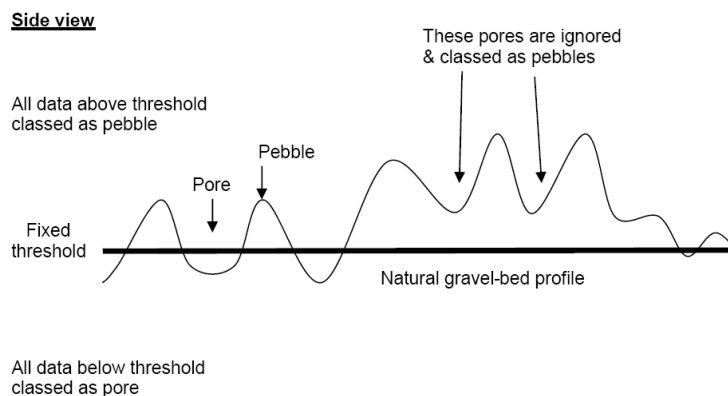
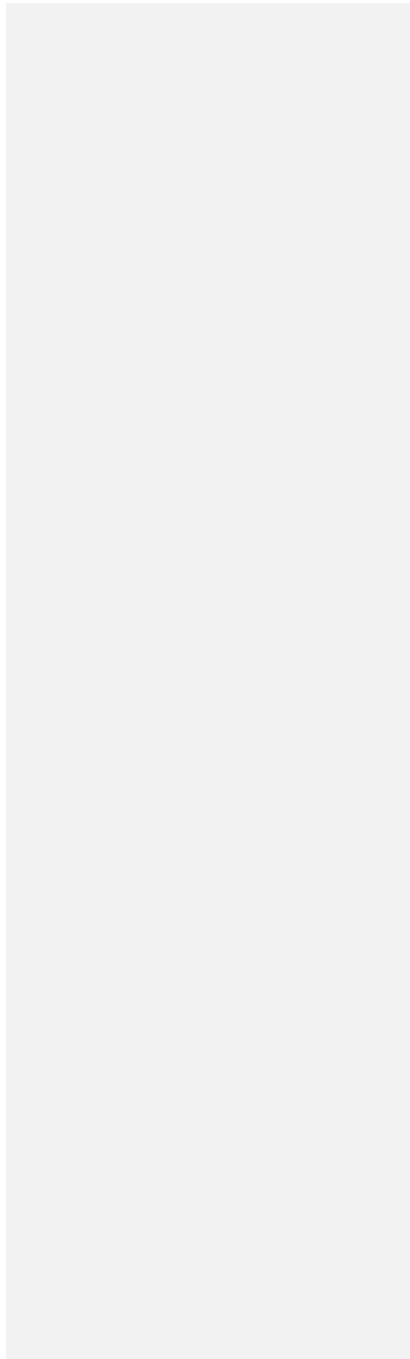


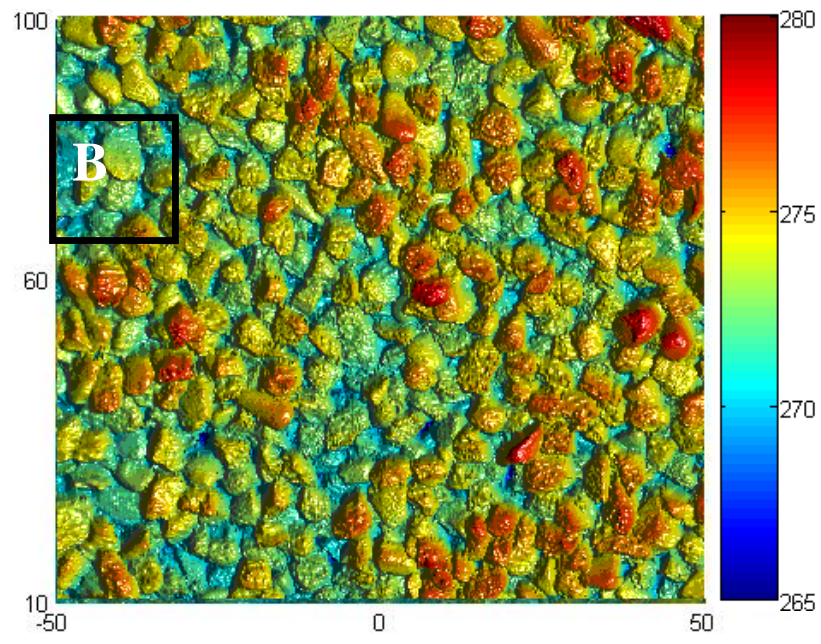
Figure 6-11: Schematic showing the problems of applying a fixed threshold to a natural gravel bed (after Rollinson 2006).

Example results are shown by Figure 6-12 to Figure 6-14 using data from the all three beds after 960 minutes of antecedent flow. The left-hand figure of each image pair shows the DEMs plotted in mm above and arbitrary datum with red being areas of high relief and blue being areas of low relief. The right-hand figure shows the same bed but with the thresholding technique applied so as to show the spatial porosity; black areas are defined as pores whilst white areas are denoted as grains.

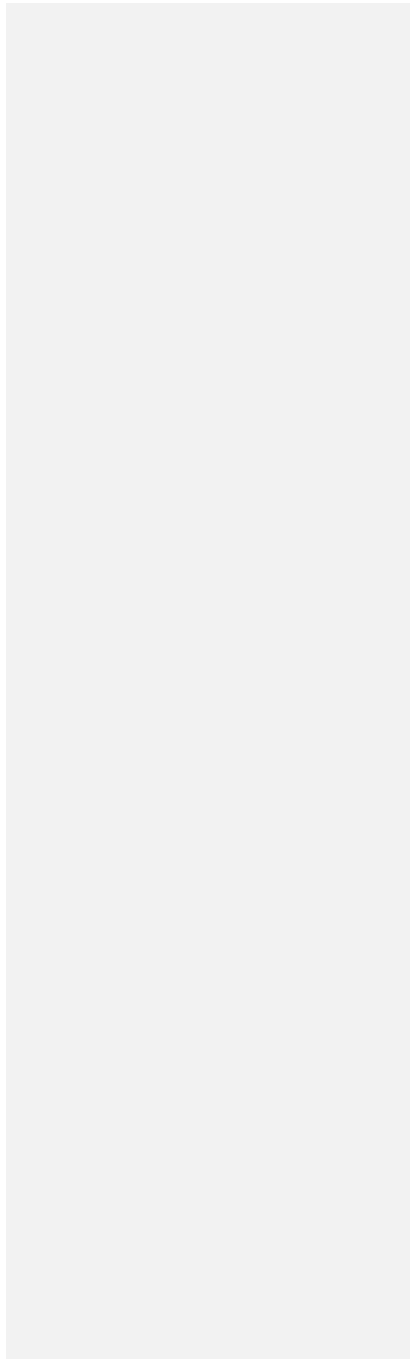
In the uniform bed, in general there is an obvious relationship between colour-coding of red/orange of high elevation grains in the DEM to the ‘grains’ depicted using the thresholding technique. Similarly there is an obvious relationship between the blue/green low relief areas on the DEM to the ‘pores’ depicted using the thresholding technique. However there is a significant overestimation of actual pores (coloured only as very dark blue on DEM) which is especially apparent where the grains lie at a lower relief (which must be below the mean elevation) on the bed surface; where this is the case grains are correctly labelled as pores. In the graded beds differentiation of grains and pores below the mean elevation are particularly badly defined with large areas depicted as being pores when there are clearly visible grains on the surface just located at lower than average elevations. This becomes especially apparent in the images of the graded sediment where the smaller grains within the image are poorly depicted. Indeed Graham *et al.*, (2005) noted that the smallest grains had to be removed from their study of field data as significant error was introduced when trying to delimit small grains from pores.

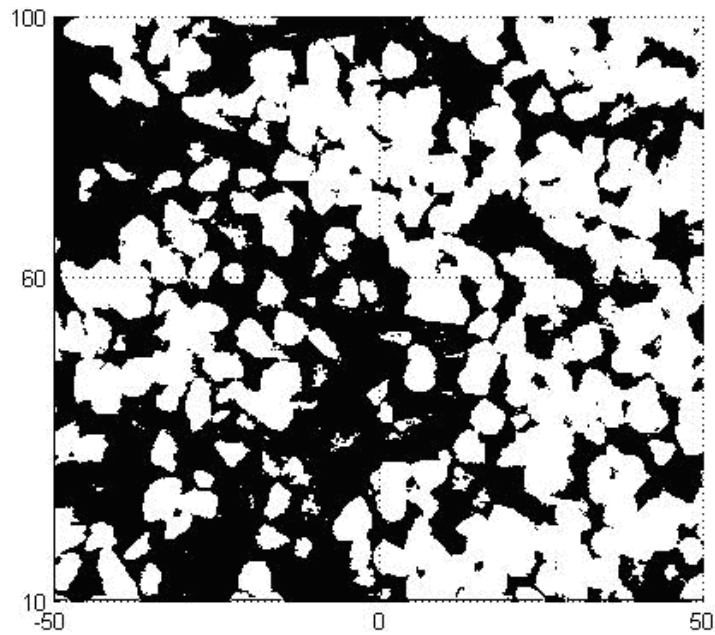
Thus from all three figures it can be seen that defining porosity using the fixed method approach can be used to plot the porosity spatially; however, a number of limitations are noted. Firstly topography which falls beneath the average bed elevation is badly affected by the threshold technique with differentiation of pores and grains proving impossible below the threshold value. In addition, the process produces pores that are spatially contiguous; thus, individual pores cannot be delimited to analyse individual pore attributes. As such, this technique falls a long way short of being able to differentiate pores and grains on the bed surface; it is therefore incapable of analysing individual pore attributes. Thus a method is needed which is not based on global bed average; instead it should be able to account for local topographic variability by way of a moving average threshold technique.





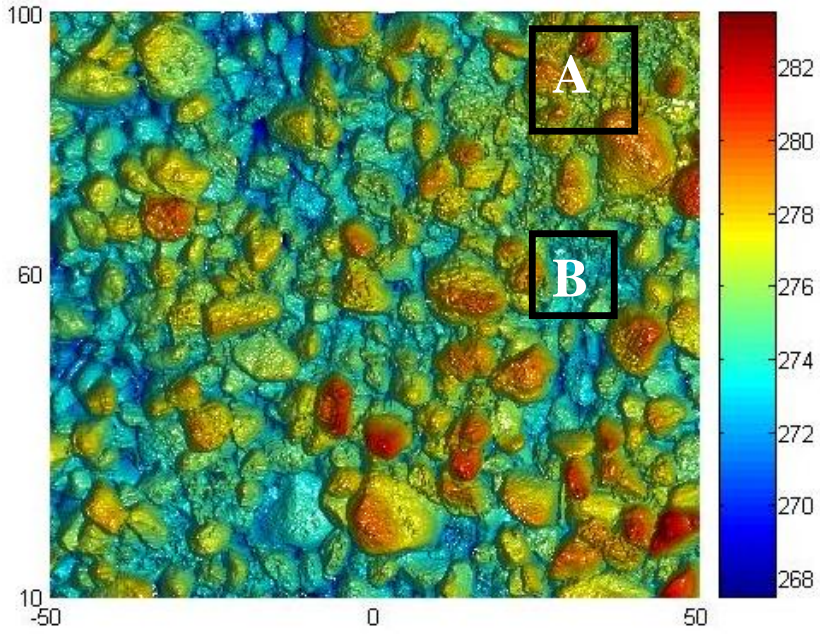
B





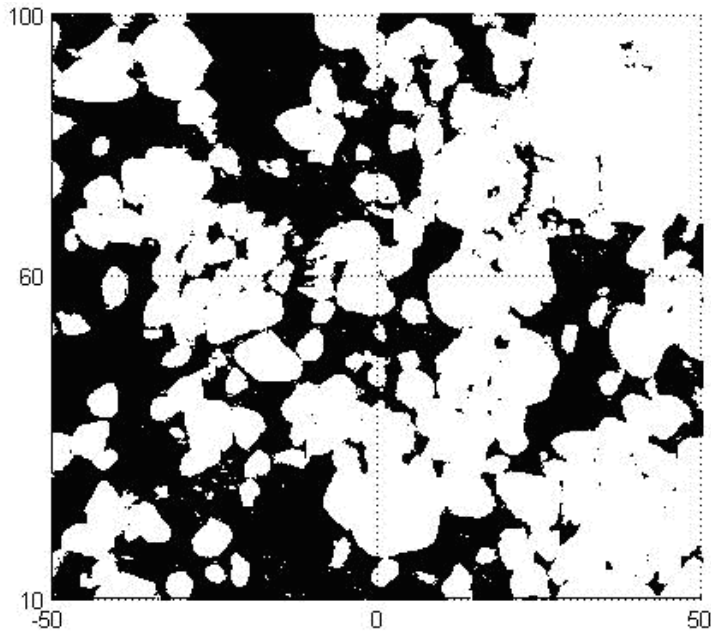
Areas of maximum and minimum elevation are often incorrectly assigned as a grain (as indicated by region A on both images) or pore respectively (as indicated by region B on both images).

Figure 6-12; Digital elevation model of the uniform bed shown in the left hand image with comparable image of the spatial porosity shown in the right hand image.



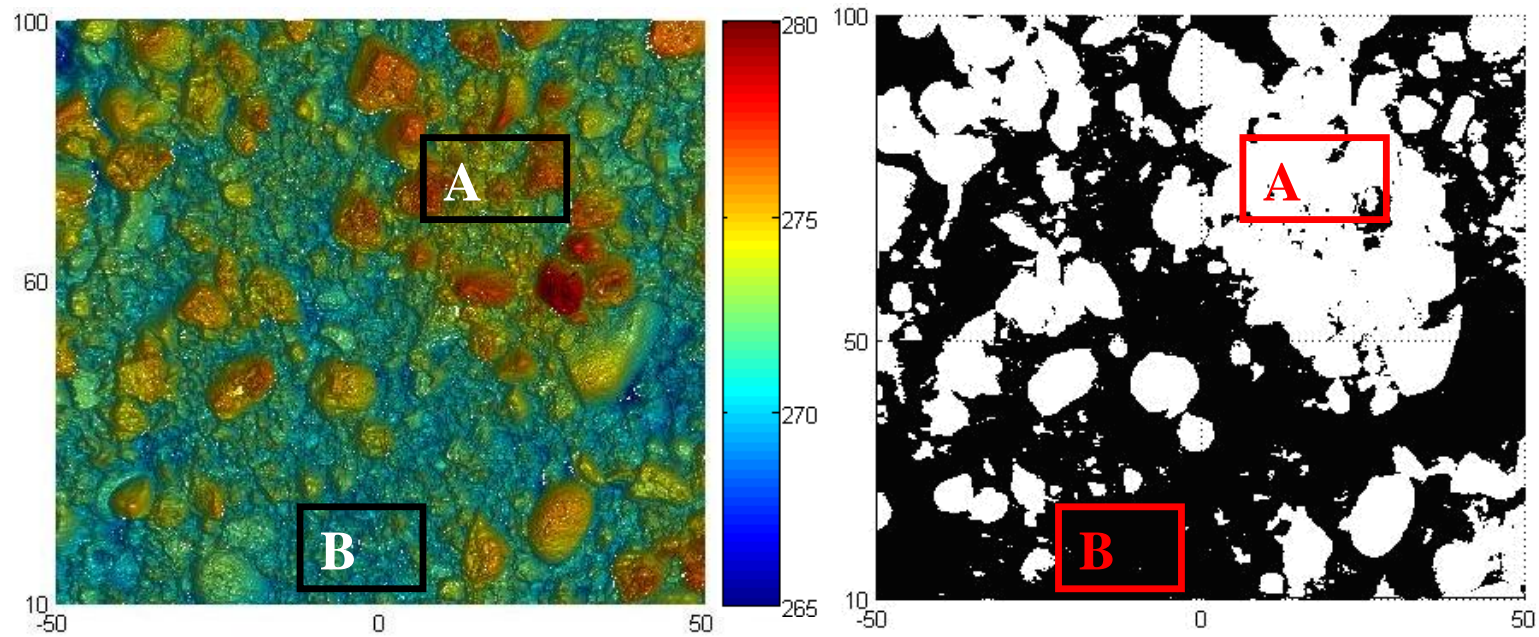
A

B



Areas of maximum and minimum elevation are often incorrectly assigned as a grain (as indicated by region A on both images) or pore respectively (as indicated by region B on both images).

Figure 6-13; Digital elevation model of the unimodal bed shown in the left hand image with comparable image of the spatial porosity shown in the right hand image.



Areas of maximum and minimum elevation are often incorrectly assigned as a grain (as indicated by region A on both images) or pore respectively (as indicated by region B on both images).

Figure 6-14; Digital elevation model of the bimodal bed shown in the left hand image with comparable image of the spatial porosity shown in the right hand image.

(ii) *Moving average threshold* - this uses the local topography upon which to base the threshold elevation value (Graham *et al.*, 2005; Rollinson 2006), thus overcoming the problems of the fixed threshold method. The moving average threshold was created by smoothing the original DEM based on a neighbourhood basis (i.e. the points surrounding the specific location in question). For a given point on the bed surface the threshold value adopted is based on a consideration of the elevation values surrounding that cell at a user defined radius thus creating a dynamic threshold. The radius was chosen based on a value of 0.325 of the D_{50} ; and was akin to the search radius as used by Rollinson (2006) who worked with the same grain sizes as in this thesis. All data above this dynamic threshold are classified as grains and all below as pores (Figure 6-15). Results using this thresholding technique are shown in Figure 6-16 to Figure 6-18 for all three beds subsequent to 960 minutes of antecedent flow; black areas defined as pores and white areas denoted as grains.

Side view

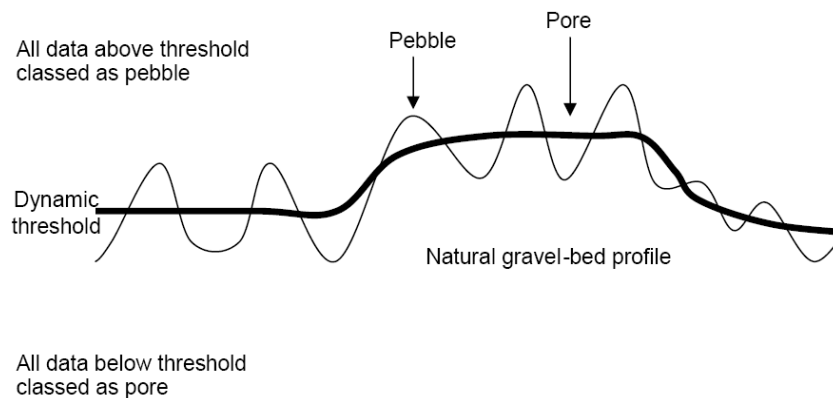
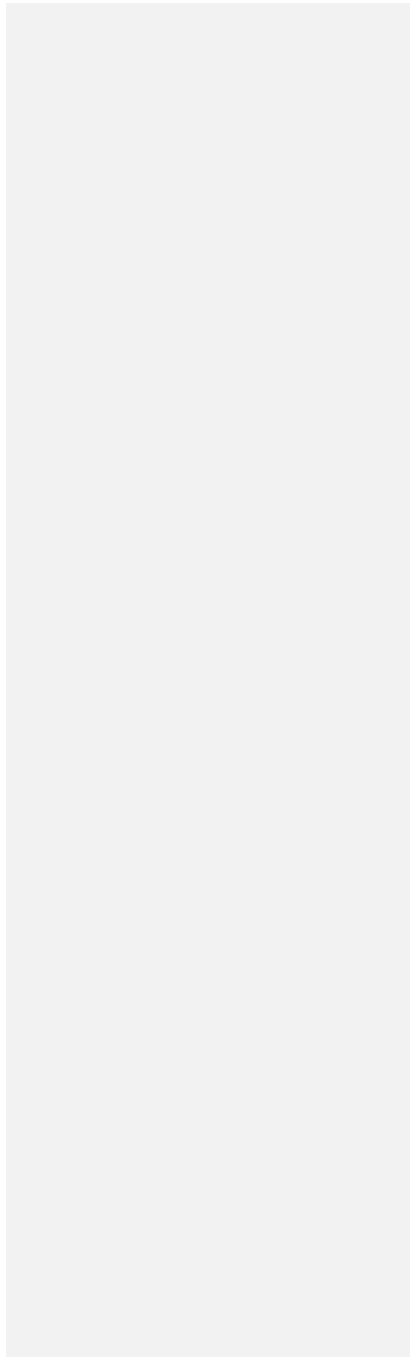
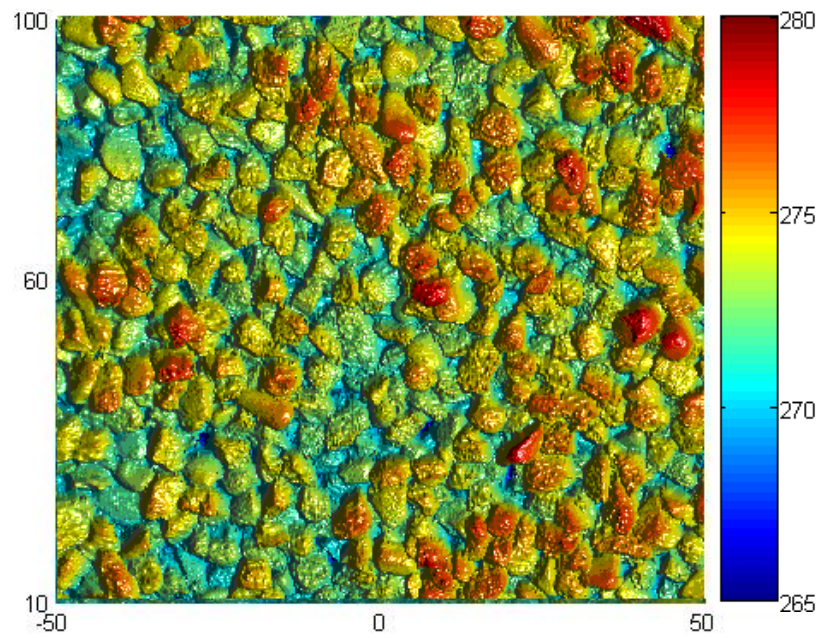


Figure 6-15; Schematic showing the dynamic threshold approach to separating gravels from pores (after Rollinson, 2006).





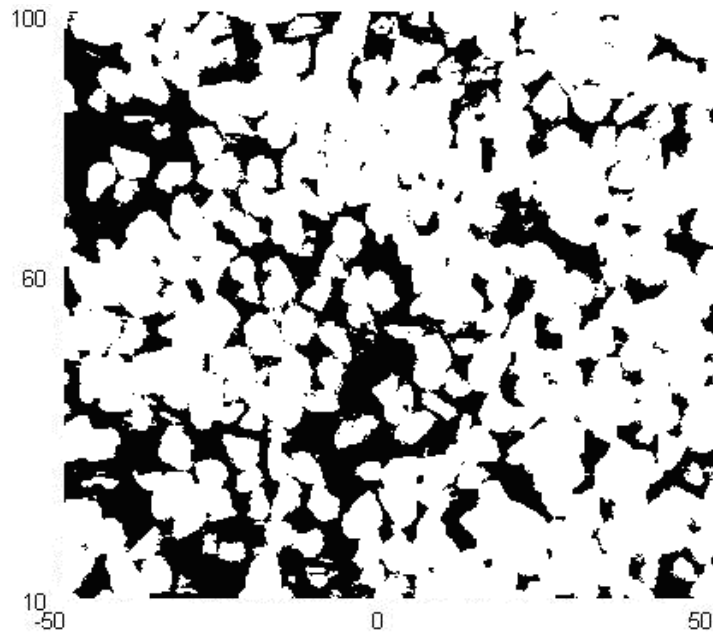
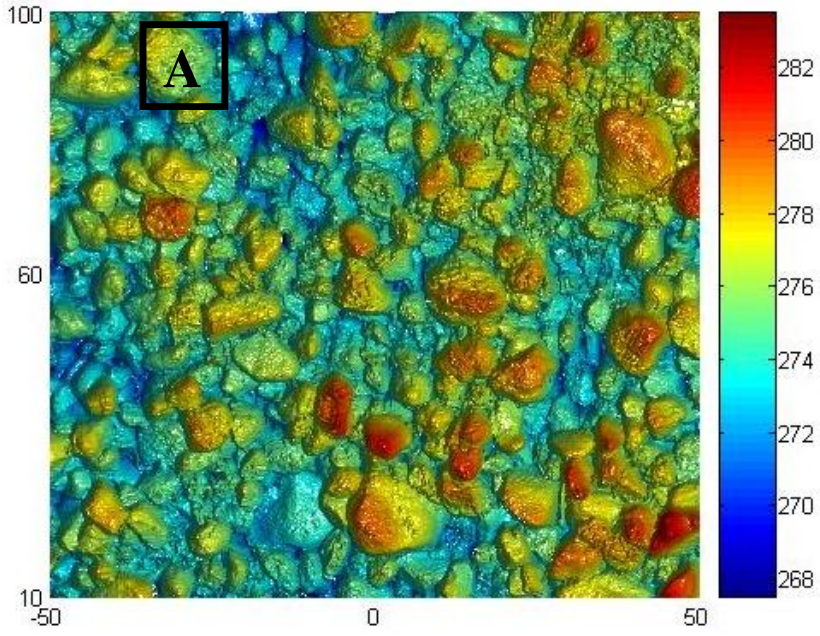
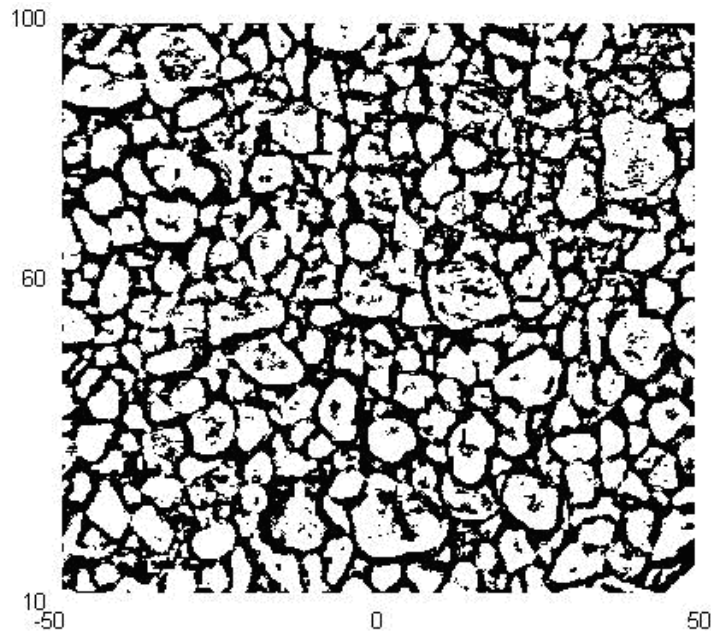


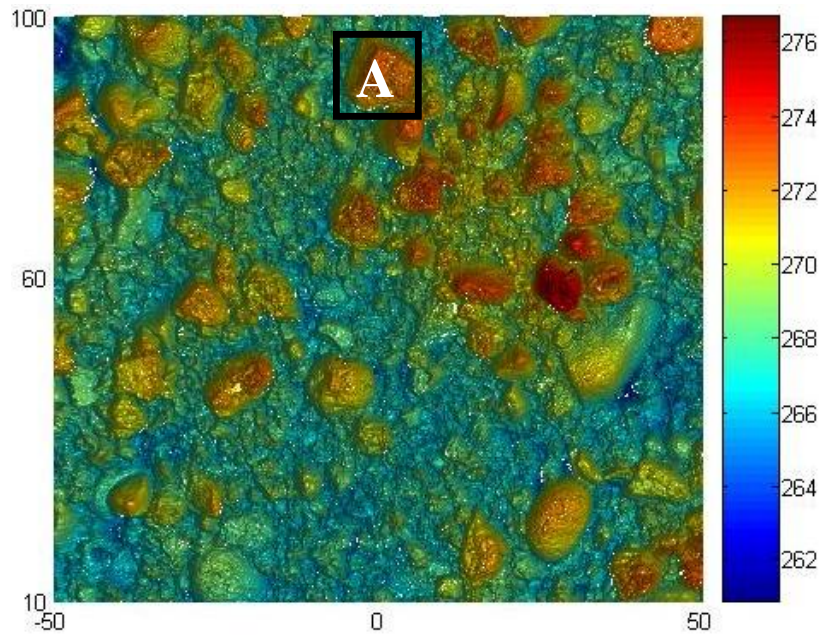
Figure 6-16; Digital elevation model of the uniform bed shown in the left hand image with comparable image of the spatial porosity shown in the right hand image.

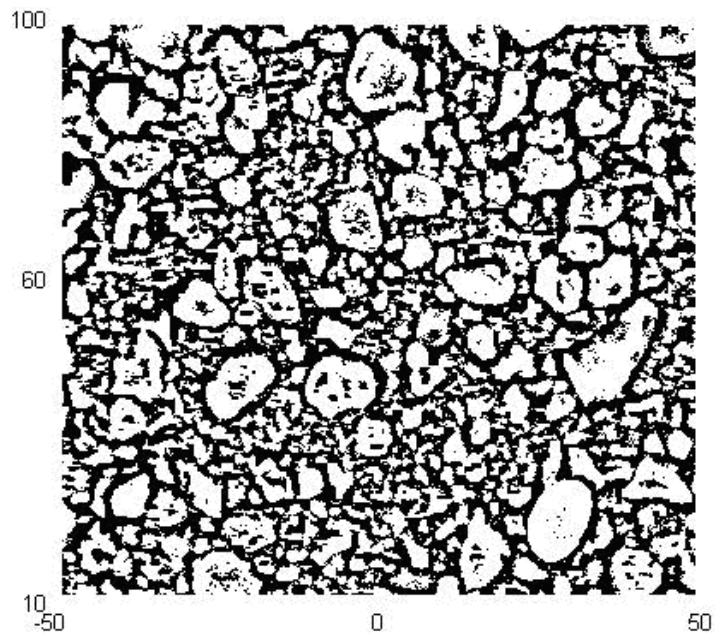




Although grains and pores are better delimited on the bed surface 'pits' on the grain surfaces are also incorrectly assigned as pores (as indicated by region A on both images).

Figure 6-17; Digital elevation model of the unimodal bed shown in the left hand image with comparable image of the spatial porosity shown in the right hand image.





Although grains and pores are better delimited on the bed surface 'pits' on the grain surfaces are also incorrectly assigned as pores (as indicated by region A on both images).

Figure 6-18; Digital elevation model of the bimodal bed shown in the left hand image with comparable image of the spatial porosity shown in the right hand image.

It is clear to see from the exemplar figures that using this thresholding technique it is possible to better demarcate the pores from the grains on the bed surface however it is still not possible to delimit individual pores; this limitation is noted by Rollinson (2006). Specifically, two features of the moving average threshold data are highlighted:

Firstly, 'halos' of pore surround each grain. This is because grains, by their nature have a peak in the grain centre and an edge leading to lower relief locations of contact with the neighbouring grains. Depending on where the threshold elevation is located, all inter-grain low relief areas are accounted for as pores, rather than isolating just the deepest areas of relief (dark blue pockets on the DEMs). This results in an overestimation of pore spaces in the bed surface.

Secondly, 'pits' (of falsely attributed pores) appear on the grain surfaces. This is liable to be a facet of the filter size applied; a filter size which is too large will not pick up the local topography and will act in a similar manner as the globally applied filter (i.e. the fixed threshold method). Conversely a filter size which is too small will pick out small scale features on the bed surface which are not relevant. In order to rectify this two filters would have to be applied; a low pass filter, as applied to derive the figures above, followed by a high pass filter applied at a smaller spatial resolution to correctly identify the missed points. This latter step was not undertaken since it would still not yield individual pore attributes which was the overall aim of the thresholding exercise. Thus, although the moving average thresholding technique has yielded improved information about the spatial porosity of the bed surface as compared to the fixed threshold technique, it still does not produce discrete pores thus precluding analysis of individual pore properties such as size and depth.

(iii) *Hydrological watersheding* - this is the most sophisticated thresholding technique to specifically delineate pore edges and thus yield information about individual pore attributes such as number, depth and size. This method uses hydrological modelling tools within the software *ArcMap*. Akin to image analysis techniques which defined grain boundaries by looking for 'edge characteristics', this method of pore derivation uses the topography of the bed surface to define where water would flow if dropped onto the surface. This technique creates 'watersheds' to define pores where a pore is defined as being composed of grains at the edge of the watershed which descend into a deeper hole (Rollinson, 2006). Watersheds are generated in a three step process:

Step 1; a grid of flow directions was determined from the DEM on a neighbourhood basis where each output cell value is relative to its eight neighbours. Flow direction was determined by finding the direction of steepest descent from each cell (ESRI, 2004).

Step 2; a grid of 'sinks' for the DEM was generated, using the output from the flow direction step. A sink is a cell or set of spatially connected cells whose flow direction cannot be assigned using the flow direction step; this occurs when all neighbouring cells are higher than the processing cell and so cannot be assigned a flow direction. For this study the sinks are significant since they represent the maximum pore depth.

Step 3; to execute a watershed command which uses both the flow direction and sink grids to calculate the contributing area for each sink. The watershed of each sink therefore defines the boundary of each pore thus making a watershed equal to a pore. This method has been successfully employed for similar work by Rollinson (2006).

The output image divides the DEM into watersheds (Figures 6-22 to 6-24). Open (i.e. partial) watersheds at the scan edges were ignored; the percentage of area lost because of this will vary according to the size of the pores which are located at the edge of the image but typically this varied between a 3% and 10% of the total area of the scan. This is in line with the findings of Rollinson (2006). The accuracy of the output is dependent upon the input DEM as, to define pores, a smoothed bed morphology was needed. This was generated (in a similar manner to the dynamic pore technique) by the DEM being re-sampled at a resolution commensurate with 'user defined' needs; these were set a 0.5mm ($<D_{min}$), 1mm (equal to D_{min}) and 4.8mm (D_{50}) and a sensitivity analysis undertaken. Figure 6-19 indicates that 1mm is the best resolution to identify and threshold each pore; Figure 6-20 shows that if the original scan data was used with no smoothing (0.5mm grid) then the bed was split into too many small and unrealistic pores included erroneous pitted surface data, whilst too much smoothing (Figure 6-21) produced pore sizes that included larger scale bedform features which served to obliterate the smaller scale details such as the bed surface pores.

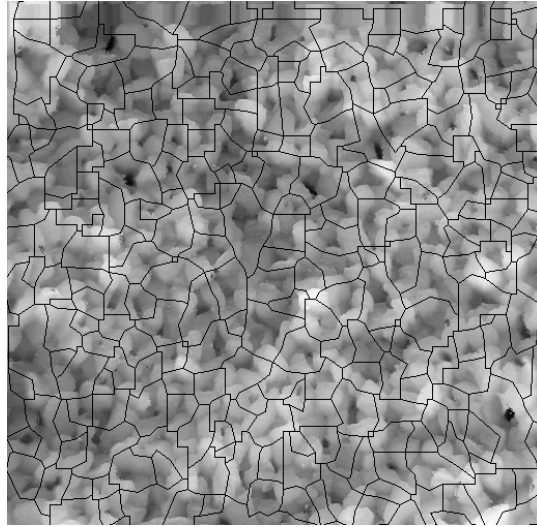


Figure 6-19; Image of the gravel bed DEM overlain by the derived watersheds representing the pores using a smoothing radius of 1.0 mm. Close inspection of the derived watersheds appear to show a faithful representation of the delineation of deeper areas representing pores on the bed surface.

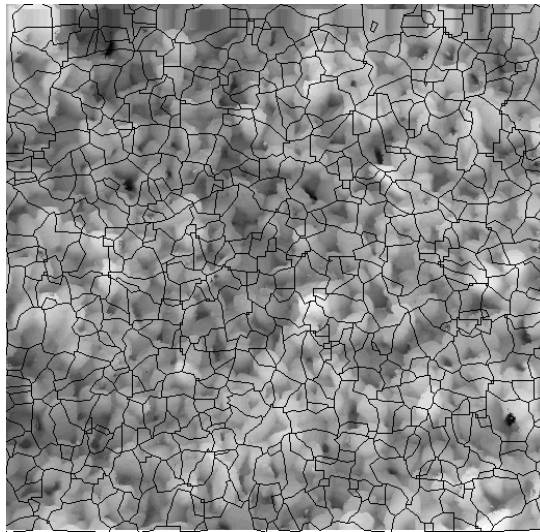


Figure 6-20; Image of the gravel bed DEM overlain by the derived watersheds representing the pores using a smoothing radius of 0.5mm. Close inspection of the derived watersheds appear to show watersheds which are split into too many unrealistic pore boundaries.

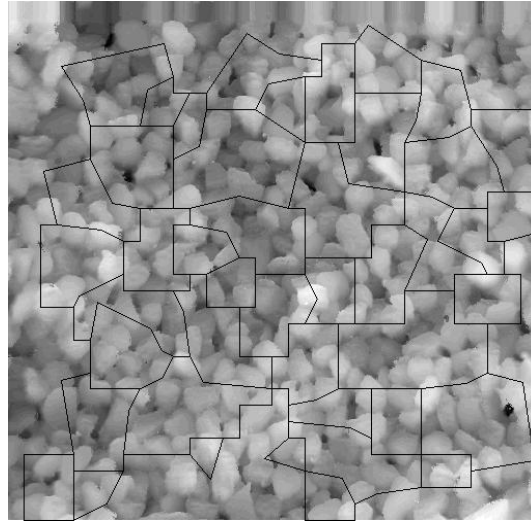


Figure 6-21; Image of the gravel bed DEM overlain by the derived watersheds representing the pores using a smoothing radius of 4.8mm (representative value of the bed D_{50}). Close inspection of the derived watersheds appear to show watersheds which are split into unrealistic larger pores missing some detail at the smaller scale.

Using this thresholding technique Rollinson (2006) proposed a new pore definition where a pore was defined according to its depth. Shallow pores were defined as having a depth $<$ the D_{50} of the bed material whereas a deep pore has a depth $>$ D_{50} of the bed material. As such, according to Carling (1984) shallow pores are defined to include minor depressions and such that any sediment, especially fine sediment, has a high chance of being entrained. Conversely deep pores extend below the D_{50} of the bed, such that fine sediment has a low chance of being entrained (Carling, 1984). The depth of the pore was taken from the highest bed elevation within the specific watershed (termed Z_{max}) such that the depth respective to the D_{50} was defined as being $Z_{max} - D_{50}$. Given that the D_{50} is the same in all three grain size distributions this descriptor was deemed suitable such that a direct comparison could be made between the beds however any grain fraction could be taken. Consequently, the results are analysed in two ways; firstly analysing pore depth in relation to the mean bed elevation and the D_{50} and, secondly, analysing the size of the pores, as shown by Table 6-3.

Grain Size Distribution	Descriptor	Antecedent. duration (Minutes)	Start of Antecedent. Period	End of Antecedent. Period	Absolute difference	Relative difference
Uniform	% below Z_b	60	97.94	96.03	-1.91	-1.99
	% below D_{50}		14.15	10.71	-3.44	-32.12
	% below Z_b	960	95.98	95.35	-0.63	-0.66
	% below D_{50}		11.76	9.26	-2.50	-27.00
Unimodal	% below Z_b	60	87.70	94.56	6.86	7.25
	% below D_{50}		5.89	22.50	16.61	73.82
	% below Z_b	960	84.20	86.39	2.19	2.54
	% below D_{50}		3.80	4.36	0.56	12.84
Bimodal	% below Z_b	60	86.81	89.96	3.15	3.50
	% below D_{50}		0.00	0.87	0.87	100.00
	% below Z_b	960	92.30	93.74	1.44	1.54
	% below D_{50}		4.56	4.61	0.05	1.08

Table 6-3; Summary of the pore properties of the three beds for experiments running 60 and 960 minutes antecedent flow duration.

Considering the proportion of area defined by pores three findings are apparent from Table 14; grade dependency, temporal dependency and that pore spaces are most affected by antecedent flow in the unimodal bed. Firstly, uniform beds indicate that the percentage of pores extending below the average bed elevation (Z_b) decreases ($< 2\%$) after antecedent flow is applied (Table 14); conversely, graded beds show an increase (up to 6.52%; Table 13). This appears similar in trend to the k value trends showing the range of bed elevations in Table 13; k (i.e. bed roughness) reduces in uniform beds but increases in graded beds. Within the uniform beds this cannot be as a result of relative size effects, thus changes must be by grain rearrangement towards a bed of either lower roughness or tighter packing density, or both. It follows that if grains are repositioned/displaced to less exposed locations on the bed surface during antecedency (as proven in Section 6.3.1), the revised average bed elevation sits lower in the bed surface; thus, even if there are no other changes to the bed surface, there will be a reduced number of pores extending below Z_b . Alternatively, more whole scale rearrangement of the bed surface by the observed slight vertical settlement (Table 13) and rearrangement may increase packing density and reduce pore extent. Conversely within the graded beds pore depth increases with applied flow with the magnitude of change decreasing with increasing antecedent flow; this is akin to the change to roughness noted within section 6.3.2.1. This two stage response was noted

within section 6.3.2.1 and was postulated to be due to (i) rapid evolution of the bed surface as a ‘first response’ to the new imparted flow which appears linked to vertical settlement; this supports the entrainment analysis (Chapter 4) which notes the greatest rate of change in bed stability at the start of the flow antecedent period; (ii) a counter secondary response to temper the roughness change caused by vertical settlement; dilation; repositioning/loss of surface grains, changes to the overlying turbulence and/or infill of bed pores by fines (Aberle and Nikora, 2006; Cooper and Tait, 2008) would be likely responsible mechanisms. The unimodal bed exhibits the greatest overall change to pore properties; this is also correlated to bed roughness data from Section 6.3.2.

Analysing the maximum depth of the pore sizes over time reveals further differences between the three sediment beds (the cumulative distribution curves plotting percentage of pores against their size are shown in Appendix E). In terms of absolute depth the deepest pore spaces are found within the uniform ($2.19D_{50}$ to $2.50D_{50}$) and unimodal beds ($1.94D_{50}$ to $2.57D_{50}$); whilst the bimodal beds have slightly shallower pores ($1.82D_{50}$ - $1.99D_{50}$). This trend would be expected and can be analysed in relation to the different packing arrangements of the three beds. Given that regions of fine grains on the bed surface would limit pore depth significantly more than an open coarser framework, it follows that beds with greater proportions of fines (i.e. the bimodal bed) would have smaller pore depth statistics. The temporal aspect of this trend notes that the uniform bed pore depths become shallower with increased antecedent duration (by 0.06 to 1.46mm). This can be explained in terms of an increased packing density and removal of exposed grains as antecedent duration is increased in line with findings in section 6.3.2.1. Conversely within the graded beds the pores become deeper with increased antecedent flow. The unimodal shows the greatest change (up to 2.12mm deeper) with this graded dependent response in line with previous findings noted throughout Chapter 6. It would be assumed that if the changes to the pore size were purely related to an increase in the packing density pore depth would decrease with increased antecedent durations however this is not the case. As postulated earlier it could be that dilation of the bed surface may explain this response (Allan and Frostick, 1999).

In summary the analysis from the pore data reveals four main trends;

- The number of deep pores (i.e. below Z_b or D_{50}) decreases in the uniform bed yet increases in graded beds following applied antecedent flow. This is supported by the changes in bed roughness (k value data from Section 6.3.2)

-
- There is an inverse relationship between the degree of change in the number of deep pores and the antecedent duration. This suggests a two-stage bed response cycle to the application of a new shear stress as already described in Section 6.3.2.
 - Absolute pore depths range from $1.82D_{50}$ to $2.57D_{50}$. The shallowest pores are found in the bimodal grade; this is likely due to the higher proportion of fines within the distribution which block pores near the surface.
 - Following antecedent flow, pores shallow in the uniform bed (due to loss of exposed grains and increased packing density of the surface) yet deepen in the graded bed possibly linked to a change in packing.

6.3.3 *Small scale grain reorientation and displacement*

From the analysis so far in this Chapter antecedent stability gains have been shown to relate to bed elevation change, roughness change and porosity change. These changes appear to be of small magnitude, but the use of average statistics (section 6.3.2.1) has the potential to be misleading. Cooper *et al.*, (2008) noted that it is possible for beds to have the same statistical distribution of bed surface elevations and volumetric grain size distributions, yet have a very different structure due to the arrangement of grains on the bed surface. In addition, the visual analysis in section 6.3.1 also showed that grains were reorientated and/or displaced from the bed surface and Section 6.3.2 indicated that this local mobility alters the statistical properties of analysis undertaken for the other variables. Consequently, Section 6.3.3 seeks to use spatial analytical techniques to specifically analyse antecedent-induced bed stability in terms of: (i) DEM's of Change in terms of time-lapse image subtraction and examination of particle reorientation; (ii) Multiparticle Structure Analysis in terms of bed surface fractional analysis, cluster formation and 2D structure functions.

6.3.3.1 *Digital Elevation Models of Change*

Figure 6-22 presents Digital Elevation Models (DEMs) that spatially represent the relative change in bed topography after each antecedent period for each bed. These DEMs were calculated in ArcGIS software, where the interpolated grid from the end of the antecedent period was subtracted from the interpolated grid derived from the beginning of the antecedent period. In order that the images be subtracted from each other the two images had to be geo-referenced such that they could be directly compared from the same arbitrary coordinate system; eight control points with low residual values (i.e. a good

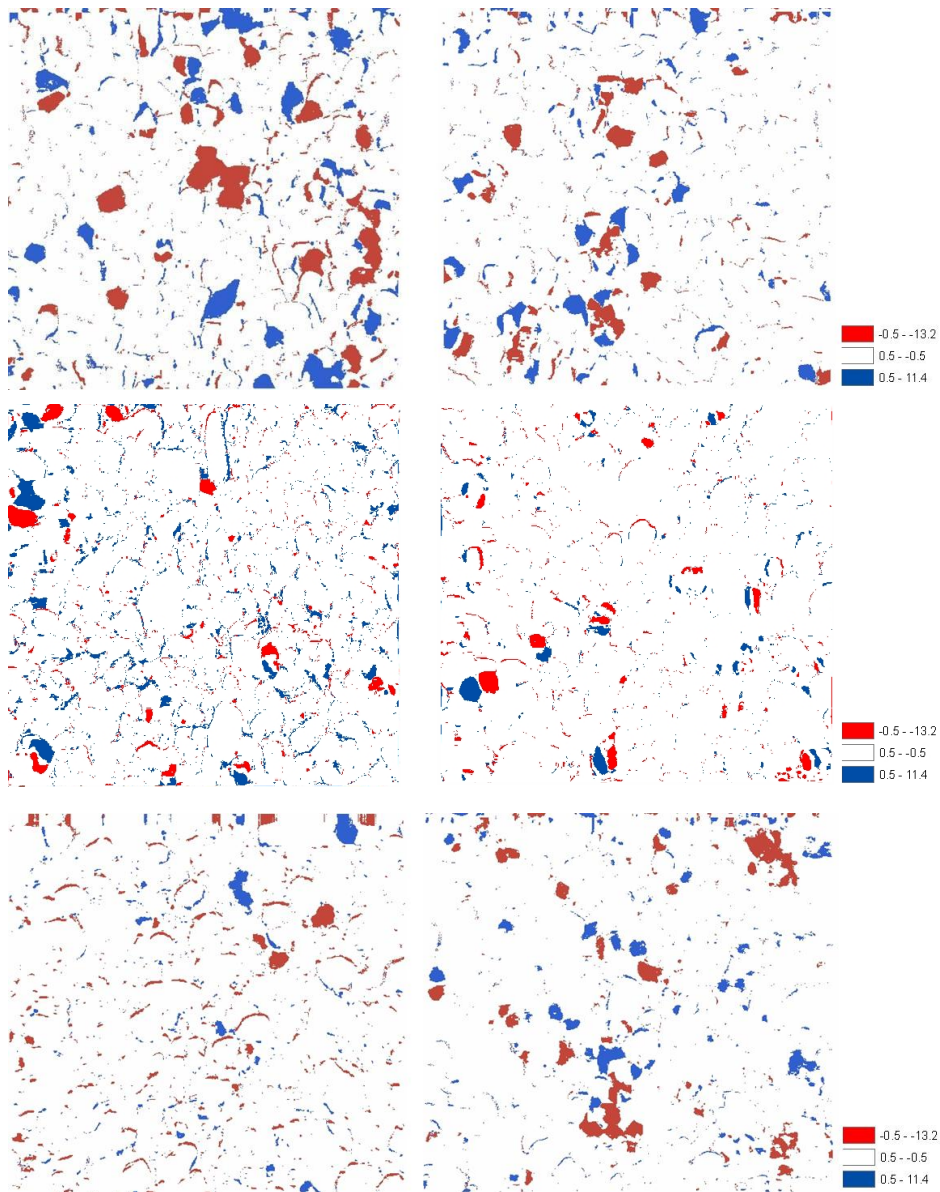
match) were located and employed for geo referencing (Ladd *et al.*, 2006). Yet, it is important to note that geo referencing is a trade off between the number of control points (taking the investment of significant time and effort) and the accuracy of the geo - referenced image output. Thus, fine ‘halos’ are typically a facet of where geo referencing leaves images slightly mis-matched and are therefore not indicative of actual changes to the bed surface; however it is impossible to determine this conclusively as they may also depict grain rotation. Given the ArcGIS methodology, areas of red indicate that the bed elevation has decreased in this location due to rotation, flipping or entrainment; areas of blue therefore indicate that the bed elevation has increased suggesting rotation, flipping or deposition. This is clear from Figure 6-22. Entrainment or deposition is identified on the images as an isolated particle moving in (blue) or out (red) of a location. Flipping of particles can be identified as generally a mirror image of a blue shape sits adjacent to an equivalent red shape. Reorientation is more difficult, but a line or crescent around the whole or part of a grain edge would be symptomatic. All these manifestations can be seen in Figure 6-22.

Figure 6-22 shows that local absolute topographic changes are far in excess (+11.4 mm (+2.4D₅₀) to -13.2 mm (-2.75D₅₀)) of the global average data implied in Table 12 earlier in Chapter 6. This suggests that the use of average statistics masks changes to the bed surface and is inappropriate in terms of accurate analysis of mechanistic processes pertaining to stress history. Typically changes noted within Figure 6-22 manifests as three different types of grain movement; (i) the overturning of a grain which manifests as blue area mirror image of neighbouring red area; (ii) the movement of a grain into or out of the field of view and; (iii) the rotation of a grain which manifests as a halo of blue and red areas around the edge of grains. The type and degree of change will be grade dependent. Specifically in the uniform bed there is evidence of all three types of grain movement with the most noticeable change being the displacement of grains either into or out of the field of view. This type of movement occurs both as individual grains as well as groups of grains moving which links well with the visual analysis of the bed in section 6.3.2. In general, the graded bed data appear ‘noisy’; this is either a facet of geo - referencing inaccuracy or that the bed surface is more changeable and hence rearranging to a greater extent. This is more likely to be a problem in the graded beds where the smaller grains on the bed surface make geo-rectifying the image more difficult. Given the pattern of the ‘noise’ appears to be concentrated around the edge of grains it would suggest the former

mechanism as being responsible for the output image rather than a more active bed surface. In unimodal beds antecedent flows (60 or 960 minutes) show that grains flipping over appears the dominant rearrangement mechanism; this appears to affect the coarser grains of the surface given their greater likelihood for over-exposure. There is no obvious migration of grains moving into or out of the field of view, despite slight indication of this section 6.3.1 In the bimodal bed both images (60 and 960 minutes) indicate evidence of grains moving into and out of the field of view; this is observed to be the dominant form of rearrangement of the bed surface in line with Section 6.3.1. Again, this mainly affects the coarser fractions due to their propensity for over-exposure and resultant susceptibility to higher shear stresses.

In summary, this DEM analysis is more quantitative than the visual analysis in Section 6.3.1 and indicates the following:

- Localised bed elevations change by $2.4-2.75D_{50}$ indicating spatially heterogeneous bed response to antecedent flow; this is significantly greater than the data yielded by global averages.
- Graded beds suffer georeferencing 'noise' more than uniform beds due to the wider grain size distribution
- Mobility of over-exposed fractions is the dominant antecedent rearrangement mechanism in both the uniform and bimodal beds; yet, grain flipping is more common in the unimodal bed.
- It appears that it is the coarse grains that are rearranged the most under antecedent flow
- The bimodal bed appears to continue to rearrange over the longest timeframes, with more significant rearrangement noted on the 960min image; this is in agreement with Section 6.3.1 and 6.3.2.



The overturning of a grain into a more stable position is represented by a blue area which is the mirror image of a neighbouring red area. Secondly particle rotation is visualised by 'halos' of blue and red around the edges of a grain.

Figure 6-22; DEM's of difference for the uniform (upper image pair), unimodal (middle image pair) and bimodal (bottom image pair) beds after 60mins (left hand of the image pairs) and 960mins (right of the image pairs) antecedent flow.

However although DEM's of change yield information regarding the spatial configuration of the changes to the bed surface and indicate that changes are in excess of those suggested by the average statistics in section 6.3.2.1 it is difficult to quantify, unambiguously, how many of each type of grain movements occur within each image. In order to use DEM's of change to a greater extent image matching algorithms would need to be used to match the shape of areas eroded with those associated with an area of deposition. This is in essence a relatively simple procedure and has been supported within the literature in such fields as population ecology where the characteristics of individual animal coats/skins species are frequently required (e.g. Hiby *et al.*, 2010). However where irregular shaped objects are used, such as with grains in this instance, pattern matching becomes an exceedingly difficult problem; if a grain overturns it is unlikely to have the exact same 'footprint' and hence the pattern of deposition will differ from the erosion pattern. In addition there would need to be greater accuracy with the geo referencing; which increases processing time required or needs revised instrumentation set-up to synchronise the stepper motor and laser (Chapter 3). Neither were undertaken here as the underpinning problem of footprint would still not be resolved. Consequently other techniques are needed to assess the type and magnitudes of grain movements on the grain surface. Section 0 uses a manual digitisation technique of individual grains to begin to assess how particles are repositioned on the bed surface.

6.3.3.2 Particle repositioning

Paphitis and Collins (2005) proposed that if it is accepted that a certain level of particle movement can occur even in sub-threshold antecedent flows, then the most unstable grains can re-orientate into positions where they have improved positions from the overlying flow; this has been shown to hold true in Section 6.3.1. It should follow that the longer the antecedent period, the more opportunity grains have to re-orientate such that particles should: (i) display a progressively increasing degree of flow alignment as antecedent duration is increased; and/or (ii) a greater proportion of grains on the bed surface will show alignment as the antecedent duration is increased.

To quantify reorientation 50 grains were manually digitised from each laser scan surface to analyse the orientation of the longest exposed axis, relative to the direction of downstream flow. A grid was placed over the image to allow a repeatable sampling procedure; grains were chosen at each of the nodes of the grid hence there was no bias towards grain size.

The orientation of the grains was measured by fitting an ellipse to the grain area (using the Matlab function 'regionprops'). Although the orientation of the grains is calculated according to the long axis of the grain (a-axis) it is recognised that if the grain is tilted, imbricated or partially obscured, this assumption may not be accurate (Ibbeken and Schleyer, 1986) and may result in the researcher analysing the intermediate axis without realising. In addition to the possible inaccurate delimitation of the a axis there is also the possibility that the manual digitisation was inaccurate. This is especially true where grains are rounded with very little difference between the a and b-axis lengths. Li and Komar (1986) clearly state that a grain preferentially aligns its b-axis with the flow (typically within 0-15° of the flow direction); this means that the a-axis will be orientated perpendicular to flow direction and expected to align within the angles 75°-105° and 255°-285° in Figure 6-23 through Figure 6-25 when most stable. This granular arrangement is increasingly referred to in the literature as dynamic armour (Allen, 1982; Komar and Li, 1986; Robert, 1991; Aberle and Nikora, 2006). This is distinct from static armour which is characterised with the a-axis being flow-aligned and the b axis perpendicular to the flow (e.g. Nikora *et al.*, 1998; Smart *et al.*, 2004). The implications for this type of armour will be analysed in the discussion of this Chapter (Section 6.4).

Orientation data shows that for all three beds there is a progressive change to the reorientation of the long axis with increasing antecedent duration. In addition Figure 6-23 through Figure 6-25 quantifies the effect of screeding upon the bed surface structure. It is hoped that screeding would not introduce any directionality to the grains on the bed surface such that the change seen after the application of the antecedent period is purely a facet of the antecedent period rather than the starting condition of the bed. Indeed all three figures show that there appears to be a random orientation to the grains on the bed surface as exhibited by the large amounts of scatter in the analysed orientations. In response to the application of the antecedent period, in the uniform beds (Figure 6-23), there appears to be a high degree of scatter within the datasets. However after 60 minutes of antecedent flow the a axis of the grains appear to be aligned with the flow whilst after 960 minutes antecedent duration, although flow alignment of the grains is still noted, there is an increase in scatter in the grain orientation. Both data suggest the formation is akin to a static armour although there is no obvious temporal effect suggesting that it is not the reorientation of grains which is responsible for stabilisation gains within a uniform bed. Within the unimodal bed (Figure 6-24), the a axis of the grains appear to be perpendicular

to flow direction after 60 minutes antecedent flow duration suggestive of a configuration akin to a dynamic armour; this configuration remains similar after 960 minutes of antecedent flow. It is interesting note that these results suggest that even after 960 minutes of antecedent flow the bed is still not at its most stable granular configuration; this concept will be further discussed in section0. Conversely within the bimodal bed (Figure 6-25), a change from a dynamic to static armour is noted as antecedent duration is increased from 60 to 960 minutes of antecedent flow. Given that a static armour is the most stable granular configuration, this supports data in both section which suggested that the processes acting to stabilise the bed are acting over longer time periods and that the bimodal bed is the most responsive to stress history.

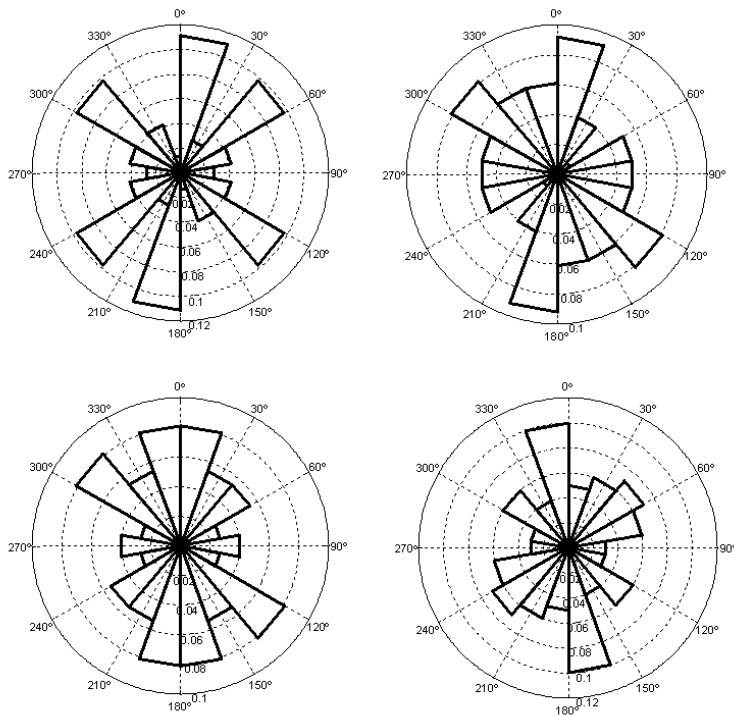


Figure 6-23; Orientations of the long a-axis of 50 grains manually digitised from laser scans for the uniform bed. Image pairs show the bed before (left hand of the image pair) after (right hand of the image pair) the application of 60 minutes (top of the image pair) and 960 minutes (bottom of the image pair) antecedent flow. Flow is along the 0 – 180 line.

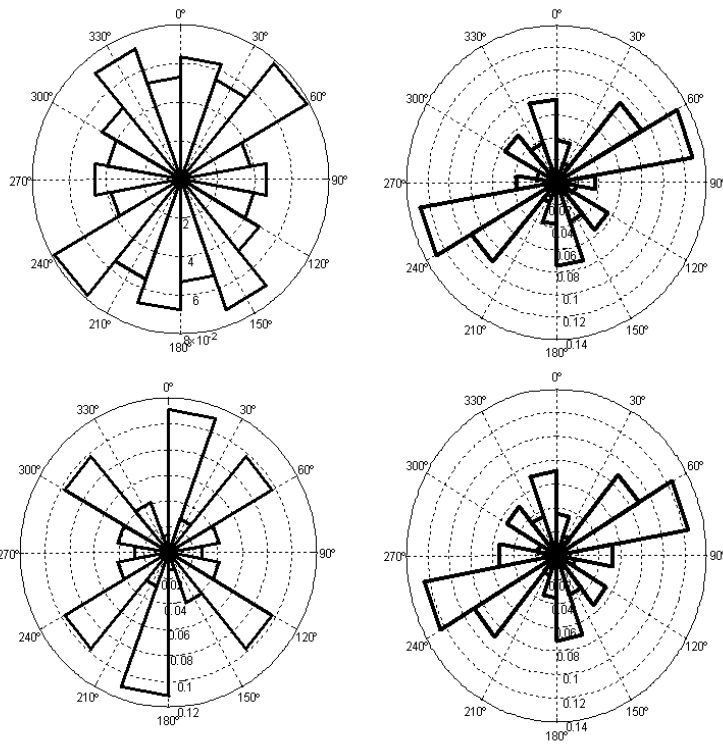


Figure 6-24; Orientations of the long a-axis of 50 grains manually digitised from laser scans for the unimodal bed. Image pairs show the bed before (left hand of the image pair) after (right hand of the image pair) the application of 60 minutes (top of the image pair) and 960 minutes (bottom of the image pair) antecedent flow. Flow is along the 0 – 180 line.

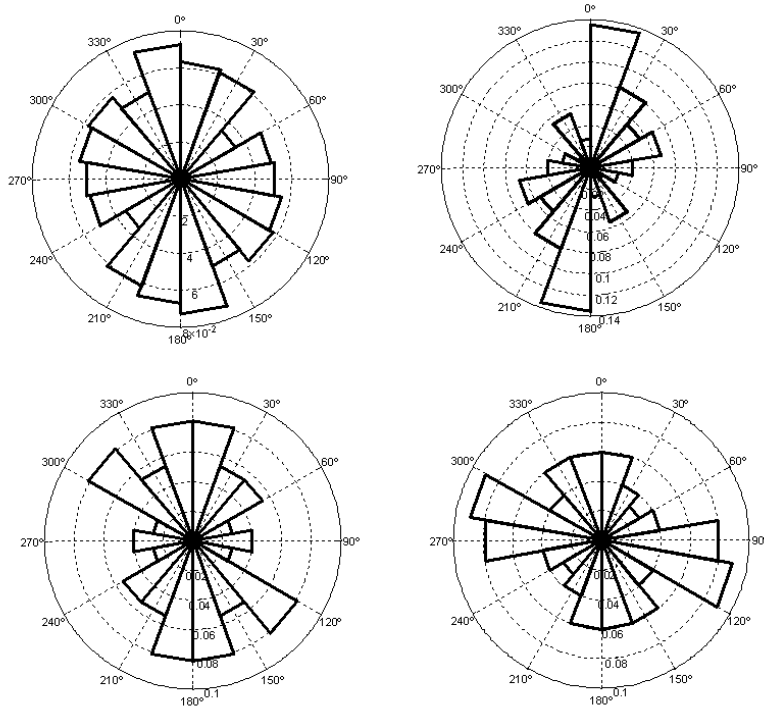


Figure 6-25; Orientations of the long a-axis of 50 grains manually digitised from laser scans for the bimodal bed. Image pairs show the bed before (left hand of the image pair) after (right hand of the image pair) the application of 60 minutes (top of the image pair) and 960 minutes (bottom of the image pair) antecedent flow. Flow is along the 0 – 180 line.

In summary, particle reorientation for both the uniform and unimodal beds reveal little change to the grain orientation with increasing antecedent flow albeit with the uniform bed exhibiting grains aligned with flow as compared to the unimodal bed where grains are aligned perpendicular to flow. Conversely a more complicated response is noted within the bimodal bed where a change from a dynamic to static armour configuration is noted. This is in line with the DEM's of change where it was noted that the stabilisation of the bimodal bed was operating over longer timescales. However it is reiterated that it is not possible to definitively know whether it was the long or intermediate axis which was measured in this analysis and as such this may partially explain the differences noted.

6.3.4 Large scale structuring

Given that the data to date have shown there to be mobility of grains on the bed surface, it is possible that discrete movements of individual grains could interact with other particles on the bed surface. This has already been alluded to in section 0 where it has been observed that it is not just individual grains which move on the bed surface but moreover groups of particles. The result of this interaction might be to develop either individual discrete structures (Reid *et al.*, 1992) or multi particles structures which take the form of pebble clusters (Lawless and Robert, 2000; Hassan and Church, 2000; Papanicolaou *et al.*, 2003). Regardless of their composition such structures have been noted to influence the surrounding flow field and any sediment transport in that they act to stabilise the bed surface (Kuhnle, 1996; Gomez and Phillips, 1999; Strom *et al.*, 2004). An alternative configuration to discrete pebble clusters but still that which could be classed as multi particle interactions would be the development of a surface where the grain arrangement itself acts to increase stability e.g. preferential orientation or imbrication (e.g. Hassan and Church, 2000; Cooper and Tait 2008; Cooper and Frostick, 2009) Again this has already been postulated in section 6.3.3.2 where the alignment of individual grains were analysed and shown to change as a result of the imposed fluid flow regime. However section 0 considered single grains in isolated yet it is noted that such alignment is a common feature at scales greater than the individual grain scale (Marion *et al.*, 2003, Cooper and Frostick 2009).

As such the last two sections of this thesis will analyse both types of multi particle organisations described above. Section 6.3.4.1 will analyse the fractional response of the bed surface in terms of analysing the changes to the number of two fractions (D_{50} and D_{90}) on the bed surface whilst Section 6.3.4.2 uses two-dimensional second order structure functions to analyse the global organisation of the particles on the bed surface. Given the shear stresses associated with the antecedent flows employed are set to be 50% that of the critical entrainment threshold of the D_{50} data have shown only occasional grain motion; thus, it seems unlikely that any significant particle clusters would be apparent on the bed surface and the bed would be rather stabilised by specific particle organisation in the bed surface as noted in earlier sections of Chapter 6. Yet, it is important to conclusively ascertain the correctness of this assumption.

6.3.4.1 Fractional Analysis

In order for all the development of clusters to be estimated the grains of interest needed to be isolated on the bed surface such that their size, area and x,y, coordinate locations could be extracted from the photographs. Given that both the D_{50} and the D_{90} were painted and hence identifiable on the bed surface, analysis in this section concentrates on using image analysis to extract information regarding their number and total area over time. Since both parameters being analysed in the subsequent sections rely upon the relationship between different grain sizes only the graded beds can be examined.

The grain fractions of interest were extracted using Image J, a freely available image analysis software developed by the US National Institute of Health, with extracted parameters further interrogated in ArcGIS and Matlab. As both the D_{50} and the D_{90} size fractions were painted different colours it was possible to threshold each image so that only the particles of the required size fraction were highlighted. Within Image J this was done using the threshold tool where the image can be altered using the hue, saturation and brightness (Cheng *et al.*, 2001) to isolate the grains of a specific colour according to their spectral signature. Once the optimum settings were found they were kept consistent throughout the sequence of images to be processed in order that a valid comparison be drawn between sequential images; this is appropriate given the constancy of lighting, bed drainage, camera set-up, paint etc. Once the particles were isolated from the photograph a filter was passed over the image to remove any small areas of the image which were highlighted by the thresholding technique due to their colour signature but which are not actually grains of interest. A median filter with a user-defined radius of $0.5D$ was set; this was chosen to correlate to with the radius of the grain size being isolated i.e. 2.4mm for the D_{50} and 4.8mm for the D_{90} respectively based on grain diameters of 4.8mm and 9.6mm for the D_{50} and D_{90} respectively; this was in line with the methodology of Rollinson (2006). Each image was manually checked to correct for grains which suffered from merged outlines due to contact with a neighbouring grain. Files were exported into ArcGIS was and interrogated to calculate the change in number and area.

Analysis of the total number, total area and ratio of $D_{50}:D_{90}$ at the start and finish of the antecedent period for the 60 and 960 minutes antecedent duration experiments are detailed in Table 6-4. Three patterns emerge from the compositional data; firstly the absolute number of both the D_{50} and D_{90} particles increase on the bed surface from the start to the

finish of the antecedent period which is reflective of in/out migration and/or exposure of sub-surface grains; this net change was difficult to quantify by previous methods of Section 6.3.1 and 6.3.2. Secondly, similar to the total number trends, the total area of the bed covered by both the D_{50} and D_{90} increases with applied antecedent duration; this is specifically compared to the statistics for the number of grains to try to isolate changes by grain movement from those caused by exposure. Finally the ratio of $D_{50}:D_{90}$ decreases with applied antecedent flow indicative of bed coarsening.

Distribution	Antecedent Duration		D_{50} number	D_{50} area	D_{90} number	D_{90} area	$D_{50}:D_{90}$ number	$D_{50}:D_{90}$ area
Unimodal								
	60 Minutes	Start	378	80142	142	14641	2.66	5.47
		Finish	382	84530	146	16853	2.62	5.02
	960 Minutes	Start	397	80689	162	19447	2.45	4.15
		Finish	400	82280	164	20743	2.44	3.97
Bimodal								
	60 Minutes	Start	133	2778	197	8719	0.68	0.32
		Finish	136	3028	206	9941	0.66	0.30
	960 Minutes	Start	136	1754	198	4786	0.69	0.37
		Finish	139	1789	205	4989	0.68	0.36

Table 6-4; Analysis of the total number, the total area and the ratio of the $D_{50}:D_{90}$ for the D_{50} and D_{90} at the start and finish of 60 and 960 minutes antecedent flow. Area is in arbitrary units.

Table 6-4 indicates the total number of D_{50} and D_{90} grains increased by between 2 and 9 grains by net in-migration of particles to the field of view or by exposure of subsurface. The magnitude of change in the unimodal bed appears relatively insensitive to antecedent duration applied with both highlighted fractions exhibiting a similar magnitude change in particle count. However, the bimodal bed indicates that the D_{90} shows 2-3 times the change of the D_{50} , although trends also appear independent of applied antecedency. Comparatively, it is the D_{90} of the bimodal bed that appears slightly more responsive than the equivalent unimodal bed; this is in agreement with evidence from Section 6.3.1. Akin to the total number trends, the total area of the bed covered by both the D_{50} and D_{90} also increases with applied antecedent flow. Table 6-4 indicates the greatest response is to the unimodal (+13.13%) and bimodal (+12.29%) beds after 60 minutes of applied antecedency. From this data it is possible to see that although the trends to the change in area are similar to those noted with the change in total numbers, the magnitude of response for the area is larger. Whilst the change in grain numbers may be net in-migration or exposure of new grains from the sub-surface, the relatively greater response of change in

area strongly advocates a dominance of exposure as the mechanism of change for both the D_{50} and D_{90} . This finding is important in determining the mechanism of surface coarsening and aid explanation of increased be stability during antecedent flows.

Analysis of the $D_{50}:D_{90}$ shows that the unimodal has higher ratios than the bimodal; this is purely related to the grain size distribution (Chapter 3) of the beds. Yet, the relative changes to the ratio of $D_{50}:D_{90}$ (in terms of both total number and total area) indicates that the bed surface is likely to be coarsening as shown by the decrease in ratio over time. It can be seen from the data in Table 6-4 that there is a reduction to both the ratio of the total numbers and the total area although the magnitude of change is greater in the ratio of total areas; this is expected given the absolute data. It is clear that the bimodal bed response is significantly greater than that observed in the unimodal bed. Ratios indicate that the rate of coarsening is slightly higher in 0-60min runs than in 0-960min runs, again suggesting this two-stage response-recovery cycle to the application of antecedent flow.

Comment [HH1]: ? I might be wrong, but is the middle section of this para a duplicate of the last para? Please check to see if this is the case.

A summary of findings to the changes occurring to the bed during the antecedent period is therefore as follows.

- In both beds the total numbers of the D_{50} and D_{90} grains increase with applied antecedent flow and, although this change is small in magnitude, it is greatest after the shortest antecedent periods; this is in line with the entrainment data (section 5.4.1)
- Akin to the total number analysis the total area of the D_{50} and D_{90} also increases with applied antecedent duration however the magnitude of this change is higher than the change noted for the total number analysis. This yields important information about the processes which are occurring as it implies that although a small number of grains are being actively entrained this change is less significant than then change to in-situ exposure. As such there is an increase in the surface area of the D_{50} and D_{90} to the flow without significantly increasing their number on the bed surface.
- A reduction in the $D_{50}:D_{90}$ ratio is noted for both the total number and total area. This confirms that the surface is slightly coarsening during antecedent flow.

Taking all three variables into consideration it can be seen that the bed surface slightly coarsens as evidenced through the change in the ratio of $D_{50}:D_{90}$ on the bed surface. The

data indicates that this coarsening is mainly by passive exposure of the coarser fractions in response to the vertical and lateral winnowing of fines from their bed surface. This is in comparison to active processes where grains are actively entrained and hence can form particle clusters. However it is not possible to definitively analyse if cluster structures are forming on the bed surface; only by using more complex orientation and structure analysis as defined in the following sections can it be determined if cluster structures form.

6.3.4.2 *2-D Second Order Structure Functions*

Theory would suggest that water working of a gravel bed causes progressive reorganisation of grains on the bed surface such as to increase bed stability (Hassan and Church, 2000; Schmeckle and Nelson, 2003; Cooper and Frostick, 2009). Results to date have provided evidence to support this supposition revealing the beds to stabilise as the result of applied antecedent flow by a number of processes; vertical settlement which causes increased roughness (section 6.3.2), grain displacement in to a more stable location on the bed surface (section 6.3.1) and small scale grain reorientation (section 6.3.3.2). Given that all three processes described imply a certain amount of mobility on the particles on the bed surface there is the possibility that rearrangement will occur such as to form an organised bed surface where grains are preferentially aligned or structured. Indeed section 0 has shown that isolated grains on the bed surface reorientation with the application of an antecedent period; the alignment of this reorientation is affected by grain size distribution with both uniform and unimodal beds showing a dynamic armour arrangement whilst the bimodal bed shows a change from a dynamic to a static armour arrangement. Section 0 has eluded to the scale and type of this change; through the analysis of the spatial organisation of certain grain fractions on the bed surface (D_{50} and D_{90}) it has been noted that no specific clusters were found on the bed surface such that it seems unlikely that the bed is stabilising as the result of large grain scale structures on the bed surface. Instead it appears more likely that the geometrical properties of the bed surface are responsible for the increased bed stability. An analytical method to examine both the scale of bed structuring and detail of particle organisation therefore appears appropriate; traditionally this has been assessed through the use of 2-D second order structure functions. This methodology is a more advanced method or orientation analysis in comparison with the axial analysis described earlier (section 6.3.3.2) as it takes into account the elevations of the whole bed surface rather than discrete particles as well as giving an idea of the scale or the rearrangement. Although it is not expected that full scale structures such as particle

clusters will not be formed during the antecedent period due to the sub-threshold shear stresses it has already been shown that particles re-align in the cross stream or downstream directions in response to stress history (section 6.3.3.2). 2D functions will augment this analysis by not only using the showing the scale of the change but also any directionality to the scaling on the bed surface in the dominant grain alignment direction.

Second order structure functions were introduced by Kolmogorov in 1941 to describe the scaling behaviour of complex systems e.g. small scale turbulence. More recently second order structure functions have been used to describe the scaling behaviour of gravel bed rivers where surfaces can be described in as either isotropic or anisotropic. The former refers to a surface for which scaling characteristics are independent of direction while the latter refers to a surface in which there is a directionality to scaling. Gravel bed rivers would be expected to be anisotropic as both individual grains and bedforms will tend to become orientated with their formative flow direction (Butler *et al.*, 2001). If different processes are operating at different scales multi fractal behaviour might be expected. This describes grain roughness of individual particles at the smallest spatial lags the and particle orientation at larger lags (Robert, 1988). Differentiation between these two scales can therefore be of use in determining if a structure is developing on the bed surface together with the associated length scales of the structures. Results have been suggested to depend upon surface forming processes, particle size distribution, shape and particle imbrication (Butler *et al.*, 2001).

The structure function $D_b(l_x, l_y)$ of bed surface elevation $z_b(x, y)$ is defined as;

$$D_b(l_x, l_y) = \frac{1}{(N_b - n_b)(M_b - m_b)} \sum_{i=1}^{N_b - n_b} \sum_{j=2}^{M_b - m_b} \{z_b(x_i + n_b \delta x, y_j + m_b \delta y) - z(x_i, y_j)\}^2$$

(Equation 21)

Where $l_x = n_b \delta x$, and $l_y = m_b \delta y$ are spatial lags n_b m_b are multiplying coefficients, δx δy are the sampling intervals, and N_b and M_b are the total number of measured bed elevations on the Streamwise x and lateral y directions respectively. The second order structure function of a globally homogenous random field has the following relationship with correlation function $R_b(l_x, l_y)$

$$D_b(l_x, l_y) = 2[\sigma_{z_b}^2] - R_b(l_x, l_x) \quad (\text{Equation 22})$$

Thus, at large lags l_x and l_y when $R_b(l_x, l_y) \rightarrow 0$ and $D_b \rightarrow 2\sigma_{z_b}^2$ the data are spatially uncorrelated and the lags l_x and l_y at which $D_b \rightarrow 2\sigma_{z_b}^2$ can be used to derive characteristic streamwise and lateral length scales (Nikora *et al.*, 1998). Low values of $D_b(l_x, l_y)/2\sigma_{z_b}^2$ indicate high levels of correlation with l_x and l_y such that the value of zero (a perfect correlation) exists. As $D_b(l_x, l_y)/2\sigma_{z_b}^2$ increases to unity, the degree of correlation decreases such that the bed elevations have no correlation and the bed surface topography can sensibly be considered random in organisation although this transition is very rarely abrupt (Nikora *et al.*, 1998).

It is understood that all second order structure functions can be subdivided into scaling, transition and saturation regions (Robert, 1998; 1991; Nikora *et al.*, 1998; Butler *et al.*, 2004; Nikora *et al.*, 1998, Nikora and Walsh, 2004). The region at small spatial lags, where the structure functions can be approximated by the power function $D_b(l_x, l_y = 0)/2\sigma_{z_b}^2 \propto l^{2H_x}$ and $D_b(l_x = 0, l_y)/2\sigma_{z_b}^2 \propto l^{2H_y}$ (Nikora *et al.*, 1998, Nikora and Walsh, 2004), corresponds to the scaling region, while at larger spatial lags the structure function approach the saturation region. Between these two regions, the structure functions are curved in the transition zone. The scaling exponent, H , known as the Hurst component can be analysed in relation to the scaling region and can be interpreted as a measure of complexity in topography with larger values of H_x and H_y indicating a less complex topography (Bergeron, 1996). The scaling (Hurst) components H_x and H_y can be estimated from the condition that $D_b(l_x, l_y = 0)/2\sigma_{z_b}^2 \propto l^{2H_x}$ and $D_b(l_x = 0, l_y)/2\sigma_{z_b}^2 \propto l^{2H_y}$ within the scaling region. In the context of this research it is hypothesised that the bed will show a greater degree of structural complexity after exposure to the antecedent flow with the degree of complexity being commensurate with antecedent flow durations. For this hypothesis to be true the correlation lengths of the bed surface elevations should increase with antecedent duration whilst the Hurst Components should decrease. This will however be contingent upon the grain size distribution employed as it has already been noted in Section 5.4.1 that there is a difference between the responses of the graded beds as compared to the uniform beds.

By plotting the second order structure functions of the bed elevations it is possible to see how variance changes as a facet of lag in both the streamwise and lateral directions. A comparison between the uniform beds at 60 and 960 minutes antecedent duration (Figure 6-26) for both the streamwise and lateral directions shows the parallel nature of the curves together with a similarity in the extent of the scaling region which indicates an isotropic scaling at small spatial lags, also observed by Nikora *et al.*, (1998); Butler *et al.*, (2004); Nikora and Walsh, (2004) and Cooper, (2008). This is consistent orientation data plotted in 0 which suggests that there is no dominant orientation to the grains on the bed surface and that the observed scaling lengths are describing the individual grain roughness. Within the unimodal bed (Figure 6-27) the curves are again very similar to one another in the scaling and saturation regions suggesting that is only minimal increase to the length scales and hence limited orientation of the grains with flow on the bed surface. This is particularly so with the curves for the 960 minute data where there is very little change to the curve after the application of the antecedent duration. This is commensurate with the findings in section 0 where it was noted that the alignment of the grains does not change with time and are not aligned with flow, more that they exhibit dynamic armouring tendencies. Conversely, in the bimodal bed (Figure 6-28) although the curves are again very similar to one another at small spatial lags in both the streamwise and lateral directions, longer transition zones are seen in both the streamwise and lateral directions as compared, particularly to the uniform bed. This suggests that the length scales involved in the bimodal bed are greater than the other two beds and is this indicative of structure orientated in the flow direction i.e. a static armour which is not present on the surface of the other two beds.

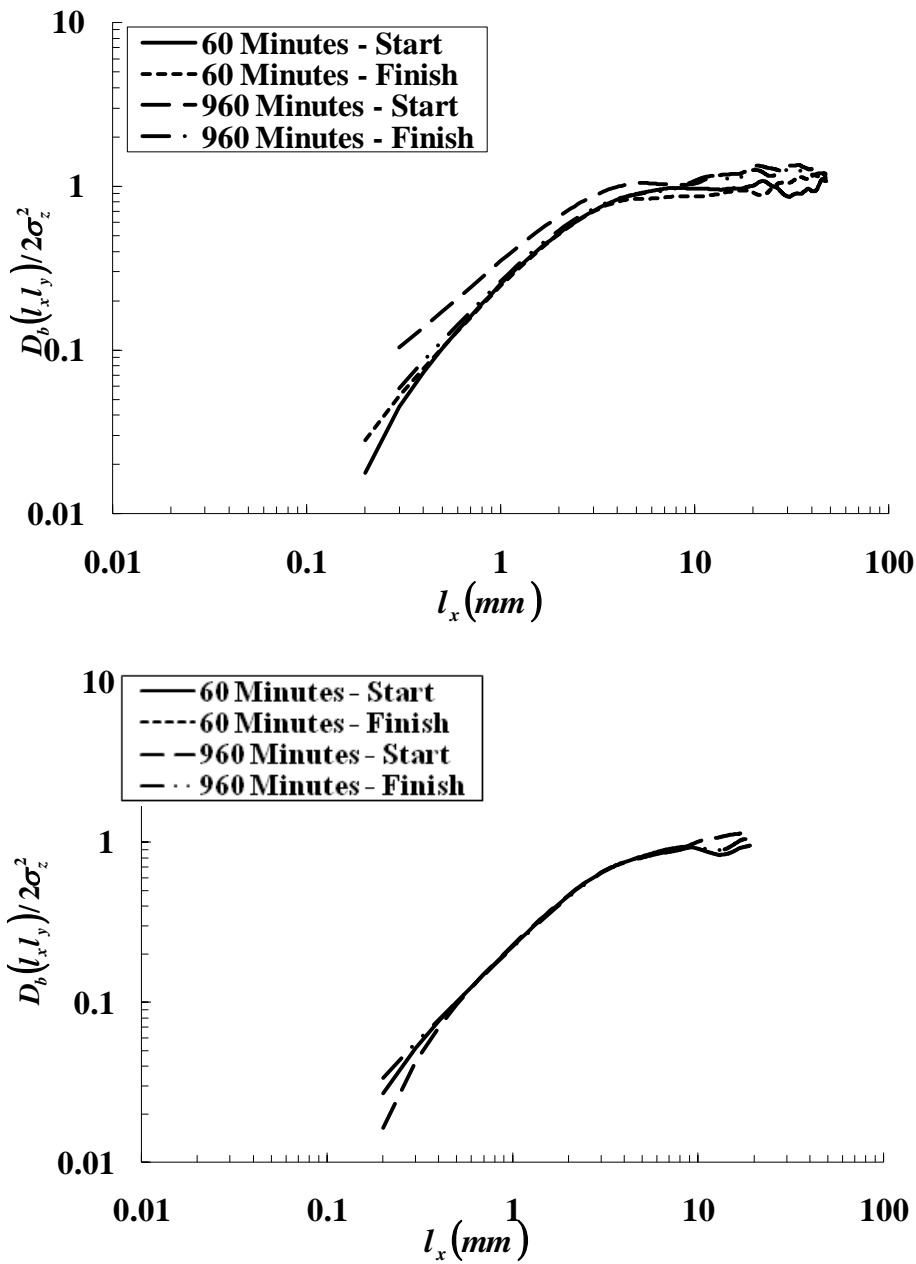


Figure 6-26; Second order structure functions D_b of the bed surface elevations for the uniform bed before and after 60 and 960 minutes antecedent flow duration for the streamwise (top of the image pair) and lateral (bottom of the image pair). D_b is normalised by $2\sigma_{Zb}^2$ for l_x and l_y where σ_{Zb} is the standard deviation of the bed surface elevations and l_x and l_y is the spatial lag in the streamwise and lateral directions respectively.

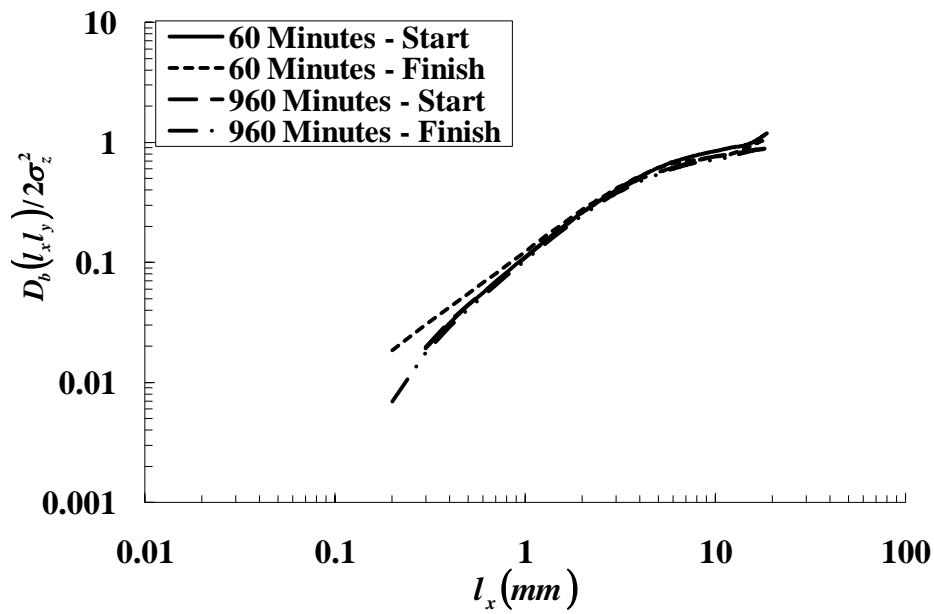
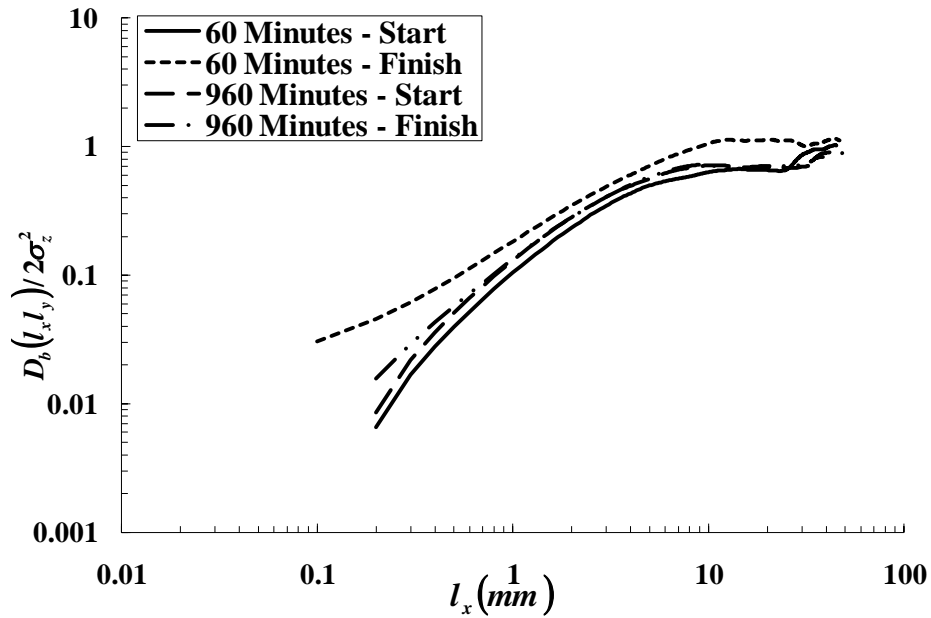


Figure 6-27; Second order structure functions D_b of the bed surface elevations for the unimodal bed before and after 60 and 960 minutes antecedent flow duration for the streamwise (top of the image pair) and lateral (bottom of the image pair). D_b is normalised by $2\sigma_{Zb}^2$ for l_x and l_y where σ_{Zb} is the standard deviation of the bed surface elevations and l_x and l_y is the spatial lag in the streamwise and lateral directions respectively.

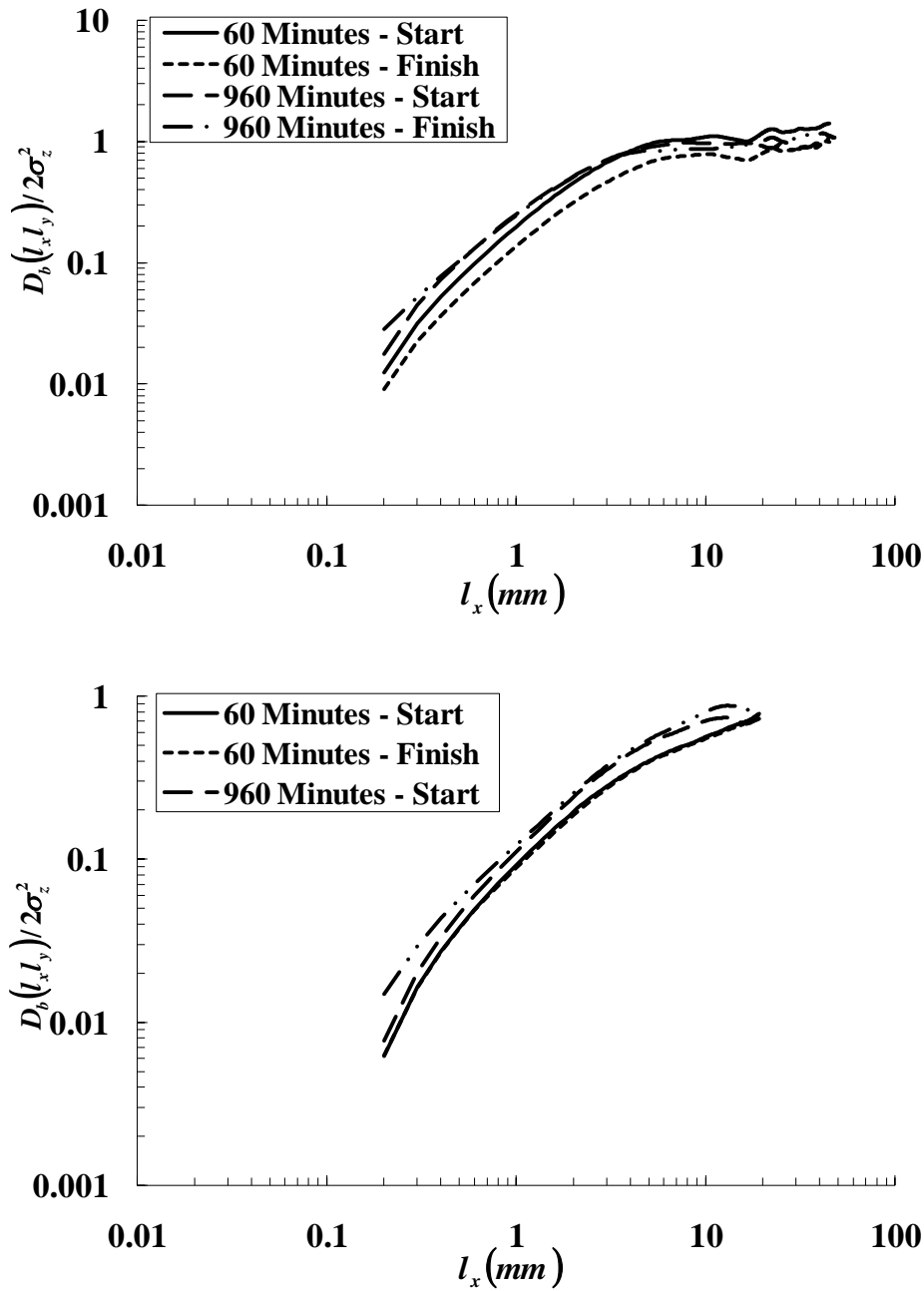


Figure 6-28; Second order structure functions D_b of the bed surface elevations for the bimodal bed before and after 60 and 960 minutes antecedent flow duration for the streamwise (top of the image pair) and lateral (bottom of the image pair). D_b is normalised by $2\sigma_{z_b}^2$ for l_x and l_y where σ_{z_b} is the standard deviation of the bed surface elevations and l_x and l_y is the spatial lag in the streamwise and lateral directions respectively.

Using the curves a number of parameters can be derived including the correlation lengths, l_{x0} and l_{y0} of the bed elevations, the horizontal roughness lengths (l_{x0}/σ_b , l_{y0}/σ_b) and the scaling (Hurst) components for both the streamwise and lateral directions (H_x and H_y) as denoted in Table 6-5 and discussed below.

			l_x	l_y	l_{x0}/σ_b	l_{y0}/σ_b	H_x	H_y
Uniform	60 Minutes	Start	4.00	2.86	2.07	1.78	0.87	0.77
		Finish	4.00	3.44	2.07	1.76	0.79	0.73
	960 Minutes	Start	3.60	3.34	2.04	1.78	0.89	0.81
		Finish	3.93	3.83	1.86	1.73	0.87	0.79
Unimodal	60 Minutes	Start	7.69	6.25	4.03	3.40	0.78	0.76
		Finish	8.51	6.49	4.46	3.70	0.68	0.67
	960 Minutes	Start	7.44	6.25	6.61	5.20	0.86	0.88
		Finish	7.94	7.17	3.68	3.68	0.85	0.83
Bimodal	60 Minutes	Start	7.86	5.99	3.57	3.34	0.78	0.81
		Finish	9.72	8.41	5.16	3.81	0.57	0.78
	960 Minutes	Start	7.27	6.62	3.99	3.50	0.76	0.56
		Finish	7.55	7.06	3.91	3.80	0.59	0.54

Table 6-5; A summary of the bed surface properties derived from the second order structure functions for the uniform, bimodal and unimodal beds where l_x and l_y are the spatial lags in the streamwise direction in the streamwise and lateral directions respectively, l_{x0} and l_{y0} are the correlation lengths of z_b in the streamwise and lateral directions respectively, σ_b is the standard deviation and H_x and H_y are the Hurst exponents for the streamwise and later variations in Z_b respectively.

The difference in spatial lags at which $D_b(l_x, l_y)/2\sigma_b^2$ the lower limit of the saturation region, reflects the difference in the correlation lengths of the bed surface elevations. The streamwise correlation length l_{x0} and the later correlation length, l_{y0} , can be estimated from the curves in Figure 6-26 to Figure 6-29 following the method outlined in Nikora *et al.*, (1998). These values are given in Table 6-5 where it is shown that there is considerable difference between the uniform and graded beds. Three trends are noted within the correlation lengths of the three beds provided in Table 6-5. Firstly, correlation lengths in the streamwise direction, (l_{x0}) are consistently larger than the corresponding lateral (l_{y0}) length scales in all beds; this is consistent with previous findings (e.g. Nikora and Walsh, 2004; Cooper and Frostick, 2009; Hodge *et al.*, 2009). Secondly there is an obvious difference between the correlation length of the uniform and graded beds. In the uniform

bed the correlation length approximates to the grain scale (~4mm) as compared to correlation lengths approximately twice this in both graded beds. This is indicative of there being a greater scale structure in the bed surface elevations of the graded beds as compared to the uniform bed. Thirdly, it is typically noted that an increase in correlation length is seen in all beds after the application of the antecedent flow period, with the exception of the uniform bed after 60 minutes. Specifically, the magnitude of the structuring is larger in graded beds. These results support the notion that beds reorganise into a more structured surface as antecedent duration is increased, thereby supporting similar findings relating to increased periods of degradational armouring (Marion *et al.*, 2003; Aberle and Nikora, 2006; Copper *et al.*, 2009). Yet, the magnitude of response decreases with increasing antecedent duration, similar to other structural data obtained so far in Chapter 6.

The horizontal roughness lengths however show a more distinct difference between the behaviour of the uniform and graded beds. In the uniform bed the horizontal roughness lengths decrease with applied antecedent duration which increases over time suggesting that the bed is becoming smoother in both the streamwise and lateral directions; this is commensurate with findings in section 6.3.2.1 where it was noted that the range of bed elevations decreased and the bed underwent vertical settlement. In contrast the horizontal roughness lengths of the graded beds increase with applied antecedent flow although the magnitude of change decreases with increased antecedent duration. These results suggest that the beds progressively offer greater flow resistance through developing roughness (Cooper and Frostick, 2009). This is also in line with the findings in section 6.3.2.1 where it was noted that roughness increased with applied antecedent flow but that the magnitude of change decreases with increasing antecedent flow. Also akin to those findings is the fact that the unimodal bed shows the greatest vertical roughness as compared to the bimodal bed. Whilst the unimodal bed has greater overall stability (section 5.4.1) which has been linked to the overall percentage of fines within the distribution, the greater vertical roughness acts to exacerbate the vertical component of turbulence and decrease the responsiveness of the unimodal bed to stress history.

Finally it has already been noted that surface complexity is inversely related to the value of the Hurst component. Consequently it would be expected that the value of the Hurst component would decrease with applied antecedent flow and with increasing antecedent

duration as the beds become more topographically complex. In all of the beds the Hurst components decrease over the applied duration of flow, in both the lateral and streamwise directions. This indicates increasing bed complexity and confirms bed restructuring even under sub-threshold flows. However, data interpretation with respect to stress history duration indicates that there remains some degree of grade dependent control on the changes to the change in the structural complexity of the bed surfaces. Streamwise data (H_x) for both the uniform and unimodal beds show that extending the antecedent period appears to have little effect upon the magnitude of change in surface complexity, with changes always ≤ 0.1 . Yet, the bimodal bed shows a more marked response to the temporal effects of the antecedent flow (i.e. a decrease in H_x of 0.03 after 60 minutes and 0.17 after 960 minutes); this in line with previous findings which have demonstrated that the bimodal bed is most responsive to the temporal effects of antecedent flow. Results therefore show two main findings: firstly, that the uniform and unimodal beds shows very little increase in surface complexity in either the streamwise or lateral directions irrespective of antecedent duration. Secondly, in the bimodal bed there is more marked evidence of the development of some form of structuring aligned with flow as evidenced by the Hurst components being larger in the downstream direction as compared to the cross stream direction.

Despite results suggesting that there are differences in the scaled parameters discussed they are unlikely to fully explain the differences in the stability of the three deposits. Consequently consideration is needed of the geometrical arrangement of the surface topography (Cooper and Frostick, 2009). As pertained to earlier observations suggest that individual particles on the bed surface have preferential alignments; in a dynamic armour the a axis is perpendicular to the flow the b axis is parallel to the flow direction and the c axis is orthogonal to the flow direction (Allen, 1982; Marion *et al.*, 2003; Aberle and Nikora, 2006). Conversely under a static armour the a axis is noted to be parallel to the flow, the b axis is perpendicular and the c axis orthogonal. Regardless of whether the structure is akin to either static or dynamic armouring such a prevailing arrangement should reveal itself in the contour plots of $D_b(I_x I_y) / 2\sigma_{zb}^2$ shown in Figure 6-29 to Figure 6-32. Particles which are not orientated in a prevalent direction are represented by circular contours whereas grains orientated in a prevalent direction are represented by elliptical contours.

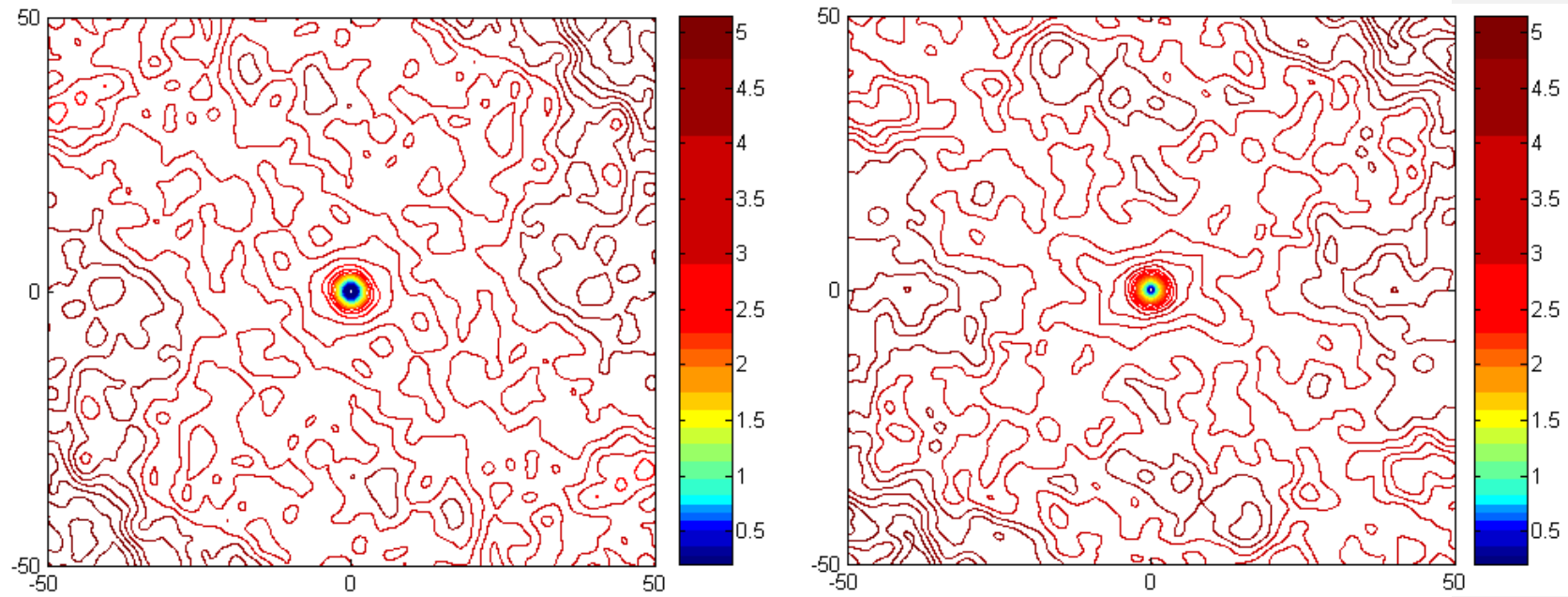


Figure 6-29; Isopleth plots of $D_b(l_x, l_y) / 2\sigma_{zb}^2$ for the uniform bed before (left hand of the image pair) and after (right hand of the image pair) 60 minutes of antecedent flow. Flow is from left to right.

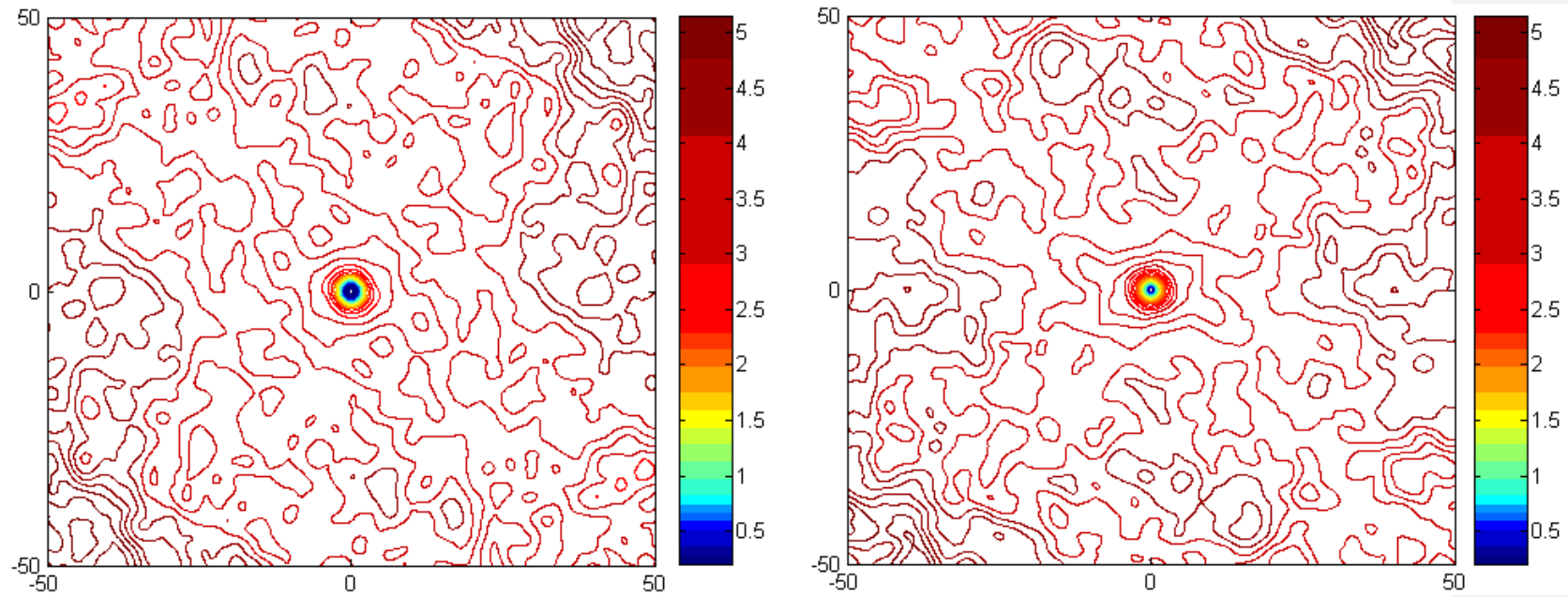


Figure 6-30; Isopleth plots of $D_b(l_x l_y) / 2\sigma_{zb}^2$ for the uniform bed before (left hand of the image pair) and after (right hand of the image pair) 960 minutes of antecedent flow. Flow is from left to right.

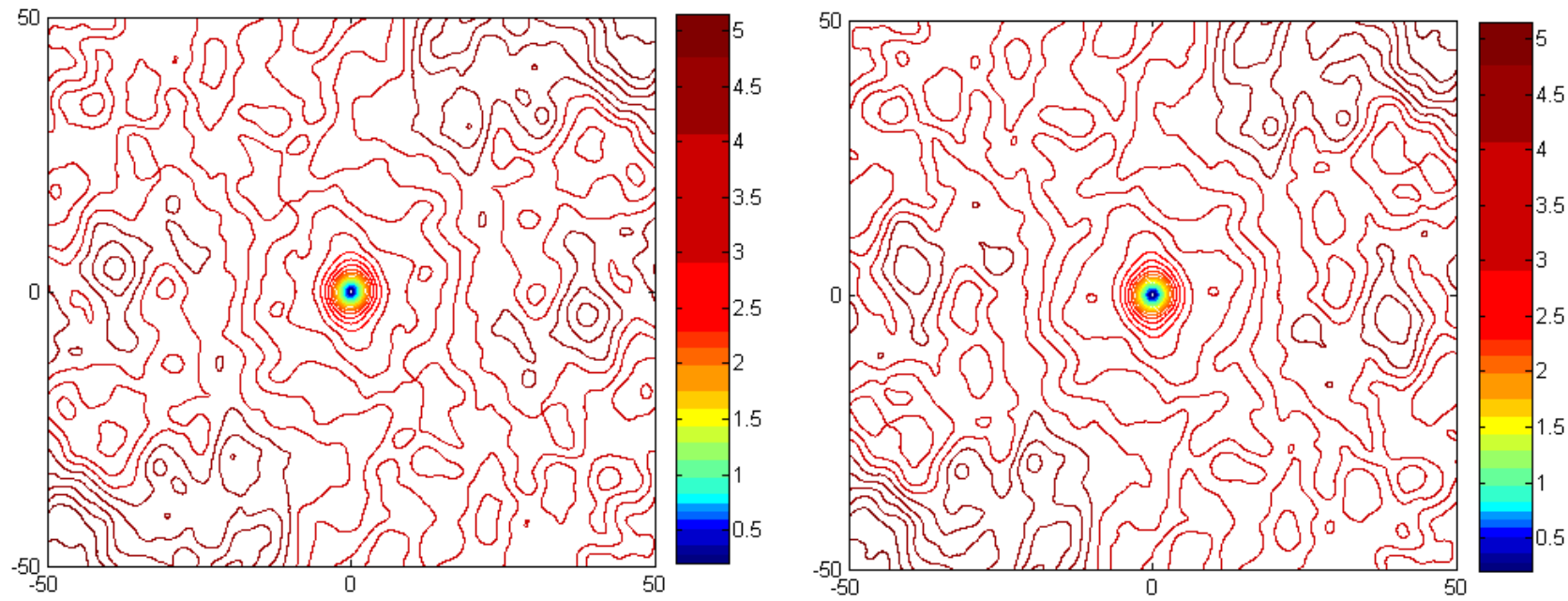


Figure 6-31; Isopleth plots of $D_b(l_x l_y) / 2\sigma_{zb}^2$ for the unimodal bed before (left hand of the image pair) and after (right hand of the image pair) 60 minutes of antecedent flow. Flow is from left to right.

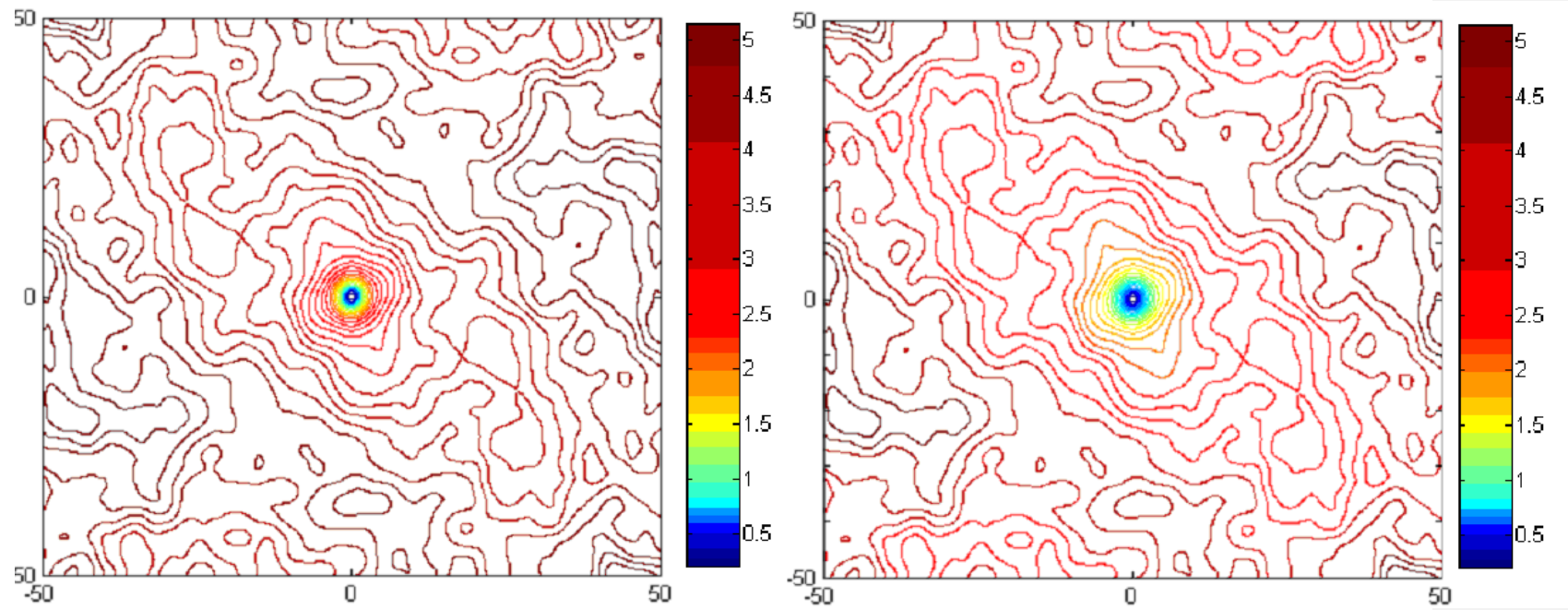


Figure 6-32; Isopleth plots of $D_b(l_x l_y) / 2\sigma_{zb}^2$ for the unimodal bed before (left hand of the image pair) and after (right hand of the image pair) 960 minutes of antecedent flow. Flow is from left to right.

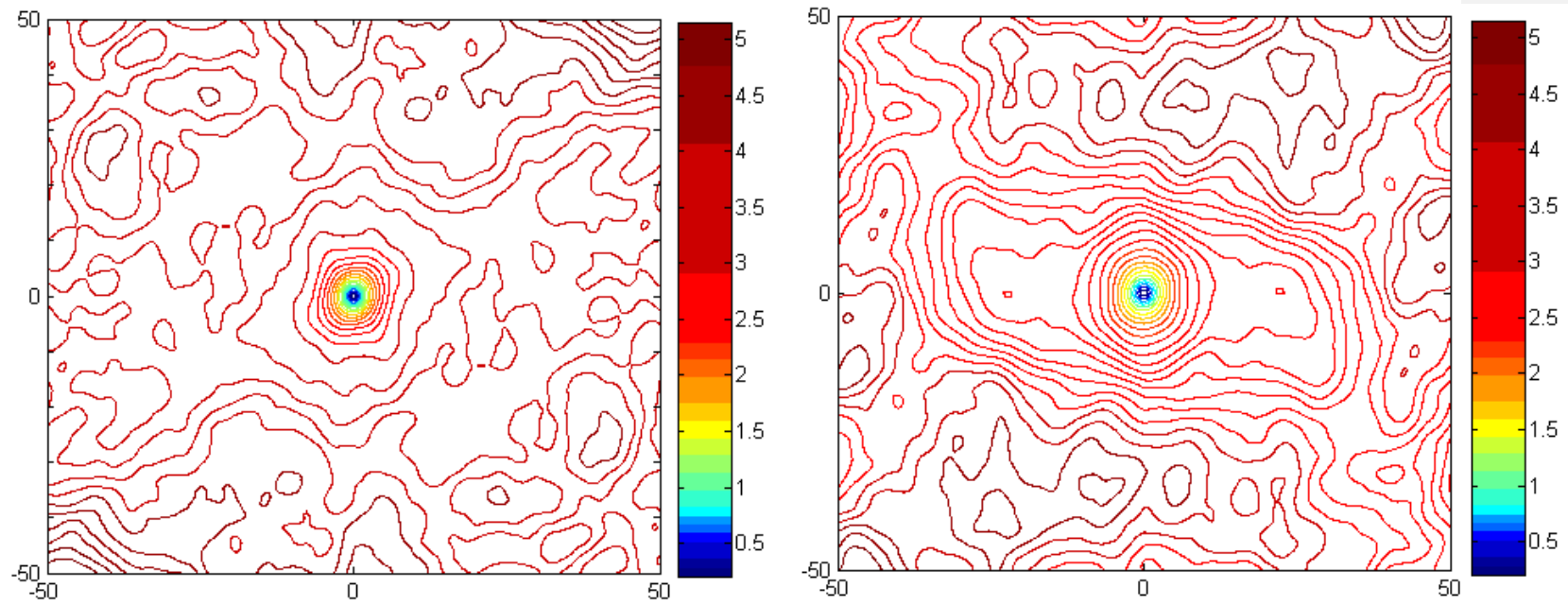


Figure 6-33; Isopleth plots of $D_b(l, l_y) / 2\sigma^2_{zb}$ for the bimodal bed before (left hand of the image pair) and after (right hand of the image pair) 60 minutes of antecedent flow. Flow is from left to right.

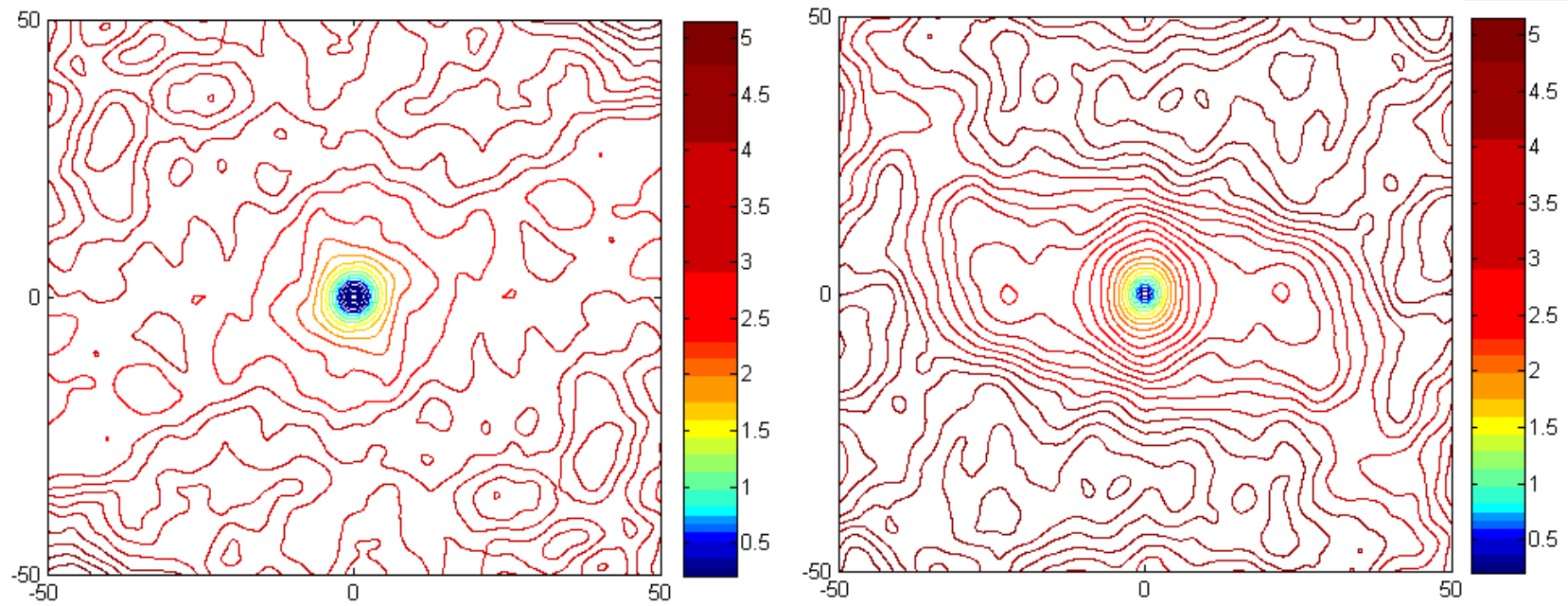


Figure 6-34; Isopleth plots of $D_b(l_{x,y})/2\sigma_{zb}^2$ for the bimodal bed before (left hand of the image pair) and after (right hand of the image pair) 960 minutes of antecedent flow. Flow is from left to right.

In the uniform bed (Figure 6-29 and Figure 6-30), regardless of the antecedent duration employed the contour lines of the 2D structure function are circular suggesting that there is no prevailing grain orientation. This indicates an isotropy in the surface structure and hence a random organisation. The correlation between z_b and $l_x l_y$ rapidly falls away with increasing spatial lags such that there are areas of separately formed circular patterns which are up to the size of the maximum grain size in the bed mixture. Similar patterns have been observed before and have been associated with depressions on the bed surface between the particles (Nikora and Walsh, 2004; Cooper and Tait, 2008). This is akin to the results presented in Table 6-5 where it was noted that the correlation lengths and the Hurst components changed very little over time.

Conversely within the graded beds a different pattern of surface organisation is noted. In the unimodal beds very little difference is noted between the start and finish of the 60 minute (Figure 6-31) antecedent flow duration. Before the antecedent period is applied the contours are largely circular suggesting that there is no prevalent orientation present on the bed surface. After the antecedent period, although there is no increase in the scale at which the correlations are present at the smallest spatial lag, at the larger spatial lags the isopleths start to describe an elliptical shape with their major axis aligned diagonally across the plot. A similar pattern is noted for the 960 minute (Figure 6-32) experiment although the contours of the bed surface before the applied antecedent period note similar diagonal tendencies at the larger spatial lags. These tendencies become more pronounced after the antecedent period where it is also noted that different elliptical shapes develop at the grain and micro-bedform scale. At the grain scale the isopleths reveal grains to be preferentially aligned with the flow direction whereas at the larger scales the alignment of the isopleths is diagonally across the plot. This suggests that the micro-bedforms or particle imbrication tend to rest in an orientation not defined by a typical armour configuration and it is likely to be a facet of the screeding of the bed surface (Cooper, Pers. Comms. 2011)

Within the bimodal beds after before both 60 minutes (Figure 6-33) and 960 minutes (Figure 6-34) of antecedent flow the bed shows a surface where the contours are circular at the smallest spatial lags suggestive of an isotropic surface related to the similarly properties associated at the individual grain scale. However after both antecedent periods the contours become elliptical and suggestive of an anisotropic surface where the grains have a prevalent orientation. The major axis of the elliptical isopleths are aligned in the

direction of flow (aligned with increasing l_x) indicating that the majority of particles rest with their a axis parallel to the flow. The minor axis of the isopleths is aligned with the prevailing orientation of their b axis, which is perpendicular to the flow. At the smallest spatial lags the streamwise and lateral coherency are similar in magnitude however as the spatial lag is increased the coherency in the streamwise directions becomes stronger and the values of $D_b(l_x, l_y) / 2\sigma_{zb}^2$ reduce more slowly in the lateral direction. This is indicative of static armouring in line with results from section 0. Contrary to the results from section 0 the time of the antecedent duration seems to make little difference to the spatial organisation of the surface after the antecedent period has been employed.

Findings from the 2D second order structure functions can be summarised as follows;

- The correlation length scales of all three beds in both the streamwise and lateral directions increase with applied antecedent flow. The lengths scales are however longer in the graded beds as compared to the uniform bed. This suggests that the grains are organising on the bed surface such as to increase stability at scales larger than the individual grain scale in the graded beds but at scales commensurate with the individual grain scale in the uniform beds.
- The horizontal roughness scales increase with applied antecedent flow in the graded beds although the magnitude of change decreases with increased antecedent duration. This is akin to the results indicating a two stage change in roughness where roughness was originally seen to increase as fines winnowed through the bed but then as pores filled the bed became smoother. Additionally the unimodal bed is comparatively most responsive in this parameter which is in line with the roughness findings. Conversely horizontal roughness decreases within the uniform bed indicating a smoother bed which becomes progressively smooth over time.
- The Hurst components, inversely proportional to bed complexity, decrease with time in all the beds in both the lateral and streamwise directions. This suggests that the beds are becoming more complex with increased antecedent flow. The uniform bed shows the smallest magnitude response suggesting the organisation of the particles does not change with applied antecedent flow. Conversely within the unimodal bed the organisation of the grains appears to be greater in the cross stream direction which is the opposite of the bimodal bed where grains are organised so the dominant organisation is in the streamwise direction.

-
- The contour plots of $D_b(I_x I_y) / 2\sigma_{zb}^2$ reveal that the organisation and alignment of the grains on the bed surface differ significantly between the beds and support the Hurst component analysis. In the uniform beds an isotropic surface is noted suggesting that there is no structure. Within the unimodal bed the contours do show increased coherency at small spatial lags suggesting that individual grains are organised on the bed surface. However there is no overall alignment of the grains with flow direction suggesting that the surface of the bed is not at its most stable granular configuration. Conversely within the bimodal bed there is alignment of the grains with flow direction suggesting that a static armour layer has formed on the bed surface. The length antecedent period does not appear to matter which supports the previous findings suggesting that the majority of rearrangement happens under the shortest antecedent periods and given that static armour formed under these time periods further change cannot occur within increasing antecedent durations.

6.4 Discussion

The aim of Chapter 6 was to provide the first insights into the mechanisms which are responsible for stabilisation as a result of applied antecedent flow. Specifically the findings in Chapter 6 have noted that the bed stabilises through four main mechanisms; vertical settlement, changes to bed porosity, grain displacement and grain reorientation. This discussion will therefore focus upon (i) the likely causes of these underpinning processes; (ii) how they change in light of applied antecedent flow and (iii) how the relative magnitude of the changes are the result of grade dependent controls.

6.4.1 *Small scale stabilisation processes; the effect of vertical settlement, changes to bed roughness and changes to bed porosity*

In all three grain size distributions, irrespective of the antecedent duration employed, a reduction in the mean bed elevation is noted over time suggesting the bed is vertically settling and therefore becoming increasingly consolidated (by up to $0.27D_{50}$) during applied antecedent flow. This is in line with the changes of Rollinson (2006) who ran experiments using uniform and unimodal gravels (D_{50} 6mm) where flow was set to $\sim 60\%$ τ_c of the D_{50} for up to 4361 minutes. His research noted up to a 7% decrease in mean bed

elevation ($\sim 0.2D_{50}$) which was attributed to increased bed consolidation as the result of particles jostling under sub threshold flow conditions. Increased antecedent duration increases the degree of settlement in all beds however graded beds show a greater degree of vertical settlement. In explanation, observations noted grain vibrations caused by the overlying fluid flow leading to an increase in friction angles and a tighter packing arrangement (Kirchner *et al.*, 1990; Paphitis and Collins, 2005) allowing the bed to seek a configuration of greater structural strength (Visscher and Bolsterli 1972; Cumberland and Crawford, 1987). In terms of the graded beds used in this research it is proposed that the finer fractions would preferentially exploit surface pores packing them more tightly between larger grains (Fraser, 1935; Hecht, 2004) in such a way that they are vertically winnowed to deep within the bed resulting in very high pivoting angles (Kirchner *et al.*, 1990). This local settlement of fines would be implicit to the decrease in global average data of elevation and therefore explain why graded beds appear more responsive. Further, research has shown that the more heterogeneous and more poorly sorted a gravel bed is the greater the amount of structural change that would occur during vibration under sub threshold flows (Hecht, 2004; Rollinson, 2006). This is supported by the data collected in this thesis where the graded beds undergo the greatest amount of vertical settlement. However this effect does not fully explain the differential response of the beds given that the uniform bed is more responsive to stress history, in terms of changes to average critical bed shear stress, than the graded beds. As such it is suggested that stability gains are not just a facet of the packing density but may be linked to other properties of the bed surface. One such bed surface property is bed roughness.

Changes to bed roughness in response to vertical settlement of the bed has been highlighted in analysis of the range of data (k) which have been used as a proxy for bed roughness (Aberle and Nikora, 2006; Cooper and Tait, 2008). Data indicates that uniform beds develop a smoother bed surface in response to antecedent flow as compared to increasingly rough surfaces in graded beds. The increased, tighter packing arrangement generated by uniform beds reduces the relative depth of localised pores, thus explaining reduced k values (Li and Komar, 1986; Kirchner *et al.*, 1990). The resulting smoother bed surface changes the characteristics of the overlying fluid flow field such that 'skimming' flow develops where it is noted that the free stream skims over the top of the bed elements such as to produce a quasi smooth flow with lower resistance (Papanicolaou *et al.*, 2001). Consequently a smoother bed surface would cause a decrease in both the shear stress

magnitude and variability across the bed (Rollinson, 2006) and may explain why a uniform bed's resistance to entrainment is most responsive to stress history. Conversely, the vertical settlement of fines in graded beds (Reid *et al.*, 1985; Marion *et al.*, 2003; Haynes and Pender, 2007) increases bed roughness to produce a coarser surface. This leads to increased flow resistance and hence elevated destabilising bed shear stresses. Specifically, directly over the top of the highest roughness elements flow depth is reduced and flow is accelerated. Immediately downstream of the element flow expansion occurs such that a flow separation zone is generated in the lee of roughness element (Bennett and Best, 2005). Re-circulating eddies in this region generate strong turbulent intensities, high Reynolds shear stresses and high magnitude quadrant events (Buffin-Belanger and Roy, 1998). The bed immediately behind the roughness element is therefore more susceptible to sweeps acting to promote the ingress of fine material deeper within the bed. This acts to further exacerbate the destabilising development of roughness. The ingress of finer material however, counteracts to some degree the destabilising forces as the tighter packing of the fines acts to consolidate and stabilise the framework gravels (e.g. Reid *et al.*, 1985; Allan and Frostick, 1999; Haynes and Pender 2007). Further the higher shear stresses may permit exposed coarser grains the ability to adjust to more stable positions on the surface (Brayshaw *et al.*, 1983; Li and Komar, 1986; Dietrich *et al.*, 1989; Fenton and Abbott, 1997). These counter processes explain why stress history stability gains are also observed in graded beds, yet they may be of lesser magnitude than in uniform beds (Ockelford and Haynes, 2010). Further, that there is a grade dependent response in the graded beds, where the bimodal bed shows a greater overall roughness supports the concept that the overall stability of the bed links to the proportion of the fines within the bed. Given the higher proportion of finer grains in the unimodal bed, the ingress of finer material into the interstices serve to consolidate the bed into a more stable configuration as compared to the bimodal bed. However despite a smaller overall fine fraction the bimodal bed shows a greater response in terms of increased critical bed shear stress in response to stress history than the unimodal bed. This suggests that it is not just the infiltration of fines that increase stability but the arrangement of grains on the bed surface (Buffington *et al.*, 1992; Church *et al.*, 1998; Marion *et al.*, 2003).

However the magnitude of roughness increase is inversely proportional to the length of the antecedent duration employed in the graded beds such that a temporally dependent two-stage process in response is noted. This is especially important in the light of the stability

response of critical bed shear stress where, akin to bed response, the most rapid stability gains are after the shortest antecedent durations (60 minutes). Thus, surprisingly, this advocates that rapid changes to the bed surface (60 minute data) are subsequently tempered following longer applied duration of antecedent flow (i.e. sometime between 60 and 960 minutes). The degradational armouring work by Marion *et al.*, (2003) supports this finding where they note that bed surface adjustments may be reversible. In their work they ran experiments of up to 80 hours to investigate the effects of feed rates on armour development using a unimodal sediment mixture ($D_{50} = 4\text{mm}$). Their results revealed that under purely degradational conditions, i.e. with no sediment feed, akin to results presented in this thesis laser scans of the bed surface revealed that after 13 hours of flow the bed had undergone rapid evolution. This was evidenced by a change to the probability density functions of the bed surface elevations which became flatter and wider indicating a surface which is composed of a larger number of coarser clasts. This supports the first response noted in this thesis where a rapid change to the bed surface occurs after the shortest antecedent conditions. However they also note that after exposure to the very longest flow durations (80 hours) the probability density functions of the bed surface elevations become increasingly peaky akin to the initial distribution in response to a change in sediment mobility and suggestive of a smoother bed surface. Whilst the flow durations and conditioning discharges were longer and higher than those used in this thesis it does prove that there is the potential for a dual response to be noted. In this thesis the rapid evolution of the bed surface appears to be a 'first response' to short-term increases in pressure and turbulence instabilities immediately following a change in flow; this is in agreement with Paphitis and Collins (2005). Second-stage moderation of these changes is more difficult to reason. Framework dilation, repositioning of particles, winnowing of surface grains, changes to the overlying turbulence and/or infill of bed pores by fines (Allan and Frostick, 1999; Aberle and Nikora, 2006; Cooper and Tait, 2008) would be possible mechanisms. Allan and Frostick (1999) observed an 8.6mm gravel framework lift and dilate just before entrainment by up to 50% (120mm flow depth at 85% τ_c) allowing fine grains to settle deeper into the bed as framework with Brasington *et al.*, (2000) noting that the dilation of the framework causes negative pore pressure that triggers fluid inrush which carries fine sediment and reinforces the dilation effect. Given that flows during the antecedent period used in this thesis are significantly below that needed to entrain even the D_{50} it is unlikely that this is the dominant mechanism responsible for the noted response. In addition the experiments of Brasington *et al.*, (2000) introduced sand grains to a consolidated gravel

matrix which is known to initiate the transport of previously stable gravel bed surfaces (Jackson and Beschta, 1984; Ikeda and Iseya, 1988; Wilcock, 1988; Curran, 2005) and may partially explain the dilation effects. The effects of the changes to the overlying fluid flow regime have been postulated above however were not the explicit focus of this thesis.

The change in bed porosity in response to both vertical settlement and bed roughness change is noted within all three beds with the response, as expected, being both grade and temporally dependent. In the uniform bed, pores are deeper in absolute terms than the graded beds. This is in line with the findings of Rollinson (2006) who noted that in a uniform bed (D_{50} 8mm) as compared to a bimodal bed of comparative D_{50} the pore spaces were both larger (by up to 3%) and deeper (by up to 5%) in the uniform bed after being exposed to up to 4361 minutes of sub-threshold flow duration. This is supported by Cuthbertson and Ervine (1999) and Cuthbertson (2001) who suggest that large scale coherent vortex structures generated in the pores of a bed are stronger the larger the pore. Further, beds with deeper pores are more likely to experience stronger vertical flow velocities as supported by Carling (1984) acting to influence the lift forces exerted upon particles and hence alter the potential for entrainment or deposition of particles (Wohl and Ikeda, 1998). In response to applied antecedent flow the numbers of deep pores decreases in the uniform beds commensurate with Rollinson (2006) who noted that as beds were water worked the percentage of deep pores decreased due to vibration of particles and hence increased packing density as described above. Further the removal of exposed grains as antecedent duration is increased would also explain this trend. This is in line with the visual analysis of the bed surface DEM's where it was noted that grain displacement occurs in areas of higher relative elevations. Conversely, in the graded beds the absolute depth of the pores is comparatively smaller than the uniform bed. This trend is well noted within the literature, typically analysed in relation to the different packing arrangements of the three beds (Kirchner *et al.*, 1990; Kleinhans *et al.*, 2008; Frings *et al.*, 2008; Haynes *et al.*, 2009). Specifically it is the regions of fine grains on the bed surface which limit pore depth significantly more than an open coarser framework such that it follows that beds with greater proportions of fines (i.e. the bimodal bed) would have smaller pore depth statistics as demonstrated here. Interestingly however there is an inverse relationship between the degree of change in the number of deep pores and the antecedent duration. This suggests a two-stage bed response cycle as already described in

relation to the temporal bed roughness development with similar mechanisms responsible for the reaction.

6.4.2 *Large scale process; the case for bed stabilisation as a result of grain rearrangement*

A by product of the changes to the bed surface in response to vertical settlement, roughness and porosity changes, is the change to the projection and exposure of the grains on the bed surface (Gomez, 1995; Kirchner *et al.*, 1990; Carling *et al.*, 1992). In turn this can mean that either grains are displaced or they can re-orientate into a more stable position on the bed surface. Typically these processes are noted to occur under higher shear stresses than those reported in this thesis where both Marion *et al.*, (1997); Carling *et al.*, (1992) and McEwan *et al.*, (2004) all report similar findings as those reported in this thesis despite flow being sub threshold in the reported experiments. Grain displacement is noted to occur within all three beds although the mechanisms responsible are different between the uniform and graded beds. Specifically in the uniform beds, given that relative grain effects cannot alter the relative projection and exposure of different grain fractions, displacement is likely to be linked to the removal of grains which are of a higher elevation (as a result of the screeding process) and hence exhibiting a greater form drag (Schmeeckle and Nelson, 2005; Bottacin *et al.*, (2008). Given that form drag is strongly correlated with the downstream velocity which is in turn strongly related to grain displacement it is assumed that an increase in relative exposure and hence form drag would cause displacement of the grains (Clifford *et al.*, 1992; Nelson *et al.*, 1995; Sterk *et al.*, 1998). This is confirmed by Bottacin *et al.*, 2008 who noted that as a grain moves 90% of the changes to the overlying fluid velocity were associated with the streamwise component and only 10% with changes to the cross products of the streamwise and traverse fluctuations. Conversely within the graded beds, as flow is imposed upon the bed infiltration of the fines will occur deeper within the bed such as to increase the exposure and hence form drag of the largest grains (Carling *et al.*, 1992, Gomez, 1995; Haynes and Pender, 2007) over a prolonged period of time as described above. In turn the removal of the roughest elements would cause the bed to become smoother again after the long periods of flow exposure. Whilst this is in line with findings noted for the uniform bed, the two stage roughness response of the graded beds suggests that only the grains with the very highest exposure and form drag would be destabilised and rather than be displaced the grains would be re-orientated so as to impose less resistance upon the overlying fluid flow. This is confirmed using visual analysis which shows that only a small number of displaced grains were noted so as to support the

postulation that only the most unstable grains on the bed surface will be displaced and that bed stability gains, particularly in the graded beds is in response to grain reorientation (Buffington *et al.*, 1992; Church *et al.*, 1998; Marion *et al.*, 2003).

Skewness (Sk_b) data confirms that graded beds develop a structured surface layer composed of larger grains with finer particles filling the depressions between, (Brown and Willetts, 1997; Nikora *et al.*, 1998; Marion *et al.*, 2003; Aberle and Nikora, 2006). That the bimodal bed appears to be significantly more structured (with skewness values three to four times those of other grade-time combinations) is likely a facet of the separation of fine and coarse modes implicit to a bimodal distribution. Secondly, the graded beds become progressively positively skewed with increased antecedent duration. Marion *et al.*, (2003) support this finding; during their experiments unimodal beds ($D_{50} \sim 4\text{mm}$, akin to the D_{50} used in this research) were exposed to up to 80 hours at conditions close to critical entrainment. Their bed surface topography was measured using laser displacement scanning taken at discrete intervals through the degradation process. Their results confirmed that skewness does increase with increased antecedent duration although the magnitude of change is not calculated. They support the supposition that this change is caused by an increase in the number of coarser grains being present on the bed surface with progressive armour development. However interestingly, rather than following the two-stage temporal response of Z_b and k , results in this thesis note a positive correlation with antecedent duration. This indicates that the timescale needed to develop significant bed structuring is much longer than both vertical settlement and roughness development, therefore suggesting that structuring is underpinned by other mechanisms such as particle orientation. This is supported by Marion *et al.*, (2003) who note that the majority of the changes to the bed surface occur during the first 15% of the experiment (in terms of the total experiment duration). Given that the *pdf's* of the bed surface only showed what they considered to be a 'true signature of a degraded armoured surface' after the longest flow durations (between 80-100% of the total experiment time) it was assumed that the majority of the changes occurring on the bed surface were small scale changes such as vertical settlement rather than larger scale reorganisation. Given that no observable coarse grain scale structures were noted to form on the bed surface during the course of the experiments reported herein it is postulated that it is not the reactivity of the coarse grains in isolation which serves to increase bed stability (if this were to be the case a much greater change would be expected in the skewness values). This is particularly apparent in the unimodal

beds where the degree of surface coarsening is considerably less than the bimodal bed and hence bed stability gains must be linked to some other property of the bed surface, such as the surface organisation (Pender *et al.*, 2001; Marion *et al.*, 2003).

The appearance and extent of such surface organisation can be analysed by assessing the length scales present on the bed surface with the scale of this organisation critical to overall bed stability. In the uniform bed the correlation length approximates to the grain scale (~4mm) as compared to correlation lengths approximately twice this in both graded beds (~2D₅₀). This is indicative of there being a greater scale structure in the graded beds as compared to the uniform bed. The graded bed relationship is supported by Cooper and Tait (2008) who compared the statistical properties of a unimodal and bimodal distribution (D₅₀ of 4.8 and 4.4mm for the unimodal and bimodal bed respectively) which were degraded under sediment feed conditions until a stable armour had formed on the bed surface. Despite the difference in the feeding conditions of this experiment and those reported in this thesis they note length scales to be in the region of 2D₅₀ as reported in this thesis, a likely facet of the similar D₅₀ grain sizes used. Typically uniform beds are not investigated within the literature so it is difficult to draw comparisons with previous findings. However results do support previous postulations that the uniform beds stabilise by vertical settlement, increased packing density and decreased bed roughness whereas the graded beds stabilise in a different manner, linked to the organisation of the grains on the bed surface (Rollinson, 2006; Cooper and Frostick, 2009). Once more the bimodal bed shows greater length scales as compared to the unimodal bed further supporting the skewness data in suggesting that the underpinning mechanisms responsible for bed stabilisation may be intrinsically different for this grade. Although Cooper and Tait (2008) note the opposite such that their length scales are larger for their unimodal bed (9.69mm) as compared to the bimodal bed (7.64mm) it is becoming more widely known that these beds stabilise in different manners (Cooper and Frostick, 2009) which may explain the differential response under sub-threshold flow conditions. Further, results show that irrespective of grain size distribution, the length scales in both the streamwise and lateral directions increase with increasing antecedent duration. These results support the notion that beds reorganise into a more structured surface as antecedent duration is increased, thereby supporting similar findings relating to increased periods of degradational armouring (Marion *et al.*, 2003; Aberle and Nikora, 2006; Copper *et al.*, 2009). In addition, data shows that surface organisation increases in topographic complexity with

increased antecedent duration, most notably within the graded beds and particularly the bimodal bed i.e. not only are beds becoming more organised but that they are becoming more topographically complex. This is in contrast to the armouring experiments of Aberle and Nikora (2006) who noted that despite an increase in geometrical roughness, as evidenced by an increase in the roughness length scales, the bed surface became topographically more simple. Given that Aberle and Nikora's (2006) relationship is the accepted norm for armouring relationships, stress history data would therefore indicate that the surface must be stabilising by different mechanisms than the active surface coarsening (armouring) under sub-threshold flow conditions as advocated by Aberle and Nikora (2006). However although the length scales increase in response to antecedent duration in the graded beds no information is given about the spatial organisation of the grains on the bed surface which is of fundamental importance if we are to fully understand why the different grades respond in such a different manner to the imposed flow regime.

Surface organisation can be effective in inducing bed stabilisation at both the individual grain scale (akin to direct sheltering described by McEwan *et al.*, 2004) as well as the multiple grain scale (akin to remote sheltering described by McEwan *et al.*, 2004) with the interaction of individual grains on the bed surface with each other providing the conceptual link between the two scales; given that no larger scale structures were noted in any of the beds it would be expected that the most likely type of stabilisation would be from direct sheltering. However as the graded beds, especially the bimodal bed, do develop length scales which approximate to $2 D_{50}$ it could be postulated that remote sheltering is beginning to develop. Consequently, taking this concept further, the contour plots of $D_b(l_x, l_y) / 2\sigma_{zb}^2$ reveal that the spatial organisation and alignment of the grains are highly grade rather than temporally dependent such that it seems that it is grade rather than antecedent duration which controls the overall organisation of the bed surface. It has been proven within the literature that such alignment of grain is of fundamental importance to the overall stability of the bed (Allen, 1982; Marion *et al.*, 2003; Aberle and Nikora, 2006).

In the uniform bed there is no obvious wholesale alignment of grains on the bed surface which is logical given that the bed becomes smoother due to grains interlocking over the shortest antecedent flow durations (Rollinson, 2006). Once the bed has become smooth there is little that increasing the antecedent duration will contribute to in terms of increasing spatial reorganisation. This is indirectly supported in the literature which

suggests that once a bed has stabilised it requires wholesale entrainment of the bed to further re-organise it. Although this is typically talked of in terms of the re-entrainment of fine grains during the full mobilisation of a coarse framework (Jackson and Beschta, 1984; Ikeda and Iseya, 1988; Wilcock, 1988) it logically follows for this research given that the former is the result of a feedback between the bed surface roughness and overlying turbulent flow regime. In the unimodal bed, despite increased coherency of contours at small spatial lags suggesting that individual grains are organised on the bed surface in response to an imposed antecedent flow there is no overall alignment of the grains with flow direction. This configuration is not temporally sensitive such that even after the longest antecedent durations there is still no dominant alignment direction of grains on the bed surface. Conversely within the bimodal bed the a-axis are flow-aligned and the b axis perpendicular to the flow (e.g. Nikora *et al.*, 1998; Smart *et al.*, 2004) in a configuration akin to that of a static armour after the application of the shortest applied antecedent flow durations. Akin to the unimodal bed this configuration is temporally insensitive.

The overall difference between the response of the unimodal and bimodal beds have been linked in previous literature to the different arrangement of the grains on the bed surface (e.g. Marion *et al.*, 2003; Cooper and Frostick, 2009). This difference has primarily been linked to the difference in the exposed areas of the grains on the bed surface. That, at the larger scale the unimodal bed does not show any significant grain alignment on the bed surface suggest grains are more likely to have larger exposed areas and hence experience greater form drag. Conversely the grains in the bimodal bed show progressive alignment with flow and hence a decreasing form drag. In explanation Cooper *et al.*, (2010) note that form induced stresses are larger at comparable relative submergences in a bed where grains are dynamically armoured such that flow retardation is higher and there are larger roughness effect in the flow. Comparatively beds which are statically armoured (bimodal bed in this research) are noted to be hydraulically smoother because of the particle reorientation; this confirms the roughness data discussed earlier where the unimodal bed was rougher than the bimodal bed. This is primarily linked to the effect of relative protrusion into the flow where it has been recorded that the sediment entrainment strongly correlates with some aspect of streamwise velocity (Nelson *et al.*, 1995; Schmeeckle and Nelson, 2003; Bottacin-Busolin *et al.*, 2008; Cooper and Tait, 2010). Where a grain exhibits greater form drag due to a greater exposed area, as in the unimodal deposit, it is therefore more likely to be destabilised as compared to a bed which exhibits smaller

amounts of form drag as in the bimodal deposit described herein. This supports the hierarchy of response to stress history where the bimodal bed is comparatively more responsive as compared to the unimodal bed and suggests that this fundamental difference is vital to stress history induced response. Further this supports the notion that the smoother bed surface generated in the uniform bed decreases the form drag and hence the destabilisation probability and produces the most responsive bed to stress history.

That there is not a temporal response to the graded beds is perhaps surprising. Given that the unimodal bed exhibits no apparent large scale alignment two theories are proposed to explain this finding; (i) the unimodal bed may not have attained its most stable granular configuration (a static armour) within the investigated timescales (as evidenced by an increase in the bed roughness). This supports the unimodal bed findings of Marion *et al.*, (2003) who note that in order for a unimodal bed to achieve a true equilibrium it will need to be exposed to flows for a considerable time. Further, the work of Cooper and Frostick (2009) who note that unimodal beds take approximately 40% longer to reach a static armour as compared to a bimodal bed of comparable D_{50} . (ii) that processes such as vertical winnowing of fines and the development of hiding effects are the most important control on bed stability, not the organisation of surface grains *per se*. This latter postulation is supported by the roughness data where it is noted that the unimodal bed is rougher than the bimodal bed with the overall magnitude of change being greater in response to antecedent duration. To the contrary, within the bimodal bed there is evidence of a distinctive structure of static armour having developed after only 60 minutes antecedent flow, with roughness development continuing. Cooper and Frostick (2009) suggest that the differences in the force contributions between the bimodal and unimodal bed deposits may explain the appearance of a different response to applied antecedent flow. In their experiments a unimodal and bimodal bed of comparative D_{50} (6.19mm) were degraded until a static armour had formed and the bedload transport rate diminished to a low level (up to 630 minutes). They note that within their bimodal deposit, after 120 minutes of flow it is more susceptible to entrainment than the unimodal deposit. This was ascribed to be due to a higher proportion of the fluid force was being carried by the finer grain fractions and a lower proportion carried by the larger grain fractions such that it was more unstable. However after 180 minutes of armouring the difference in the force distributions between the two beds reduced such that a static armour developed and the fluid force distributions became similar (630 minutes in the unimodal bed and 390 minutes

in the bimodal bed). Given that the unimodal bed took longer to reach static armour the bimodal bed must evolve from being more mobile at comparable time frames to less susceptible to movement as it approaches the development of a static armour layer. This supports the previous findings suggesting that the majority of rearrangement happens under the shortest antecedent periods. Further, this data is clearly supportive of the comparative complexity of the bimodal bed response as noted within this thesis such that it is a combination of spatial organisation and small scale grain rearrangement via fine grain infiltration which control the response to the imposed flow regime. It also suggests that the unimodal bed used in this research may not have been exposed to a long enough flow duration for a static armour to form further supporting the work described earlier by Marion *et al.*, (2003).

6.5 Chapter Summary

Data given in this chapter has confirmed that non-cohesive granular beds locally restructure in response to a sub-threshold applied flow. They have also provided the first quantitative insight into the mechanisms responsible for enhanced bed stabilisation as a result of antecedent flow duration. The argument made, although complex, suggests that the beds reorganise by (i) vertical settlement causing a change to the packing arrangement, (ii) a change to porosity, (iii) grain displacement and (iv) changes to the arrangement of the grains on the bed surface, particularly orientation. Each mechanism is likely to act as a feedback to the other, particularly packing and porosity and so the relative effects of each are difficult to differentiate between. However, all three beds have shown notable changes to the mechanisms which are responsible for stabilisation due to prolonged exposure to sub threshold flow. The magnitude of the change is responsive to both the period of applied antecedent flow as well as being significantly affected by the grade.

The uniform bed is seen to be most responsive to antecedent flow. In response to applied antecedent flow the bed undergoes vertical settlement similar in magnitude to the graded beds which becomes exacerbated with increased flow duration. However in response to vertical settlement the bed becomes smoother. Hand in hand with the decrease to roughness is a decrease in bed porosity. This suggests that the bed is becoming increasingly consolidated in response to the antecedent flow where grain pivot angles increase and hence stability increases. Since the bed becomes smoother grain protrusion decreases such that destabilisation by grain displacement occurs only in very localised

areas typified by higher initial relative elevations. Further, very little evidence points towards the stabilisation of uniform beds being as the result of grain reorientation. As such it has been assumed that it is the change to the bed surface in response to applied antecedent flow which exacerbates the effects of the overlying fluid flow regime such that it is the interaction with the fluid flow in the uniform bed rather than a change to the structure *per se* which is responsible for bed stabilisation in response to antecedent flow.

Conversely within the graded beds different mechanisms are noted to cause bed stabilisation in response to applied antecedent duration. Vertical settlement of the bed increases packing density and increases pivot angles akin to that noted within the uniform beds. However, because of relative grain effects the vertical settlement is spatially heterogeneous controlled by the range of grain sizes present on the bed surface. Therefore although the magnitude of bed settlement is positively correlated with antecedent duration, due to relative size effects, the bed roughness increases. This magnitude of bed roughness increase is however both temporally and grade sensitive. The unimodal bed becomes rougher than the bimodal bed and the magnitude of roughness change decreases with increased antecedent duration. The difference between the unimodal and bimodal bed is the likely effect of the proportion of sand with the bed whereas the temporal response is initially linked to a rapid response to applied antecedent flow as the result of vertical settlement and tempered by a counter secondary response where the magnitude of roughness changes decreases. The dual nature of this response is difficult to understand although it has been linked to vertical settlement; dilation; repositioning/loss of surface grains, changes to the overlying turbulence and/or infill of bed pores by fines. This differential fractional response of the grains on the bed surface means that there is a change to the relative exposure and projection of grains on the bed surface such that reorientation and alignment with flow is possible.

In the unimodal bed, at the large scale, there is no preferential grain direction which supports the hypothesis that the timescales needed to create an armoured surface are in excess of those durations employed in this research. Conversely within the bimodal bed a configuration akin to a static armour is developed suggesting that even though individual grains on the bed surface may still be mobile, the timescales involved over which stabilisation occurs is much shorter than that of the unimodal bed, a potentially fundamental finding. As such these results show that the more complex the grain size

distribution, the more complex the bed surface response to stress history. Further, it assumed that, in bimodal beds it is the reorganisation of the bed surface in response to applied antecedent flow which plays a greater controlling mechanism to enhanced bed stability than the interaction with the fluid flow *per se* as in the uniform beds.

Chapter 7 Conclusions and Future Research

This PhD thesis has provided direct experimental evidence of the stabilising effects of antecedent flow. Primarily this has been shown through three main metrics; entrainment threshold, transported bedload and bed structure. The following section presents a summary of the work undertaken and highlights the main results and conclusions drawn from data collected. It finishes with identifying suggestions for future avenues of research.

7.1 Experimental summary

Two discrete sets of experiments have been undertaken in two different flume facilities to comprehensively investigate the effects of antecedent duration upon bed stability. The first set of experiments used short antecedent flow durations and five different grain size distributions to quantify the effect of stress history upon grain size distribution. Three grain size distributions with median grain sizes (D_{50}) of 4.8mm [uniform ($\sigma_g = (D_{84}/D_{16})^{0.5} = 1.13$; bimodal ($\sigma_g = 2.08$); and, unimodal ($\sigma_g = 1.63$)] were compared. Two further grades were employed, a coarse distribution and a fine distribution to assess the impact of fines on the distribution. Beds were exposed to antecedent durations of between 0 (benchmark) and 60 minutes, where the applied shear stress was set to 50 % of the critical threshold for entrainment of the median grain size. The second set of experiments used the same near-uniform, unimodal and bimodal grain size distributions but antecedent duration was increased to up to 960 minutes (to assess the possibility of a stability maxima being reached). In both sets of experiments average critical bed shear stress, total transported load and bed surface photographs were taken at discrete periods during the experiment. During the second set of experiments two laser scans of the bed surface were taken immediately prior to and subsequent to the antecedent period in order to quantify changes to the bed surface as a result of the applied antecedent flow. In total, 128 experiments have been extensively discussed in Chapter 4 (effect of grain size distribution and stress history), Chapter 5 (effect of extended antecedent durations on bed stability) and Chapter 6 (quantifying the mechanisms of bed stabilisation).

7.2 Effects of stress history upon entrainment threshold

Results from both sets of experiments were analysed to investigate the effect of stress history upon entrainment threshold in terms of both antecedent duration and grain size

distribution. Stability gains were measured in terms of a change to average critical bed shear stress. The main conclusions are discussed below;

- Increasing the duration of antecedent flow increases the structural resistance of the bed to entrainment by fluid flow. The magnitudes of response noted within this thesis range from between + 25% in the uniform bed to +2% in the coarse bed.
- The rate of response to stress history is inversely proportional to applied antecedent duration, suggesting that the greatest changes to stability occur over the shortest antecedent time frames.
- The increase in average bed shear stress is seen to be grade dependent whereby the uniform beds are at least twice as responsive as graded beds, a facet of the ability of the bed to rearrange (uniform (+25%) > bimodal (+9%) > unimodal (+8%) > fine distribution (+8%) > coarse distribution (+2%) after the shortest antecedent durations and uniform (+14.2%) > bimodal (+11.5%) > unimodal (+7.3%) after the longest antecedent durations). However, end member distributions employed (coarse and fine distributions) do not respond in a consistent trend to stress history suggesting that the ratio of coarse to fine sediment within a grain size distribution appears to influence the magnitude of the response to stress history.
- Despite evidence supporting the possible attainment of a stability maxima, data in this current thesis never reaches this stabilised value, suggesting that value is in excess of 960 minutes of applied antecedent flow.

7.3 Effects of stress history upon transported bedload

Bedload data has been used to support entrainment findings, acting as a proxy for bed stability. The main results are discussed below;

- Increasing the duration of antecedent flow reveals a reduction in the transport rate as a function of antecedent duration.
- The rate of response to stress history is inversely proportional to applied antecedent duration suggesting that the greatest changes to stability occur over the shortest antecedent time frames; this is consistent with the entrainment data.
- The response of total transported load to the imposed stress history regime shows significant grade dependency; this is supportive of earlier entrainment threshold analysis. Specifically, extending the antecedent flow period results in the transported bedload reducing by the following grade-specific hierarchy: bimodal (-94%) > unimodal (-90%) > fine (-70%) > coarse (-59%) after the shortest

antecedent durations and bimodal (-89%) > uniform (-65%) > unimodal (-50%) after the longest antecedent durations. The difference between the two sets of results is thought to be due to the different overlying fluid flow properties as a result of the different flume facilities.

- Increasing the duration of antecedent flow typically results in a systematic decrease in the geometric standard deviation suggesting enhanced size selectivity of transport. There is, however, a significant grade dependency, suggesting that there is also a dependence on the relative position of a grain fraction within the grain size distribution rather than σ_g alone.
- As total bedload transported decreases as a function of stress history there is a general change to the selectivity of the transport which is occurring. This is particularly notable in the unimodal, bimodal and coarse beds after the shortest antecedent durations and in both the unimodal and bimodal beds after the longest antecedent durations. This suggests that hiding effects are developing. As this typically goes hand-in-hand with hiding development the effect is on mobility of the middle fractions of the transported distribution. Data for the fine bed is subtly different in that, from a start point of equal mobility, selective entrainment only develops progressively during the antecedent period.
- Despite a reduction in the total load with increased antecedent duration, evidence suggests that a stability maxima will never be reached and that a background transport rate will always be observed. This implies that the bed will continue to transport sediment even though it may be at its most stable granular configuration as evidenced by the attainment of a stability maxima in the shear stress values.

7.4 Effects of stress history upon bed structure

This thesis has shown the first real insight into the mechanism of stress history induced stability by way of quantifying the associated changes to bed topography. The main conclusions are discussed below;

- Sediment beds, regardless of antecedent duration, reorganise by three main mechanisms; (i) vertical settlement causing a change to the packing arrangement and porosity, (ii) grain displacement and (iii) changes to the arrangement of the grains on the bed surface, particularly orientation. However, although all three beds exhibit all three types of change, the magnitude of the change is responsive to

both the period of applied antecedent flow as well as being significantly affected by the grade.

- In the uniform beds;
 - In response to applied antecedent flow the bed undergoes vertical settlement and the bed becomes smoother and exacerbated with increased flow duration. Hand in hand with the decrease in roughness is a decrease in bed porosity. This suggests that the bed is becoming increasingly consolidated in response to the antecedent and hence stability increases.
 - Since the bed becomes smoother grain protrusion decreases such that destabilisation by grain displacement occurs only in very localised areas typified by higher initial relative elevations.
 - Very little evidence points towards the stabilisation of uniform beds being as the result of grain reorientation.
- In the graded beds;
 - Vertical settlement of the bed increases packing density akin to that noted within the uniform beds. However because of relative grain effects the vertical settlement is spatially heterogeneous controlled by the range of grain sizes present on the bed surface and the bed roughness increases. The temporal response, however, sees the magnitude of roughness change decrease with increasing antecedent duration. This advocates a two stage response; an initial rapid response to applied antecedent flow as the result of vertical settlement tempered by a counter secondary response postulated to be caused by vertical settlement; dilation, repositioning/loss of surface grains, changes to the overlying turbulence and/or infill of bed pores by fines.
 - This differential fractional response of the grains on the bed surface means that there is a change to the relative exposure and projection of grains on the bed surface such that reorientation and alignment with flow is possible. In the unimodal bed this reorientation occurs such that individual grains are aligned transverse to the flow direction, akin to a dynamic armour configuration, which is not temporally sensitive. This suggests that either this is the most stable granular configuration or the timescales needed to develop a static armour exceed those timescales used in this thesis. However, at the larger than grain scale there is no preferential grain

direction which supports the hypothesis that the timescales needed to create an armoured surface are in excess of those durations employed in this research. Conversely, within the bimodal bed, realignment of flow is temporally sensitive at the individual grain scale such that after the shortest antecedent durations the alignment of the grains is transverse to the flow. However as antecedent duration is increased, particles align with the flow direction akin to the configuration typically associated with a static armour. At the larger scale, a configuration akin to a static armour is developed suggesting that even though individual grains on the bed surface may still be mobile, the timescales involved over which stabilisation occurs are much shorter than those of the unimodal bed.

7.5 *Future Research*

This thesis has provided significant evidence to support the concept of stress history and it is clear that the level of stability attained by a sediment bed is contingent upon and specific to, the applied antecedent flow and the surface grain size distribution. As such not only is the outcome of this research pertinent to wider investigations in fluvial engineering and the management of regulated rivers but also to flume-based experimental techniques. It may also form a basis from which to increase the reliability of sediment transport models via the inclusion of a bed stability parameter. With this in mind, and in order to consolidate knowledge gained in this thesis, a number of suggestions are provided below which raise possible future research agendas;

- *Quantify the effect of the coarse and fine end members of the distribution*

Despite consistent overall trends in response to stress history it has been highlighted throughout this current thesis that the response to stress history is grade dependent. This becomes particularly apparent given the unexpected response of the uniform and graded beds where the former appear to be more responsive to stress history than the latter. However the reasoning behind the lack of response of the coarse beds and the variable response of the fine beds to stress history needs further exploration. This is especially important since it is the response of the coarse and fine fractions (in particular the latter) which have been noted to control sediment bed stability.

- *High resolution temporal measurement of bed stability*

Results have been consistent in indicating that the greatest response to stress history in terms of both changes to average critical bed shear stress, total transported load and bed

structure, occur during the shortest applied antecedent flow durations. This is an extremely interesting and vital aspect of this research, but understanding has been limited due to the temporal resolution of the measurement, particularly using the bed surface laser scans. Thus, although this thesis has provided insight into a new high speed laser technology and shown that this new technology has the capabilities to accurately and rapidly describe bed surface of different grade, size and composition, the temporal resolution of sampling has been limited; this has primarily been linked to potential issues with draining the flume. By taking more regular scans, the reasoning behind the temporal stabilisation of the bed could be fully quantified. As such, and especially since there are now new technologies becoming increasingly available which allow laser scans of the bed surface to be taken through the water column, future research should concentrate on increasing the temporal resolution of bed surface sampling.

- *Link changes to the bed surface with the changes to the overlying fluid flow properties*

Results have consistently been linked to the interaction between the bed surface and the overlying fluid flow regime. This has been postulated to be especially linked to the turbulent properties of the flow. Whilst speculative postulations have been forwarded to explain the potential impact of turbulence upon the stability gains in response to stress history, only direct analysis of the fluid column during the progression of an experiment could fully explain this possible link. As such the use of technologies such as PIV could be used to not only quantify the turbulent properties of the fluid but also to link these properties with the temporal evolution of the bed fabric and investigate how the fluid force distribution changes with flow duration and magnitude. This is particularly pertinent given the difference in the results gained from the two different flume facilities, especially in uniform bed where it was postulated that width depth ratios have a fundamental effect upon the stability attained due to the differences in the overlying fluid dynamics.

- *Quantify the effect of sediment feed and recirculation experiments*

Although results have pointed towards stress history as being an important parameter in controlling bed stability, previous research (e.g Wilcock and Southard, 1989) illustrate that degradation (as used in this thesis), feed and re-circulating sediment systems produce very different equilibrium sediment transport conditions. As such further research is needed to quantify the effects of stress history when the sediment feed conditions are altered.

-
- *Development of a stress history term into incipient motion equations*

The findings presented in this thesis are fundamental to the accurate prediction of the transition between river bed stability and instability. Yet prediction of such a transition is complicated by the data that are available and the uncertainty which surrounds analysis of incipient motion. As such it is proposed that future research in this area of sediment analysis could begin to provide guidance as to the best practice for incorporating such a variable into existing entrainment / transport equations via the inclusion of a bed stability parameter defined from stress history analysis.

- *Validating the results in the field*

Indirect evidence from the field already supports the concept of stress history (e.g. Reid and Frostick, 1984 and Reid *et al.*, 1985), however no direct evidence exists to record the effects of stress history. If the effects of stress history in terms of entrainment thresholds and total transported load are to ultimately be included in incipient motion and sediment transport equations it is vital that data be available to calibrate and validate proposed models.

Appendix A

A.1 Experimental Programme

Experiments highlighted in black formed the first part of this thesis performed in the 0.3 m wide flume whilst experiments highlighted in blue form the second part of this thesis performed in the 1.8m wide flow.

Experiment number	Grain Size Distribution	Bed slope	Bedding In Period (Minutes)	Antecedent Period	Stability Test Duration (Minutes)
				Duration (Minutes)	
1	Uniform	1/200	10	0	85
2	Uniform	1/200	10	0	85
3	Uniform	1/200	10	0	85
4	Uniform	1/200	10	0	85
5	Uniform	1/200	10	10	90
6	Uniform	1/200	10	10	90
7	Uniform	1/200	10	10	90
8	Uniform	1/200	10	20	120
9	Uniform	1/200	10	20	120
10	Uniform	1/200	10	20	120
11	Uniform	1/200	10	40	125
12	Uniform	1/200	10	40	125
13	Uniform	1/200	10	40	125
14	Uniform	1/200	10	60	130
15	Uniform	1/200	10	60	130
16	Uniform	1/200	10	60	130
17	Unimodal	1/200	10	0	90
18	Unimodal	1/200	10	0	90
19	Unimodal	1/200	10	0	90
20	Unimodal	1/200	10	0	90
21	Unimodal	1/200	10	10	100
22	Unimodal	1/200	10	10	100
23	Unimodal	1/200	10	10	100
24	Unimodal	1/200	10	20	110
25	Unimodal	1/200	10	20	110
26	Unimodal	1/200	10	20	110
27	Unimodal	1/200	10	40	110
28	Unimodal	1/200	10	40	110
29	Unimodal	1/200	10	40	110
30	Unimodal	1/200	10	60	115
31	Unimodal	1/200	10	60	115
32	Unimodal	1/200	10	60	115
33	Bimodal	1/200	10	0	60
34	Bimodal	1/200	10	0	60
35	Bimodal	1/200	10	0	60

36	Bimodal	1/200	10	0	60
37	Bimodal	1/200	10	10	65
38	Bimodal	1/200	10	10	65
39	Bimodal	1/200	10	10	65
40	Bimodal	1/200	10	20	75
41	Bimodal	1/200	10	20	75
42	Bimodal	1/200	10	20	75
43	Bimodal	1/200	10	40	75
44	Bimodal	1/200	10	40	75
45	Bimodal	1/200	10	40	75
46	Bimodal	1/200	10	60	80
47	Bimodal	1/200	10	60	80
48	Bimodal	1/200	10	60	80
49	Coarse	1/200	10	0	155
50	Coarse	1/200	10	0	155
51	Coarse	1/200	10	0	155
52	Coarse	1/200	10	0	155
53	Coarse	1/200	10	10	155
54	Coarse	1/200	10	10	155
55	Coarse	1/200	10	10	155
56	Coarse	1/200	10	20	170
57	Coarse	1/200	10	20	170
58	Coarse	1/200	10	20	170
59	Coarse	1/200	10	40	160
60	Coarse	1/200	10	40	160
61	Coarse	1/200	10	40	160
62	Coarse	1/200	10	60	170
63	Coarse	1/200	10	60	170
64	Coarse	1/200	10	60	170
65	Fine	1/200	10	0	60
66	Fine	1/200	10	0	60
67	Fine	1/200	10	0	60
68	Fine	1/200	10	0	60
69	Fine	1/200	10	10	70
70	Fine	1/200	10	10	70
71	Fine	1/200	10	10	70
72	Fine	1/200	10	20	65
73	Fine	1/200	10	20	65
74	Fine	1/200	10	20	65
75	Fine	1/200	10	40	60
76	Fine	1/200	10	40	60
77	Fine	1/200	10	40	60
78	Fine	1/200	10	60	70
79	Fine	1/200	10	60	70
80	Fine	1/200	10	60	70
81	Uniform	1/200	30	0	85
82	Uniform	1/200	30	0	85
83	Uniform	1/200	30	0	85
84	Uniform	1/200	30	0	85

85	Uniform	1/200	30	60	90
86	Uniform	1/200	30	60	90
87	Uniform	1/200	30	60	90
88	Uniform	1/200	30	120	120
89	Uniform	1/200	30	120	120
90	Uniform	1/200	30	120	120
91	Uniform	1/200	30	240	130
92	Uniform	1/200	30	240	130
93	Uniform	1/200	30	240	130
94	Uniform	1/200	30	960	140
95	Uniform	1/200	30	960	140
96	Uniform	1/200	30	960	140
97	Unimodal	1/200	30	0	70
98	Unimodal	1/200	30	0	70
99	Unimodal	1/200	30	0	70
100	Unimodal	1/200	30	0	70
101	Unimodal	1/200	30	60	70
102	Unimodal	1/200	30	60	70
103	Unimodal	1/200	30	60	70
104	Unimodal	1/200	30	120	80
105	Unimodal	1/200	30	120	80
106	Unimodal	1/200	30	120	80
107	Unimodal	1/200	30	240	80
108	Unimodal	1/200	30	240	80
109	Unimodal	1/200	30	240	80
110	Unimodal	1/200	30	960	80
111	Unimodal	1/200	30	960	80
112	Unimodal	1/200	30	960	80
113	Bimodal	1/200	30	0	40
114	Bimodal	1/200	30	0	40
115	Bimodal	1/200	30	0	40
116	Bimodal	1/200	30	0	40
117	Bimodal	1/200	30	60	40
118	Bimodal	1/200	30	60	40
119	Bimodal	1/200	30	60	40
120	Bimodal	1/200	30	120	50
121	Bimodal	1/200	30	120	50
122	Bimodal	1/200	30	120	50
123	Bimodal	1/200	30	240	50
124	Bimodal	1/200	30	240	50
125	Bimodal	1/200	30	240	50
126	Bimodal	1/200	30	960	50
127	Bimodal	1/200	30	960	50
128	Bimodal	1/200	30	960	50

Table A1; Experimental variables detailing grain size distribution, bed slope and sampling durations.

A.2 Data Collected

Experiment Number	Data Collected				
	Critical Entrainment Threshold (Yalin)	Bedload (Total Load)	Bedload (Composition)	Bed Composition (photographs)	Laser Scan
1	X	n/a	n/a	n/a	n/a
2	X	n/a	n/a	n/a	n/a
3	X	n/a	n/a	n/a	n/a
4		n/a	n/a	n/a	n/a
5	X	n/a	n/a	n/a	n/a
6	X	n/a	n/a	n/a	n/a
7		n/a	n/a	n/a	n/a
8	X	n/a	n/a	n/a	n/a
9	X	n/a	n/a	n/a	n/a
10		n/a	n/a	n/a	n/a
11	X	n/a	n/a	n/a	n/a
12	X	n/a	n/a	n/a	n/a
13		n/a	n/a	n/a	n/a
14	X	n/a	n/a	n/a	n/a
15	X	n/a	n/a	n/a	n/a
16		n/a	n/a	n/a	n/a
17	X				n/a
18	X				n/a
19	X				n/a
20		x	x	x	n/a
21	X				n/a
22	X				n/a
23		x	x	x	n/a
24	X				n/a
25	x				n/a
26		x	x	x	n/a
27	X				n/a
28	X				n/a
29		x	x	x	n/a
30	X				n/a
31	X				n/a
32		x	x	x	n/a
33	X				n/a
34	X				n/a
35	X				n/a
36		x	x	x	n/a
37	X				n/a
38	x				n/a
39		x	x	x	n/a
40	X				n/a
41	x				n/a
42		x	x	x	n/a

43	X				n/a
44	X				n/a
45		x	x	x	n/a
46	X				n/a
47	X				n/a
48		x	x	x	n/a
49	X				n/a
50	X				n/a
51	X				n/a
52		x	x	x	n/a
53	X				n/a
54	x				n/a
55		x	x	x	n/a
56	X				n/a
57	x				n/a
58		x	x	x	n/a
59	X				n/a
60	X				n/a
61		x	x	x	n/a
62	X				n/a
63	X				n/a
64		x	x	x	n/a
65	X				n/a
66	X				n/a
67	X				n/a
68		x	x	x	n/a
69	X				n/a
70	x				n/a
71		x	x	x	n/a
72	X				n/a
73	x				n/a
74		x	x	x	n/a
75	X				n/a
76	X				n/a
77		x	x	x	n/a
78	X				n/a
79	X				n/a
80		x	x	x	n/a
81	X				
82	X				
83	X				
84		x	n/a	x	x
85	X				
86	x				
87		x	n/a	x	x
88	X				
89	x				
90		x	n/a	x	x
91	X				

92	X				
93		x	n/a	x	x
94	X				
95	X				
96		x	n/a	x	x
97	X				
98	X				
99	X				
100		x	X	x	x
101	X				
102	x				
103		x	X	x	x
104	X				
105	x				
106		x	X	x	x
107	X				
108	X				
109		x	X	x	x
110	X				
111	X				
112		x	X	x	x
113	X				
114	X				
115	X				
116		x	x	x	X
117	X				
118	x				
119		x	x	x	X
120	X				
121	x				
122		x	X	x	x
123	X				
124	X				
125		x	X	x	x
126	X				
127	X				
128		x	X	x	x

Table A2; Experimental variables detailing the measurements which were taken for each experimental run.

Appendix B; Cumulative Grain Size Distribution Graphs for the Unimodal, Bimodal, Coarse and Fine Beds

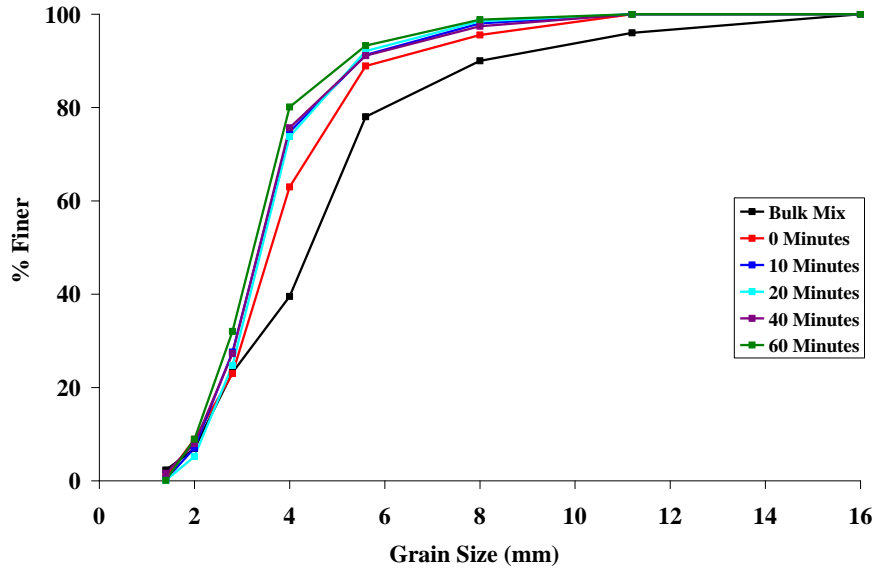


Figure B1; Bedload Composition for the unimodal bed subject to a range of antecedent durations.

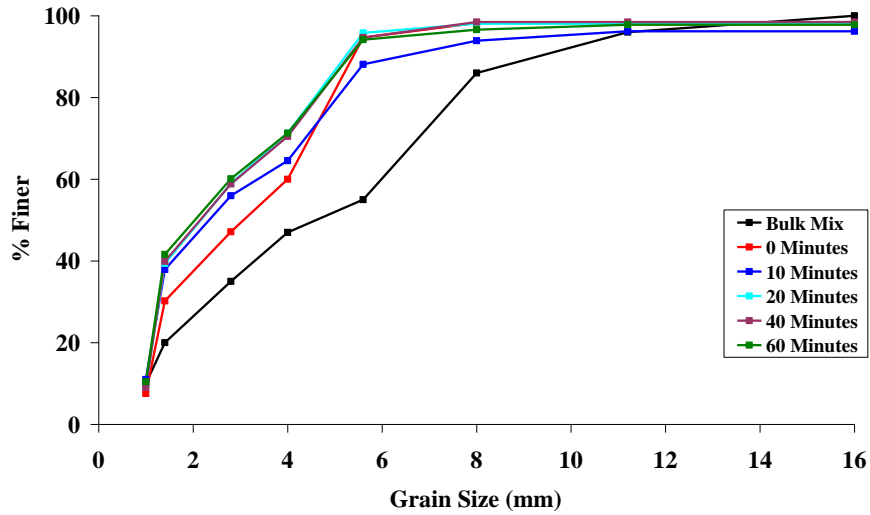


Figure B2; Bedload Composition for the bimodal bed subject to a range of antecedent durations.

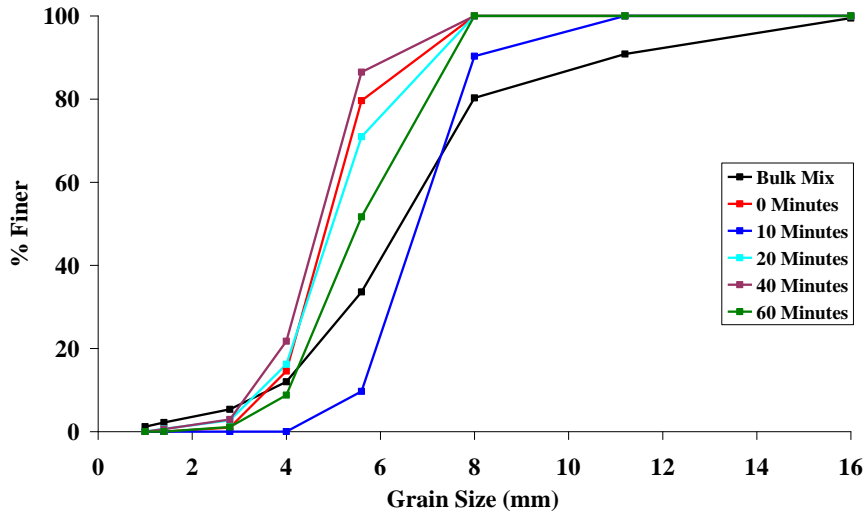
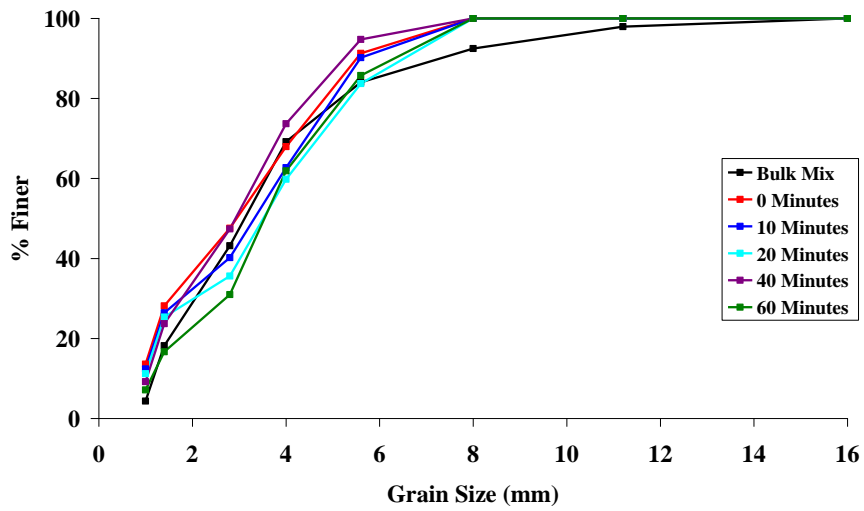


Figure B3; Bedload composition for the coarse bed subjected to a range of antecedent durations.



FigureB4; Bedload Composition for the fine bed subject to a range of antecedent durations.

Appendix C; Cumulative Grain Size Distribution Graphs for the Unimodal and Bimodal Beds

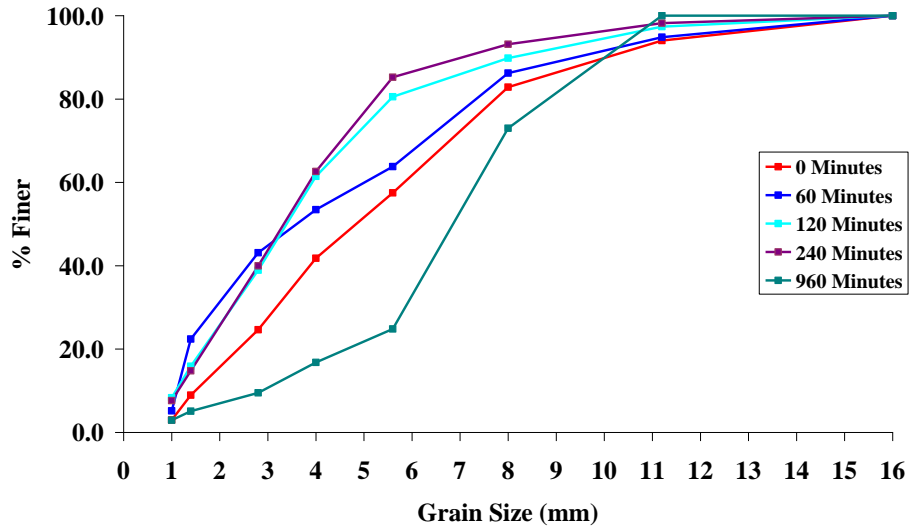


Figure C1; Bedload Composition for the bimodal bed subject to a range of antecedent durations.

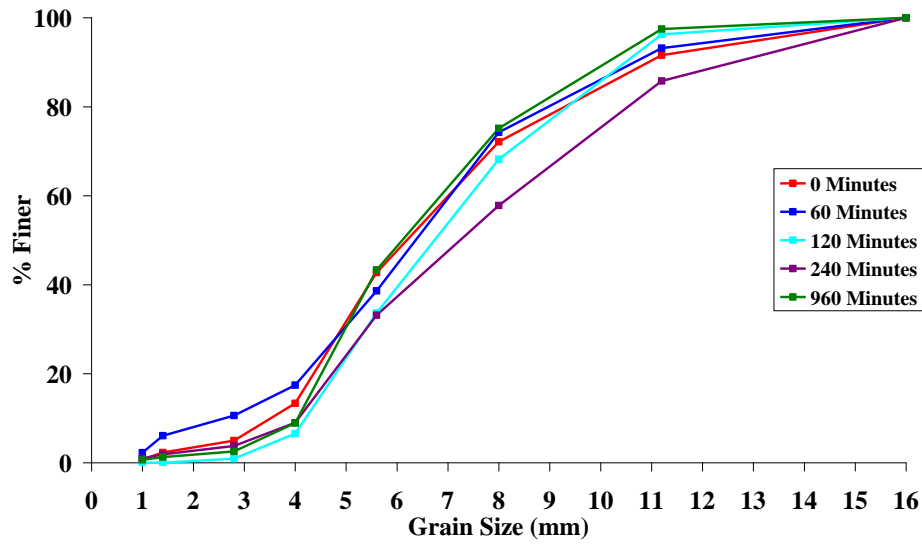


Figure C2; Bedload Composition for the unimodal bed subject to a range of antecedent durations.

Appendix D; Probability Density Functions of Normalised Elevation for the Uniform, Unimodal and Bimodal Beds

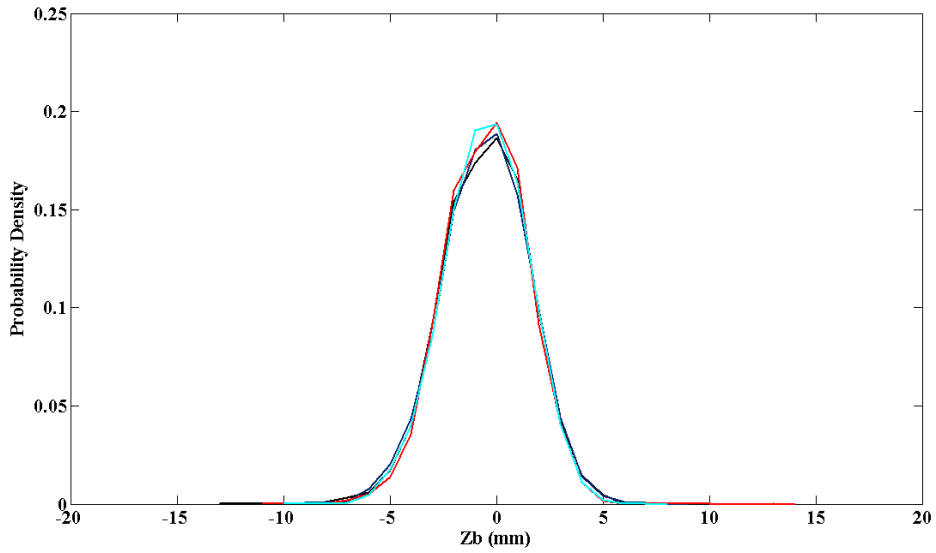


Figure D1; Probability density functions for the uniform beds plotted for the start and finish of the 60 and 960 minute antecedent duration experiments respectively.

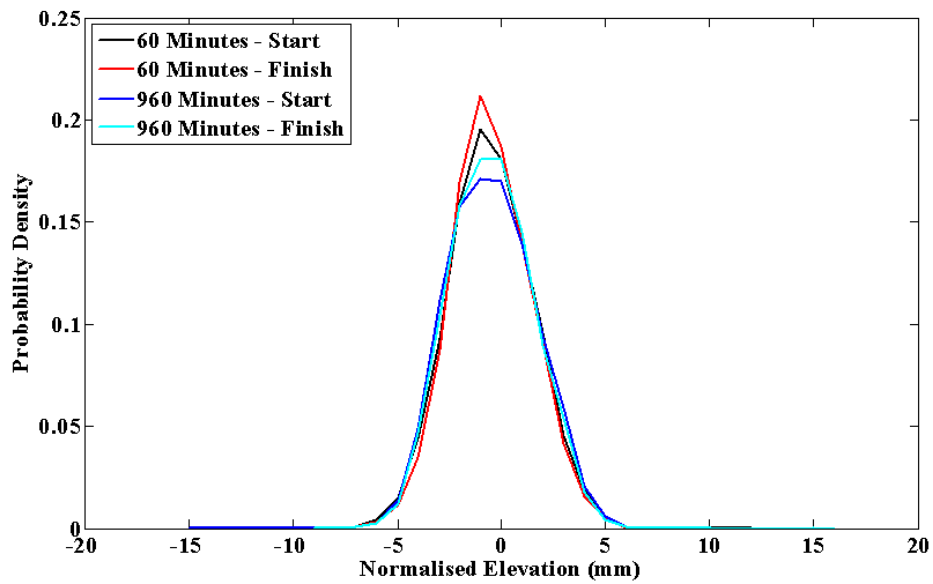


Figure D2: Probability density functions for the unimodal beds plotted for the start and finish of the 60 and 960 minute antecedent duration experiments respectively.

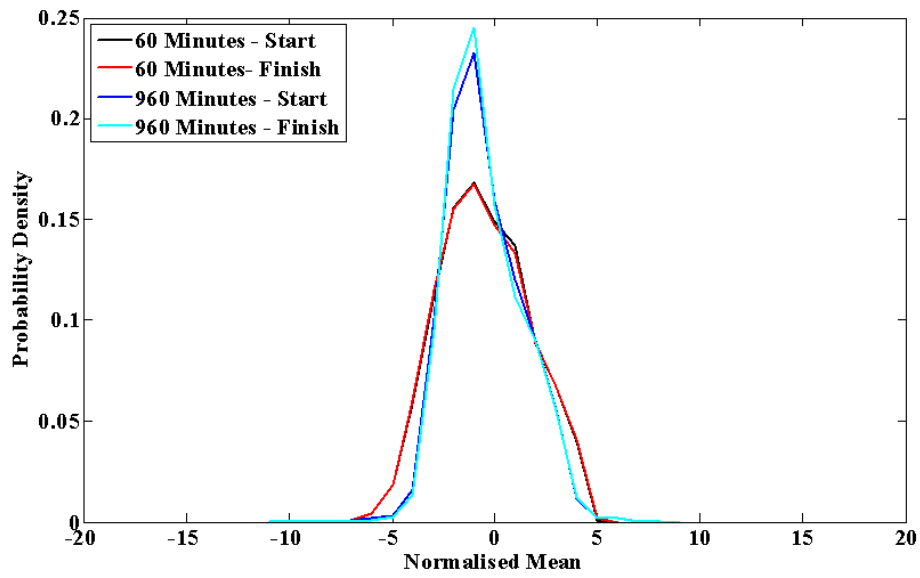


Figure D3; Probability density functions for the bimodal beds plotted for the start and finish of the 60 and 960 minute antecedent duration experiments respectively.

Appendix E; Cumulative Distribution Graphs plotting pore size as a function of applied antecedent flow for the Uniform, Unimodal and Bimodal Beds

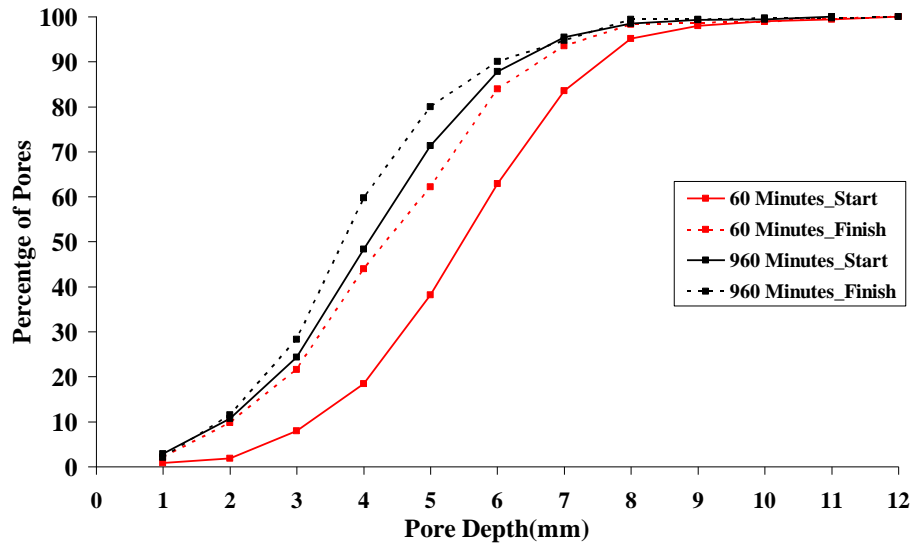


Figure E1; The change in pore depth as a function of applied antecedent flow plotted against the percentage of pores at that depth in the uniform bed.

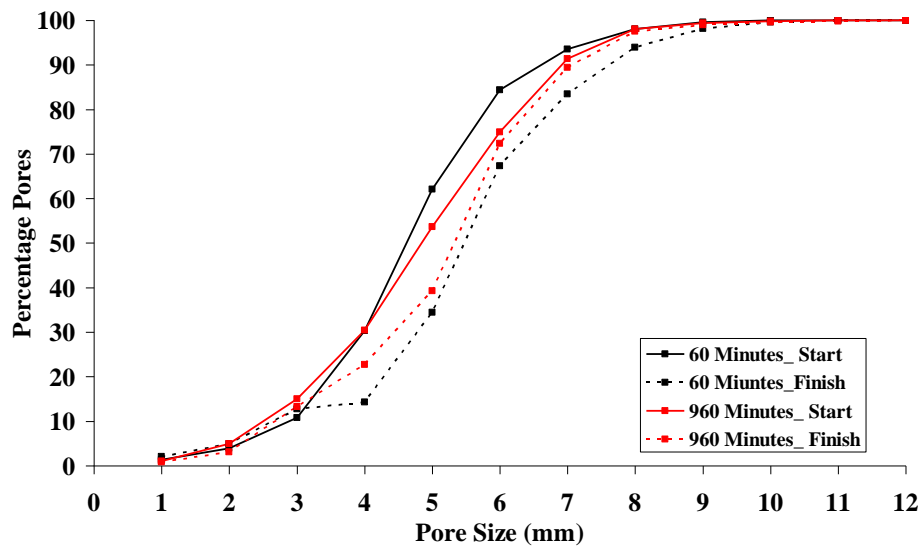


Figure E2; The change in pore depth as a function of applied antecedent flow plotted against the percentage of pores at that depth in the unimodal bed.

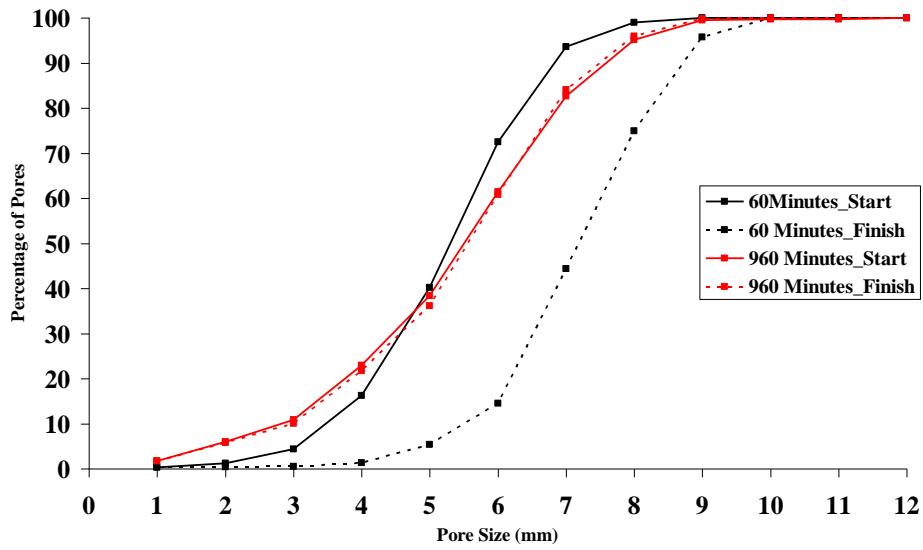


Figure E3; The change in pore depth as a function of applied antecedent flow plotted against the percentage of pores at that depth in the bimodal bed.

References

- Aberle, J.** (2007). Measurements of armour layer roughness geometry function and porosity. *Acta Geophysica*. 55(1); 23-32.
- Aberle, J. and K, Koll.** (2004). Double-averaged flow field over static armour layers In the Proceedings of the International Conference on Fluvial Hydraulics River Flow 2004. Vol. 1; 225– 233.
- Aberle, J. and Nikora, V.** (2006) Statistical properties of armored gravel bed surfaces. *Water Resources Research*. 42; DOI: 10.1029/2005WR004674
- Aberle, J.** Personal Communication February 2010.
- Acreman, M.C.** (2000). Guidelines for the Sustainable Management of Groundwater-fed Catchment. Report to European Union. Institute of Hydrology, United Kingdom.
- Acornley, R.M. and Sear, D.A.** (1999). Sediment transport and sedimentation of Brown trout (*Salmo trutta* L.) spawning gravels in chalk streams. *Hydrological Process*. 13; 447–458.
- Allen, J.R.L.** (1970). *Physical processes of sedimentation: an introduction*. Allen and Unwin, London, UK.
- Allen, J. R. L.** (1982). *Sedimentary Structures; Their character and physical basis*. In *Developments in Sedimentology*. Vol. 30B, Elsevier, New York.
- Allan, A.F. and Frostick, L.E.** (1999). Framework dilation, winnowing and matrix particle size: the behaviour of some sand-gravel mixtures in a laboratory flume. *Journal of Sedimentary Research*. 69; 21–26.
- Almedeij, J., Diplas, P. and Al-Ruwaih, F.** (2006). Approach to separate sand from gravel for bed-load transport calculations in streams with bimodal sediments. *Journal of Hydraulic Engineering*. 132 (11); 1176-1185.
- Ashida, K., and Michiue, M.** (1972). Study on hydraulic resistance and bedload transport rate in alluvial streams. *Transactions of the Japanese Society of Civil Engineering*. 206; 59-69
- Ashworth, P.J. and Ferguson, R.I.** (1989). Size selective entrainment of bedload in gravel bed streams. *Water Resources Research*. 25:627–634.
- Andrews, E. D.** (1983). Entrainment of gravel from naturally sorted riverbed material. *Geological Society of America Bulletin*. 94; 1225-1239.
- Andrews, E.D. and Erman, D.C.** (1986). Persistence in the size distribution of surficial bed material during extreme snowmelt floods. *Water Resources Research*. 22; 191-97

Andrews, E. D. and Parker, G. (1987). Formation of a coarse surface layer as the response to gravel mobility. In Thorne, C. R., Bathurst, J.C. and R. Hey. (Eds). *Sediment transport in gravel-bed rivers*. John Wiley & Sons. Chichester, UK. 269–325.

Bauer, B.O., Sherman, D.J. and Wolcott, J.F. (1992). Sources of uncertainty in shear stress and roughness length estimates derived from velocity profiles. *Professional Geographer*. 44; 453–464.

Bennett, S.J. and Best, J.L. (1995). Mean flow and turbulence structure over fixed, two-dimensional dunes: implications for sediment transport and bedform stability. *Sedimentology*. 42; 491–513.

Bottacin-Busolin, A., Tait, S.J., Marion, A., Chegini, A., and Tregnaghi, M. (2008). Probabilistic description of grain resistance from simultaneous flow field and grain motion measurements. *Water Resources Research*. doi: 0.1090.2007WR006224

Bridge, J.S. and Bennett, S.J. (1992). A model for the entrainment and transport of sediment grains of mixed sizes, shapes and densities. *Water Resources Research*. 28; 337–363.

Brayshaw, A.C., Frostick, L.E. and Reid, I. (1983). The hydrodynamics of particle clusters and sediment entrainment in coarse alluvial channels. *Sedimentology*. 30; 137–140.

Brown, A and Willetts, B. (1997). Sediment flux, grain sorting and the bed condition. In *Environmental and Coastal Hydraulics: Protecting the Aquatic Habitat*. Wang, S.S.Y. and Carstens, T. (Eds). American Society of Civil Engineers. 2: 1469–1474.

Buffin-Bélanger, T., Roy, A.G. (1998). Effects of a pebble cluster on the turbulent structure of a depth-limited flow in a gravel-bed river. *Geomorphology*, 25, 249–267.

Buffington, J. (1999). The legend of A. F. Shields. *Journal of Hydraulic Engineering*. 125; 376–387.

Buffington, J.M., Dietrich, W.E. and Kirchner, J.W. (1992). Friction angle measurements on a naturally formed gravel streambed; Implications for critical boundary shear stress. *Water Resources Research*. 28; 411–425

Buffington, J.M. and Montgomery, D.R. (1997). A systematic analysis of eight decades of incipient motion studies, with special reference to gravel-bedded rivers. *Water Resources Research*. 33; 1993–2029.

Buffington, J.M. and Montgomery, D.M. (1999). Effects of sediment supply on surface textures of gravel-bed rivers. *Water Resources Research*. 35; 3523– 3530.

Bullock, A., Gustard, A. and Grainger, E.S. (1991). *Instream Flow Requirements of Aquatic Ecology in Two British Rivers*. Institute of Hydrology. Wallingford, Oxfordshire. 115; 138.

Bunte, K. and Abt, S.R. (2001). Sampling surface and subsurface particle-size distributions in wadable gravel-and cobble-bed streams for analyses in sediment transport,

hydraulics and streambed monitoring. General Technical Report 74. Department of Agriculture, Forest Service, Rocky Mountain Research Station. Fort Collins; U.S.

Butler, J.B., Lane, S.N., Chandler, J.H. (1998). Assessment of DEM quality characterizing surface roughness using close range digital photogrammetry. *Photogrammetric Record*. 19: 271–291.

Butler, J.B., Lane, S.N. and Chandler, J.H. (2001). Automated extraction of grain-size data for gravel surfaces using digital image processing. *Journal of Hydraulic Research*. 39; 519-529.

Carbonneau, P., Lane, S. and Bergeron, N. (2003). Cost-effective non metric close-range digital photogrammetry and its application to a study of coarse gravel river beds. *International Journal of Remote Sensing*. 24; 2837-2854.

Carling, P.A. (1983). Particulate dynamics, dissolved and total load, in 2 small basins, northern Pennines, UK. *Hydrological Sciences Journal*. 28; 355-375.

Carling, P. A. (1984). Deposition of fine and coarse sand in an openwork gravel bed. *Canadian Journal of Fisheries and Aquatic Sciences*. 4; 263–270.

Carling, P.A. (1989). Bedload transport in two gravel-bedded streams. *Earth Surface Processes and Landforms*. 14; 27-39.

Carson, M.A. and Griffiths, G.A. (1987). Bedload Transport on gravel channels. *Journal of Hydrology*. 79; 375-378.

Carling, P. A., A. Kelsey, and Glaister, M.S. (1992). Effect of bed roughness, particle shape and orientation on initial motion criteria. In *Dynamics of Gravel-bed Rivers*. Billi, P., Hey, R.D., Thorne, C.R. and Tacconi, P, (Eds). Wiley; Chichester. 24–39.

Chandler, J.H., Shiono, K., Rameshwaren, P. and Lane, S.N. (2001). Measuring flume surfaces for hydraulics research using a Kodak DCS460. *Photogrammetric Record*. 17; 39-61.

Chien, N. and Wan, Z. (1999). *Mechanics of sediment transport*. ASCE; Va.

Chin, C.O., Melville, B.W. and Raudkivi, A.J. (1994). Stream bed armouring. *Journal of Hydraulic Engineering*. 120; 899–918.

Church, M. (1978). Palaeohydraulic Reconstructions From a Holocene Valley Fill. In: *Fluvial Sedimentology*; Miall, A.D. (Eds). Canadian Society of Petroleum Geologists. Calgary. Canada. 743–772.

Church, M., Hassan, M.A. and Wolcott, J.F. (1998). Stabilizing self organized structures in gravel-bed stream channels: Field and experimental observations. *Water Resources Research*. 34; 3169-3179

Cho, V.T. (1959). *Open Channel Hydraulics*. New York. McGraw-Hill.

Clifford, N. J., Richards, K. S. and Robert, A. (1992). The influence of microform bed roughness elements on flow and sediment transport in gravel bed rivers. *Earth Surface Processes and Landforms*. 17; 529-534.

Cooper, J.R., Tait, S.J. and Marion A. (2005). The influence of relative submergence on the near-bed flow field: implications for bed-load transport, *Eos Transactions. AGU*. 52; H51H-07

Coleman, S.E. and Nikora, V.I. (2008). A unifying framework for particle entrainment. *Water Resources Research*. 44; doi:10.1029/2007WR006363.

Colombini, M. (1993). Turbulence-driven secondary flows and formation of sand ridges. *Journal of Fluid Mechanics*. 254; 701-719.

Colombini, M. and Parker, G. (1995). Longitudinal streaks. *Journal of Fluid Mechanics*. 304; 161-183.

Cooper, J.R. (2008). Spatially-induced Momentum Transfer over Water-worked Gravel Beds. Unpublished Ph.D. Thesis. Department of Civil and Structural Engineering. The University of Sheffield.

Cooper, J.R. and Tait, S.J. (2008). Water worked gravel beds in laboratory flumes- a natural analogue?. *Earth Surface Processes and Landforms*. 34: 384-397.

Cooper, J.R., Aberle J., Koll K., McLelland S.J., Murphy B.J., Tait S.J. and Marion, A. (2008). Observation of the near-bed flow field over gravel bed surfaces with different roughness length scales, 4th International Association of Hydraulic Research River Flow Conference. Cesme-Izmir; Turkey.

Cooper, J.R. and Frostick, L.E. (2009). The difference in the evolution of the bed surface topography of gravel and gravel-sand mixtures, 33rd IAHR Congress: Water Engineering for a Sustainable Environment. International Association of Hydraulic Engineering & Research. Vancouver, Canada.

Cooper, J.R. and Tait, S.J. (2010). Examining the physical components of boundary shear stress for water-worked gravel deposits. *Earth Surface Processes and Landforms*. 35; 1240-1246.

Culbertson, J. K. (1967). Evidence of secondary circulation in an alluvial channel. U.S. Geological Survey Professional Paper. 57; 214-216.

Cumberland, D.J. and Crawford, R.J. (1987). The Packing of the Particles. *Handbook of Powder Technology*. 6; 24-25.

Cuthbertson, A.J.S. (2001). The motion of fine sand particles in turbulent open channel shear flows over porous bed conditions. Unpublished Ph.D. Thesis. Department of Civil Engineering, University of Glasgow.

Cuthbertson, A.J.S. and Irvine, D.A. (1999). The interaction between turbulent vortices and fine sediment particles—A possible reason for enhanced settling characteristics. *Proceedings of the 27th IAHR Congress*. Graz. Austria. D; Paper D5.

-
- Detert, M., Klar, M., Wenka, T. and Jirka, G.H.** (2008). Pressure- and velocity-measurements above and within a porous gravel bed at the threshold of stability. *Developments in Earth Surface Processes*. 11; 85-107
- Dietrich, W.E., Kirchner, J.W., Ikeda, H. and Iseya, F.** (1989). Sediment supply and the development of the coarse surface layer in gravel-bedded rivers. *Nature*. 340; 215-217
- Diplas, P., and Parker, G.** (1985). Pollution of gravel spawning grounds due to fine sediment. St. Anthony Falls Hydraulic Laboratory Project Report 240. University of Minneapolis.
- Drake, T.G., Shreve, R.L., Dietrich, W.E., Whiting, P.J. and Leopold, L.B.** (1988). Bedload transport of fine gravel observed by motion picture photography. *Journal of Fluid Mechanics*. 192;193-217.
- Egiazaroff, I.V.** (1965). Calculation of non-uniform sediment concentrations. *Journal of the Hydraulics Division, Proceedings of the American Society of Civil Engineers*, 91; 225-247.
- Einstein, H.A.** (1942). Formulas for the transportation of bed load. *Transactions of the American Society of Civil Engineers*. 107; 561–597.
- Einstein, H.A.** (1950). The bed load function for sediment transportation in open channels. *Technical Bulletin 1026*. U.S. Department of Agriculture Soil and Conservation Service. Washington D.C.
- Fenton, J. D. and Abbott, J. E.** (1977). Initial movement of grains on a stream bed: the effect of relative protrusion. *Proceedings of the Royal Society of London*. 352; 523–537.
- Ferguson, R.I.** (2003). The missing dimension: effects of lateral variation on 1-D calculations of fluvial bedload transport. *Geomorphology*. 56: 1–14.
- Ferguson, R.I., K. Prestegard, K. and Ashworth, P.J.** (1989). Influence of sand on hydraulics and gravel transport in a braided gravelbed river. *Water Resources Research*. 25; 635–643.
- Fraser, H.F.** (1935). Experimental study of the porosity and permeability of clastic sediments. *Journal of Geology*. 83; 910-1010.
- Frey, P. and Church, M.** (2009). How River Beds Move. *Science*. 325, 1509-1510.
- Frings, R., Kleinhans, M. and Vollmer, S.** (2008). Discriminating between pore-filling load and bed-structure load: a new porosity-based method, exemplified for the river Rhine *Sedimentology*. 77;1–23.
- Frostick, L.E., Lucas, P.M. and Reid, I.** (1984). The infiltration of fines into coarse-grained alluvial sediments and its implications for stratigraphical interpretation. *Journal of the Geological Society of London*. 141; 955-965.

Gessler, J. (1971). Beginning and ceasing of sediment motion. In Shen, H.W. *River Mechanics*. Fort Collins; Colorado. 7:1–7:22.

Gibbons, C.N., Soulsby, C., Jeffries, M.J, and Acornley, R. (2001). Developing ecologically acceptable river flow regime: a case study of Kielder reservoir and Kielder water transfer system. *Fisheries Management and Ecology*. 8; 463-485.

Gilvear, D.J. (1994). River Flow Regulation. In Maitland, P.S., Boon, P. and McClusky, D.S. (Eds) *The Freshwaters of Scotland; A National Resource of International Significance*. J Wiley & Sons; UK. 463-488

Gomez, B. (1983). Temporal variations in the particle size distribution of the surficial bed material: the effect of progressive armouring. *Geografiska Annaler*. 65; 183-192.

Gomez, B. and Phillips, J.D. (1999). Deterministic uncertainty in bedload transport. *Journal of Hydraulic Engineering*. 125; 305-308.

Graf, W. (1971) *Hydraulics of sediment transport*. McGraw-Hill; NewYork.

Graf, W. H. (1998). *Fluvial hydraulics. Flow and transport processes in channels of simple geometry*. J Wiley & Sons; UK.

Graf, W.H. and Pазis, G.C. (1977). Deposition and erosion in an alluvial channel. *Journal of Hydraulic Research*. 15; 151-166.

Graham, D.J., Reid, I. and Rice, S.P. (2005). Automated Sizing of Coarse-Grained Sediments: Image-processing procedures. *Mathematical Geology*. 37; 1-28.

Grass, A.J. (1970). Initial instability of fine bed sand. *Journal of the Hydraulics Division; American Society of Civil Engineering*. 96; 619-632;

Hassan, M.A. and Church, M. (2000). Experiments on surface structure and partial sediment transport on a gravel bed. *Water Resources Research*. 36; 1885-1895.

Hassan, M.A., Egozi, R. and Parker, G. (2006). Experiments on the effect of hydrograph characteristics on vertical grain sorting in gravel bed rivers. *Water Resources Research*. 42; doi: 10.1029/2005WR004707.

Haynes, H. and Ockelford, A. (2009). A Comparison of Time-Induced Stability Differences Between a Framework-Supported and a Matrix-Supported Gravel:Sand Mixture. 33rd IAHR Congress: Water Engineering for a Sustainable Environment. International Association of Hydraulic Engineering & Research. Vancouver, Canada.

Haynes, H. and Pender, G. (2007). Stress history effects on graded bed stability. *Journal of Hydraulic Engineering*. 33; 343-349.

Haynes, H., Vignaga, E. & Holmes, W.M. (2009). Magnetic Resonance Imaging of 3D River Bed Structure. *Sedimentology*, 56; 1961-1975.

-
- Hecht, C.A.** (2004). Geo-mechanical models for clastic grain packing. *Pure and Applied Geophysics*. 161; 331-349.
- Henning, M., Hentschel, B. and Hüsener, T.** (2008). Determination of channel morphology and flow features in laboratory models using 3D-photogrammetry. 4th International IAHR River Flow Conference. Cesme-Izmir; Turkey.
- Henning, M., Hentschel, B. and Hüsener, T.** (2009). Photogrammetric System for Measurement and Analysis of Dune Movement. 33rd IAHR Congress: Water Engineering for a Sustainable Environment. International Association of Hydraulic Engineering & Research. Vancouver, Canada.
- Hey, R.** (1996). Environmentally sensitive river engineering. In: Petts, G.E. and Calow, P. (Eds) *River Restoration*. Blackwell Science. 80 –105.
- Hiby, L., Lovell, P., Patil, N.S., Gopalaswamy, A.M. and Ullas Karanth, K.** (2009). A tiger cannot change its stripes: using a three-dimensional model to match images of living tigers and tiger skins. *Biological Letters*. 23; 283-286.
- Hodge, R., Brasington, J. and Richards, K.,** (2009). Analysing laser-scanned Digital Terrain Models of gravel bed surfaces: Linking morphology to sediment transport processes and hydraulics. *Sedimentology*. 56; 2024 – 2043.
- Hoey, T.B. and Ferguson, R.** (1994). Numerical simulation of downstream fining by selective transport in gravel bed rivers: model development and illustration. *Water Resources Research*. 30; 2251–2260,
- Humphreys, F.J., Huang, Y., Brough, I. and Harris, C.** (1999). Electron backscatter diffraction of grain and sub-grain structures; resolution considerations. *Journal of Microscopy*. 195; 212–216.
- Hunziker, R., and Jaeggi, M.N.R.** (2002). Grain sorting processes. *Journal of Hydraulic Engineering*. 128;1060-1068.
- Ibbeken, H., Warnke, D.A. and Diepenbroek, M.** (1998). Granulometric study of the Hanaupah Fan, Death Valley, California. *Earth Surface Processes and Landforms*. 23; 481-492.
- Ikeda, S.** (1981). Self-formed straight channels in sandy beds. *Journal of the Hydraulics Division, Proceedings of the American Society of Civil Engineers*. 107; 389-406.
- Ikeda, H. and Iseya, F.** (1988). Experimental study of heterogeneous sediment transport. Environmental Research Centre Paper 12. University of Tsukuba; Japan.
- Jackson, W. L., and Beschta, R.L.** (1984). Influences of increased sand delivery on the morphology of sand and gravel channels. *Journal of the American Water Resources Association*. 20; 527–533.
- Johnston, C.E., Andrews, E.D. and Pitlick, J.** (1998). In situ determination of particle friction angles of fluvial gravels. *Water Resources Research*. 34; 2017-2030.

-
- Junk, W.J., Bayley, P.B. and Sparks, R.E.** (1989). The flood pulse concept in river-floodplain systems. *Canadian Special Publications of Fisheries and Aquatic Sciences*. 106;110-127.
- Jones, R.R., Wawrzyniec, T.F., Holliman, N.S., Kenneth J.W., Imber, J.I. and Holdsworth, R.E.** (2008). Describing the dimensionality of geospatial data in the earth sciences - Recommendations for nomenclature. *Geosphere*. 4; 354-359.
- Kaftori, D., Hetsroni, G. and Banerjee, S.** (1995). Particle behavior in the turbulent boundary layer. Part I: Motion, deposition, and entrainment. *Physics of Fluids*. 7;1095–1106.
- Karcz, I.** (1973). Reflections on the origin of source; Small-scale longitudinal streambed scours. IN *Fluvial Geomorphology*. Morisawa, M. (Eds). 4th Annual Geomorphology Symposia Series. 149-173.
- Kirchner, J.W., Dietrich, W.W., Iseya, F. and Ikeda, H.** (1990). The variability of critical shear stress, friction angle, and grain protrusion in water-worked sediments. *Sedimentology*. 37; 647–672.
- Kleinhans, M.G., Jeukens, C., Bakker, C., and Frings, R.** (2008). Magnetic Resonance Imaging of coarse sediment. *Sedimentary Geology*. 208; 69-78.
- Koll K., Tait S.J., Cooper J.R., Aberle J., and Marion A.** (2008). Comparison of turbulence characteristics measured using LDA and PIV systems over a gravel sediment surface. 4th International IAHR River Flow Conference. Cesme-Izmir; Turkey.
- Kuhnle, R.A.** (1992). Fractional transport rates of bedload on Goodwin Creek. In *Dynamics of Gravel-bed Rivers*. Billi, P., Hey, R.D., Thorne, C.R. and Tacconi, P, (Eds). Wiley; Chichester. 141-151.
- Kuhnle, R.A.** (1993). Incipient motion of sand-gravel sediment mixtures. *Journal of Hydraulic Engineering*. 119; 400–415.
- Komar, P.D.** (1987). Selective grain entrainment by a current from a bed of mixed sizes: a reanalysis. *Journal of Sedimentary Petrology*. 57; 203-211.
- Komar, P.D. and Li, Z.** (1986). Pivoting analysis of the selective entrainment of sediments by shape and size with application to gravel threshold. *Sedimentology*. 33; 425–436.
- Komar, P.D. and Shih, S.** (1992). Equal mobility versus changing bed load grain sizes in gravel-bed stream. In *Dynamics of Gravel-bed Rivers*. Billi, P., Hey, R.D., Thorne, C.R. and Tacconi, P, (Eds). Wiley; Chichester. 73–93.
- Kramer, H.** (1935). Sand mixtures and sand movement in fluvial models. *Transactions of the America Society of Civil Engineers*. 100; 798–878.
- Ladd, G., Nagchaudhuri, A. and Earl, T. Rectificaion** (2006). Georeferencing and mosaicing of images acquired with remotely operated aerial platforms. *American Society for Photogrammetry and Remote Sensing Annual Conference*. Reno; Nevada.
-

-
- Laronne, J. B., Reid, J., Yitshak, Y. and Frostick, L.E.** (1994). The non-layering of gravel streambeds under ephemeral flood regimes. *Journal of Hydrology*. 159: 353-363.
- Lane, S.N., Chandler, J.H. and Porfiri, K.** (2001). Monitoring river channel and flume surfaces with digital photogrammetry. *Journal of Hydraulic Engineering*. 127: 871-877.
- Lawless, M. and Robert, A.** (2001). Three-dimensional flow structure around small-scale bedforms in a simulated gravel-bed environment. *Earth Surface Processes and Landforms*. 26; 507-522.
- Leeder, M.R.** (1983). On the interactions between turbulent flow, sediment transport and bedform mechanics in channelized flows. In: *Modern and Ancient Fluvial Systems*. Collinson, J.D and Lewin, J. (Eds). Special Publication of the International Association of Sedimentologists. 6; 5-18.
- Legleiter, C.J., Phelps, T.L. and Wohl, E.E.** (2007). Geostatistical analysis of the effects of stage and roughness on reach-scale spatial patterns of velocity and turbulence intensity. *Geomorphology*. 83; 322-345.
- Li, Z. and Komar, P.D.** (1986). Laboratory measurements of pivoting angles for applications in selective entrainment of gravel in a current. *Sedimentology*. 33; 5917-5929.
- Lisle, T.E., Nelson, J.M., Pitlick, J., Madej, M.A. and Barkett, B.L.** (2000). Variability of bed mobility in natural gravel-bed channels and adjustments to sediment load at the local and reach scales. *Water Resources Research*. 36; 3743 - 3756.
- Livesey, R.H.** (1963). Channel armouring below Fort Randall Dam, U.S. Department of Agriculture Report. 970; 461-470.
- Lorang, M.S. and Hauer, F.R.** (2001). Flow Competence and Streambed Stability: An Evaluation of Technique and Application. *Journal of the North American Benthological Society*. 22; 475 -491.
- Marion, A., Tait, S. J. and McEwan I. K.** (1997). On the competitive effects of particle rearrangement and vertical sorting. *Proceedings of the 27th IAHR Congress, International Association for Hydraulic Research*. Madrid. Spain. 2; 1493-1498.
- Marion, A., Tait, S.J. and McEwan, I.K.** (2003). Analysis of small-scale gravel bed topography during armouring. *Water Resources Research*. 39; 1334-1345.
- Mao L., Cooper, J.R. and Frostick L.E.** (2009). Armour layer development during sediment starvation and recirculation flume experiments. *33rd IAHR Congress: Water Engineering for a Sustainable Environment*. Vancouver; Canada.
- McEwan, I.K., Sheen, T.M., Cunningham, G.J. and Allen, A.R.** (2000). Estimating the size composition of sediment surfaces through image analysis. *Proceedings of the Institution of Civil Engineering*. 142;189-195.

McEwen, I.K., Sorensen, M., Heald, J., Tait, S.J., Cunningham, G.J., Goring, D.G. and Willetts, B.B. (2004). Probabilistic modeling of bed-load composition. *Journal of Hydraulic Engineering*. 130; 129-139.

McLelland, S.J., Ashworth, P.J. and Best, J.L. (1999). Flow structure and transport of sand-grade suspended sediment around an evolving braid bar, Jamuna River, Bangladesh. In *Fluvial Sedimentology VI*, International Association of Sedimentologists Special Publication. 28; 43-57.

Measures, R. and Tait, S.J. (2008). Quantifying the role of bed surface topography in controlling sediment stability in water worked gravel deposits. *Water Resource Research*. 44; 4413;4430.

Miller, L. and Byrne, R.J. (1966). The angle of repose for a single grain on a fixed rough bed. *Sedimentology*. 6; 303-314.

Miller, M.C., McCave, I.N. and Komar, P.D. (1977). Threshold of sediment motion under unidirectional currents. *Sedimentology*. 24; 507-527.

Misri, R.L., Garde, R.J. and Ranga Raju, K.G. (1983). Experiments on bed load transport of nonuniform sands and gravels. *Proceedings of the Second International Symposium on River Sedimentation*. Beijing, China. 440-450.

Monteith, H. (2005). Experimental investigation into the effect of antecedent flow conditions on the stability of graded sediment beds; stress history. Unpublished Ph.D. Thesis, Department of Civil Engineering, Heriot-Watt University.

Monteith, H. and Pender, G. (2005) Flume investigation into the influence of shear stress history. *Water Resources Research*. 41, doi:10.1029/2005WR004297.

Muller, A. and Studerus, X. (1979). Secondary Flow in an Open-channel. *Proceedings of the 18th International Association of Hydraulic Research Congress*. Cagliari. 19-24.

Nakagawa, H. and Nezu, I. (1977). Prediction of the contributions to the Reynolds stress from bursting events in open-channel flows. *Journal of Fluid Mechanics*. 80; 99-128.

Neill, C.R. and Yalin, M.S. (1969). Quantitative definition of bed movement. *Journal of the Hydraulics Division, American Society of Civil Engineers*. 95; 581-588.

Nelson, J.M., Shreve, R.L., McLean, S.R. and Drake T.G. (1995). Role of near-bed turbulence structure in bed transport and bed form mechanics. *Water Resources Research*. 31; 2071-2086.

Nezu, I. and Rodi, W. (1985). Experimental study on secondary currents in open channel flow. *Proceedings of 21st Congress of International Association of Hydraulic Research*. Melbourne, Australia. 114-119.

Nezu, I. and Nakagawa, H. (1993). *Turbulence in Open-Channel Flows*. A. A. Balkema (Eds). Rotterdam. The Netherlands.

-
- Nicholas, A.P.** (2000). Modelling bedload yield in braided gravel bed rivers. *Geomorphology*. 36; 89-106.
- Nikora, V.I., Goring, D.G. and Biggs, B.J.F.** (1998). On gravel-bed roughness characterization. *Water Resources Research*. 34; 517–527.
- Nikora, V., Goring, D., McEwan, I. and Griffiths, G.** (2001). Spatially averaged open channel flow over rough bed. *Journal of Hydraulic Engineering*. 127; 123-133.
- Nikora, V.I. and Walsh, J.** (2004). Water-worked gravel surfaces: high-order structure functions at the particle scale. *Water Resources Research*. 40;doi: 10.1029/2004WR003346.
- Ockelford, A. and Haynes, H.** (2008). The Effect of Grain Size Distribution Modality on the Relationship Between Stress History and Entrainment Threshold. 4th International Association of Hydraulic Research River Flow Conference. Cesme-Izmir; Turkey.
- Ockelford, A., Haynes, H., Hodge, R. and Haynes, R.** (2010). Using high resolution laser scanning to indicate mechanisms of stabilisation under varying sub threshold flow exposures. 17th Congress of the Asia and Pacific Division of the International Association of Hydro-Environment Engineering and Research. Auckland; New Zealand
- Ockelford, A. and Haynes, H.** (2011). The impact of stress history on bed structure. Submitted to *Earth Surfaces Processes and Landforms*.
- Oldmeadow, D.F. and Church, M.** (2006). A field experiment on streambed stabilization by gravel structures. *Geomorphology*. 78; 335–350.
- Packman, A.I., and Brooks, N.H.** (2001). Hyporheic exchange of solutes and colloids with moving bedforms. *Water Resources Research*. 37; 2591-2605.
- Packman, A.I., Brooks, N.H., and Morgan, J.J.** (1997). Experimental techniques for laboratory investigation of clay colloid transport and filtration in a stream with a sand bed. *Water, Air, and Soil Pollution*. 99; 113-122.
- Paintal, A.S., (1971).** A stochastic model for bed load transport. *Journal of Hydraulic Research*. 9; 527–553.
- Paola, C. (1996).** Incoherent structure: turbulence as a metaphor for stream braiding. In Ashworth, P.J., Bennett, S.J., Best, J.L. and McLelland, S.J. (Eds.). *Coherent flow structures in open channels*. Wiley. Chichester.705-723.
- Paola, C. and R. Seal.** (1995). Grain size patchiness as a cause of selective deposition and downstream fining. *Water Resource Research*. 31; 1395–1407.
- Paphitis, D. and Collins, M.B.** (2005). Sand grain threshold, in relation to bed stress history: an experimental study. *Sedimentology*. 52; 827 838.
- Papanicolaou, A.N., Diplas, P., Dancy, C.L. and Balakrishnan, M.** (2001). Surface roughness effects in near-bed turbulence: implications to sediment entrainment. *Journal of Engineering Mechanics*. 127; 211-219.

Papanicolaou, A.N., Diplas, P., Evaggelopoulos, N. and Fotopoulos, S. (2002). Stochastic incipient motion criterion for spheres under various packing conditions. *Journal of Hydraulic Engineering*. 128; 369-381.

Parker, G. (1990). Surface-based bed load transport relation for gravel rivers. *Journal of Hydraulic Research*. 28; 417-436.

Parker, G., Klingeman, P.C. and McLean, D.G. (1982). Bedload and size distribution in paved gravel-bed stream. *Journal of the Hydraulic Division of the American Society of Civil Engineers*. 108; 544-571.

Parker, G. Personal communication September 2009.

Patel, P. L. and Ranga Raju, K. G. (1999). Critical tractive stress of non-uniform sediments. *Journal of Hydraulic Research*. 37; 39–58.

Petts, G.E. (1984). *Impounded Rivers*. John Wiley & Sons; Chichester.

Pender, G. and Li, Q. (1995). Comparison of two hiding function formulations for non uniform sediment transport calculations. *Proceedings of the Institute of Civil Engineers; Water, Maritime and Energy*, 112; 127-135.

Pender, G., Hoey, T.B., Fuller, C. and Mcewan, I.K. (2001). Selective bedload transport during the degradation of a well sorted graded sediment bed. *Journal of Hydraulic Research*. 39; 269-277

Powell, D.M. (1998). Patterns and processes of sediment sorting in gravel-bed rivers. *Progress in Physical Geography*. 22; 1 – 32.

Powell, D.M. and Ashworth, P.J. (1995). Spatial pattern of flow competence and bedload transport in a divided gravel bed river. *Water Resources Research*. 31: 741-752.

Powell, D. M., Reid, I. and Laronne, J. B. (1999). Hydraulic interpretation of cross-stream variations in bed-load transport. *Journal of Hydraulic Engineering*. 125; 1243-1252.

Prandtl, L. (1952). *Essentials of Fluid Dynamics*. London: Blackie.

Proffitt, G. T., and Sutherland, A. J. (1983). Transport of non uniform sediments. *Journal of Hydraulic Research*. 21; 33–43.

Raudkivi, A.J. (1991). *Loose boundary hydraulics*. 4th Edition. Balkema; Netherlands.

Reid, I. and Frostick, L.E. (1984). Particle interaction and its effects on the thresholds of initial and final bedload motion in coarse alluvial channels. *Sedimentology of Gravels and Conglomerates*. In Koster, E.H and Steel, R.J.S. (Eds). *Canadian Society of Petroleum Geologists Memoir*. 10: 61-68.

-
- Reid, I., Frostick, L.E. and Layman, J.T.** (1985). The incidence and nature of bedload transport during flood flows in coarse-grained alluvial channels. *Earth Surface Processes and Landforms*. 10: 33-44.
- Richards, K.** (1982). *Rivers - Form and Process in Alluvial Channels*. Methuen and Co; New York.
- Righetti, M. and Lucarelli, C.** (2007). May the Shields theory be extended to cohesive and adhesive benthic sediments?. *Journal of Geophysical Research*. 112 doi:10.1029/2006JC003669
- Robert, A.** (1990). Boundary roughness in coarse-grained alluvial channels. *Progress in Physical Geography*. 14; 42-70.
- Robert, A.** (1991). Fractal properties of simulated bed profiles in coarse-grained channels, *Mathematical Geology*. 23; 367-382.
- Rollinson, G.K.** (2006). Bed structure, pore spaces and turbulent flow over gravel beds. Unpublished Ph.D. Thesis. Department of Civil Engineering. The University of Hull.
- Rumsby, B.T., Brasington, J., Langham, J.A., McLelland, S.J., Middleton, R and Rollinson G.** (2008). Monitoring and modelling particle and reach-scale morphological change in gravel-bed rivers: Applications and challenges. *Geomorphology*. 93; 40-54.
- Saadi, Y.** (2002). The influence of different time varying antecedent flows on the stability of mixed grain size deposits. PhD thesis Department of Civil and Structural Engineering. University of Sheffield.
- Sambrook Smith, G.H., Nicholas, A.P. and Ferguson, R.I.** (1997). Measuring and defining bimodal sediments: problems and implications. *Water Resources Research*. 33 1179-1185.
- Sarmiento, O.A. and Falcon, M.A.** (2006). Critical bed shear stress for unisize sediment. *Journal of Hydraulic Engineering*. 132; 172-179.
- Schmeeckle, M.W. and Nelson, J.M.** (2003). Direct numerical simulation of bedload transport using a local, dynamic boundary condition. *Sedimentology*. 50; 279-301.
- Schmeeckle, M.W., Nelson, J.M. and Shreve, R.L.** (2007). Forces on stationary particles in near-bed turbulent flows. *Journal of Geophysical Research*. 112; doi:10.1029/2006JF000536.
- Shaw, J. and Kellerhals, R.** (1982). The composition of recent alluvial gravels in Alberta River beds. *Alberta Research Council Bulletin*. 41; 151.
- Schoklitsch A.** (1962). *Handbuch des Wasserbaues*. 3rd Edition. Springer-Verlag: Vienna.
- Shvidchenko, A. B.** (2000). Incipient motion of streambeds. PhD thesis. University of Glasgow, UK.

-
- Shvidchenko, A.B., and Pender, G.** (2000) Flume study of the effect of relative depth on the incipient motion of coarse uniform sediments. *Water Resources Research*. 36; 619 - 628.
- Scvidchenko, A.B., Pender, G. and Hoey, T.B.** (2001). Critical shear stress for incipient motion of sand/gravel streambeds. *Proceedings of the Institute of Civil Engineering; Waters and Maritime Engineering*. 142; 217-227.
- Shields, A.** (1936). Application of Similarity principles and Turbulence research to bedload Movement. *Hydrodynamics laboratory. California Institute of Technology*. 167; 36.
- Smart, G.M., Aberle, J., Duncan, M. and Walsh, J.** (2004). Measurement and analysis of alluvial bed roughness. *Journal of Hydraulic Research*. 43; 227 – 237.
- Sousa, W.P.** (1984). The role of disturbance in natural communities. *Annual Review of Ecology and Systematics*. 14; 353-391.
- Sterk, G., Jacobs, A.F.G. and Van Boxel, J.H.** (1998). The effect of turbulent flow structures on saltation transport in the atmospheric boundary layer. *Earth Surface Processes and Landforms*. 23; 877–887.
- Swales, S.** (1989). The Use of In stream Habitat Improvement Methodology in Mitigating the Adverse Effects of River Regulation on fisheries. In Gore, J. A. and Petts, G.E. (Eds). *Alternatives in Regulated River Management*. CRC Press; Florida.
- Sime, L.C. and Ferguson, R.I.** (2003). Information on Grain Sizes in Gravel-Bed Rivers by Automated Image Analysis. *Journal of Sedimentary Research*. 73; 630-636.
- Soulsby, C. and Malcolm, I.A.** (2001). Fine sediment influence on spawning habitat in a lowland regulated stream: a preliminary assessment. *Science of the Total Environment*. 265; 295–307.
- Sutherland, A.J.** (1987). Static armour layers by selective erosion. *Sediment Transport in Gravel-Bed Rivers*. C.R. Thorne et al., Wiley, Chichester, 243-60
- Sutherland, A.** (1991). Hiding functions to predict self armouring. *Proceedings, International Grain Sorting Seminar*. ETH Zürich. 117; 273-298.
- Tait, S. J., and Willetts, B.B.** (1991). Characterization of armoured bed surfaces. *Proceedings of the Internatial Grain Sorting Seminar*. Monte Verità. Switzerland.
- Tait, S.J., Willetts, B.B. and Maizels, J.K.** (1992). Laboratory observations of bed armouring and changes in bedload composition. In *Dynamics of Gravel-bed Rivers*. Billi, P., Hey, R.D., Thorne, C.R. and Tacconi, P, (Eds). Wiley; Chichester. 205-225.
- Van Rijn, L.C.** (1989). *Handbook of Sediment Transport by Currents and Waves*. Delft Hydraulics Report. Aqua Publications; The Netherlands.
- Vanoi, V.A., Benedict, P.C., Bondurant, D.C. McKee, J.E., Piest, R.F. and Smallshaw, J.** (1971). *Sediment Transport Mechanics; Hydraulic Relations for alluvial streams*.

Journal of the Hydraulic Division of the American Society of Civil Engineers. 97; 101-141.

Veličković, B., (2005). Colmation as one of the processes in interaction between the groundwater and surface water. *Architecture and Civil Engineering*. 3; 165–172.

Visscher, W.M. and Bolsterli, M. (1972). Random Packing of Equal and Unequal Spheres in Two and Three Dimensions. *Nature*. 239; 504–507.

Vollmer, S. and Kleinhans, M. G. (2007). Predicting incipient motion, including the effect of turbulent pressure fluctuations in the bed. *Water Resources Research*. 43; doi:10.1029/2006WR004919.

Wallbridge, G., Voulgaris, B.N., Tomlinson, B. and Collins, M.B. (1999). Initial motion and pivoting characteristics of sand particles in uniform and heterogeneous beds: experiments and modelling. *Sedimentology*. 46; 17–32.

Wathen, S.J., Ferguson, R.I., Hoey, T.B., and Werritty, A. (1995). Unequal mobility of gravel and sand in weakly bimodal river sediments. *Water Resources Research*. 31; 2087-2096

Webb, R.H., Schmidt, J.C., Marzolf, G.R. and Valdez, R.A. (1999). The Controlled Flood in Grand Canyon. *Geophysical Monograph Series*. 110; 368.

White, W. R. and Day, T.J. (1982) Transport of graded gravel bed material. Gravel-bed rivers. Hey, R.D., Bathurst, J.C. and Thorne, C.R. (Eds) John Wiley and Sons; London

Whiting, P. and King, J. (2003). Surface particle sizes on armoured gravel streambeds: Effects of supply and hydraulics. *Earth Surface Processes and Landforms*. 28:1459–1471.

Wilcock, P.R. (1988). Methods for estimating the critical shear stress of individual fractions in mixed-size sediment. *Water Resources Research*. 24; 1127-1135.

Wilcock, P.R. (1992). Experimental investigation of the effect of mixture properties on transport dynamics. In *Dynamics of Gravel-bed Rivers*. Billi, P., Hey, R.D., Thorne, C.R. and Tacconi, P. (Eds). Wiley; Chichester. 109–139

Wilcock, P.R. (1993). Critical shear stress of natural sediments. *Journal of Hydraulic Engineering*. 119: 491-505.

Wilcock, P.R. (1996). Estimating local bed shear stress from velocity observations. *Water Resources Research*. 32; 3361-3366.

Wilcock, P. R. and Southard, J. B. (1988). Experimental study of incipient motion in mixed-size sediment. *Water Resources Research*. 24; 1127-1135.

Wilcock, P.R. and Southard, J.B. (1989). Bedload transport of mixed size sediment: fractional transport rates, bed forms, and the development of a coarse bed surface layer. *Water Resources Research*. 25;1629 – 1641.

Wilcock, P. R., Barta, A.F., Shea, C.C., Kondolf, G.M., Matthews, G.V. and Pitlick, J. (1996). Observations of flow and sediment entrainment on a large gravel-bed river. *Water Resources Research*. 32; 2897–2909.

Wilcock, P.R. and McArdell, B.W. (1993). Surface-based fractional transport rates: Mobilization thresholds and partial transport of a sand-gravel sediment. *Water Resources Research*. 29; 1297–1312.

Wilcock, P. R. and McArdell, B.W. (1997). Partial transport of a sand/gravel sediment. *Water Resources Research*. 33; 235-245.

Wilcock, P.R., Kenworthy, S.T. Crowe, J.C. (2001). Experimental study of the transport of mixed sand and gravel. *Water Resources Research*. 37; 3349-3358.

Wilcock, P.R. and Crowe, J.C. (2003). Surface-based transport model for mixed-size sediment. *Journal of Hydraulic Engineering*. 129; 120–128.

Willetts, B.B., Maizels, J.K. and Florence, J. (1987). The simulation of stream bed armouring and its consequences. *Proceedings of the Institute of Civil Engineering*. 1; 799-814.

Wohl, E.E. and Ikeda, H. (1998). Patterns of bedrock channel erosion on the Boso Peninsula, Japan. *Journal of Geology*. 106:331–45.

Yalin, M.S. (1972). *Mechanics of Sediment Transport*. Pergamon; New York

Yalin, M.S. and E. Karahan, E. (1979). Inception of sediment transport. *Journal of the Hydraulic Division of Civil Engineering*. 105; 1433–1443.

Yalin, M.S. and da Silva, A.M.F. (2001). *Fluvial processes*. IAHR Monograph. Delft; The Netherlands

Yang, C.T. (1996). *Sediment transport: Theory and practice*. McGraw-Hill; New York.